



Universitat de Girona

THEORETICAL STUDY OF CATALYTIC REACTIONS OF CARBENES: HAPTOTROPIC REARRANGEMENTS AND THE DÖTZ REACTION

José Óscar Carlos JIMÉNEZ HALLA

ISBN: 978-84-693-0034-3

Dipòsit legal: GI-1353-2009

<http://www.tesisenxarxa.net/TDX-0112110-135752/>

ADVERTIMENT. La consulta d'aquesta tesi queda condicionada a l'acceptació de les següents condicions d'ús: La difusió d'aquesta tesi per mitjà del servei TDX (www.tesisenxarxa.net) ha estat autoritzada pels titulars dels drets de propietat intel·lectual únicament per a usos privats emmarcats en activitats d'investigació i docència. No s'autoritza la seva reproducció amb finalitats de lucre ni la seva difusió i posada a disposició des d'un lloc aliè al servei TDX. No s'autoritza la presentació del seu contingut en una finestra o marc aliè a TDX (framing). Aquesta reserva de drets afecta tant al resum de presentació de la tesi com als seus continguts. En la utilització o cita de parts de la tesi és obligat indicar el nom de la persona autora.

ADVERTENCIA. La consulta de esta tesis queda condicionada a la aceptación de las siguientes condiciones de uso: La difusión de esta tesis por medio del servicio TDR (www.tesisenred.net) ha sido autorizada por los titulares de los derechos de propiedad intelectual únicamente para usos privados enmarcados en actividades de investigación y docencia. No se autoriza su reproducción con finalidades de lucro ni su difusión y puesta a disposición desde un sitio ajeno al servicio TDR. No se autoriza la presentación de su contenido en una ventana o marco ajeno a TDR (framing). Esta reserva de derechos afecta tanto al resumen de presentación de la tesis como a sus contenidos. En la utilización o cita de partes de la tesis es obligado indicar el nombre de la persona autora.

WARNING. On having consulted this thesis you're accepting the following use conditions: Spreading this thesis by the TDX (www.tesisenxarxa.net) service has been authorized by the titular of the intellectual property rights only for private uses placed in investigation and teaching activities. Reproduction with lucrative aims is not authorized neither its spreading and availability from a site foreign to the TDX service. Introducing its content in a window or frame foreign to the TDX service is not authorized (framing). This rights affect to the presentation summary of the thesis as well as to its contents. In the using or citation of parts of the thesis it's obliged to indicate the name of the author.

UNIVERSITAT DE GIRONA

FACULTAT DE CIÈNCIES

Institut de Química Computacional



**THEORETICAL STUDY OF CATALYTIC
REACTIONS OF CARBENES: HAPTOTROPIC
REARRANGEMENTS AND THE DÖTZ REACTION**

**MEMÒRIA que per optar al grau de DOCTOR per la
UNIVERSITAT DE GIRONA presenta**

I.Q. JOSE OSCAR CARLOS JIMENEZ HALLA

Thesis Supervisors:

Prof. Dr. Miquel Solà Puig

Prof. Dr. Juvencio Robles García



UdG

Institut de Química Computacional
Departament de Química

El professor Miquel Solà i Puig, catedràtic d'Universitat a l'Àrea de Química Física de la Universitat de Girona i el professor Juvencio Robles García, catedràtic de la Facultat de Química de la Universidad de Guanajuato certifiquen que:

En **José Oscar Carlos Jiménez Halla**, llicenciat en Enginyeria Química pel Instituto Tecnológico de Oaxaca, ha realitzat sota la nostra direcció, a l'Institut de Química Computacional i al Departament de Química de la Facultat de Ciències de la Universitat de Girona, el treball d'investigació que porta per nom:

*Theoretical Study of Catalytic Reactions of Carbenes:
Haptotropic Rearrangements and the Dötz Reaction*

que es presenta en aquesta memòria per optar al Grau de Doctor en Química.

I perquè consti a efectes legals, signem aquest certificat.

Girona, 30 de juny de 2009

Prof. Miquel Solà i Puig

Prof. Juvencio Robles García

PREFACE

February 2004. I came to Girona, Catalonia to take some doctoral courses as a part of my Master degree formation in Guanajuato, Mexico when Prof. Miquel Solà told me about past projects he was involved in. I found them not only very interesting but a real big challenge to continue developing some organometallic reaction mechanisms as I previously did study reaction mechanisms of palladacycle chemistry in Guanajuato, so I decided to follow up my Ph.D. degree at *Institut de Química Computacional (IQC)*. One year later, I started my new research project at Girona. This Thesis dissertation gathers together some of my work during last four years derived from initial ideas I took from Prof. Solà's vision.

The first part of this document deals with Fischer carbene chemistry. Particularly, about the addition of acetylenes to such carbenes in cycloannulation reactions to give five- and six-membered rings where the most important is the benzannulation also called the Dötz reaction. I explored through several reaction mechanisms on the most exemplary substituents ruling out the electronic structure of Fischer carbenes to get deeper in understanding the regioselectivity found in these reactions.

Chapter one presents an introduction to Fischer carbene chemistry for the reader not familiarized with the issues raised in this Thesis. It describes briefly the synthesis, chemical properties and the most typical reactions in Fischer carbene complexes. Dötz benzannulation reaction as well as other cycloannulation reactions are exposed for very important applications in organic synthesis. This Chapter also contains the proposed reaction mechanisms most commonly found in literature and the earlier work done in this research group and others.

Chapter two reviews briefly the modern theoretical methods of quantum mechanics applied to the computational chemistry in this research. The density functional approach was applied successfully to compile a methodology capable of finding not only transition states of old-proposed reaction mechanisms but also a detailed potential energy surface of the new reaction pathways reported here.

Chapter three collects the results of the effect in changing the substituents X and R of Fischer carbenes of general formula $(\text{CO})_5\text{Cr}=\text{C}(\text{X})\text{R}$ in cycloannulation reactions focusing on the Dötz reaction. Classically, alkoxycarbenes ($\text{X}=\text{OR}'$) and aminocarbenes ($\text{X}=\text{NR}'_2$) control the electronic effects on the carbenoid carbon whereas the bulkiness of R groups define mostly of the steric effects and both substituents serve for tuning the chemical reactivity of these species. We demonstrate how these particular combinations affect the experimental product distribution through an analysis of the kinetics of the reaction. This Chapter is the result of that initial proposal Prof. Solà and me defined that February 2004 and can be regarded as the sequel of Maricel Torrent's work.

Chapter four contains the work developed at University of North Texas in collaboration with Prof. Thomas Cundari and Prof. Brent Gunnoe from North Carolina State University, USA about the catalytic cycle of a variety of carbene nitrogen-containing chain, or isonitrile, that is arylated in presence of the $\text{TpRu}(\text{PMe}_3)(\text{NCMe})\text{Ph}$ complex {Tp = hydridotris(pyrazolyl)borate} acting as the catalyst. This non-photolytic, intramolecular addition of an activated C-H bond to the isonitrile to produce an isoquinolinyl derivative represents other metal-mediated cycloannulation reaction. Other route also explored but not reported here can be found in Chapter eight.

Chapter five is one of my first works dealing with the most direct application of cyclopentannulated and benzannulated products of cyclization of Fischer carbenes: the haptotropic rearrangement of $\text{Cr}(\text{CO})_3$ moiety once the product of reaction is obtained. Our first intent was to explore what could happen when the number of rings increased as we knew (from Introduction) that synthesis of new products by using the Dötz methodology leads to big systems and/or polyheterocycles. The discussion of the effect of the curvature was also reported for this stage.

Chapter six is a continuation of our initial effort to elucidate all the pathways governing the movement of tricarbonylchromium through polycyclic aromatic hydrocarbons. We delimited the subject of study from naphthalene, the simplest polycyclic system, to four six-membered organic rings. Intermolecular haptotropic migrations studied in this Chapter were also dismissed from the aromaticity and orbital

interaction point of views as well since not only pure energetic reasons give a big picture of the whole process. Until here, the reader is submerged into the applicability of the final stage of Dötz reaction where more than one ring is formed.

Chapter seven relates on a research made for bimetallic complexes complexed on the acenes and curved arenes studied in the prior Chapter. The main contribution was to analyze the effect on the electronic structure that presents the coordination of two tricarbonylchromium complexes to either the same or the opposite face of the arene.

Chapter eight summarizes all the results shown in this Thesis and useful discussions of some non-reported works yet which can contribute to the entire vision of the previous Chapters of this Thesis.

Finally, conclusions of this Thesis as well as acknowledgements to the people that supported me during these years in this work can be found at the final pages. I really wish this work can stimulate future generations of IQCians enjoying research in theoretical chemistry field, especially those who dedicated hours of fun and creativity elucidating reaction mechanisms coming from imagination and chemical intuition. My *kunda-kalari* or particular time-space configuration is with all you.

J. Oscar C. Jiménez-Halla
Girona, July 2009.

A la luz hermosa de mi vida:

Maribel Contreras-Arana

A mi madre y a mi padre:

Luz Ma. Halla-Barriguet

Oscar Fco. Jiménez-Aquino

SUMMARY

Table of Abbreviations.....	5
-----------------------------	---

1 Fischer Carbene Chemistry

1.1 Structure, properties and organic reactions of Fischer carbenes.	
1.1.1 Structure of Fischer carbenes and chemical properties.....	11
1.1.2 Reactions of organic synthesis in Fischer carbenes.....	15
1.2 Cycloannulation reactions catalyzed by Fischer-like metal carbenes.	
1.2.1 Benzannulation Dötz reaction and its applications.....	22
1.2.2 Other cycloannulation reactions.....	27
1.3 Proposed reaction mechanisms of cycloannulation reactions.	
1.3.1 Experimental and theoretical research reported in the literature.....	32
1.3.2 Contributions made on the past years in our research group (IQC).....	38
References.....	41

2 Computational Methods

2.1 A brief theoretical background of quantum mechanics.	
2.1.1 Hartree-Fock theory and post <i>ab-initio</i> methods.....	51
2.1.2 Density Functional Theory.....	53
2.1.3 Types of basis sets and nomenclature.....	57
2.1.4 Non-relativistic pseudopotentials.....	59
2.2 Methods for exploring potential energy surfaces.	
2.2.1 Searching transition states.....	62
2.2.2 Proposing a reaction step to create a reaction mechanism.....	63
References.....	66

3 Dötz Benzannulation Reaction: Heteroatom and Substituent Effects In Fischer Carbene Complexes.

3.1	Introduction.....	71
3.2	Computational methodology.....	77
3.3	Results and discussion.	
3.3.1.	Initial part of the reaction.....	78
3.3.2.	Chromium-mediated cycloannulation reactions of Fischer carbenes.	
3.3.2.1.	Vinylcarbenes.....	86
3.3.2.2.	Phenylcarbenes.....	93
3.4.	Concluding Remarks.....	109
	Appendix.....	111
	References.....	116

4 Reactivity of TpRu(L)(NCMe)R (L = CO, PMe₃; R = Me, Ph) Systems with Isonitriles: Experimental and Computational Studies Toward the Intra- and Intermolecular Hydroarilation of Isonitriles.....

137

5 Coordination and Haptotropic Migration of Cr(CO)₃ in Polycyclic Aromatic Hydrocarbons: The Effect of the Size and the Curvature of the Substrate.....

151

Addendum..... 163

6 Intramolecular Haptotropic Rearrangements of the Tricarbonylchromium Complex in Small Polycyclic Aromatic Hydrocarbons.....

167

7	Coordination of bis(Tricarbonylchromium) Complexes to Small Polycyclic Aromatic Hydrocarbons: Structure, Relative Stabilities, and Bonding.	181
----------	--	-----

8 Discussion of Results.

9.1	Effects of heteroatom, substituents and asymmetric acetylene for Fischer carbenes in cycloannulation reactions.....	193
9.2	Catalytic reaction of an isonitrile cyclization reaction.....	199
9.3	Haptotropic rearrangements as the last step in Dötz reaction.....	207
	Appendix.....	223
	References.....	232

	General conclusions of this Thesis.	237
--	--	-----

	Acknowledgments.	241
--	-------------------------------	-----

ABBREVIATIONS

- AO(s):** Atomic Orbital(s)
BDE(s): Bond Dissociation Energy(-ies)
BSSE: Basis Set Superposition Error
B3LYP: Becke **three**-parameter correlation + Lee-Yang-Parr exchange functionals
DFT: Density Functional Theory
EDA: Energy Decomposition Analysis
FCC(s): Fischer Carbene Complex(es)
FLU: aromatic FLUctuation index
GGA: Generalized Gradient Approximation
HF: Hartree-Fock
HOMA: Harmonic Oscillator Model of Aromaticity
HOMO: Highest Occupied Molecular Orbital
IRC: Intrinsic Reaction Coordinate
IRHR(s): Inter-Ring Haptotropic Rearrangement(s)
LUMO: Lowest Unoccupied Molecular Orbital
MCI: Multi-Center Index
MEP: Minimum Energy Path
MO(s): Molecular Orbital(s)
n-**MR(s):** *n*-Membered Ring(s)
NICS: Nucleus-Independent Chemical Shifts
PAH: Polycyclic Aromatic Hydrocarbon
PDI: *para*-Delocalization Index
PES: Potential Energy Surface
SOMO: Single Occupied Molecular Orbital
STQN: Synchronous Transit-guided Quasi-Newton
 Tp: Tris-pyrazolylborate ligand
TS: Transition State
TM: Transition Metal

CHAPTER 1

FISCHER CARBENE CHEMISTRY

Carbenes –molecules with a neutral bicoordinated carbon atom, having 6 electrons in the valence shell, which generates a deficit of electron charge, also named alkylidenes– play an important role in all fields of chemistry since the new discoveries on the synthetic organic field envisaged a plethora of compounds which could be functionalized by profiting the chemical properties that the two unpaired electrons confer to the carbene carbon. They were introduced to organic chemistry by Doering and Hoffmann¹ in 1954 and subsequently to organometallic chemistry when the first metallocene carbene was reported by Fischer and Maasböl² in 1964. Its rich chemistry became more attracted when the first applications catalyzed by metal complexes started at the 1970s.³ Metal carbenes were reported as potential precursors in the preparation of carbo- and heterocycles.⁴ Wanzlick showed that the stability of carbenes depends on the substituents in the vicinal position,⁵ which provide π -donor/ σ -acceptor character, since they stabilize the lone pair by filling the p-orbital of the carbene carbon (*vide infra*). The negative inductive effect reduces the electrophilicity and therefore also the reactivity of the singlet carbene.

On the other hand, carbenes also become stabilized when they act as ligands in the coordination sphere of transition metals. In a general way, the combination of a metal and a carbene ligand in a metal complex consists in a donor σ -type bond from the ligand to the metal and a π bond established by back-donation from an occupied d -orbital of the metal to the LUMO of carbene ligand (see Figure 1). Thus, metal carbenes can be classified in groups as a function of the metal's ability to accept σ -electrons from carbene ligand and of its ability of π back-donation to the empty p-orbital of the carbenoid carbon. Thereby we can consider four cases: 1) Good σ -acceptor and good π back-donation; 2) Poor σ -acceptor and good π back-donation; 3) Good σ -acceptor and poor π back-donation; and 4) Poor σ -acceptor and poor π back-donation.

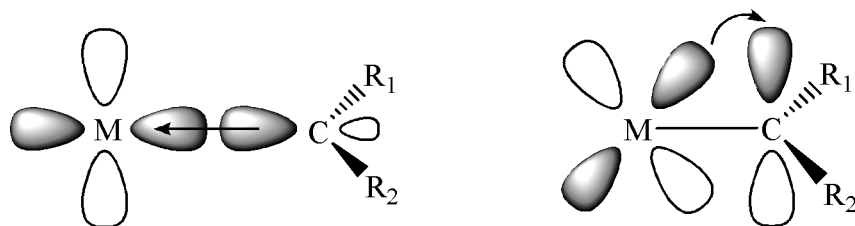


Figure 1. Properties of metal carbene bond.

The first case belongs to the Schrock carbenes characterized by stronger M=C bonds between a triplet metal fragment and a 3B_1 triplet carbene. These compounds are most prone to nucleophilic attacks. The second group is for the Grubbs' catalysts, used in reactions of olefin metathesis, which also present a nucleophilic character but weaker M=C bonds. In the third case we find the electrophilic carbenes, that is, Fischer-type metal carbene complexes (which are polarized with a positive charge on the carbenoid carbon) and those from the reaction of Rh(II) and Pd(II) carboxylates with diazoalkanes are typical examples of carbenes that belong to this group. The fourth type is for carbenes that present a very weak interaction metal-carbene.

In this Thesis, the subject of study is just one part of carbene (also called alkylidene) chemistry, dealing with the third case above mentioned. In fact, we can say a Fischer carbene is a derivation of alkylidenes (see Figure 2), where the organic chain R is substituted by a heteroatom as functional group mainly O, S or N (at this point, the resulting species is named a carbene ligand) and the α -hydrogen by another R substituent like alkyl, aryl or other functional group.

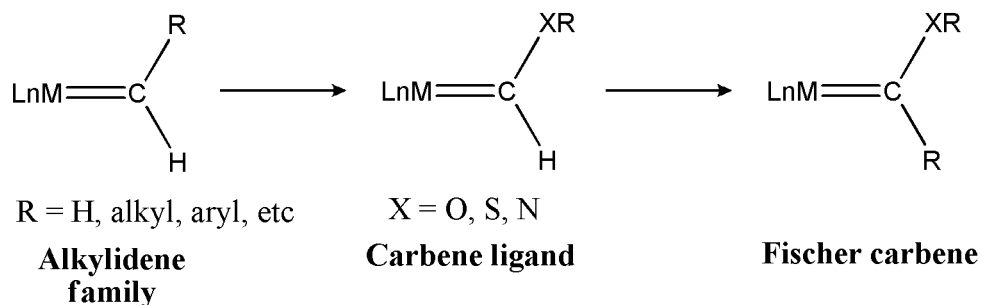


Figure 2. Derivation of Fischer carbenes.

Next, a brief description of Fischer carbene chemistry and general proposals of reactions mechanisms reviewed from literature are presented to introduce the reader into the theoretical framework of the area of research in this Thesis memory.

1.1 Structure, properties and organic reactions of Fischer carbenes.

1.1.1 Structure of Fischer carbenes and chemical properties.

Fischer-like metal carbene complexes contain in its structure one transition metal from Group VI to VIII in a low oxidation state bound to the carbenoid carbon and stabilized by means of ligands with strong acceptor character (generally these groups are CO). The polarity of M=C bond in Fischer carbenes [metal(δ^-)-carbene(δ^+)], contrary to Schrock carbenes [metal(δ^+)-carbene(δ^-)], makes carbenoid carbon electrophilic and therefore susceptible of nucleophilic attacks in that position.

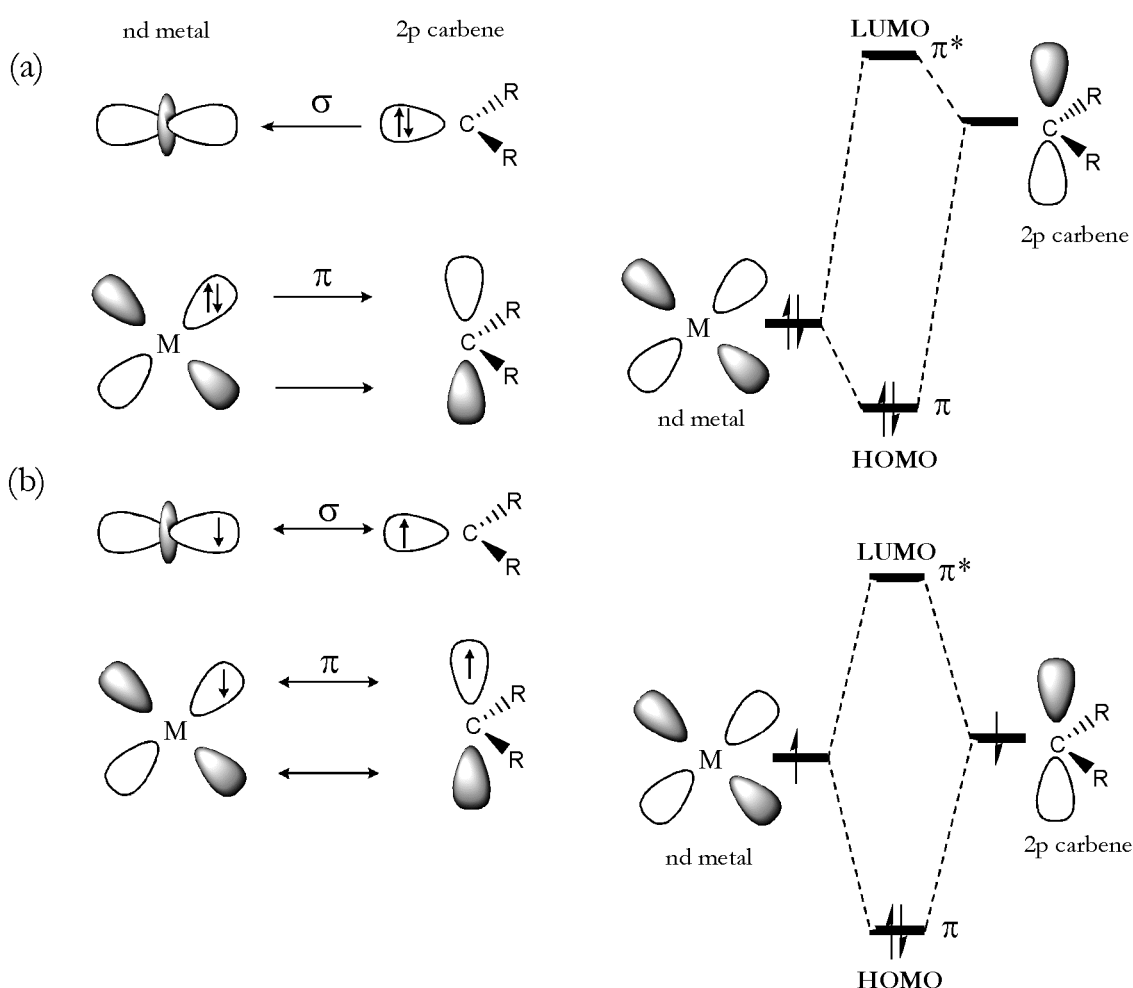


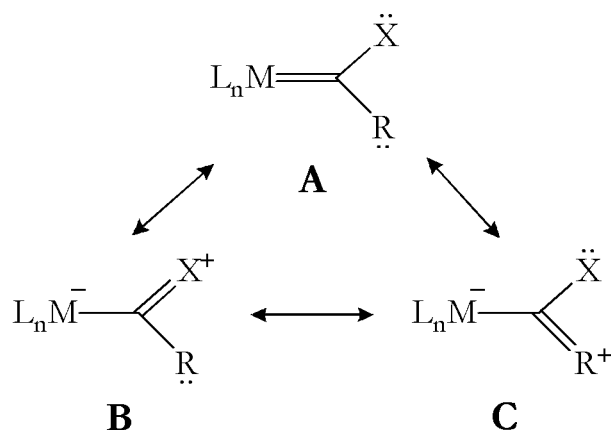
Figure 3. Orbital interactions between metal center and carbene carbon for (a) Fischer carbenes compared against (b) Schrock carbenes.

Thus, Fischer carbenes donate electron charge from the carbenoid carbon to the metal complex becoming partially positive and metal back-donates charge from nd

orbitals to the empty $2p$ orbitals of carbene (see Figure 3, left side). Moreover, this interaction in a Fischer-like complex is not quite effective because of the large energy difference, which originates by overlapping a LUMO of low energy that is a target for reactions with nucleophilic reagents (see Figure 3, right side). Thus, this orbital interaction and the influence of CO ligands limit the ability of back-donation of the metal, which explains the electrophilicity of carbenoid carbon. Charge deficiency in this carbon atom is compensated somewhat by electron transfer from heteroatom which acts as a stabilizing agent for these types of complexes. Therefore, reactivity in Fischer carbenes against nucleophilic attacks increases when the ability of electron donation of the heteroatom directly bound to the carbenoid carbene diminishes.

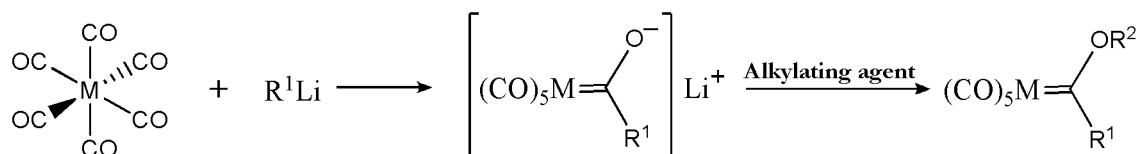
In the same way, Schrock carbenes can be conceivable like less polarized species joining a covalent bond between triplet fragments as shown in Figure 3, left side. They have a very effective overlapping due to the small difference in energy between SOMO of metal atom and SOMO of carbenoid carbon, which originates a LUMO higher in energy for the whole complex not suitable for reactions with nucleophilic reagents (Figure 3, right side).⁶ In other words, the nucleophilic character of Schrock carbenes is the result of a strong $M=C$ π -bond that allows an efficient electron transfer from the metal to the carbenoid carbon making it more accessible to electrophilic reagents.

It is well known that carbenoid carbons in Fischer-like complexes possess sp^2 hybridization. Theoretical calculations as well as experimental data obtained from X-ray diffraction show that the bond order between carbenoid carbon and heteroatom corresponds to an average value between a single bond and a double one.⁷ Therefore, Fischer carbenes can be described as resonance hybrids between structures **A** and **B** from Scheme 1. Electron delocalization is also evident from the restricted rotation (barrier of 14 – 25 $\text{kcal}\cdot\text{mol}^{-1}$) around the carbenoid carbene – heteroatom bond.



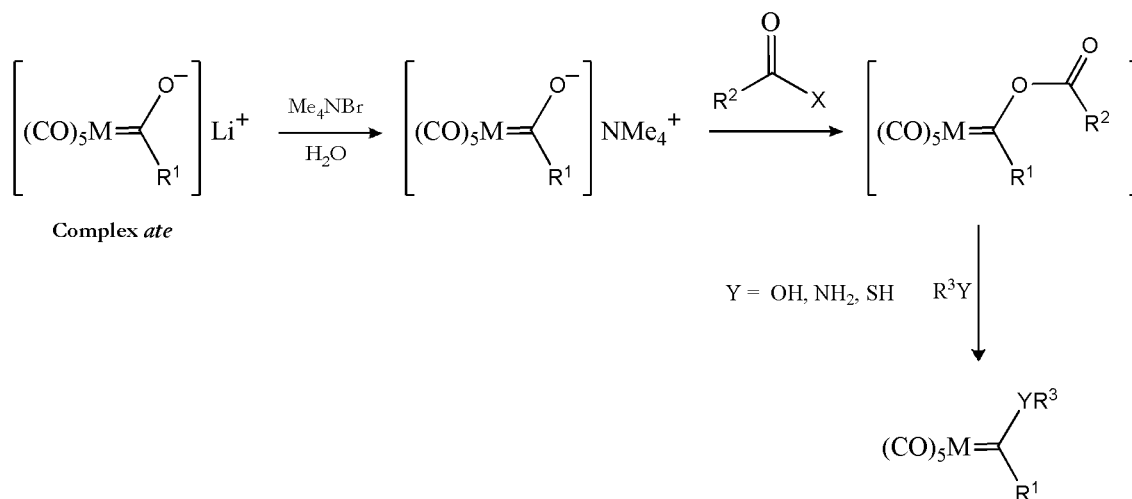
Scheme 1. Resonance hybrids in Fischer carbenes.

On the other hand, the procedure most often used for preparing these compounds is that described by Fischer and Maasböl² (Scheme 2). Regarding to this method, it starts from hexacarbonyl metal that reacts with an organolithium reagent to produce a lithium acyl metalate called complex *ate*. Due to the strength of the ionic pair⁸ (oxygen and lithium), *o*-alkylation from this complex requires the use of strong alkylating agents such as trimethyloxonium, dimethyl sulfate, methyl triflate, methyl fluorosulfonate or diphenylsulfonium salts, to give the corresponding alkoxy carbene complex in excellent yields.⁹



Scheme 2. Most common method for preparing Fischer carbenes.

For convenience, the complex *ate* is more used experimentally as the tetramethylammonium salt which also increases notably its reactivity. That is, the ionic pair formed with ammonium is bulkier and weaker and hence the complex can be easily acylated with acid halides. Acylcarbenes produced in this way are usually less stable thermally and the acyloxy groups can be replaced by nucleophilic agents such as alcohols, amines or thiols to generate new heterosubstituted metal carbene complexes (see Scheme 3).¹⁰

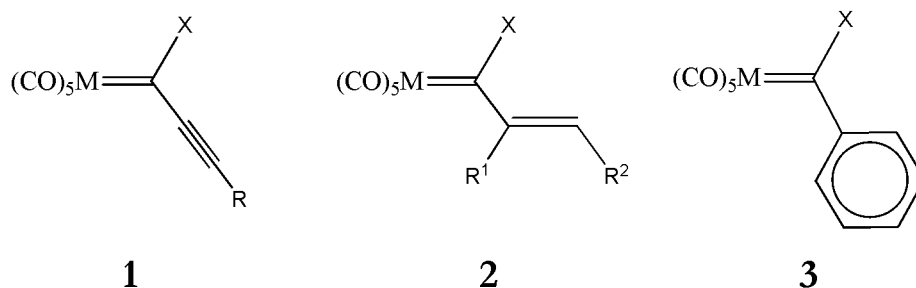


Scheme 3. Alcoholysis of acyloxy metal carbenes.

Chemically, Fischer carbenes show a behavior qualitatively similar to that of carboxylic esters even though quantitatively are completely different because of the much stronger electron withdrawing effect of the $(\text{CO})_5\text{M}$ moiety compared to that of a carbonyl oxygen. This is reflected in the strong acidity of the hydrogen in the α position with respect to the carbenoid carbon, i.e. thermodynamic acidities of ionizable Fischer carbenes are 14 $\text{p}K_{\text{a}}$ units higher in average than that of ethyl acetate¹¹ and the equilibrium constants for nucleophilic additions are *ca.* 10^9 -fold higher than for the corresponding carboxylic esters.¹² In fact, Bernasconi and coworkers reported in the last decade a number of studies on addition of a variety of nucleophiles as an important effort exploring the factors that determine the reactivity of Fischer carbene complexes.^{13,14} Recently, Zoloff Michoff and co-workers¹⁵ showed that there is a linear dependence between rate constants of alkaline hydrolysis of Fischer carbenes and bulkiness of R groups. Thus, the difference in reactivity has been attributed more to the contribution of steric factors than to the π -donor properties of heteroatom. However in our group, Cases *et. al.*^{7d} demonstrated that there is a correlation between back-donation and the heteroatom group attached to the carbenoid carbon also shown by the values of the electrophilicity index, which in consequence indicates that the heteroatom substituent has a larger effect on the M-C bonding than the R group. This means that it is possible to tune the strength of M-C bonding (through donation and back-donation) depending on the type of heteroatom used and direct the reactivity properties by taking into account the bulkiness of R group of the Fischer carbene. Yet, similar conclusions were obtained extending the study to Schrock carbenes as well.¹⁶

1.1.2 Reactions of organic synthesis in Fischer carbenes.

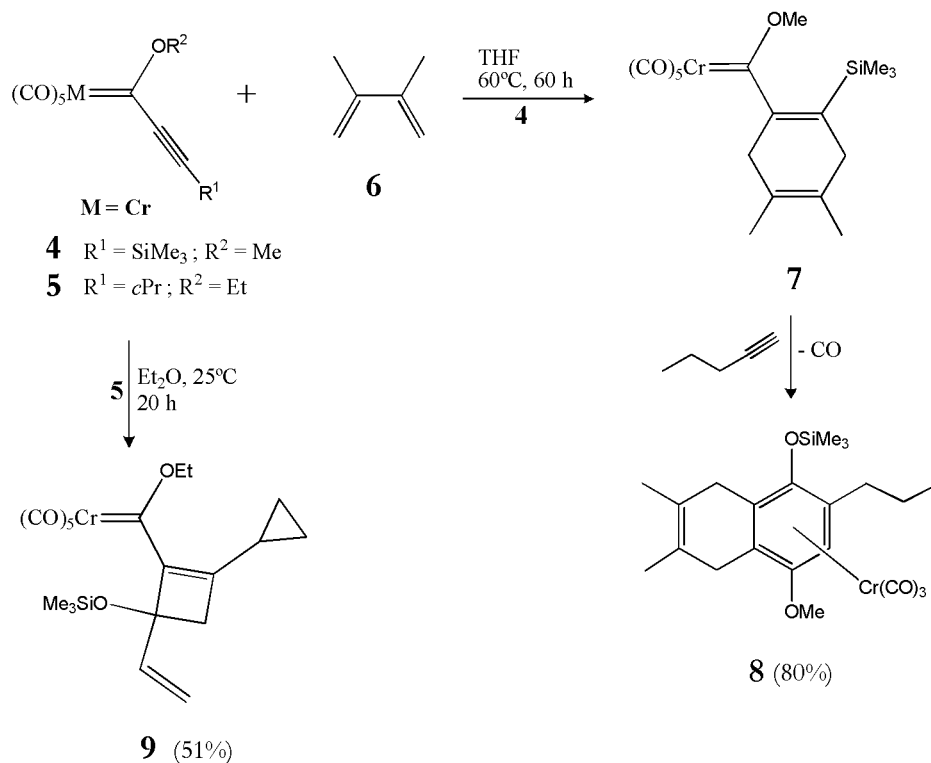
Chemical properties of Fischer carbene complexes (FCCs), as aforementioned above, lead to nucleophilic attacks on the carbenoid carbon but it is also probable that multiple bonds neighboring this carbene center can be also activated and therefore, they present a richer chemistry in formal cycloaddition reactions of organic synthesis. For instance, nucleophilic additions to the triple bond of the alkynylcarbene complexes **1** result in the α -alkenylcarbene complexes **2** which subsequently can participate in tandem cycloaddition processes with alkynes with the inclusion of the carbenoid carbon and a CO ligand even. Whereas the reactions of complexes **1** are dominated by the strong polarization of the triple bond, for complexes **2** and the analogous aryl complexes **3** the metal center almost always plays a role by coordinating with some reaction partners or stabilizing reactive intermediates by strong interactions.



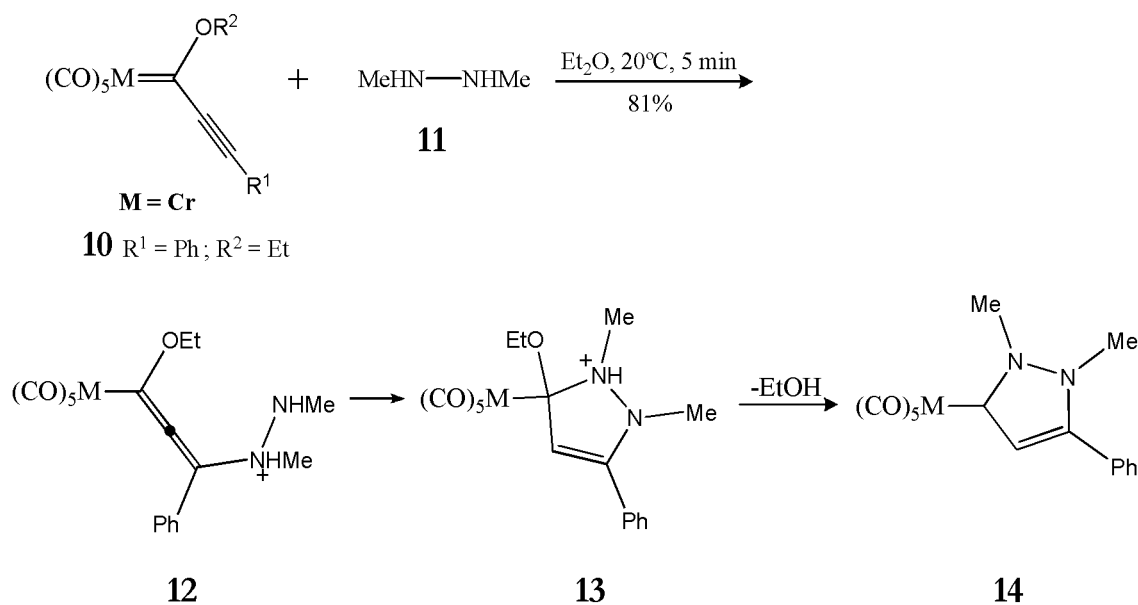
Due to the big amount of published work of a new range of organic products and functionalities since the discovery of FCCs forty five years ago, this Section only deals with a brief summary of organic reactions of the most common Fischer carbenes, complex types **1**, **2**, and **3** precisely.

In view of the strong electron withdrawing influence of the pentacarbonylmetal moiety on the carbene ligand in FCCs it seems to be obvious to use α,β -unsaturated complexes of this type as dienophiles in Diels-Alder reactions. For instance, 2-(trimethylsilyloxy)butadiene (**6**), known for its high diene reactivity, can react in different way with alkynylcarbene complexes **1** depending on R^1 and R^2 substituents. With the (trimethylsilylethynyl)carbene complex **4** it forms a [4 + 2] cycloadduct **7** product which immediately reacts with the added 1-pentyne to obtain the complexed dihydronaphthalene derivative **8** whereas the cyclopropyl-substituted complex **5** reacts

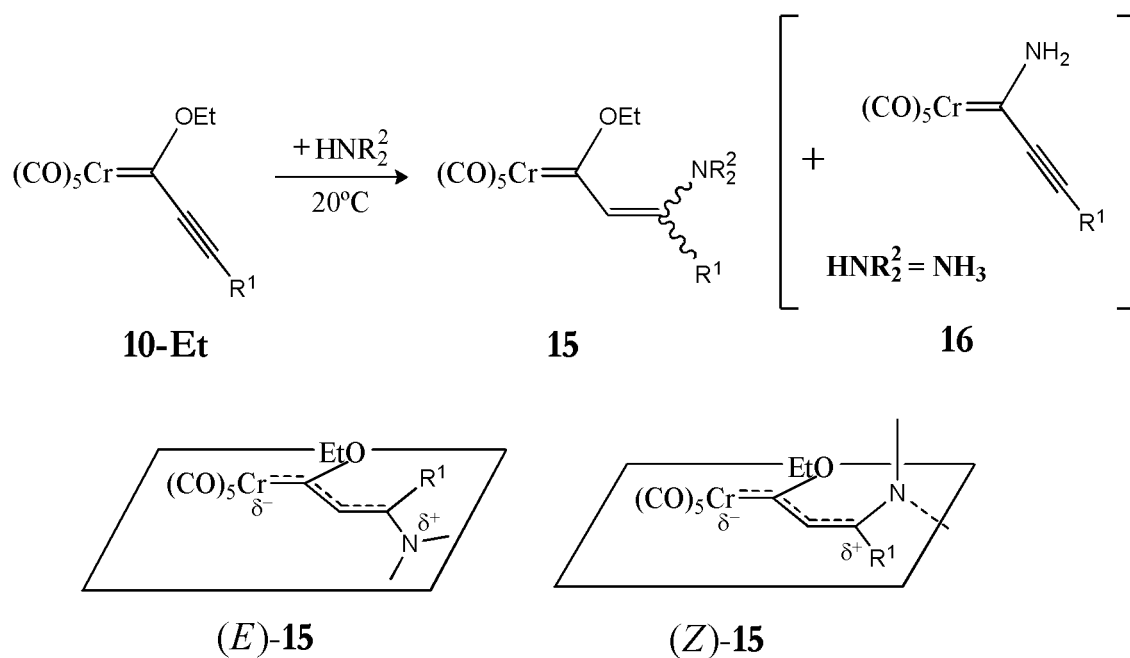
regioselectively with the electron-rich double bond in **6** ([2 + 2] cycloaddition) to give **9**.^{17,18} Faron and Wulff¹⁹ also observed a [2 + 2] addition of 2,3-bis (tert-butyl)dimethylsilyloxy)butadiene to a complex akin to **5** (but in this case, R² = Me).



Later, it was observed that the reaction of compounds containing nitrogen as azadienes, enamines, ammonia, imines and hydrazines with alkynylcarbene complexes provoke the formation of ring-annulated cyclopentadienes after formal [3 + 2] cycloaddition in most of the cases. For example, alkynylcarbene chromium complexes such as **10** react with 1,2-dimethylhydrazine **11** to produce a Michael addition product **12** which in turn, after a formal substitution on the carbenoid carbon atom by the second secondary amino group to form the betaine complex **13**, it follows by elimination the dihydropyrazolynylidenechromium complex **14**.²⁰



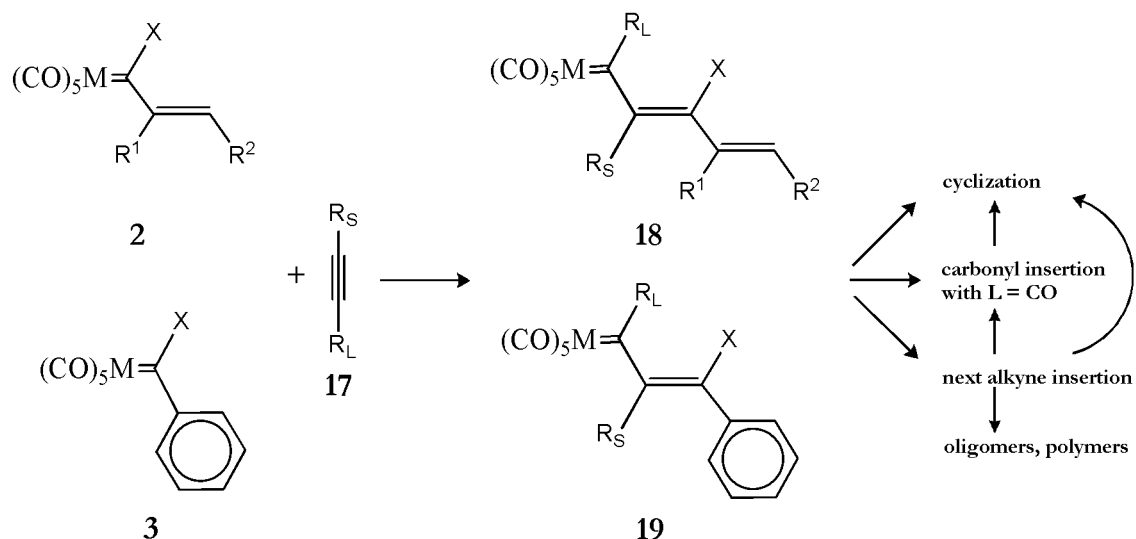
For the insertion of secondary amines in complexes like **10-Et**, it was found that the insertion formed almost without exception the products **15** as a single diastereomer, usually the *E*-isomer,^{21,22} if R^1 is not too large and the amine is a secondary one. In this case a coplanar arrangement with optimal conjugation including that of the lone electron pair on the nitrogen atom is possible (Figure 4). Whether R^1 is tertiary or extremely sterically demanding (*e.g.* $R^1 = \text{CH}(\text{Me})\text{OSiMe}_2t\text{Bu}$), the products **15** with *Z*-configuration are obtained.²¹ In (*Z*)-**15** the substituents on the amino group are rotated out of the plane so that the interaction of the lone electron pair with the 1-metalla-1,3-diene system is greatly reduced. When R^1 represents large tertiary substituents in **10-Et** side products are formed in this reaction, which with suitable choice of amine and/or temperature, can become the main products.²² Actually, by using ammonia and excess of diethyl ether, the reaction always gives considerable proportions of the respective formal substitution products **16** (Figure 4) and exclusively *Z*-isomers of **15** are observed in these cases precisely for the bulkier R^1 groups.

For 10-Et + NH₃

R ¹	15 [%]	16 [%]
Ph	86	13
<i>n</i> Pr	31	63
<i>c</i> Pr	28	70
<i>t</i> Bu	60	35

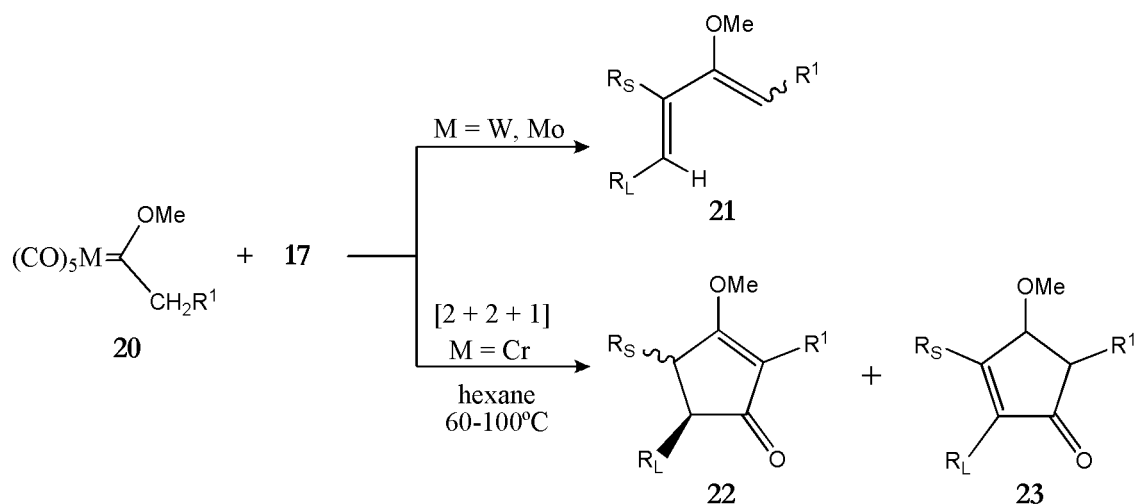
Figure 4. Steric effects in *E*- and *Z*-configured pentacarbonyl(3-dialkylamino-1-ethoxyprop-2-enylidene)chromium complexes **15** (up) and product ratios of the reaction of alkynylcarbene complexes **10-Et** with ammonia (down).

Carbenes complexes **2** and **3** of Group VI metals insert alkynes **17** into the metal – carbene double bond to form the alkenylcarbene complexes **18** and **19**, respectively. Depending upon the nature of the complex, this alkyne insertion can be either repeated reiteratively or multiply, leading finally to alkyne oligomers or polymers.²³ Alternatively, one of the intermediates cyclizes –possibly with the insertion of a carbonyl ligand– to afford an organic product after reductive elimination of the metal fragment.

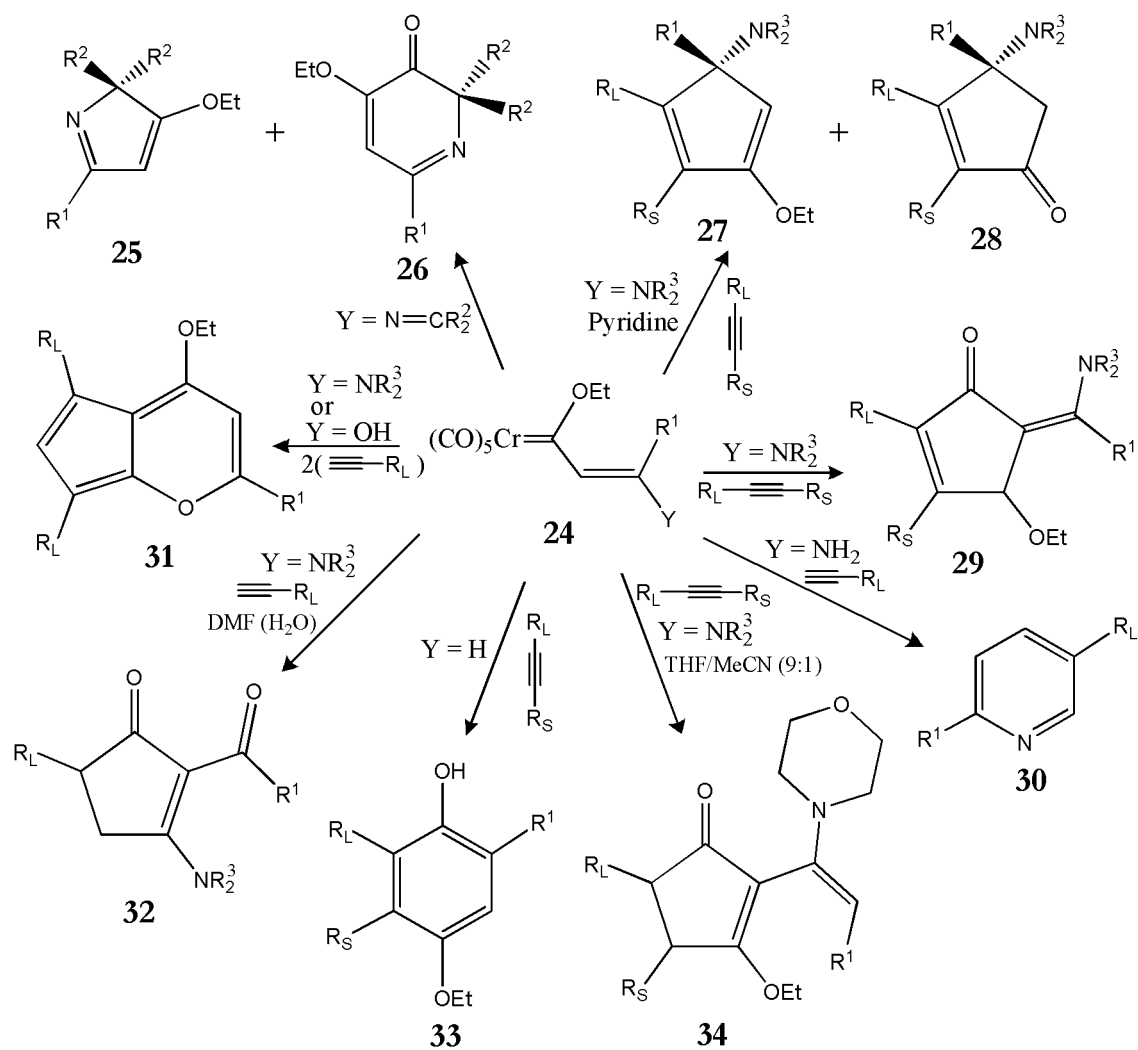


Examples of all three follow-up reactions after the first alkyne insertion illustrated above are known for alkenyl- and phenylcarbene pentacarbonylchromium complexes. They may be classified as formal $[k + m + n]$ cycloadditions, where k , m and n represent the respective number of atoms from the carbene ligand (k), the alkyne (m), and the carbonyl ligand (n) which will form the new ring.

Furthermore, each transition metal (TM) can influence the catalysis of reactions in several ways. For instance, treatment of alkyl chromium FCCs **20** ($R^1 = H, n\text{-Pr, Ph}$), bearing a α -hydrogen in the alkyl group, with 1-2 equivalents of alkyne **17** ($R_L = Et, n\text{-Pr, } i\text{-Pr, } t\text{-Bu, Ph}$ and $R_S = H, Et, n\text{-Pr, } n\text{-Hex, } n\text{-Hep, Ph}$) in a non-polar solvent such as hexane and employing diluted conditions (0.05 M) produce cyclopentenones **22** and **23** obtained in good yields. When using tungsten or molybdenum, reaction usually provides either dienes **21** or their corresponding hydrolysis products in a wide range of yields from 23 to 60%.²⁴ The formation of cyclopentenones requires the metal-mediated activation of the α -hydrogen of the alkyl group and then, due to the decrease of the electron-withdrawing character in TMs ($W < Mo < Cr$), this C-H bond activation is less achieved. Some molybdenum FCCs have some exceptions to this behavior performing $[2+2+1]$ cyclization reactions at low yields.²⁵



Finally, as can be seen in references 4c and 26, every FCC have a great versatility to undergo cycloaddition reactions and hence these kinds of complexes have been labeled as ‘chemical multitalents’ serving in multi-component reactions to construct organic building blocks. For the case of 3-(diorganylmethylenamino)-substituted complexes **24**, the metal catalyzes the cyclization even in the absence of alkynes (see Scheme 4). By using ketimines, which are known for 1,4-additions only to highly reactive Michael acceptors,²⁷ they rather cyclizes to *2H*-pyrroles **25** mainly and complexes **26** in minor scale.²⁸ Adding primary amino groups first rearrange and then cycloadd to yield pyridines **30**.²⁹ Especially with a morpholinyl group, dialkylamino-substituted complexes catch internal as well as terminal alkynes with carbonyl insertion to selectively give –each one under different set of reaction conditions– either 5-(1'-dialkylaminoalkylidene)cyclopent-2-enones **29**³⁰ or 3-ethoxy-1-(1'-morpholinyl-1'-alkenyl)cyclopent-2-enones **34**³¹ or 2-acyl-3-dialkylaminocyclopent-2-enones **32**.³² Extremely bulky groups at R^1 in complexes **24** favor the (*Z*)- rather than (*E*)-configuration and prefer to insert two molecules of the alkyne and CO to finally yield cyclopenta[*b*]pyrans **31**. The ready accessibility of 5-dialkylamino-3-ethoxycyclopentadienes **27** and **28** is particularly noteworthy.³³ These compounds are enol ethers of cyclopentenones and can also be regarded as protected cyclopentadienones (or precursors thereof), which are in a sense templates assembled from one alkyne and one carbon monoxide stemming from hexacarbonylchromium. This process is similar to the Dötz product **33**, a metal-assisted assembly of an alkyne, a carbon monoxide and a carbene.

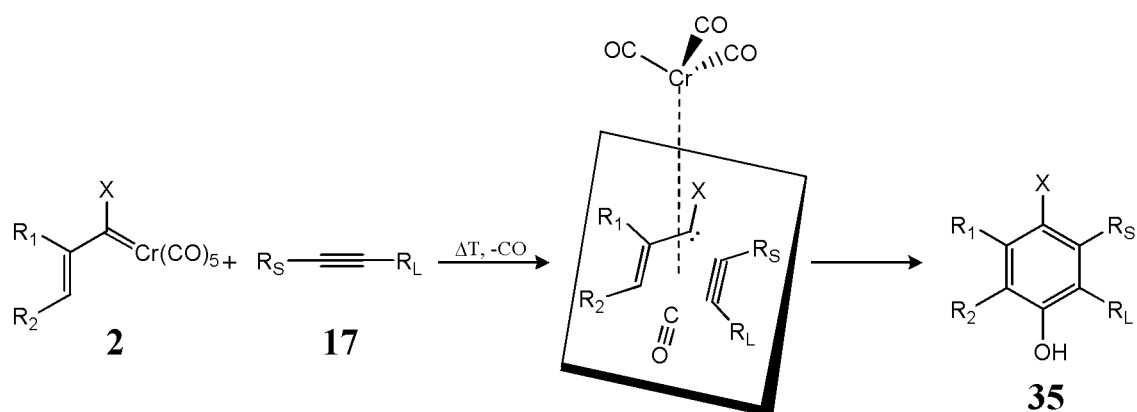


Scheme 4. Versatility of β -amino substituted α,β -unsaturated chromium FCCs and alkynes to generate new different products under variable conditions. Note that superscripts stand for labelled R substituents.

1.2 Cycloannulation reactions catalyzed by Fischer-like metal carbenes.

1.2.1 Benzannulation Dötz reaction and its applications.

Perhaps the most important reaction of FCCs is the benzannulation of complexes **2**, unique in its genre, which consists in an ensemble with an alkyne **17** and a carbon monoxide (from pentacarbonylchromium) providing a one-pot process to densely substituted oxygenated arenes **35** as products (Scheme 5). Such a reaction was introduced to the organometallic chemistry in 1975 by K.H. Dötz³⁴ and since then, the so-called Dötz benzannulation reaction has gained considerable attention in stereoselective synthesis.^{35,36}



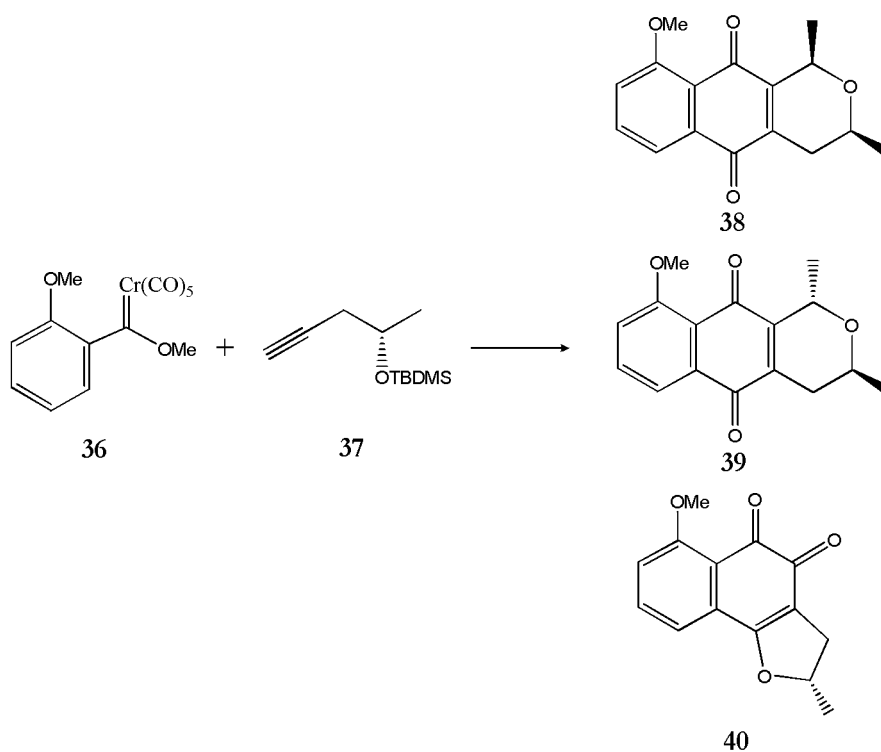
Scheme 5. Schematic representation of chromium-mediated benzannulation reaction.

Chromium is the most used metal template for benzannulation because it allows excellent chemo- and regioselectivity under mild conditions (*tert*-butyl methyl ether, 50°C). When molybdenum carbenes are used, furans are usually obtained in moderate yields because the cocyclization of carbene, carbonyl and alkyne ligands is favored. For the case of tungsten carbenes, due to its increased thermostability, the CO incorporation fails and usually products of formal [3+2] cycloaddition (*e.g.* cyclopentadienes) in good yields are obtained. Other metals require additional electrophilic activation for the carbenoid carbon under more drastic thermal (or photochemical) conditions giving only poor annulation yields like manganese.³⁷

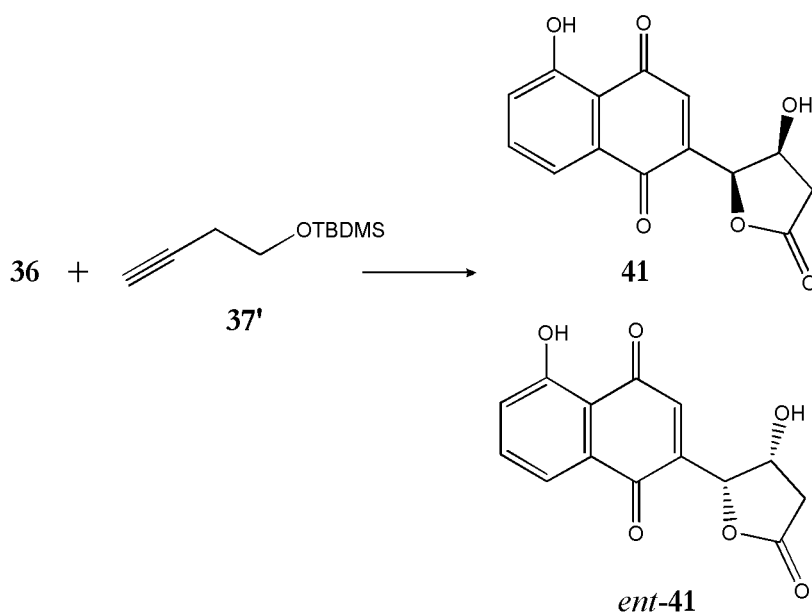
The character of chromium-mediated Dötz benzannulation reaction can be tuned by changing both alkyne and the unsaturated side group of carbene and has been a subject of interest in substitution pattern studies.³⁸ Aryl carbene complexes usually react with methyl, methoxy, naphthyl and heteroaryl substituents in the *ortho*-, *para*-, or *meta*-position to give apart of benzannulated products, furans, pyrroles, pyrazoles and indoles, among others. Vinyl carbene complexes have been studied extensively bearing alkyl substituents in a variety of cyclic and acyclic systems with a major regioselectivity. Moreover, benzannulation gives from moderate to excellent yields with substituted alkynes bearing aryls, esters, lactones, ketones, amides, acetals, α -ethers, enol ethers, sulfides, tosylates, and nitrile or isonitrile groups. There is an obvious dependence on both their steric and electronic properties; *ortho*-substituted arylalkynes and strong electron-withdrawing substituents, if not compensated by donor functionalities in either the carbene ligand or the alkyne,³⁹ result in low or poor yields.⁴⁰

In some cases, dry-state,⁴¹ photo-irradiation,⁴² ultrasonication,⁴³ and microwave-conditions⁴⁴ have been experimentally reported techniques to give similar or even superior yields of benzannulation products. However, in general, decomplexation of Cr(CO)₃ metal complex occurs under mild conditions affording uncoordinated phenyl derivatives **35** or – after oxidative work-up – quinones.

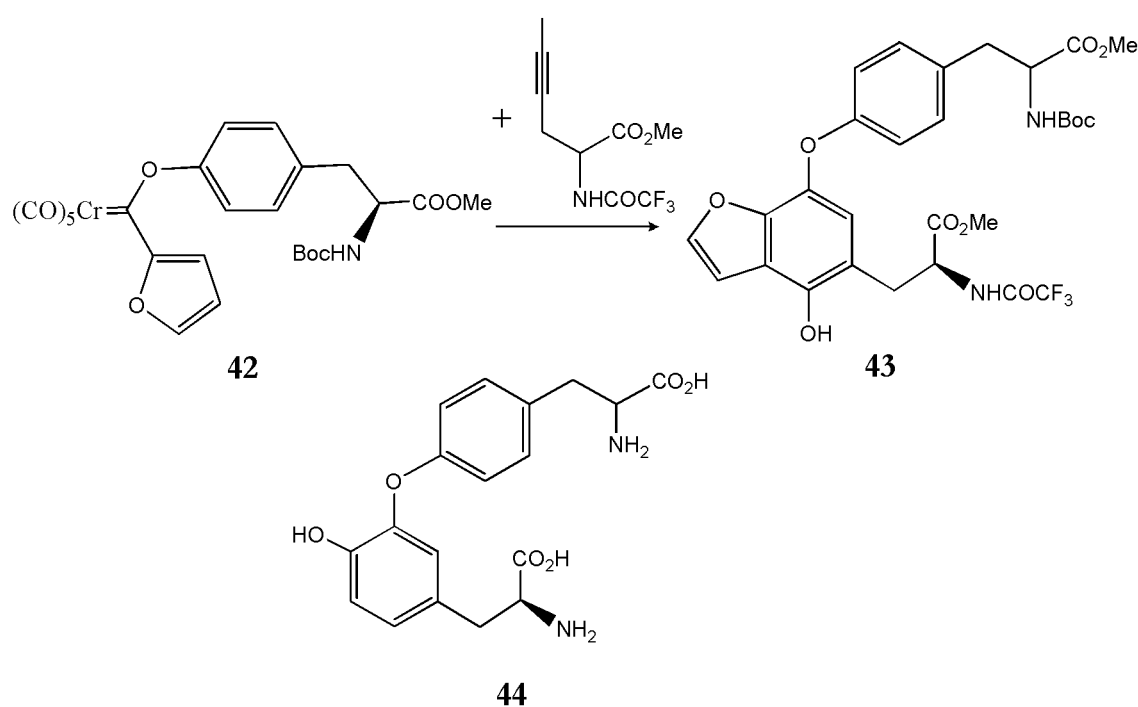
Because of many organic molecules of great interest in biochemistry have hydroquinoid, quinoid or fused phenolic rings, Dötz benzannulation reaction is a good strategic choice for an intermediate step in order to synthesize biological molecules in pharmacological or medical fields. In this sense, the Fischer carbene complex **36** was condensed with the chiral alkyne **37** (1.5 equiv.) to create the naphthalenic skeleton as a precursor of antibiotics (+)-eleutherin **38** and (+)-allo-eleutherin **39** at room temperature for 14 h to give a mixture (easily separated by preparative TLC) in good yields (86% and 89%, respectively).⁴⁵ Under more acidic conditions, these reagents can also bring up the formal synthesis of (+)-nocardione B **40**, which is an enzymes' inhibitor and also possesses moderate antifungal and cytotoxic activities.⁴⁶



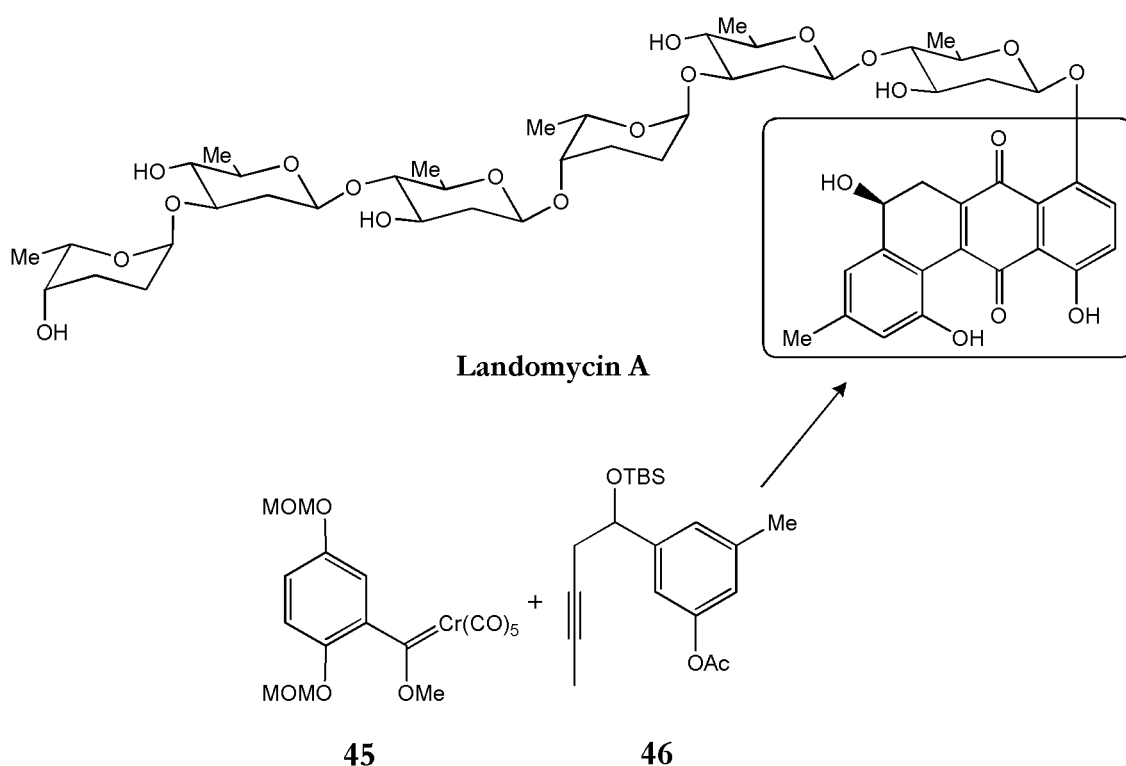
Other reaction very similar using a slightly modified achiral alkyne **37'** was reported to promote a highly enantioselective synthesis of both (-)-juglomycin A **41** and its unnatural isomer (+)-*ent*-**41** via an asymmetric dihydroxylation and Dötz benzannulation reaction. These compounds have exhibited antitumor activity as well as antibacterial activity.⁴⁷



Furthermore, by using a Dötz benzannulation approach, several subunits of numerous biologically active macromolecules containing an endocyclic diaryl ether can be synthesized. The key step is utilized to simultaneously construct an aromatic ring and a diaryl ether linkage at the same time. For instance, Boc-tyrosine FCC **42** undergoes benzannulation by heating with the proper alkyne under argon at 60°C for 20 h to furnish the diaryl ether **43** in 60% yield. This is the precursor, after Boc ligand deprotection, of the aryloxyphenol moiety of (*S,S*)-isodityrosine **44** which in time, is used to assemble complex polycyclic glycopeptide antibiotics.⁴⁸

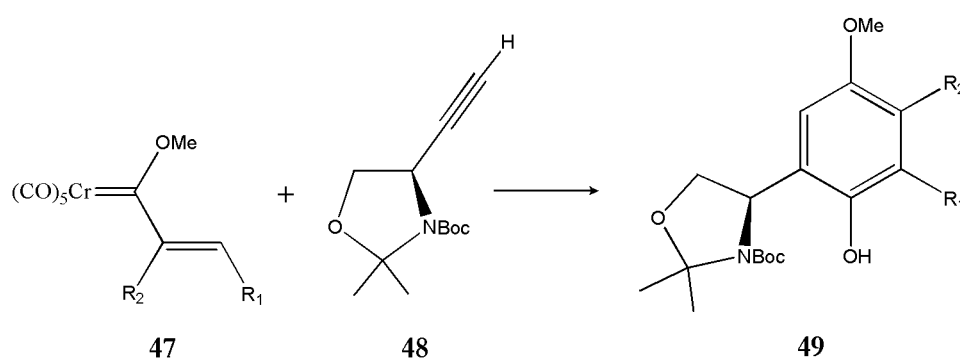


Another example comes from the reported synthesis of landomycin A aglicone,⁴⁹ an antibiotic and a potential antitumor agent. The arene fragment of this macromolecule, landomycinone, is obtained from metal carbene **45** and acetylene derivative **46** heating in heptane at 55°C followed by oxidation with ceric ammonium nitrate and an intramolecular Michael-type addition. Even though this reaction was tested with other solvents and reaction conditions, the 40% yield indicates a moderate regioselectivity along with other products that have been not identified.



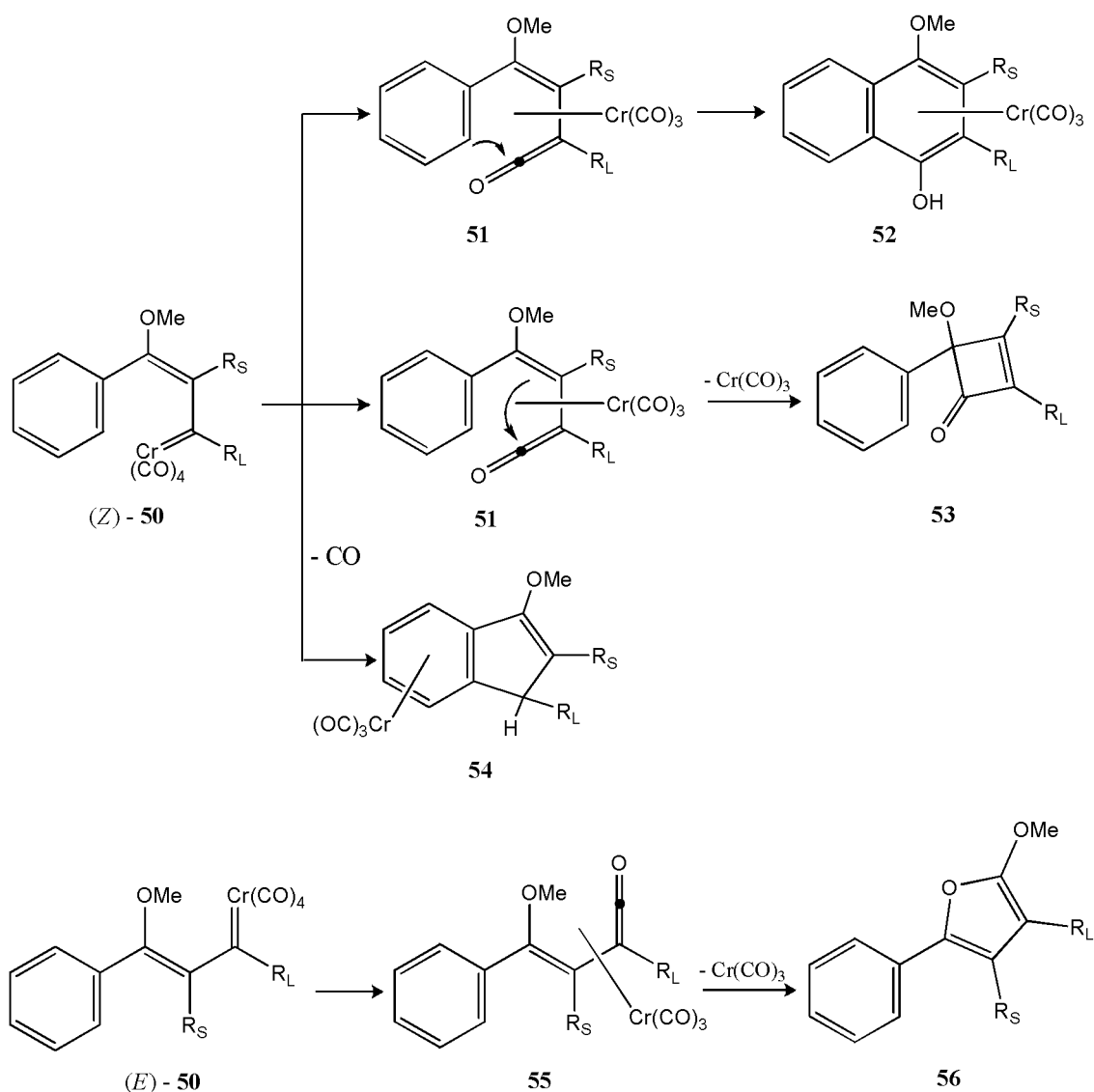
Dötz benzannulation reaction has been used as well in the synthesis of other antibiotics like aflatoxin B₂,^{50,51} family of carbazolquinones,⁵² and fredericamycin A,⁵³ among others. This strategic methodology has also been employed to get essential components of metabolites like (-)-kendomycin,⁵⁴ and natural products like derivatives of (-)-curcuquinone,⁵⁵ and alkaloids extracted from plants like bulgaramine.⁵⁶

Dötz and coworkers reported the synthesis of vitamins E and K⁵⁷ by means of this reaction. More recently, biologically active α -amino acids like arylglycines have been obtained under this approach.⁵⁸ Interestingly, these compounds are presented in the core of antibiotics like vancomycin, ristocetin, teicoplanin, nocardicin and also can be found in the side chain of penicillins and cephalosporins. Fischer carbenes **47** react with alkyne **48** in the Dötz benzannulation fashion to produce the aromatic skeleton of arylglycines **49** at the intermediate stage of the production of these antibiotics. Thus, Dötz reaction has been proved to be very useful as a synthetic method for mild conditions and good yields (70 – 80%) in such processes.



1.2.2 Other cycloannulation reactions.

The benzannulation affords the most valuable product but has to compete with the formation of four-, five- and even eight-membered rings.^{4c} Most of these reactions have a common η^3 -allylidene intermediate **50** formed upon alkyne insertion. These pathways are outlined in Scheme 6. Insertion of CO into the (*Z*)-isomer generates the vinyl ketene complex **51** which by 6π -benzannulation produces the aforementioned Dötz product **52** but if 4π -electrocyclization is followed, then it gives cyclobutenone **53**. When the carbon monoxide fails to be inserted, (*Z*)-**50** affords indene **54** by direct electrocyclic ring closure and after reductive elimination and tautomerization. A route which has been less explored starting from the (*E*)-isomer of **50**, where the CO insertion is achieved at the alkyl chain near to the methoxy group in **55**, is believed to be responsible for the formation of the furan skeleton **56**.⁵⁹

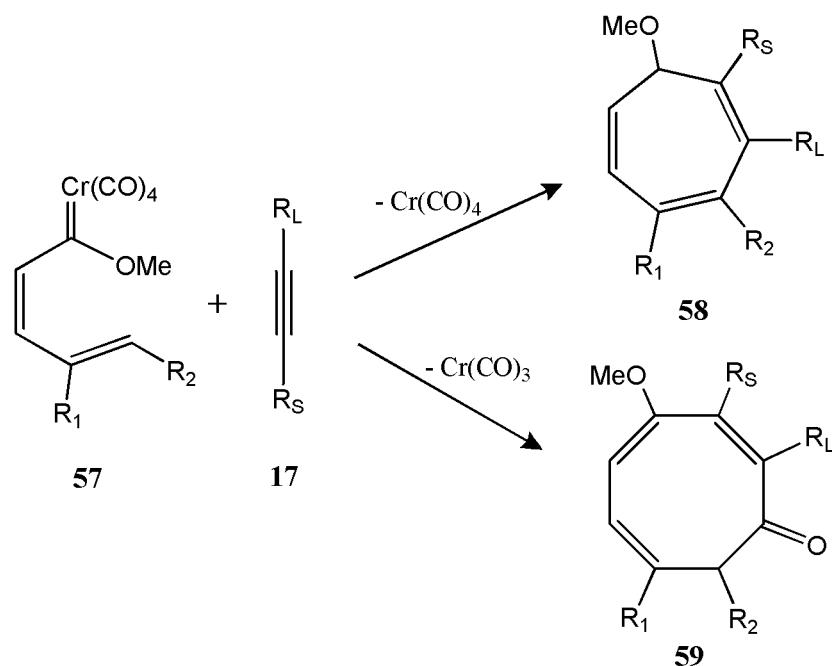


Scheme 6. Competitive reactions of benzannulation **52**, cyclobutenones **53**, cyclopentannulation **54** and furan **56** products.

Additionally, FCCs intermediates like **57** possess one extra double bond before insertion of alkyne **17** that participates in the electrocyclic ring closure. This process can be viewed as an extension of the Dötz benzannulation or the cyclopentannulation reaction, where carbocycle formation occurring upon CO insertion gives rise to the eight-membered product **59** otherwise when carbon monoxide fails, complexes **58** are obtained.⁶⁰

The chemoselectivity depends on the nature of the metal fragment, the substituents of the carbene and the reaction conditions. Besides the concentration and

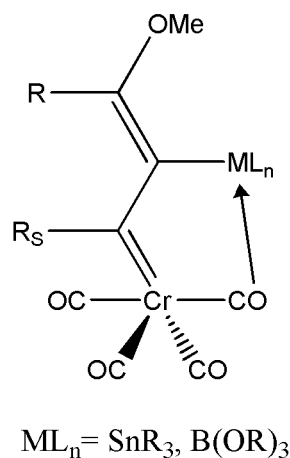
the temperature used, the solvent has been recognized to play a major role.⁶¹ Donor solvents like ethers favour selective benzannulation whereas a non-coordinating solvent (like hexane) increases the amount of four- and five-membered ring products and for the latter, a more polar solvent such as DMF is the medium of choice. This is because the experimental hypothesis points out that from intermediate **50**, the coordination of a molecule of solvent (or also of alkyne, due to high concentrations of this one) accelerates the CO insertion step thus leading to greater proportions of benzannulated product and vice versa for the case of less- or non-coordinating solvents. This mechanistic reason is called the *allochemical effect*^{62a} and has been proposed specially to explain the competition of benzannulation and cyclooctannulation, which are the products most commonly obtained for chromium alkoxy- and aminocarbene complexes.



Scheme 7. Annulation reactions of Fischer carbene complexes leading to cycloheptatrienes **58** and cyclooctatrienones **59**.

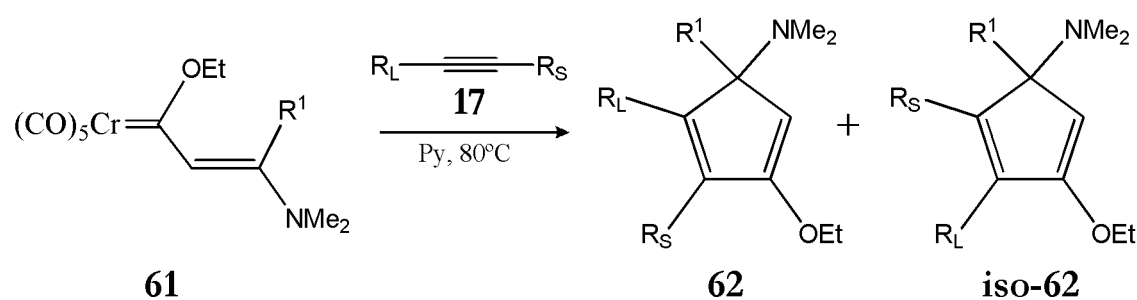
In fact, it has been found that (alkyl)thiocarbene complexes give a different reactivity pattern than (alkyl)alkoxycarbene complexes due to kinetically unstable formed products and a thermodynamically more favored cycloannulation pathway for the former whereas it is the inverse trend for the latter.⁶²

Furthermore, the use of unsymmetrical alkynes adds another dimension of regioselectivity to the cycloannulation reactions. The major regioisomer generally bears the larger alkyne substituent close to the metal complex whereas the shorter one is next to the heteroatom group. This has been rationalized in terms of the minimization of the repulsive steric interaction between the alkyne substituents and the carbonyl ligands of the metal fragment when the insertion is carried out. This argument takes into account the fact that the smaller alkyne substituent R_S is closer to the apical CO ligand than the larger R_L is to the equatorial CO ligand.⁶³ Thus, synthetically useful regioselectivities are encountered with terminal alkynes which give a single regioisomer whereas unsymmetrical internal alkynes generally afford regioisomeric mixtures. The steric control reaches its limits if diarylalkynes bearing two electronically different *para*-substituents were incorporated.⁶⁴ For alkynylstannanes⁶⁵ and alkynylboronates,⁶⁶ this steric preference is inverted as an exception. This outcome was rationalized in terms of a carbonyl oxygen to tin or boron Lewis acid/base interaction in the metallahexatriene intermediate **60**.

**60**

More interestingly, a wide range of 5-dialkylamino-3-ethoxycyclopentadienes **62** accessible in high yields from β -amino-substituted α,β -unsaturated FCCs **61** in pyridine, and terminal as well as internal alkynes, has been reported.^{37a,67} It is noteworthy that the effect of β -amino-substituted groups inhibits the regiopreference for **iso-62** species even if the substituent R^1 in the complex **61** contains a triple bond (entry 10 in Scheme 8). With certain functionalities on the terminal acetylenes, the regioisomeric cyclopentadienes **iso-62** are sometimes formed as by-products. With

unsymmetrically disubstituted acetylenes the regioselectivity for the formation of **62** rather than **iso-62** can be even less pronounced.



	R ¹	R _L	R _S	62 Yield [%]
1	Me	Me	Me	82
2	Me		H	86
3	<i>n</i> Pr	Ph	Ph	80
4	<i>n</i> Pr		H	85
5	<i>c</i> Pr	Me	Me	84
6			H	77
7		Me	Me	91
8		Me	Me	79
9		Me	Me	69
10		Me	Me	46

Scheme 8. Desactivated alkyne-dependent regioselectivity is shown when using different groups at the alkyl chain of Fischer carbenes.

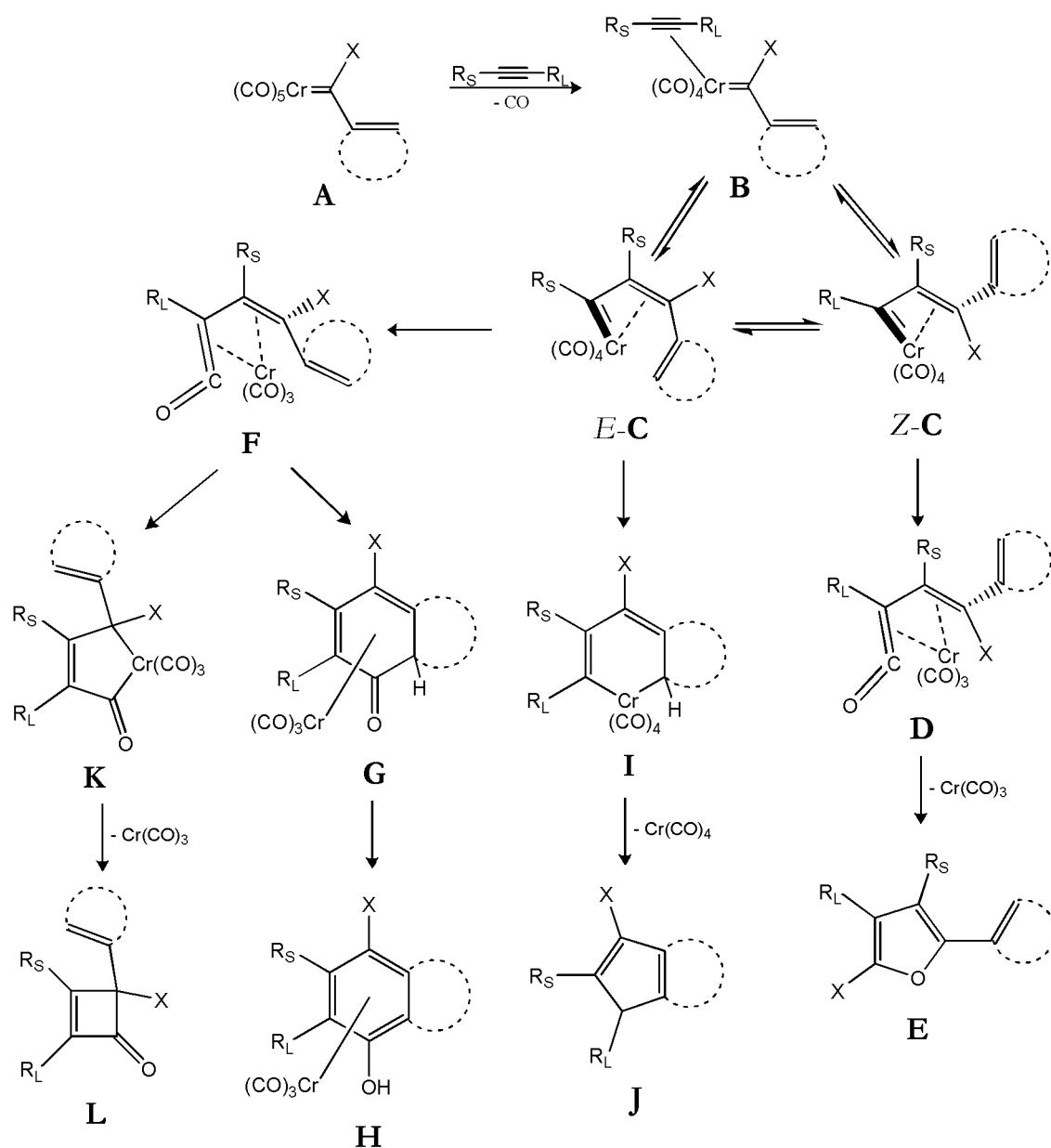
1.3 Proposed reaction mechanisms of cycloannulation reactions.

1.3.1 Experimental and theoretical research reported in the literature.

From a literature survey of mechanistic proposals, Scheme 9 depicts the generally accepted reaction pathways for chromium carbene-alkyne reactions, supported by experimental studies.^{36,64,68} Initially, an early decarbonylation from the pentacarbonyl chromium carbene complex **A** has been recognized as the rate-determining step of these reactions.⁶⁹ It is followed by the alkyne coordination into the metal sphere to give **B** complex. Subsequent insertion into the chromium-carbene bond generates a η^1, η^3 -vinylcarbene intermediate. It may be formed either as *E*- η^1, η^3 -vinylcarbene complex (*E*-**C**) or its *Z*-isomer (*Z*-**C**) and is considered as a common intermediate for the variety of products observed. This isomerization of vinylcarbene intermediates has been addressed as occurring in the alkyne de- and insertion equilibrium.^{61b}

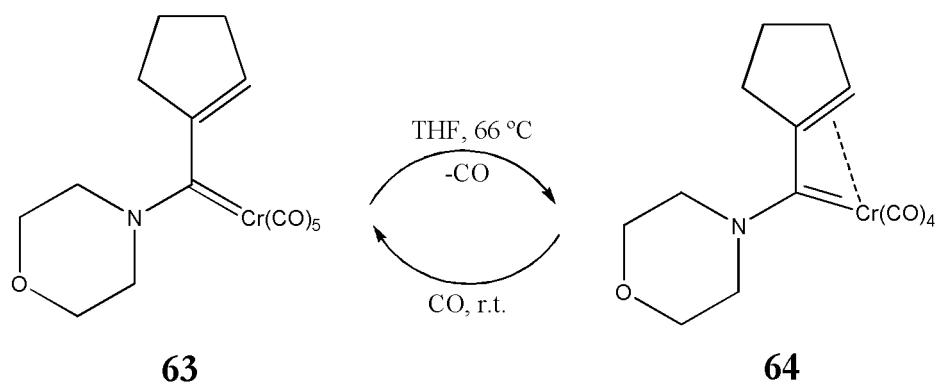
Thus, furan side product (**E**) may be traced back to *Z*-**C** when it undergoes a carbon monoxide insertion into the α -carbon to give the vinylketene **D** which by ring closure from carboxylic oxygen and migration of X group leads to the furan complex. On the other hand, CO insertion into the *E*- η^1, η^3 -vinylcarbene produces η^4 -vinylketene intermediate **F** which undergoes subsequent ring closure and tautomerization to result in phenol formation (**H**) via cyclohexadienone **G**. The cyclobutenone side product observed in rare cases even may rise from intermediate **F** by forming a metallacyclopentenone **K** that, with subsequent extrusion of chromium complex, leads to **L**.

If the CO insertion step in *E*-**C** is hampered as a result of increased stability of the Cr-CO bond, the formation of a chromacyclohexadiene intermediate **I** has been proposed that may give rise to indene formation (**J**).

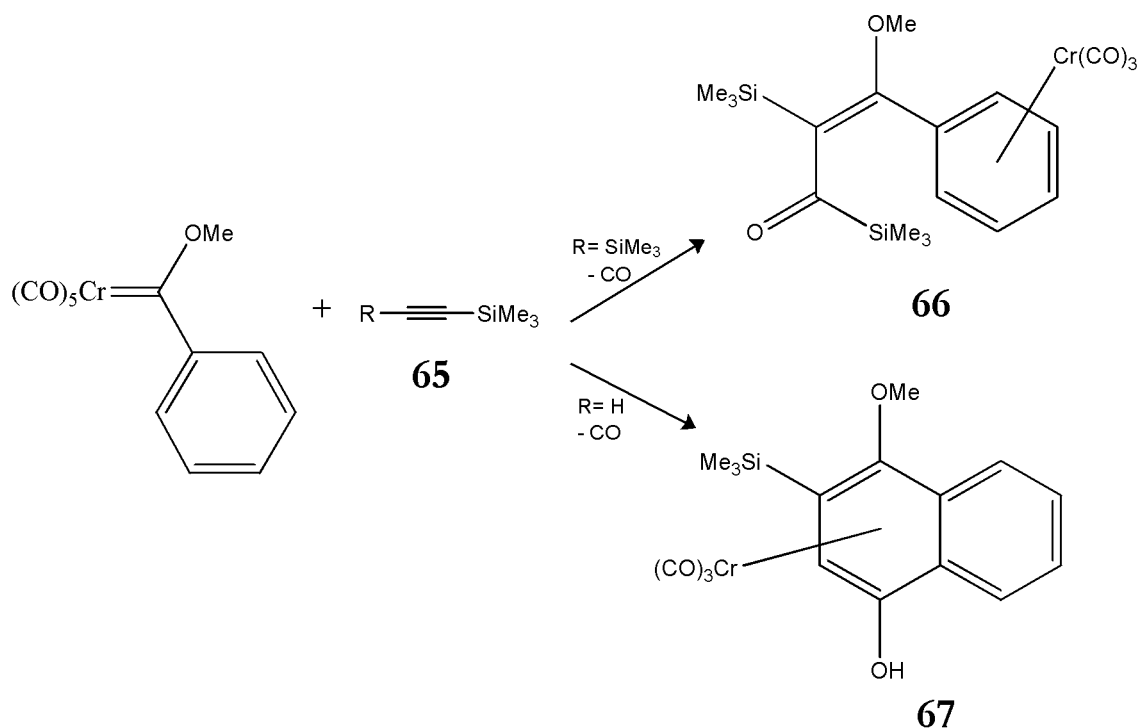


Scheme 9. Most accepted reaction mechanisms in literature for the cycloannulation reactions of Fischer carbene complexes.

Over the years all relevant types of key intermediates have been isolated and structurally characterized as model compounds. Tetracarbonyl vinylcarbene **64** has been isolated by Barluenga and coworkers by heating under reflux a solution of carbene **63** in THF and crystallizing the product in 90% yield.⁷⁰ The reaction is reverted when CO was bubbled at room temperature into a solution of **64** resulting in few minutes.



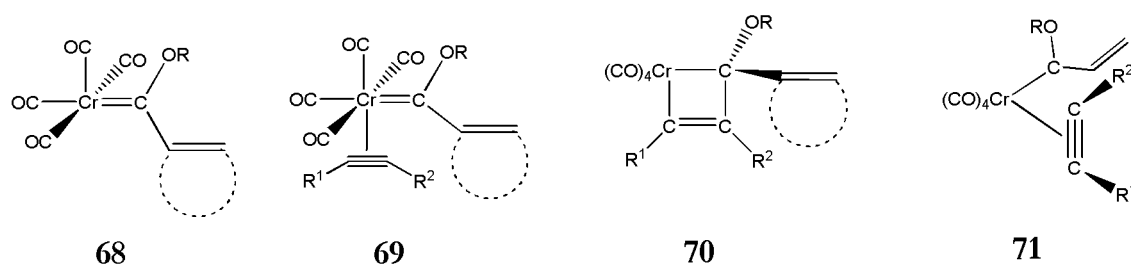
Vinylketenes as the final acyclic intermediates have been first isolated from reactions of chromium carbenes and silylalkynes **65** (Scheme 10). A vicinal disilyl substitution in **66** disfavors a vinylketene conformation required for electrocyclization; in contrast trimethylsilylethyne allows for a vinylketene intermediate bearing the phenyl ring in close proximity to the ketene group which results in clean benzannulation to **67**.⁷¹



Scheme 10. Suppressed electrocyclization in case of a vicinal disilyl substituted vinylketene.

Wulff and co-workers⁵⁹ postulated chromacyclobutene **70**, based on the stereochemistry of the electrocyclic ring opening due to the rotational mode of carbene carbon, as the key species to obtain the α,β -unsaturated vinylcarbene which is the

bottleneck responsible of all the products of cycloannulations. Nonetheless, initial theoretical works employing extended Hückel calculations created some controversy on previous steps to cycloannulation reactions, i.e., it is assumed first *cis* CO dissociation to yield tetracarbonyl carbene **68** and the insertion of alkyne into the vacant coordination site forming intermediate **69**. Hofmann and Hämmerle⁷² refuted this proposal arguing that the axial insertion (four-electron donor) of ethyne in **71** was ca. 5 kcal·mol⁻¹ (through a transition state for the rotational barrier of 23 kcal·mol⁻¹) more favorable than the “in-plane” (two-electron donor) conformation in **70**, which was postulated to be more than likely a transition state.

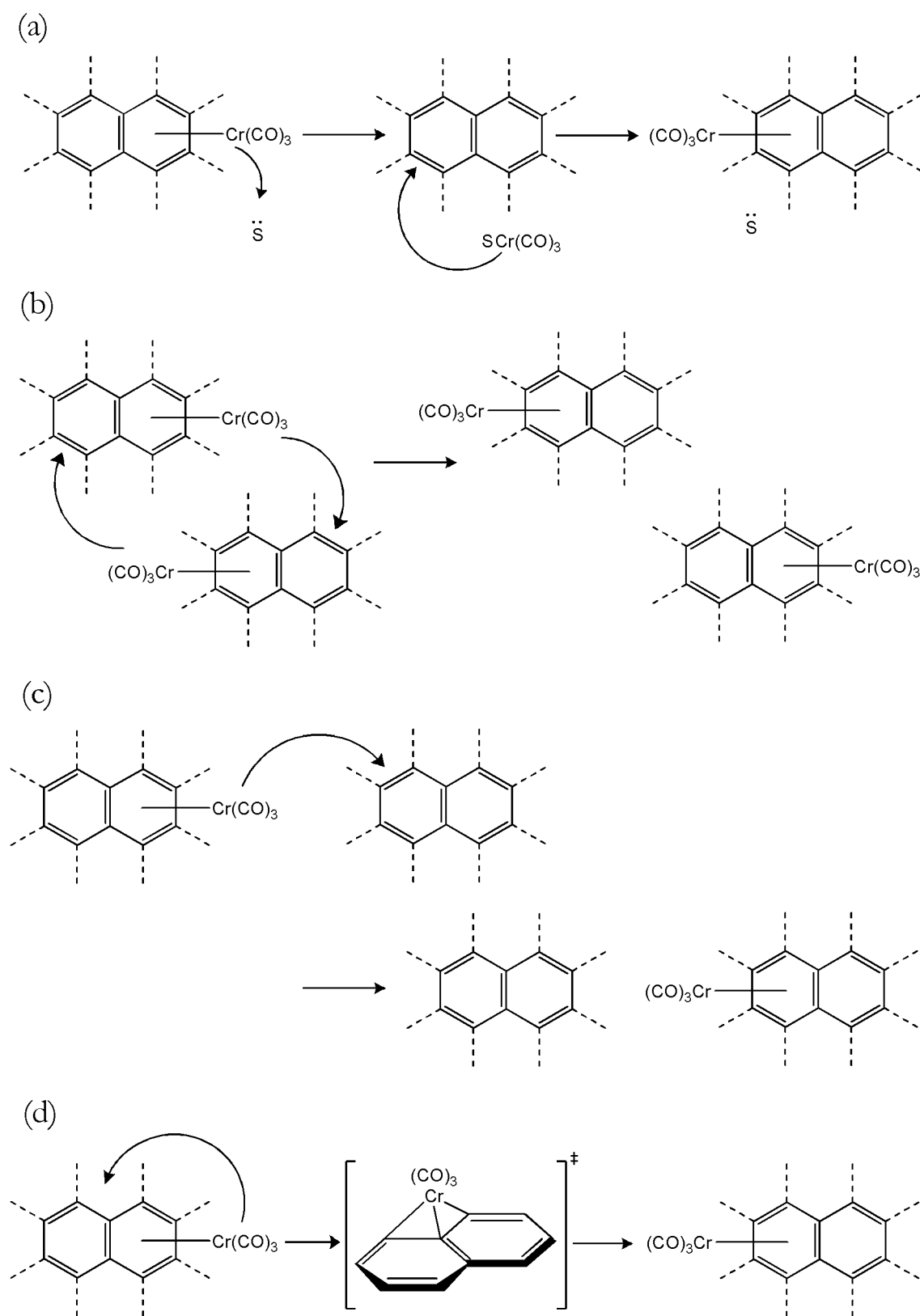


Perhaps the most important work about exploring the validity of the proposed reaction mechanism of Dötz benzannulation last decade was made by Gleichmann and co-workers.⁷³ They found that the rate-determining step is the dissociation of a *cis*-CO ligand before cycloannulation starts and the reaction mechanism was notoriously influenced by alkyl or aryl substituents. They concluded that the product of carbon monoxide insertion at the vinylcarbenes (i.e., η^4 -vinylketenes) is more stable than for phenylcarbenes, but once benzannulation takes place forming η^4 -cyclohexadienones, the process goes without any further energy barrier for vinylcarbenes whereas the route leading to η^4 -benzocyclohexadienones which are more stabilized species, for the case of phenylcarbenes, shows a significant barrier to complete benzannulation. Thus, it implies that vinylcarbenes should generally produce six-membered rings whereas benzannulation is less favored for *ortho*-substituted phenylcarbene chromium complexes. Even when they could not find the proper transition states structures to calculate the kinetics of reaction, most of the intermediates were very well discussed in terms of steric repulsions in geometries and reaction energies. Moreover, some pioneer work has been carried out on photochemical carbo- and decarbonylation reaction of FCCs by Fernández, Sierra and Cossío during last years.⁷⁴ These reaction mechanisms studied for thermal cycloadditions also complement the general overview of the work

reported in this Thesis where are not taken into account possible excited states that can generate new routes of reaction. An excellent review of these reactions has been reported by the same authors recently.⁷⁵

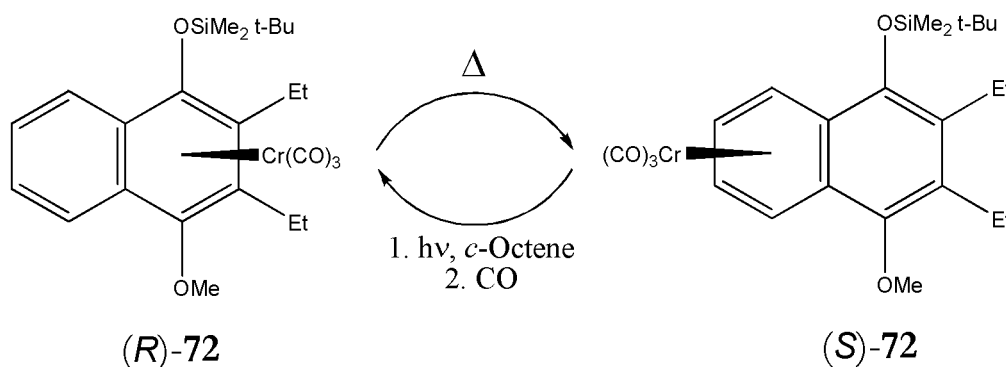
Until now, it can be seen that all those complexes undergoing benzannulation reactions end with a $\text{Cr}(\text{CO})_3$ fragment attached to the new formed ring. These compounds are suitable for haptotropic rearrangements along extended π -ligand systems and have been studied separately by several groups.⁷⁶ In general, haptotropic metal shifts are induced upon warming the arene complex to temperatures ranging from 40 °C to 100 °C; this protocol allows one to transform the thermodynamically less stable to the more stable regioisomer. If the coordination of one aromatic ring is strongly favored over the other, the haptotropic isomerization is virtually irreversible; in cases in which both isomers possess comparable thermodynamic stabilities, a dynamic equilibrium is observed. Four different mechanisms may account for the rearrangement as illustrated for a model complex in Scheme 11.

A dissociative mechanism involves the release of the metal fragment from the π -ligand followed by recomplexation (a). This path will be assisted by solvents or additives featuring donor abilities which allow a stabilization of the coordinatively unsaturated metal fragment intermediate. Bimolecular processes could be based either on the mutual exchange of the $\text{Cr}(\text{CO})_3$ fragments between two complex molecules (b) or on the transfer of the organometallic moiety to a non-coordinated π -ligand (c). Finally, the isomerization may result from an intramolecular metal shift during which the metal fragment remains coordinated to the π -electron-system (d). This implies that the metal moiety remains attached to the same face of the arene ligand throughout the whole process and thus, this mechanism fulfills the requirements of a haptotropic metal migration which has to proceed strictly intramolecularly. The extent to which intermolecular mechanisms contribute to the isomerization may increase with increasing polarity and donor properties of the solvent and with increasing temperature. Earlier theoretical studies suggested that the metal migration proceeds close to the periphery of the aromatic ligand rather than by the direct way across the central C-C bond.⁷⁷



Scheme 11. Mechanisms of haptotropic rearrangements proposed in literature.

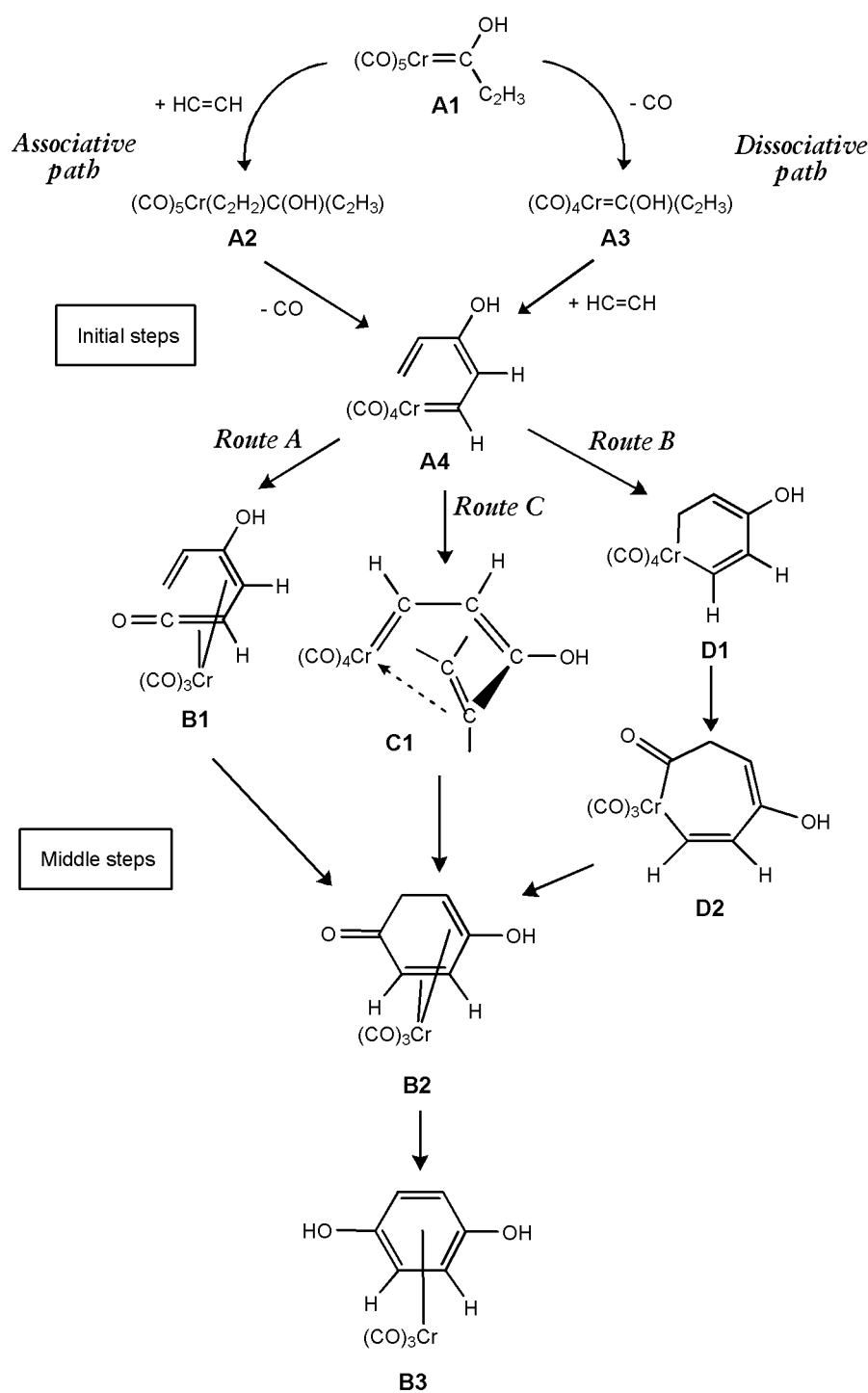
Dötz and co-workers⁷⁸ showed that the migration is governed by both the steric and the electronic properties of the ligands. In fact, the impact of substituents influencing haptotropic metal shifts in arene chromium complexes can be based on a ligand tuning of this reaction. The controllability of this kind of dynamic processes makes it suitable for applications in molecular machines. The metal migration may be rendered switchable between two specifiable isomers by internal influence, e.g. heating, emission of light or pH-change (see Scheme 12).⁷⁸ Moreover, it has been reported a novel application of controllable haptotropic migration on substituted phenanthrene rings (directly accessible from Dötz benzannulation) by substitution of one CO ligand for phosphines and phosphites showing interest in the mechanistic aspects.⁷⁹ Therefore, it becomes crucial to understand the vital points on the reaction mechanism of haptotropic migrations in order to get deeper into the design of these intermolecular switch devices.



Scheme 12. Stereospecific organometallic switch based on a reversible metal migration.

1.3.2 Contributions made on the past years in our research group (IQC).

Despite the undeniable synthetic value of the benzannulation reaction of aryl and alkenyl FCCs, the details of its mechanism at the molecular level remained to be ascertained. In view of the fact that few studies have been devoted to the analysis of reaction mechanisms of processes involving the Dötz reaction, our group contributed with some theoretical works exploring the abovementioned experimental proposals.



Scheme 13. Mechanistic diagram of the reaction pathways of Dötz benzannulation reaction explored for alkoxyvinylcarbenes in our group during last years.

Initially, it was published the first theoretical study of the early stage of Dötz reaction considering the two possible pathways from initial pentacarbonyl chromium carbene **A1**.⁸⁰ Namely, the insertion of an alkyne previous to the CO dissociation (route $\text{A1} \rightarrow \text{A2} \rightarrow \text{A4}$) called as the *associative route* or a more plausible reaction more supported by experimental work⁸¹ than the other, where the CO loss is undergone prior

to the alkyne coordination (route **A1** → **A3** → **A4**), named the *dissociative route*. From that work, it was concluded that the nucleophilic attack of alkynes on carbene complexes is not always understood as to require a vacant site of coordination at the metal center due to the high thermodynamic stability of intermediate **A2** which is the lowest minimum in the PES.

Later, it was derived a novel mechanistic proposal for the benzannulation reaction. Among the other explored routes: Dötz's original proposal³⁹ (**route A**) and Casey's pathway⁸² (**route B**), a third one was obtained in our group and named as the chromahexatriene pathway (**route C**).⁸³ All the reaction mechanisms shown in Scheme 13 were then explored, analysed and compared to discern the proper mechanistic scenario that fits better experimental observations in a next work.⁸⁴ Finally, a complete revision of all these past contributions was made in a book chapter for a complete assessment of benzannulation reaction of hydroxyvinylcarbene complex **A1**.⁸⁵

Therefore, the next approach is to explore the other reaction mechanisms of the remaining cycloannulation processes. The main goals of this Thesis are: i) Explore more routes of cycloannulation in chromium alkoxy- and aminocarbenes in order to extend the theoretical work developed last years in our group to investigate the effect of the substituents in these reactions mechanisms; ii) Discuss the competition reactions from the point of view of the product distributions experimentally reported; iii) The elucidation of the reaction mechanisms of intramolecular haptotropic rearrangements taking into account the size and the curvature of the arene fragment in order to improve the yield and applicability as was shown for the final stage of the Dötz reaction; iv) Contribute to the organometallic catalysis field and coordination chemistry by means of the study of these reactions of carbenes (or isonitriles) where a part of this knowledge can be reflected in the improvement of synthesis of natural products through fine Chemistry processes.

References.

- (1) W. v. E. Doering, A. K. Hoffmann, *J. Am. Chem. Soc.* **1954**, *76*, 6162.
- (2) E. O. Fischer, A. Maasböl, *Angew. Chem., Int. Ed.* **1964**, *3*, 580.
- (3) (a) C. P. Casey, R. L. Anderson, *J. Am. Chem. Soc.* **1971**, *93*, 3554; (b) C. P. Casey, R. L. Anderson, *J. Chem. Soc., Chem. Commun.* **1975**, 895.
- (4) (a) J. Barluenga, F. J. Fañanás, *Tetrahedron* **2000**, *56*, 4597; (b) J. Barluenga, J. Santamaria, M. Tomás, *Chem. Rev.* **2004**, *104*, 2259; (c) A. de Meijere, H. Schirmer, M. Duetsch, *Angew. Chem., Int. Ed.* **2000**, *39*, 3964; (d) K. H. Dötz, in: *Topics in Organometallic Chemistry*, K. H. Dötz ed., Springer-Verlag: Berlin/Heidelberg, **2004** vol. 13, p. 123; (e) J. W. Herndon, *Coord. Chem. Rev.* **2005**, *249*, 999; (f) M. A. Sierra, *Chem. Rev.* **2000**, *100*, 3591; (g) W. D. Wulff, in: *Comprehensive Organometallic Chemistry II*, E. W. Abel, F. G. A. Stone, G. Wilkinson eds., Pergamon Press: Oxford, **1995** vol. 12, p. 469.
- (5) (a) H. W. Wanzlick, H. J. Kleiner, *Angew. Chem.* **1961**, *73*, 493; (b) H. W. Wanzlick, E. Schikora, *Chem. Ber.* **1961**, *94*, 2389; (c) H. W. Wanzlick, *Angew. Chem.* **1962**, *74*, 129; (d) H. W. Wanzlick, H. J. Kleiner, *Chem. Ber.* **1963**, *96*, 3024; (e) H. W. Wanzlick, F. Esser, H. J. Kleiner, *Chem. Ber.* **1963**, *96*, 1208.
- (6) (a) R. J. Goddard, R. Hoffmann, E. D. Jemmis, *J. Am. Chem. Soc.* **1980**, *102*, 7667; (b) T. R. Cundari, M. S. Gordon, *J. Am. Chem. Soc.* **1991**, *113*, 5231.
- (7) (a) H. Nakatsuji, J. Ushio, S. Han, T. Yonezawa, *J. Am. Chem. Soc.* **1983**, *105*, 426; (b) H. Jacobsen, T. Ziegler, *Organometallics* **1995**, *14*, 224; (c) C.-C. Wang, Y. Wang, H.-J. Liu, K.-J. Lin, L.-K. Chou, K.-S. Chan, *J. Phys. Chem. A* **1997**, *101*, 8887; (d) M. Cases, G. Frenking, M. Duran, M. Solà, *Organometallics* **2002**, *21*, 4182.
- (8) J. P. Collman, R. G. Finke, J. N. Cawse, J. I. Brauman, *J. Am. Chem. Soc.* **1977**, *99*, 2515.
- (9) (a) C. P. Casey, C. R. Cyr, R. A. Boggs, *Synth. Inorg. Met-Org. Chem.* **1973**, *3*, 249; (b) D. F. Harvey, M. F. Brown, *Tetrahedron Lett.* **1990**, *31*, 2529; (c) H. Matsuyama, T. Nakamura, M. Iyoda, *J. Org. Chem.* **2000**, *65*, 4796.
- (10) (a) M. F. Semmelhack, J. J. Bozell, *Tetrahedron Lett.* **1982**, *23*, 2931; (b) M. A. Schwindt, J. R. Miller, L. S. Hegedus, *J. Organomet. Chem.* **1991**, *413*, 143.
- (11) T. L. Amyes, J. P. Richard, *J. Am. Chem. Soc.* **1996**, *118*, 3129.
- (12) C. F. Bernasconi, *Chem. Soc. Rev.* **1997**, *26*, 299 and references herein.

- (13) For instance, see: (a) C. F. Bernasconi, F. X. Flores, J. T. R. Gandler, A. E. Leyes, *Organometallics* **1994**, *13*, 2186; (b) C. F. Bernasconi, F. X. Flores, W. Sun, *J. Am. Chem. Soc.* **1995**, *117*, 4875; (c) C. F. Bernasconi, F. X. Flores, K. W. Kittredge, *J. Am. Chem. Soc.* **1997**, *119*, 2103; (d) C. F. Bernasconi, F. X. Flores, K. W. Kittredge, *J. Am. Chem. Soc.* **1998**, *120*, 8575; (e) C. F. Bernasconi, K. W. Kittredge, F. X. Flores, *J. Am. Chem. Soc.* **1999**, *121*, 6630.
- (14) (a) C. F. Bernasconi, M. W. Stronach, *J. Am. Chem. Soc.* **1993**, *115*, 11384; (b) C. F. Bernasconi, L. Garcia-Rio, *J. Am. Chem. Soc.* **2000**, *122*, 3821; (c) C. F. Bernasconi, G. S. Pérez, *J. Am. Chem. Soc.* **2000**, *122*, 12461; (d) C. F. Bernasconi, S. Bhattacharya, *Organometallics* **2003**, *22*, 426; (e) C. F. Bernasconi, S. Bhattacharya, *Organometallics* **2003**, *22*, 1310.
- (15) M. E. Zoloff Michoff, R. H. de Rossi, A. M. Granados, *J. Org. Chem.* **2006**, *71*, 2395.
- (16) G. Frenking, M. Solà, S. F. Vyboishchikov, *J. Organomet. Chem.* **2005**, *690*, 6178.
- (17) W. D. Wulff, D. C. Yang, *J. Am. Chem. Soc.* **1984**, *106*, 7565.
- (18) A. de Meijere, L. Wessjohann, *Synlett* **1990**, 20.
- (19) K. L. Faron, W. D. Wulff, *J. Am. Chem. Soc.* **1988**, *110*, 8727.
- (20) R. Aumann, B. Jasper, R. Fröhlich, *Organometallics* **1995**, *14*, 231.
- (21) M. Duetsch, F. Stein, R. Lackmann, E. Pohl, R. Herbst-Irmer, A. de Meijere, *Chem. Ber.* **1992**, *125*, 2051.
- (22) F. Stein, M. Duetsch, E. Pohl, R. Herbst-Irmer, A. de Meijere, *Organometallics* **1993**, *12*, 2556.
- (23) See for example: (a) T. J. Katz, S. J. Lee, *J. Am. Chem. Soc.* **1980**, *102*, 422; (b) R. Schlund, R. R. Schrock, W. E. Crowe, *J. Am. Chem. Soc.* **1989**, *111*, 8004.
- (24) (a) O. Geis, H. G. Schmalz, *Angew. Chem. Int. Ed.* **1998**, *37*, 911; (b) K. M. Brummond, J. L. Kent, *Tetrahedron* **2000**, *56*, 3263; (c) T. Sugihara, M. Yamaguchi, M. Nishizawa, *Chem. Eur. J.* **2001**, *7*, 1589; (d) S. E. Gibson, A. Stevenazzi, *Angew. Chem. Int. Ed.* **2003**, *42*, 1800.
- (25) D. F. Harvey, K. P. Lund, D. A. Neil, *J. Am. Chem. Soc.* **1992**, *114*, 8424.
- (26) J. Barluenga, M. A. Fernández-Rodríguez, E. Aguilar, *J. Organomet. Chem.* **2005**, *690*, 539.
- (27) L. Wesjohann, G. McGaffin, A. de Meijere, *Synthesis* **1989**, 359.

- (28) F. Funke, M. Duetsch, F. Stein, M. Noltemeyer, A. de Meijere, *Chem. Ber.* **1994**, *127*, 911.
- (29) M. Duetsch, F. Stein, F. Funke, E. Pohl, R. Herbst-Irmer, A. de Meijere, *Chem. Ber.* **1993**, *126*, 2535.
- (30) M. Duetsch, S. Vidoni, F. Stein, F. Funke, M. Noltemeyer, A. de Meijere, *J. Chem. Soc., Chem. Commun.* **1994**, 1679.
- (31) B. L. Flynn, C. C. Silveira, A. de Meijere, *Synlett* **1995**, 812.
- (32) B. L. Flynn, F. J. Funke, M. Noltemeyer, A. de Meijere, *Tetrahedron* **1995**, *51*, 11141.
- (33) (a) B. L. Flynn, F. J. Funke, C.C. Silveira, A. de Meijere, *Synlett* **1995**, 1007;
(b) A. G. Meyer, R. Aumann, R. Frölich, *Synlett* **1995**, 1011.
- (34) K. H. Dötz, *Angew. Chem. Int. Ed.* **1975**, *14*, 644.
- (35) K. H. Dötz, P. Tomuschat, *Chem. Soc. Rev.* **1999**, *28*, 187.
- (36) K. H. Dötz, *Angew. Chem. Int. Ed. Engl.* **1984**, *23*, 587.
- (37) B. L. Balzer, M. Cazanoue, M. Sabat, M. G. Finn, *Organometallics* **1992**, *11*, 1759.
- (38) For instance, see the review of substituted FCC in: W. D. Wulff in: *Comprehensive Organic Synthesis*, B. M. Trost, I. Fleming, L. A. Paquette eds. Pergamon Press: Oxford, **1991**, vol. 5, p. 1065.
- (39) J. Barluenga, F. Aznar, I. Gutiérrez, A. Martín, S. García-Granda, M. A. Llorca-Baragaño, *J. Am. Chem. Soc.* **2000**, *122*, 1314.
- (40) J. C. Anderson, J. W. Cran, N.P. King, *Tetrahedron Lett.* **2002**, *43*, 3849.
- (41) J. P. A. Harrity, W. J. Kerr, *Tetrahedron Lett.* **1993**, *34*, 2995.
- (42) Y. H. Choi, K. S. Rhee, K. S. Kim, G. C. Shin, S. C. Shin, *Tetrahedron Lett.* **1995**, *36*, 1871.
- (43) J. P. A. Harrity, W. J. Kerr, D. Middlemiss, *Tetrahedron* **1993**, *49*, 5565.
- (44) E. J. Hutchinson, W. J. Kerr, E. J. Magennis, *Chem. Commun.* **2002**, 2262.
- (45) R. A. Fernandes, V. P. Chavan, A. B. Ingle, *Tetrahedron Lett.* **2008**, *49*, 6341.
- (46) Y. Tanada, K. Mori, *Eur. J. Org. Chem.* **2001**, 4313.
- (47) R. A. Fernandes, V. P. Chavan, *Tetrahedron Lett.* **2008**, *49*, 3899.
- (48) A. Gupta, S. Sen, M. Harmata, S. R. Pulley, *J. Org. Chem.* **2005**, *70*, 7422.
- (49) W. R. Roush, R. J. Neitz, *J. Org. Chem.* **2004**, *69*, 4906.
- (50) S. A. Eastham, J. Herbert, S. P. Ingham, P. Quayle, M. Wolfendale, *Tetrahedron Lett.* **2006**, *47*, 6627.

- (51) S. A. Eastham, S. P. Ingham, M. R. Hallett, J. Herbert, P. Quayle, J. Raftery, *Tetrahedron Lett.* **2006**, *47*, 2299.
- (52) M. Rawat, W. D. Wulff, *Org. Lett.* **2004**, *6*, 329.
- (53) D. L. Boger, O. Huter, K. Mbiya, M. S. Zhang, *J. Am. Chem. Soc.* **1995**, *117*, 11839.
- (54) J. D. White, H. Smits, *Org. Lett.* **2005**, *7*, 235.
- (55) A. Minatti, K. H. Dötz, *J. Org. Chem.* **2005**, *70*, 3745.
- (56) M. W. Giese, W. H. Moser, *J. Org. Chem.* **2005**, *70*, 6222.
- (57) (a) K. H. Dötz, W. Kuhn, *Angew. Chem. Int. Ed. Engl.* **1983**, *22*, 732; (b) K. H. Dötz, I. Pruskil, *J. Organomet. Chem.* **1981**, *209*, C4; (c) K. H. Dötz, I. Pruskil, J. Muhlemeister, *Chem. Ber.* **1982**, *115*, 1278.
- (58) S. R. Pulley, B. Czako, G. D. Brown, *Tetrahedron Lett.* **2005**, *46*, 9039.
- (59) J. S. McCallum, F.-A. Kunng, S. R. Gibertson, W. D. Wulff, *Organometallics* **1988**, *7*, 2346.
- (60) J. Barluenga, M. Fañanás-Mastral, M. A. Palomero, F. Aznar, C. Valdés, *Chem. Eur. J.* **2007**, *13*, 7682.
- (61) (a) M. E. Bos, W. D. Wulff, R. A. Miller, S. Chamberlin, T. A. Brandvold, *J. Am. Chem. Soc.* **1991**, *113*, 9293; (b) M. L. Waters, M. E. Bos, W. D. Wulff, *J. Am. Chem. Soc.* **1999**, *121*, 6403.
- (62) B. Karatas, I. Hyla-Kryspin, R. Aumann, *Organometallics* **2007**, *26*, 4983.
- (63) P. Hofmann, M. Hämmerle, G. Unfried, *New J. Chem.* **1991**, *15*, 769.
- (64) D. H. Dötz, J. Mühlemeister, U. Schubert, O. Orama, *J. Organomet. Chem.* **1983**, *247*, 187.
- (65) S. Chamberlin, W. L. Waters, W. D. Wulff, *J. Am. Chem. Soc.* **1994**, *116*, 3113.
- (66) M. W. Davis, C. N. Johnson, J. P. A. Harrity, *J. Org. Chem.* **2001**, *66*, 3525.
- (67) Y.-T. Wu, B. Flynn, H. Schirmer, F. Funke, S. Müller, T. Labahn, M. Nötzel, A. de Meijere, *Eur. J. Org. Chem.* **2004**, 724.
- (68) (a) S. Chamberlin, W. D. Wulff, B. Bax, *Tetrahedron* **1993**, *49*, 5531; (b) J. W. Herndon, *Tetrahedron* **2000**, *56*, 1257; (c) B. L. Flynn, H. Schirmer, M. Duetsch, A. de Meijere, *J. Org. Chem.* **2001**, *66*, 1747; (d) R. Aumann, *Eur. J. Org. Chem.* **2000**, 17; (f) J. Barluenga, F. Rodríguez, F. J. Fañanás, J. Flórez, *Top. Organomet. Chem.* **2004**, *13*, 59.
- (69) (a) K. H. Dötz, H. Fischer, J. Mühlemeister, R. Märkl, *Chem. Ber.* **1982**, *115*, 1355; (b) H. Fischer, P. Hofmann, *Organometallics* **1999**, *18*, 2590.

- (70) J. Barluenga, F. Aznar, A. Martín, S. García-Granda, E. Pérez-Carreño, *J. Am. Chem. Soc.* **1994**, *116*, 11191.
- (71) K. H. Dötz, B. Fügen-Köster, *Chem. Ber.* **1980**, *113*, 1449.
- (72) P. Hofmann, M. Hämmerle, *Angew. Chem. Int. Ed. Engl.* **1989**, *28*, 908.
- (73) M. M. Gleichmann, K. H. Dötz, B. A. Hess, *J. Am. Chem. Soc.* **1996**, *118*, 10551.
- (74) (a) I. Fernández, M. A. Sierra, M. Gómez-Gallego, M. J. Mancheño, F. P. Cossío, *Chem. Eur. J.* **2005**, *11*, 5988; (b) I. Fernández, M. A. Sierra, F. P. Cossío, *J. Org. Chem.* **2006**, *71*, 6178; (c) I. Fernández, M. A. Sierra, M. J. Mancheño, M. Gómez-Gallego, F. P. Cossío, *J. Am. Chem. Soc.* **2008**, *130*, 13892.
- (75) M. A. Sierra, I. Fernández, F. P. Cossío, *Chem. Commun.* **2008**, 4671.
- (76) (a) R. U. Kirss, P. M. Treichel, Jr., *J. Am. Chem. Soc.* **1986**, *108*, 853; (b) T. G. Traylor, K. J. Stewart, *J. Am. Chem. Soc.* **1986**, *108*, 6977; (c) Z. Y. Own, S. M. Wang, J. F. Chung, D. W. Miller, P. P. Fu, *Inorg. Chem.* **1993**, *32*, 152; (d) H. C. Jahr, M. Nieger, K. H. Dötz, *Chem. Eur. J.* **2005**, *11*, 5333; (e) K. H. Dötz, J. Stendel, Jr., S. Müller, M. Nieger, S. Ketrat, M. Dolg, *Organometallics* **2005**, *24*, 3219; (f) S. Ketrat, S. Müller, M. Dolg, *J. Phys. Chem. A* **2007**, *111*, 6094; (g) I. D. Gridnev, *Coord. Chem. Rev.* **2008**, *252*, 1798; (h) Y. F. Oprunenko, I. P. Gloriov, *J. Organomet. Chem.* **2009**, *694*, 1195.
- (77) (a) T. A. Albright, P. Hofmann, R. Hoffmann, C. P. Lillya, P. A. Dobosh, *J. Am. Chem. Soc.* **1983**, *105*, 3396; (b) Y. F. Oprunenko, N. G. Akhmedov, D. N. Laikov, S. G. Malyugina, V. I. Mstislavsky, V. A. Roznyatovsky, Y. A. Ustynyuk, N. A. Ustynyuk, *J. Organomet. Chem.* **1999**, *583*, 136.
- (78) K. H. Dötz, in: *Topics in Current Chemistry*, K. H. Dötz ed., Springer Berlin/Heidelberg, **2004** vol. 248, p. 63.
- (79) O. Joistgen, A. Pflöschinger, J. Ciupka, M. Dolg, M. Nieger, G. Schnakenburg, R. Fröhlich, O. Kataeva, K. H. Dötz, *Organometallics* **2009**, *28*, 3473.
- (80) M. Torrent, M. Duran, M. Solà, *Organometallics* **1998**, *17*, 1492.
- (81) (a) J. R. Knorr, T.L. Brown, *Organometallics* **1994**, *13*, 2178; (b) C. P. Casey, M. C. Cesa, *Organometallics* **1982**, *1*, 87.
- (82) C. P. Casey, in: *Reactive Intermediates*; M. Jones, Jr. and R. A. Moss eds., Wiley: New York, **1981** vol. 2, p. 152.
- (83) M. Torrent, M. Duran, M. Solà, *Chem. Commun.* **1998**, 999.

- (84) M. Torrent, M. Duran, M. Solà, *J. Am. Chem. Soc.* **1999**, *121*, 1309.
- (85) M. Solà, M. Duran, M. Torrent, *Computational Modeling of Homogeneous Catalysis*; Kluwer Academic: Amsterdam, **2002**; Vol. 25, p. 269.

CHAPTER 2

COMPUTATIONAL METHODS

A molecular system in a stationary state is fully characterized by the solution Ψ to the many-electron Schrödinger equation

$$\hat{H}_T \Psi(\vec{R}, \vec{r}) = E_T \Psi(\vec{R}, \vec{r}) \quad (1)$$

Then, Ψ is a wave function that depends on the electronic (\vec{r}) and nuclear coordinates (\vec{R}) and \hat{H}_T is the quantum mechanical Hamiltonian of the molecule whereas E_T is the energy of the system. Usually, we consider that the motion of the electrons is much faster than the nuclei (the Born-Oppenheimer approximation¹) and is a very good simplification since for the hydrogen molecule the mass ratio is on the order of 10^{-4} but for systems with heavier nuclei, it becomes smaller. Thus, the nuclei can be fixed in space and equation 1 can be reduced to

$$\hat{H} \Psi(\vec{r}) = E \Psi(\vec{r}) \quad (2)$$

Here, E is the electronic energy $E(\vec{q}_1, \vec{q}_2, \vec{q}_3, \dots, \vec{q}_N)$ of the molecule at the nuclear coordinates $\{\vec{q}_i, i = 1, \dots, N\}$ and \hat{H} is the Hamiltonian of the molecule where the kinetic energy of the nuclei is neglected and nucleus-nucleus potential is a constant operating on the electronic wave function. The Potential Energy Surface (PES) $E(\vec{q}_1, \vec{q}_2, \vec{q}_3, \dots, \vec{q}_N)$ can be obtained in principle from the solution of equation 2 at all nuclear conformations. By expanding Ψ in terms of the so-called Slater determinants¹ D_i as

$$\Psi = \sum_{i=1}^n f_i D_i \quad (3)$$

equation 2 can be solved to any degree of accuracy. Moreover, since

$$D_i = |\varphi_{i1}(1)\varphi_{i2}(2)\varphi_{i3}(3)\dots\varphi_{in}(n)| \quad (4)$$

this determinant can be calculated once the function $\varphi_{in}(n)$ is expressed in turn as a linear combination of a set of known basis functions $\{\chi_r, r = 1, \dots, m\}$ as

$$\varphi_{in}(n) = \sum_{r=1}^m C_{in,r} \chi_r(n) \quad (5)$$

Thus, in practice, $\{\chi_r, r = 1, \dots, m\}$ is a set of atomic orbitals and the corresponding molecular orbitals $\varphi_{in}(n)$ are written as a linear combination of them. The coefficients f_i and $C_{in,r}$ of equations 3 and 5, respectively, are determined in such a way as to minimize the energy E of equation 2 (note this is not the case for other *ab initio* methods such as perturbation theory or coupled cluster). Furthermore, the number of used determinants in equation 3 defines the *ab initio* method used among other factors.

Ab initio calculations are difficult. The trouble is that the electrons have been observed to obey complicated and nonintuitive quantum mechanical laws. According to quantum theory, the electrons can only be described probabilistically. This means that the positions and velocities of the electrons cannot be known exactly at the same time with absolute precision; rather, the whole system must be described by a mathematical object: the wave function. Our physical vision of the world has shown that the wave function satisfies the Schrödinger equation to a very good approximation. Unfortunately, solving this equation to find the wave function is not generally feasible. One difficulty comes from the nature of the electrons. They are fundamentally indistinguishable. This has more than just philosophical implications. It means that all physical quantities must be left unchanged when two electrons switch places. For this to be true, the wave function can only change at most by an overall sign. The other complication arises from terms in the Schrödinger equation that describe how the electrons interact and repel each other. This mutual repulsion makes the solution grow exceedingly complex as the number of electrons increases.

Alternatives to *ab initio* methods are empirical methods such as the force field approach. These methods solve problems by parameterization of similar well-studied problems.² Since these empirical methods are designed for certain classes of systems, they are not to be trusted when applied to general situations. These methods can be designed to work at various length scales but are not the best tool to explore new scientific problems reliably.

2.1 A brief theoretical background of quantum mechanics.

2.1.1 Hartree-Fock theory and post *ab initio* methods.

In 1926, Erwin Schrödinger solved the equation for the hydrogen-like atom. The first applications of quantum mechanics to the study of the chemical bond together with valence bond theory and molecular orbital theory were barely instantaneous. In 1930, Douglas R. Hartree³ and Vladimir A. Fock⁴ proposed the Self-Consistent Field (SCF) method for numerical calculations of atomic energies, a starting point of the actual *ab initio* calculations. However, it was not operative for molecules until the introduction of the Linear Combinations of Atomic Orbitals (LCAO) method.⁵

The main contribution of the work of Hartree and Fock (HF) was to transform the time-independent, non-relativistic Schrödinger equation for polyelectronic systems into a product of single-electron functions,⁶

$$\hat{F}_i \varphi_i = \sum_{j=1}^N \lambda_{ij} \varphi_j \quad (6)$$

where $\hat{F}_i = \hat{h}_i + \sum_{j=1}^N (\hat{J}_j - \hat{K}_j)$ is the Fock operator: an effective single-electron operator that contains the terms of the kinetic energy of a single electron, the attraction of this electron with respect to all the nuclei and the repulsion with respect to the other electrons, respectively. By means of the undetermined Lagrange multipliers λ_{ij} , it is ensured that molecular orbitals (MOs) φ_i are orthonormalized and when a unitary transformation is applied to diagonalize the eigenvalue matrix, a special set of MO (φ_i') called the canonical MO emerges and equation (6) can be rewritten as

$$\hat{F}_i \varphi_i' = \varepsilon_i \varphi_i' \quad (7)$$

And the total Hartree-Fock molecular energy is given by

$$E = \sum_{i=1}^N \varepsilon_i - \frac{1}{2} \sum_{ij}^N (J_{ij} - K_{ij}) + V_{nn} \quad (8)$$

The terms J_{ij} and K_{ij} involved the calculation of bielectronic integrals (the Coulombic integral and the exchange integral, respectively) whereas V_{nn} is the constant energy of nuclear repulsion. The new multipliers ε_i are interpreted as the energies of every MO (note the sum of all of them is not the total energy). Through Koopmans'

theorem,⁷ values from both the negative of the multipliers associated to HOMO and LUMO are taken as approximations to the ionization energy or the electron affinity of the atom or molecule, respectively.

As said before, the problem of how to implement equation (7) in molecules was solved by C. C. J. Roothaan expanding every MO in terms of a set of basis functions, the referred LCAO,⁵

$$\varphi_i = \sum_{\alpha}^M c_{\alpha i} \phi_{\alpha} \quad (9)$$

where ϕ_i is an atomic orbital. By substituting eq. (9) into eq. (7) and multiplying to the left of each side by a specific base function and integrating this expression, we get the algebraic Roothaan-Hall equations (for closed-shell systems),^{5,8} that is, HF equations in the base of atomic orbitals. Commonly they are expressed in the matrix form:

$$\mathbf{FC} = \mathbf{SC}\boldsymbol{\varepsilon} \quad (10)$$

F is the Fock matrix containing each Fock operator operating over the basis functions (it involves single- and bielectronic integrals), S is the overlap matrix which contains the overlaps between basis functions and C is the matrix of coefficients of the linear combinations, eq. (9), and $\boldsymbol{\varepsilon}$ is the matrix of the orbital energies (both last terms are unknown variables). SCF iterative procedure is illustrated somewhere^{2,5,6} and basically it starts by proposing a guess density matrix, to get the Fock matrix, diagonalize it and obtain a new density matrix solving eq. (10). Then the iteration is repeated until convergence of the wave function and the total energy (see Section 2.2).

HF is an ideal method of independent particles since it does not take into account the electronic correlation energy, using just one Slater determinant and more advanced methods⁹ that expand the energy with corrective terms of second-order and so on are called *post*-HF methods. In other words, by increasing the number of Slater determinants into the expansion for Ψ given in eq. (3) makes it possible to correct the energy of the different states. Simpler correlated methods include the second-order Moller-Plesset perturbation theory¹⁰ scheme (MP2), the generalized valence bond (GVB) method¹¹ and the complete active space scheme (CASSCF).¹² These methods provide reasonable chemical accuracy with time requirements increasing as m^5 to m^{10} with the number of basis functions m . More accurate correlated methods include the

coupled-cluster scheme CCSD(T), the multireference approach (MCSCF), as well as the complete active space second-order perturbation theory (CASPT2).¹³ Especially, CCSD(T) has been shown to provide high chemical accuracy.¹⁴ Unfortunately, the CCSD(T) scheme requires large basis sets and scales as m^7 .¹⁵ Thus, CCSD(T) can only serve as a benchmark method for smaller size molecules (up to 20 atoms). The correlation between electrons at close distance (dynamic correlation) is described well by the CCSD(T) scheme. However, there are cases in which the correlation between electrons separated by long distances (nondynamic correlation) is important as well. For these cases,¹⁶ it is strongly recommended to use the MCSCF and CASPT2 approaches.

2.1.2 Density Functional Theory.

Investigations into a density-based theory of matter started about the same time as wave function quantum mechanics. In 1927, Thomas and Fermi attempted a density-based description of atoms.¹⁷ At that time, there was no known formal justification for this method. For most practical applications, Thomas-Fermi theory was inadequate. Nevertheless, the idea of a density-based theory was appealing and work continued. For example, von Weizsäcker introduced the first gradient-density functional¹⁸ in 1935. Moreover, the computer was developed in the forties and was a new tool for physics. If used properly, it could provide a quantitative theory of matter. Slater realized this and pushed for a density-based approximation to quantum theory that would be particularly compatible with computing larger systems. His X_α approximation was found to be good but, like Thomas-Fermi theory, lacked a known formal justification.¹⁹

Validation came in 1964 when Hohenberg and Kohn demonstrated that the density, as well as the potential, uniquely characterizes a non degenerated ground-state electronic structure problem.²⁰ Under this exact definition, the total electronic ground-state energy is expressed as a functional of the density

$$E^{HK}[\rho] = T[\rho] + V_{ee}[\rho] + \int v_{ext}(\vec{r})\rho(\vec{r})d\vec{r} \quad (11)$$

That is, the sum of the kinetic energy, electron-electron interaction energy and the nucleus-electron interaction energy, respectively.

The problem was that the last term of equation (11) is the only one analytically easy to calculate, the others are unknown. Then, a practical scheme to approximate these quantities was proposed by Kohn and Sham (KS)²¹ by means of a system of non-

interacting electrons and introducing the more familiar orbital approach, *i.e.*, electron density was divided into N orbital densities. Thus, eq. (11) was transformed into

$$E^{KS}[\rho] = T_s[\rho] + \int v_s(\vec{r})\rho(\vec{r})d\vec{r} + E_{xc}[\rho] \quad (12)$$

where

$$T_s[\rho] = \sum_{i=1}^N \langle \psi_i | -\frac{1}{2} \nabla^2 | \psi_i \rangle, \quad \rho(\vec{r}) = \sum_{i=1}^N |\psi_i(\vec{r})|^2 \quad (13)$$

and it is assumed the existence of an external potential v_s that can reproduce the density of the corresponding interacting system (the real one): $\rho(\vec{r}) = \rho_s(\vec{r})$.

If v_s exists the one-to-one $v \rightarrow \rho$ mapping ensures its uniqueness.

For the interacting system all those quantities (which do not have classical analogues and we called quantum effects) that eq. (12) needs to recover the total exact energy described in eq. (11) were collected in one term: the exchange-correlation energy that is defined as

$$E_{xc}[\rho] = T[\rho] - T_s[\rho] + V_{ee}[\rho] - \int \frac{\rho(\vec{r}_1)\rho(\vec{r}_2)}{|\vec{r}_1 - \vec{r}_2|} d\vec{r}_1 d\vec{r}_2 \quad (14)$$

The exchange-correlation (XC) energy is sometimes referred to as nature's glue²² because it is responsible for keeping much of matter together by counteracting some of the Coulomb repulsion. If nature only kept the classical interaction energy, then chemical bonds would be weaker and longer. The exchange-correlation contribution reduces the interaction energy because it accounts for the tendency of electrons not to collide.

By other hand, the form of v_s can be found by comparing the Euler-Lagrange for the two systems, the non-interacting and the real ones (whose solution should provide the same ground-state density) and fixing the asymptotic to zero so that $\mu = \mu_s$ (the chemical potential between electrons be the same). So the external potential of the non-interacting Kohn-Sham system v_s contains then the effect of the interaction between electrons,

$$v_s(r_1) = v(r_1) + \int \frac{\rho(r_2)}{|r_1 - r_2|} dr_2 + v_{xc}(r_1) \quad (15)$$

The only part we need to deal with is in $E_{XC}[\rho]$. Furthermore the computational scheme is quite simple requiring the self-consistent solution of the KS set of N one particle equations:

$$\left(-\frac{1}{2}\nabla^2 + v_s(\vec{r})\right)\psi_i(\vec{r}) = \varepsilon_i \psi_i(\vec{r}) \quad , \quad i = 1, \dots, N \quad (16)$$

The eigenvalues and eigenvectors of this set of equations are respectively the one electron KS orbital functions ψ_i and the KS orbital energies ε_i . The density is calculated from the occupied KS orbital functions through eq. (13).

There are different approximations to calculate the correlation-exchange energy which were classified by John Perdew²³ according to a biblical analogy (Jacob's ladder). Chemical accuracy is on top and each rung preserves the formal, exact properties of the lower rungs.

Local Density Approximation (LDA) is the lowest rung of the ladder,

$$E_{XC}^{LDA}[\rho] = \int \rho(\vec{r}) \varepsilon_{XC}(\rho) d\vec{r} \quad (17)$$

This model was derived by considering an ideal electron gas where every electron experiences the same effect from the surrounding electrons as if the electronic density was uniform and equal to the density where the affected electron is. The total interaction energy would then be an integral over all local contributions. The term ε_{XC} is the local energy per particle of a uniform electron gas of density ρ at each point in space.²⁴ The LDA is correct for the homogeneous electron gas as well as for small-gap insulators and satisfies exact constraints as the form of XC hole, electron fluctuation regime delimited by Wigner-Seitz radius and others.²⁵ It is accurate for slowly varying densities and is useful in solid-state physics as well as star clusters in astronomy. Because of its simplicity, this functional is perhaps the most reliable. However, LDA tends to over-emphasize metallic character and overestimates weak bonds like hydrogen bonds and van der Waals forces. Some successes and shortcomings of LDA are discussed in Ref. 26.

First attempts to correct the LDA by expanding the gradient near to every local point failed because some derivatives of density diverges and even so, they do not represent a more accurate scheme,^{20,21} but careful considerations lead to the generalized gradient approximations (GGA),²⁷

$$E_{XC}^{GGA}[\rho] = \int \rho(\vec{r}) \varepsilon_{XC}^{GGA}(\rho(\vec{r}), \nabla \rho(\vec{r})) d\vec{r} \quad (18)$$

GGA functionals preserve many of the exact features of LDA and provide results which are good for chemistry as well as solid-state physics.

The next rung is the meta-generalized gradient approximation (meta-GGA),

$$E_{XC}^{meta-GGA}[\rho] = \int \rho(\vec{r}) \varepsilon_{XC}^{GGA}(\rho(\vec{r}), \nabla \rho(\vec{r}), \tau(\vec{r})) d\vec{r} \quad (19)$$

which depends on the KS local kinetic energy density,

$$\tau(\vec{r}) = \frac{1}{2} \sum_{\varepsilon_i < \mu} |\nabla \phi_i(\vec{r})|^2 \quad (20)$$

meta-GGA is more accurate than GGA for slowly varying or one-electron densities. Recently, meta-GGA density-functionals have become popular in quantum chemistry.

Until now, orbital-dependent functionals of the occupied KS orbitals (hyper-GGA) are the upper step on Jacob's ladder and bring more accuracy but also more computational cost.²⁸

$$E_{XC}^{hyper-GGA}[\rho] = E_{XC}[\phi_{KS}^{Occ}\{\rho\}] \quad (21)$$

The KS orbitals are implicit functions of the density; consequently, it is a density functional. Orbital functionals are considerably more expensive to implement self-consistently; however, the non-interacting kinetic energy is a functional of the occupied KS orbitals, and the approximate KS orbitals result from any self-consistent lower-rung calculation. Consequently, using this rung non-self-consistently in addition to a self-consistent lower rung calculation does not consume significantly more computer time and resources.

Nevertheless, the exact correlation has not been described with this kind of functionals that cover only the dynamical part of the correlation.²⁹ A functional has to be found to get the remaining nondynamical part. A practical solution is to mix the exact exchange (which contains also nondynamical correlation at some extent) with a GGA exchange; those are the so-called hybrid functionals:

$$E_{XC}^{hybrid}[\rho] = E_X + a(E_X^{GGA} - E_X) + E_C^{GGA} \quad (22)$$

The nondynamical effects are then given by the difference in energy of the GGA and exact exchange energy weighted with a mixing factor a . The mixing factor a is not “universal”: the effects of nondynamical correlation depend on the type of bond and vary strongly with the bond distance. For instance, the well-known B3LYP hybrid functional³⁰ possesses the next parameterized form:

$$E_{XC} = A E_X^{Slater} + (1 - A) E_X^{HF} + B (E_X^{B88} - E_X^{Slater}) + E_C^{VWN} + C (E_C^{LYP} - E_C^{VWN}) \quad (23)$$

with $A = 0.80$, $B = 0.72$ and $C = 0.81$.

2.1.3 Types of basis sets and nomenclature.

A basis set is a group of functions used to represent the orbitals in an atom. There are two types of basis sets (also called atomic orbitals, AO, and in general they can not be considered as solutions to the atomic Schrödinger equation) commonly used in electronic structure calculations: Slater-type orbitals³¹ (STO) and Gaussian-type orbitals³² (GTO).

$$\Phi_{STO} = N Y_{lm} \sum_i C_i \sum_j C_{ij} r^{n-1} e^{-\zeta_{ij} r} \quad (24)$$

$$\Phi_{GTO} = N Y_{lm} \sum_i C_i \sum_j C_{ij} e^{-\zeta_{ij} r^2} \quad (25)$$

The functions Y_{lm} are the spherical harmonics which give the correct symmetry to the orbital (s, p, d or f). Contraction coefficients C_{ij} and exponents ζ_{ij} are defined from the beginning and remain constant when minimizing the electronic energy. Precisely, this set of coefficients and exponents is called basis set. Therefore, coefficients C_i of the molecular orbital are those to be optimized in the calculation. Whereas GTOs cannot represent properly the electron density near the nuclei and also vanish rapidly when are far from it, STOs have the correct asymptotic behavior but are computationally more expensive. However, one STO can be fixed into three GTOs using lineal combinations called contractions and then a better behavior in positions close to and far from the nucleus is achieved. The use of these contracted functions is more extended into quantum mechanic calculations.³³

Pople's basis sets are the one of the most used among all the currently available. The minimal basis sets using this nomenclature are the STO-nG.³⁴ This means that every occupied atomic orbital will be approximated to a STO using a particular contraction of n-GTOs (n= 2-6). The notation k-nlmG is more used nowadays: this is, k primitive GTOs are used to represent the core electrons and nlm defines the way by which valence orbital functions are split (nl stands for split-valence and nlm for triple-split valence). For the case of the basis set used in this work, 6-31G,³⁵ each core orbital is described by a particular contraction of six primitive GTOs, the inner part of valence orbitals by a contraction of three primitive GTOs and the external part of valence is represented by one primitive GTO. Moreover, polarization functions³⁶ are added to give more flexibility to the wave function in order to represent bonds in more directions in the space, *i.e.*, considering larger angular moments. The notation of Pople's basis set is modified adding one or two asterisks after G letter depending on whether these *d*- or *p*-extra functions of polarization are added only to atoms distinct of hydrogens or they also included, respectively. The same notation stands for one or two signs (+) placed before G letter and referred to the added diffuse functions.

There are other popular basis sets also using GTOs, like Huzinaga's basis sets³⁷ (which are non contracted), Partridge,³⁸ McLean and Chandler³⁹ and those contracted and derived from Huzinaga's basis sets by Dunning.⁴⁰ He also introduced the notation for those very useful *correlation-consistent* basis sets⁴¹ like aug-cc-pVDZ. Other well-known notation as the TZVP basis set was introduced by Alhrichs and co-workers.⁴² In general, more basis sets have appeared last years since the algorithms for parametrizing over new schemes of calculus are developed looking for a better accuracy.

When solving the Schrödinger equation considering molecular orbitals which in turn are defined by these basis sets –truncated until some extension for technical reasons– there is a part of overlapping between atomic functions that can underestimate the real molecular energy. Obviously, the more complete the basis set, the smaller the error is. This error is known as the Basis Set Superposition Error (BSSE) and it is defined from the interaction energy between two atomic or molecular fragments A and B to give the complete system AB,

$$\Delta E(AB) = E(AB) - E(A) - E(B) \quad (26)$$

There are two methods to calculate this error: The chemical Hamiltonian approach (CHA)⁴³ which replaces the conventional Hamiltonian with one designed to prevent basis set mixing *a priori*, by removing all the projector-containing terms that would allow basis set extension and the Boys and Bernardi's Counterpoise Method⁴⁴ which calculates the BSSE by re-performing *all* the calculations using the mixed basis sets, through the use of *ghost orbitals* and then subtracts this error *a posteriori* from the uncorrected energy. Thus, the correction to the energy can be defined as⁴⁵

$$\delta^{BSSE} = E_{AB}^A(A) + E_{AB}^B(B) - E_{AB}^{AB}(A) - E_{AB}^{AB}(B) \quad (27)$$

where $E_Y^Z(X)$ represents the energy of subsystem X at optimized geometry Y using the basis set Z.

2.1.4 Non-relativistic pseudopotentials.

It is well known that only valence electrons are the most important for chemical reactions due to the electron transfer undergone in these processes whereas core electrons are closer to the nuclei and are not present in reactions but represent the most part of atomic energy. Assuming this fact, the effect of core electrons can be simulated by the so-called *effective-core potentials* (ECP). All the theoretical methods based in the frozen-core approximation for calculating ECP are divided into two families: those using an orbital transformation called *pseudo-orbital transformation* are related with the Phillips-Kleinman equation.⁴⁶ These methods are known as PseudoPotentials (PP). The other family contains those methods not used in this transformation and are related with the Huzinaga-Cantu equation.⁴⁷ These methods are known as Model Potentials (MP).

For this Thesis, pseudopotentials were used in some cases to treat the core electrons of the TM. By applying a hermitian Hamiltonian operator, \hat{F} , that allows a separation of valence functions, $|\varphi_v\rangle$, and core functions, $|\varphi_c\rangle$, (orthonormal each other), that is, this Hamiltonian has the valence function $\hat{F}|\varphi_v\rangle = \varepsilon_v|\varphi_v\rangle$ and the core functions $\hat{F}|\varphi_c\rangle = \varepsilon_c|\varphi_c\rangle$ as eigenfunctions, we can define an arbitrary function called the Phillips-Kleinman *pseudo-orbital* (for the case of single-electron Hamiltonians) as a lineal combination of valence function and core functions as

$$|\tilde{\varphi}_v\rangle = a_v|\varphi_v\rangle + \sum_c a_c|\varphi_c\rangle \quad (28)$$

By multiplying this equation to the left by $\langle\varphi_c|$ and using the orthonormal conditions, we can see that $a_c = \langle\varphi_c|\tilde{\varphi}_v\rangle$ and substituting this result in the equation, we get the next expression

$$|\tilde{\varphi}_v\rangle = a_v|\varphi_v\rangle + \sum_c |\varphi_c\rangle\langle\varphi_c|\tilde{\varphi}_v\rangle \quad (29)$$

Isolating $|\varphi_v\rangle$ from here, we can rewrite the Hamiltonian operator as

$$\hat{F}^{PK}|\tilde{\varphi}_v\rangle \equiv \left\{ \hat{F} + \sum_c (\varepsilon_v - \varepsilon_c) |\varphi_c\rangle\langle\varphi_c| \right\} |\tilde{\varphi}_v\rangle = \varepsilon_v |\tilde{\varphi}_v\rangle \quad (30)$$

This is the Phillips-Kleinman equation, where can be seen that the eigenfunctions of \hat{F} are also eigenfunctions of the \hat{F}^{PK} operator, where the solutions $|\varphi_v\rangle$ and $|\varphi_c\rangle$ are degenerated with eigenvalue ε_v . Precisely the additional term comparing original \hat{F} with eq. (30) is the Phillips-Kleinman pseudopotential. In practice, this pseudopotential and those from Coulomb and core exchange are substituted together by one single operator called just pseudopotential $\hat{V}_{\mu,nl}^{PP}$. Moreover, it is not required then, that the pseudoorbitals are lineal combinations of core orbitals and valence orbitals.⁴⁸

The effective valence multi-electronic Hamiltonian, where the electron correlation is incorporated is then defined, when pseudopotential is applied, as

$$\begin{aligned} \hat{H}^{PP}(1, \dots, N_v) \equiv & \sum_{i=1}^{N_v} \left\{ -\frac{1}{2} \nabla_i^2 + \sum_{\mu} \left[\frac{-Z_{\mu}^{eff}}{|\vec{r}_i - \vec{R}_{\mu}|} + V_{\mu,nl}^{PP} \right] \right\} \\ & + \sum_{i>j=1}^{N_v} \frac{1}{r_{ij}} + \sum_{\mu>\nu} \frac{Z_{\mu}^{eff} Z_{\nu}^{eff}}{|\vec{R}_{\mu} - \vec{R}_{\nu}|} \end{aligned} \quad (31)$$

where non relativistic pseudopotential basis sets are defined as a set of core pseudopotentials, V_{nl}^{PP} (linked autoconsistently with the valence pseudo-orbitals $|\tilde{\varphi}_v\rangle$), and pseudopotential radial functions, $\tilde{R}_{nl}(r)$, this way:

$$V_{nl}^{PP} = \sum_{k=1}^{K_V} A_k^{(l)} r^{n_k} \exp(-\alpha_k^{(l)} r^2)$$

$$\tilde{R}_{nl}(r) = \sum_{k=1}^{K_R} C_k^{(l)} r^l \exp(-\zeta_k^{(l)} r^2)$$
(32)

2.2 Methods for exploring potential energy surfaces.

Geometry optimization is a general term to indicate the search of stationary points of a function, *i.e.*, points where the first derivative is zero. For most of the cases, the desired stationary point is a minimum, where all the second derivatives are positive. Essentially, most of the optimization methods used in the computational chemistry⁴⁹ assume that at least the first derivative of the function (total energy) with respect to all the variables (nuclei coordinates), the gradient \vec{g} , can be calculated analytically (which means directly, no need of numerical differentiation over each variable). Some methods also require the calculation of the second derivative matrix (of the energy), the Hessian \tilde{H} .

Since this function to optimize, and the derivative(s), are calculated with a finite precision, depending on the computational implementation, a stationary point can not be located accurately, thus only the gradient can be reduced close to zero. In the practice, the optimization is considered converged when the gradient is reduced to a limit number that is considered acceptable. This is called the convergence criteria.

There are four classes of optimization methods commonly utilized to find minima:² (1) Steepest Descent, (2) Conjugate Gradient, (3) Newton-Raphson, and (4) Direct Inversion of the Iterative Subspace (DIIS), where there are also different methods in literature to calculate the initial Hessian and the subsequent updates every optimization step. Moreover, the election of a proper system of coordinates to find the

stationary points is also very important. Pulay and co-workers' method⁵⁰ (generally implemented in the computational methodologies) suggest the use of natural internal coordinates, which are the bond distances and angles chosen as $3N - 6$ freedom degrees, especially useful to follow a reaction pathway.

2.2.1 Searching transition states.

When we speak about mapping a reaction mechanism, this means about optimizing geometries of reactants and products, to find the transition state (TS) and follow the reaction route to ensure us we got the correct TS connecting both of them. Thus, a TS or first-order saddle point is a stationary point at the PES which is a maximum in energy in one direction and a minimum in all the others, although computationally speaking, these can be very difficult to find and deserve more sophisticated algorithms than minima.

There are several different strategies to search for first-order saddle points and the optimization, in all the cases, is based on the interpolation between reactants and products. Among these methods sounded in literature, we can find the Saddle optimization,⁵¹ chain method,⁵² sphere optimization technique,⁵³ the self-penalized route,⁵⁴ etc.

For this Thesis I used the method of the synchronous transit to localize TS structures. The method of the linear synchronous transit (LST) makes an interpolated vector from the geometries of reactant and product and localizes the structure of highest energy along this line. To do this, it is supposed that all the variables change in the same proportion over the reaction route.

In general, this is not a good approximation, and just for simpler systems LST generates a reasonable estimation of the geometry of a TS. The method of quadratic synchronous transit (QST) makes a parabolic approximation of the reaction pathway instead of a straight line. After finding the maximum by using LST, the QST is generated minimizing the energy in the perpendicular directions to the LST route. Thus, QST pathway searches for the maximum in energy. Both methods are illustrated in Figure 5.

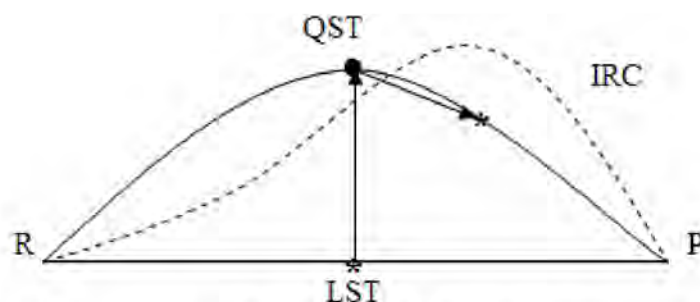


Figure 5. Linear synchronous transit and quadratic synchronous transit are used to localize transition states. The minima and the maximum in energy are denoted by the asterisks and the black dot, respectively.

Bell and Crighton⁵⁵ refined this method by performing a minimization from the maximum LST in the conjugated directions to the LST instead of the orthogonal ones, as was planned originally. A more recent variation of QST, called the synchronous transit-guided quasi-Newton (STQN)⁵⁶, uses an arc circle instead of a parabola for the interpolation and also the tangent to the circle to guide the searching to the TS region. When the point is near enough of the TS, the optimization changes to a quasi-Newton method that has a more rapid and accurate convergence at this position (it can also use the eigenvector-following algorithm when the convergence is erratic). The term *near enough* means that the Hessian must have just one negative eigenvalue and the eigenvector must be in the correct direction, over the reaction coordinate. For the search of TSs is very recommended to choose internal coordinates instead of the cartesian ones, because the use of the former sometimes diverges the calculation and by employing internal coordinates it is easier to follow the reaction coordinate.

2.2.2 Proposing a reaction step to create a reaction mechanism.

Once a TS has been obtained, it must be verified that it is connecting unequivocally to the desired minima (reactant and product), as mentioned before. For a TS, the normal coordinate of vibration associated with the negative frequency is the reaction coordinate and by inspecting the corresponding atomic displacements, we can have an approximate idea if this is the correct TS. However, if we need a rigorous prove, it is required to determine the minimum energy path (MEP) from the TS to the

minima downhill. If the MEP is performed by using weighted-mass coordinates, the following of this path is called Intrinsic Reaction Coordinate (IRC). The sketched route of IRC is very important for the dynamical studies of reactions since very often nuclei remain closer to the IRC and the model for the reaction surface can be built by expanding the energy to second-order, *e.g.*, around the points over IRC.

IRC route is defined by the next differential equation:

$$\frac{d\bar{x}}{ds} = -\frac{\bar{g}}{|\bar{g}|} = \bar{v} \quad (33)$$

Here \bar{x} is the weighted-mass coordinate, s is the length of the path and \bar{v} is the normalized gradient (in the negative direction). To determine the IRC entails to solve eq. (33) starting from a geometry slightly displaced from TS driven by the normal coordinate of the negative frequency.

The simplest method to integrate eq. (33) is Euler's scheme. A series of steps are taken from the opposite direction to the normalized gradient,

$$\bar{x}_{n+1} = \bar{x}_n + \Delta s \bar{v}(\bar{x}_n) \quad (34)$$

This is similar to a steepest descent geometry optimization but with a fixed Δs step. Since this methodology usually oscillates around the true pathway, consequently it requires a small step size to follow the IRC accurately.

A more advanced method is the *Runge-Kutta* (RK). The aim is to generate some intermediate steps which allow a better and more stable estimate of the next geometry for a given step size. *Runge-Kutta* of second order (RK2) calculates first the gradient at the point which is the half step size when using Euler's method, eq. (34). This gradient at the point the half of the step is used to take the whole step, then

$$\begin{aligned} \bar{k}_1 &= \Delta s \bar{v}(\bar{x}_n) \\ \bar{k}_2 &= \Delta s \bar{v}\left(\bar{x}_n + \frac{1}{2} \bar{k}_1\right) \\ \bar{x}_{n+1} &= \bar{x}_n + \bar{k}_2 \end{aligned} \quad (35)$$

Runge-Kutta of forth-order (RK4) generates four intermediate gradients and combines the steps as follows:

$$\begin{aligned}
\vec{k}_1 &= \Delta s \vec{v}(\vec{x}_n) \\
\vec{k}_2 &= \Delta s \vec{v}(\vec{x}_n + \frac{1}{2} \vec{k}_1) \\
\vec{k}_3 &= \Delta s \vec{v}(\vec{x}_n + \frac{1}{2} \vec{k}_2) \\
\vec{k}_4 &= \Delta s \vec{v}(\vec{x}_n + \vec{k}_3) \\
\vec{x}_{n+1} &= \vec{x}_n + \frac{1}{6} \vec{k}_1 + \frac{1}{3} \vec{k}_2 + \frac{1}{3} \vec{k}_3 + \frac{1}{6} \vec{k}_4
\end{aligned}
\tag{36}$$

Other method to calculate the IRC has been developed by González and Schlegel.⁵⁷ The idea is to generate points over the IRC by means of a series of restricted optimizations, as it is illustrated in Figure 2. A point to expand is generated by taking one step into the followed direction with a step size of $\frac{1}{2} \Delta s$. Then, the energy is minimized in a hypersphere of radius $\frac{1}{2} \Delta s$, localized in the point to expand. This is one example of a restricted optimization guided through a Lagrange multiplier. Moreover, this procedure insures us that the tangent to the IRC pathway is correct at every point.

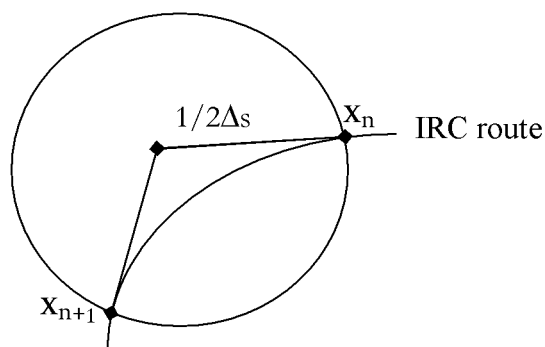


Figure 2. Sketched method of the restricted optimization of González-Schlegel to follow the IRC.

References.

- (1) I. R. Levine, *Quantum Chemistry*, 5th ed.; Prentice Hall: New Jersey, **2000**
- (2) F. Jensen, *Introduction to Computational Chemistry* Wiley & Sons ed., New York, **1999**.
- (3) D. R. Hartree, W. Hartree, *Proc. Roy. Soc.* **1935**, *A150*, 9.
- (4) V. Fock, *Z. Physik* **1930**, *61*, 126.
- (5) R. McWeeny, *Methods of Molecular Quantum Mechanics*, Academic Press, **1992**.
- (6) A. Szabo, N. S. Ostlund, *Modern Quantum Chemistry*, McGraw-Hill, **1982**.
- (7) T. A. Koopmans, *Physica* **1933**, *1*, 104.
- (8) G. G. Hall, *Proc. R. Soc. (London)* **1951**, *A205*, 541.
- (9) (a) R. J. Bartlett, J. F. Stanton, in: *Rev. Comput. Chem.* VCH Publishers, Inc. New York **1994**, vol. 5; (b) T. D. Crawford, H. F. Schaefer III, in: *Rev. Comput. Chem.* Wiley-VCH, ed., New York **2000**, vol. 14.
- (10) C. Moller, M. S. Plesset, *Phys. Rev.* **1934**, *46*, 0618.
- (11) W.A. Goddard, T. H. Dunning, W. J. Hunt, P. J. Hay, *Acc. Chem. Res.* **1973**, *6*, 368.
- (12) B. O. Ross, *Adv. Chem. Phys.* **1987**, *69*, 399.
- (13) K. Andersson, P. Å. Malmqvist, B. O. Ross, *J. Chem. Phys.* **1992**, *96*, 1218.
- (14) M. Diedenhofen, T. M. Wagener, G. Frenking, in: *Computational Organometallic Chemistry*, T. R. Cundari, ed., Marcel Dekker: Basel, **2001**, p. 69.
- (15) J. A. Pople, M. Head-Gordon, K. Raghavachari, *J. Chem. Phys.* **1987**, *87*, 5968.
- (16) K. Pierloot, in: *Computational Organometallic Chemistry*, T. R. Cundari, ed., Marcel Dekker: Basel, **2001**, p. 123.
- (17) (a) L.H. Thomas, *Proc. Camb. Phil. Soc.* **1926**, *23*, 542; (b) E. Fermi, *Zeit. Phys.* **1928**, *48*, 73.
- (18) C. F. von Weizsäcker, *Zeit. Phys.* **1935**, *96*, 431.
- (19) (a) J. C. Slater, *Phys. Rev.* **1951**, *81*, 385; (b) J. C. Slater, *Phys. Rev.* **1951**, *82*, 538; (c) J. C. Slater, *Phys. Rev.* **1953**, *91*, 52.
- (20) P. Hohenberg, W. Kohn, *Phys. Rev. B* **1964**, *136*, 864.
- (21) W. Kohn, L. J. Sham, *Phys. Rev. A* **1965**, *140*, 1133.

-
- (22) S. Kurth, J. P. Perdew, *Int. J. Quantum Chem.* **2000**, *77*, 814.
- (23) J. P. Perdew, K. Schmidt, in: *Density Functional Theory and Its Applications to Materials*, V.E. van Doren, K. van Alsenoy, P. Geerlings eds., American Institute of Physics, **2001**.
- (24) J. C. Slater, *Quantum Theory of Molecules and Solids*, McGraw-Hill: New York, **1974**.
- (25) (a) M. Ernzerhof, K. Burke, J. P. Perdew, in: *Recent Developments and Applications in Density Functional Theory*, J. M. Seminario ed., Elsevier: Amsterdam, **1996**; (b) M. Ernzerhof, J. P. Perdew, K. Burke, in: *Density Functional Theory*, R. Nalewajski, ed., Springer-Verlag: Berlin, **1996**.
- (26) U. von Barth, *Chemica Scripta* **1986**, *26*, 449.
- (27) (a) D. C. Langreth, M. J. Mehl, *Phys. Rev. B* **1983**, *28*, 1809. (b) J. P. Perdew, K. Burke, M. Ernzerhof, *Phys. Rev. Lett.* **1996**, *77*, 3865; (c) J. P. Perdew, *Phys. Rev. Lett.* **1985**, *55*, 1665.
- (28) J. P. Perdew, *Chem. Phys. Lett.* **1979**, *64*, 127.
- (29) P. R. T. Schipper, O. V. Gritsenko, E. J. Baerends, *Phys. Rev. A* **1998**, *57*, 1729.
- (30) (a) A. D. Becke, *J. Chem. Phys.* **1993**, *98*, 5648; (b) C. Lee, W. Yang, R. G. Parr, *Phys. Rev. B* **1988**, *37*, 785.
- (31) J. C. Slater, *Phys. Rev.* **1930**, *36*, 57.
- (32) S. F. Boys, *Proc. Roy. Soc. A* **1950**, *200*, 542.
- (33) See for instance: T. Helgaker, P. R. Taylor, *Modern Electronic Structure Theory, Part II*, D. Yarkony ed., World Scientific **1995**.
- (34) W. J. Hehre, R. F. Stewart, J. A. Pople, *J. Chem. Phys.* **1969**, *51*, 2657.
- (35) W. J. Hehre, R. Ditchfield, J. A. Pople, *J. Chem. Phys.* **1972**, *56*, 2257.
- (36) M. J. Frisch, J. A. Pople, J. S. Binkley, *J. Chem. Phys.* **1984**, *80*, 3265.
- (37) S. Huzinaga, *J. Chem. Phys.* **1965**, *42*, 1293.
- (38) H. Partridge, *J. Chem. Phys.* **1989**, *90*, 1043.
- (39) A. D. McLean, G. S. Chandler, *J. Chem. Phys.* **1980**, *72*, 5639.
- (40) T. H. Dunning, *J. Chem. Phys.* **1971**, *55*, 716.
- (41) (a) T. H. Dunning, *J. Chem. Phys.* **1989**, *90*, 1007; (b) A. K. Wilson, T. van Mourik, T. H. Dunning, *J. Mol. Struct.* **1996**, *388*, 339; (c) R. A. Kendall, T. H. Dunning, R. J. Harrison, *J. Chem. Phys.* **1992**, *96*, 6796.
- (42) (a) A. Schaefer, H. Horn, R. Ahlrichs, *J. Chem. Phys.* **1992**, *97*, 2571; (b) A. Schaefer, C. Huber, R. Ahlrichs, *J. Chem. Phys.* **1994**, *100*, 5829.

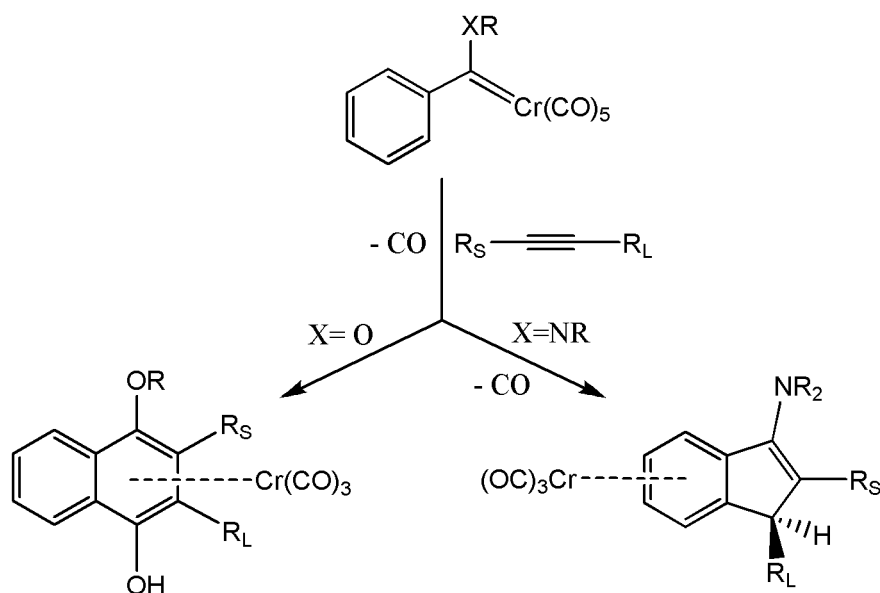
- (43) I. Mayer, *Int. J. Quantum Chem.* **1983**, *23*, 341.
- (44) S. F. Boys, F. Bernardi, *Mol. Phys.* **1970**, *19*, 553.
- (45) P. Salvador, M. Duran, *J. Chem. Phys.* **1999**, *111*, 4460.
- (46) J. C. Phillips, L. Kleinman, *Phys. Rev.* **1959**, *116*, 287.
- (47) (a) S. Huzinaga, A. A. Cantu, *J. Chem. Phys.* **1971**, *55*, 5543; (b) S. Huzinaga, D. McWilliams, A. A. Cantu, *Adv. Quantum Chem.* **1973**, *7*, 187.
- (48) M. Krauss, W. J. Stevens, *Annu. Rev. Phys. Chem.* **1984**, *35*, 357.
- (49) (a) T. Schlick, *Rev. Comput. Chem.* **1992**, *3*, 1; (b) H. B. Schlegel, *Adv. Chem. Phys.* **1987**, *67*, 249; (c) H. B. Schlegel, in: *Modern Electronic Structure Theory, Part I*, D. Yarkony ed., World Scientific: New York **1995**, p. 459; M. L. McKee, M. Page, *Rev. Comput. Chem.* **1993**, *4*, 35.
- (50) G. Fogarasi, X. Zhou, P. W. Taylor, P. Pulay, *J. Am. Chem. Soc.* **1992**, *114*, 8191.
- (51) M. J. S. Dewar, E. F. Healy, J. J. P. Stewart, *J. Chem. Soc., Faraday Trans. 2* **1984**, *80*, 227.
- (52) D. A. Liotard, *Int. J. Quantum Chem.* **1992**, *44*, 723.
- (53) Y. Abashkin, N. Russo, *J. Chem. Phys.* **1994**, *100*, 4477.
- (54) R. Czerminski, R. Elber, *Int. J. Quantum Chem. Symp.* **1990**, *24*, 167.
- (55) S. Bell, J. S. Crighton, *J. Chem. Phys.* **1984**, *80*, 2464.
- (56) C. Peng, H. B. Schlegel, *Isr. J. Chem.* **1993**, *33*, 449.
- (57) C. González, H. B. Schlegel, *J. Chem. Phys.* **1991**, *95*, 5853.

CHAPTER 3

**DÖTZ
BENZANNULATION
REACTION:
HETEROATOM AND
SUBSTITUENT EFFECTS
IN FISCHER CARBENE
COMPLEXES**

Since their discovery by Fischer and Maasböl in 1964,¹ Fischer metal-carbene complexes of general formula $(\text{CO})_5\text{M}=\text{C}(\text{X})\text{R}$ ($\text{M} = \text{Cr}, \text{Mo}, \text{W}$; $\text{X} =$ a π -donor substituent; and $\text{R} =$ a saturated alkyl or unsaturated alkenyl, alkynyl, or aryl group) have developed from exotic organometallic complexes to useful reagents with an extensive, versatile, rich, and fascinating chemistry.^{2,3} In this species, the $\text{Cr}=\text{C}_{\text{carbene}}$ bonding mechanism is similar to that of a metal-carbonyl bond; the carbene donates in a σ fashion to the metal and the metal back-donates to the unoccupied π -orbitals of carbene.³ However, at variance with the $\text{Cr}-\text{CO}$ bonding, donation is larger than back-donation in the $\text{Cr}=\text{C}_{\text{carbene}}$ bond.⁴ As a result, there is a lack of charge on the carbene carbon atom which suggests a $[(\text{CO})_5\text{Cr}^{\delta-}-\text{C}^{\delta+}(\text{X})\text{R}]$ electronic distribution and partially explains the electrophilic nature of this atom in Fischer carbenes.⁵ In these complexes, the substituent X acts as a π -donor stabilizing the electron-deficient carbene atom, while the low-valent metal center is stabilized by π -acceptor substituents such as CO .^{4,6} The $\text{Cr}=\text{C}-\text{X}$ group forms a weak 3-center-4-electron bond.⁶ The first applications assisted by these group 6 heteroatom stabilized carbene complexes started around 1970s⁷ and nowadays, after four decades, the Fischer carbenes chemistry has reached what could be considered a situation of creative maturity. These fascinating complexes are potential precursors in the preparation of many functionalized carbo- and heterocycles through thermal and photochemical procedures.⁸⁻¹⁰

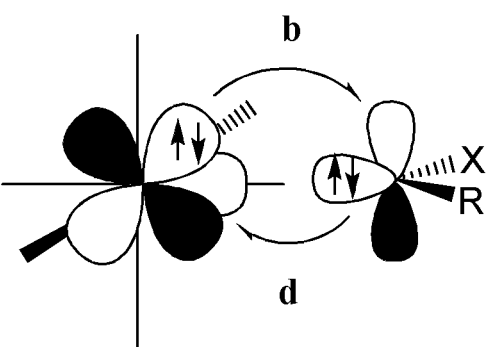
First reported in 1975,¹¹ the so-called Dötz benzannulation reaction can be regarded as the most important and synthetically useful of the Fischer carbene reactions (see refs. 12-14 for recent reviews). This reaction represents an efficient synthetic method that gives easy access to relevant antibiotics,¹⁵ natural products,¹⁶ and biologically interesting molecules.¹⁷ It consists in an ensemble between an α,β -unsaturated pentacarbonyl chromium carbene complex with an alkyne providing phenol (see Scheme 14, left side product) or indene derivatives (see Scheme 14, right side product). Although these six- and/or five-membered ring (5-MR) products of the Dötz reaction are the most frequently observed, up to twenty-one different structural types of species have been isolated and characterized in Dötz reactions.^{14,18} Among them one can find quinones, indenones, furans, cyclobutenones or cyclooctatrienones.^{19,20}



Scheme 14. Dötz benzannulation against cyclopentannulation as the most common chromium-mediated cycloaddition reactions in Fischer carbene complexes, where R are alkyl substituents and R_S and R_L are the small and the large alkyl or aryl substituent of alkyne, respectively.

Relatively minor modifications to the structure of the Fischer carbene, the alkyne or the reaction conditions can dramatically alter the product distribution of the reaction.^{12-14,21} For instance, higher temperatures, smaller alkyne concentrations, presence of non coordinating solvents, and the use of terminal instead of internal alkynes and more sterically hindered alkynes as well as heavier transition metals of group VI are all factors that favor indene products relative to phenols.^{10,12-14,18,21} Moreover, a very important characteristic is the π -donor character of the X substituent in the Fischer carbene. Thus, when amino groups are used instead of alkoxy ligands the ratio of cyclopentannulation over benzannulation increases.^{13,14,22} This is related presumably to the better π -donor capacity of nitrogen rather than oxygen as can be seen in Scheme 15 (values for the $X = N(CH_3)_2$ species were not included in the study of ref. 4). Some of us showed that, as expected from the Dewar-Chatt-Ducanson model,²³ the stronger the π -donor character of the X group, the smaller the back-donation from the metal to the carbene is as can be seen from the values of Scheme 15.^{3,4,24} As a result of the reduced carbene to metal back-donation in strong π -donors, the back-donation from the metal to the CO ligands becomes larger making the Cr–CO bonds stronger and the insertion of the CO in the new ring more difficult.²⁵ This is referred to as the heteroatom

effect and it concurs with the experimental observation that less electron-poor chromium carbenes require harsher conditions for the initial decarbonylation step of the Dötz reaction.^{13,14} However, during the last decade many cases where this explanation is not enough to distinguish why cyclopentannulation is favored over benzannulation have been reported.^{10,26-29} Values of back-donation in Scheme 15 also indicate that phenylcarbenes have slightly larger back-donation than vinylcarbenes ($\text{CH}=\text{CH}_2$ is somewhat better π -donor than Ph ³⁰). Indeed, the **R** group is also an important factor that can have an enormous influence in the product distribution. For instance, it has been found that dialkylamino arylcarbenes give exclusively indenenes^{13,21,27,31} whereas dialkylamino vinylcarbenes yield phenols and cyclohexadienones.^{27,31}



The diagram illustrates the interaction between a Fischer carbene complex and a metal center. The metal center is represented by a vertical line with a horizontal line extending to the left. The carbene complex is shown to the right, with a carbon atom bonded to a metal atom (represented by a vertical line). The carbon atom is also bonded to a group X (dashed bond) and a group R (solid wedge bond). Two curved arrows, labeled 'b' and 'd', indicate the direction of electron flow: 'b' shows donation from the carbene lone pair to the metal, and 'd' shows back-donation from the metal to the carbene's empty p-orbital. The metal has two d-orbitals shown as lobes with arrows indicating their orientation.

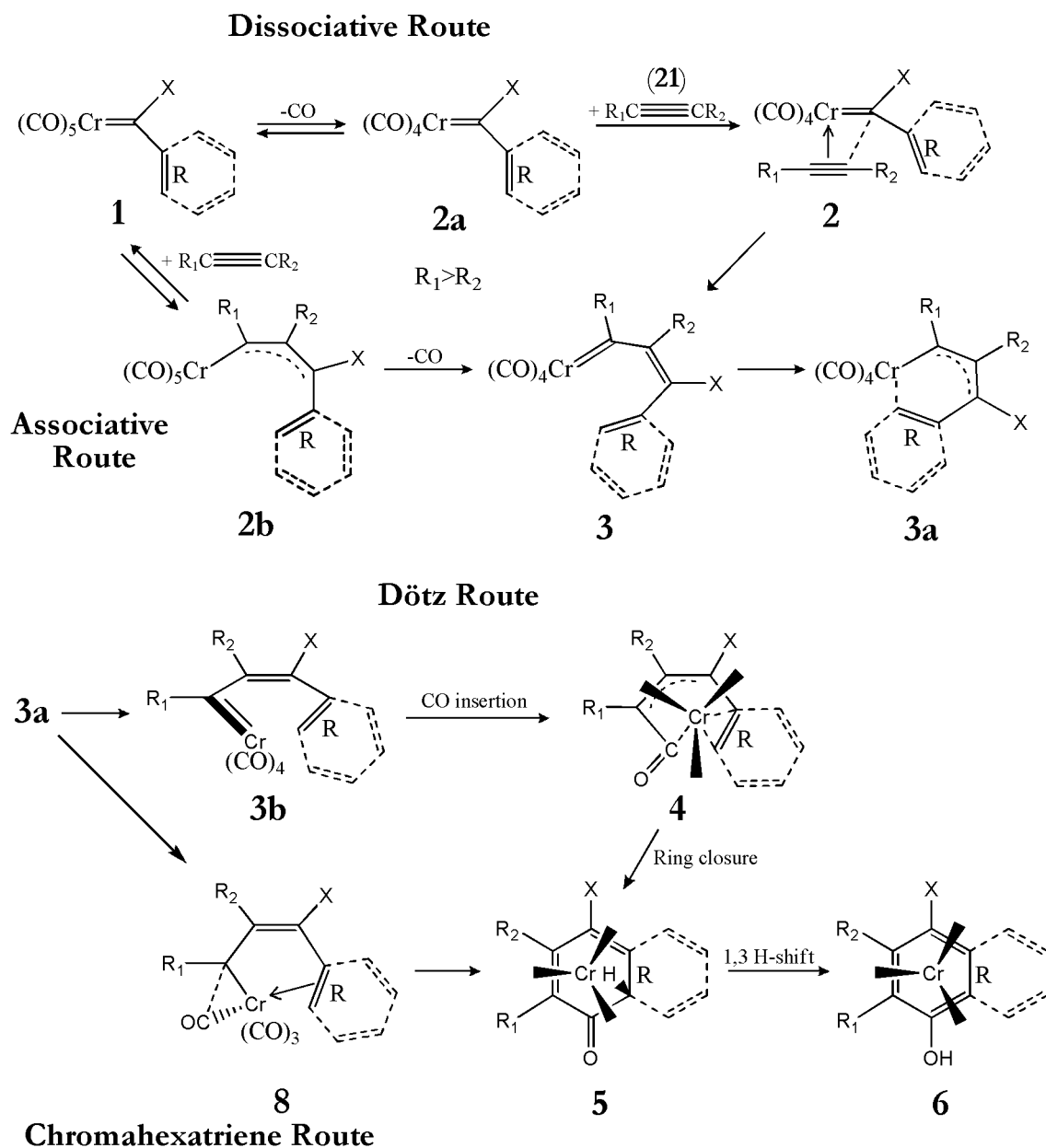
R=	H	CH=CH ₂	Ph
OH	0.499 <i>0.255</i>	0.507 <i>0.215</i>	0.503 <i>0.249</i>
OCH ₃	0.528 <i>0.244</i>	0.522 <i>0.206</i>	0.513 <i>0.243</i>
NH ₂	0.501 <i>0.214</i>	0.499 <i>0.198</i>	0.480 <i>0.229</i>
NHCH ₃	0.511 <i>0.218</i>	0.502 <i>0.191</i>	0.486 <i>0.214</i>

Scheme 15. Role of heteroatom effect on electron flow in Fischer carbenes. Data of donation and back-donation (italics) in electrons is taken from ref. 4.

A deeper understanding of the reaction mechanisms that direct the formation of the different products obtained in the Dötz reaction would be highly desirable in order to achieve a better control of the reaction outcome.^{5,32,33} To reach this knowledge from experiments only is rather difficult because the rate-limiting step of this process

involves CO loss to open a coordination site for the alkyne to bind. Then, once the alkyne is bound, very fast ring closure takes place, which makes characterization of reaction intermediates very complicated. The use of computational tools in such cases is highly recommended to help elucidating the reaction mechanisms.^{34,35} Indeed, some mechanistic details of this paradigmatic reaction have already been investigated from a theoretical point of view in the past by our group³⁶⁻³⁸ and by others.^{39,40}

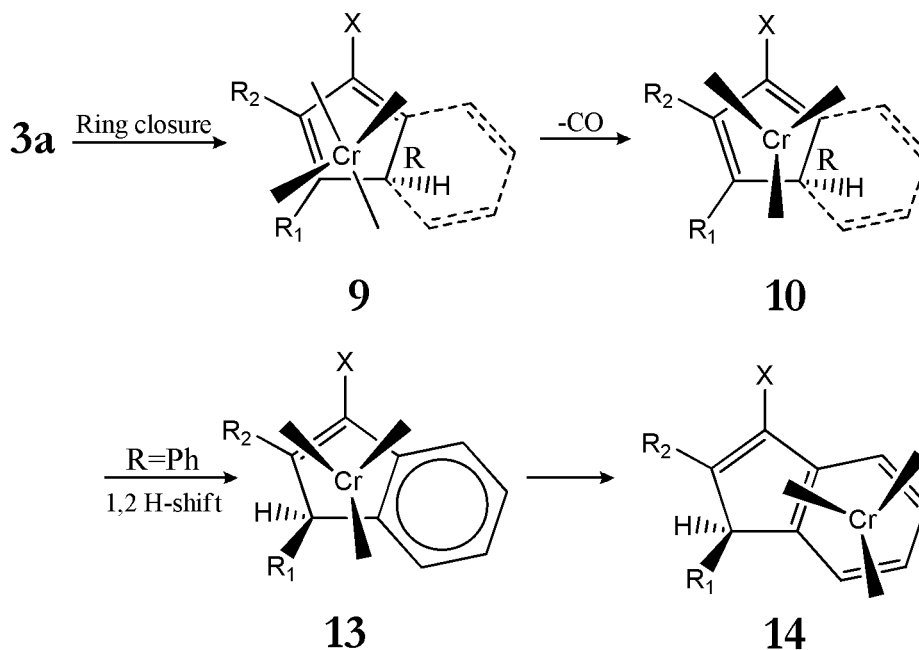
Scheme 16 shows the most viable reaction mechanism proposals which were explored in these previous works. Basically, the reaction begins with CO dissociation and alkyne insertion into the metal sphere at the vinylcarbene **1**. It is well documented that this thermally reversible stage is the rate-limiting step^{20,41} in the Dötz reaction. Depending on the order of events, it has been postulated that an initial CO dissociation in **1** leads to the unsaturated 16-electron species **2a** and subsequent alkyne coordination (**2**) and insertion into the carbene metal bond (**3**) produces an α,β -unsaturated vinyl- or phenylcarbene **3a** (Dissociative Route).^{42,43} Another possibility for this initial part of the reaction is alkyne insertion in **1** leading to the 19-electron intermediate **2b** and by CO dissociation, the reaction also results in species **3** (Associative Route).^{44,45} In the central part of the reaction, under the Dötz benzannulation mechanistic proposal, there is first a rearrangement of carbene **3a** into **3b** (bending of Cr-C(α) bond to place one of CO ligands closer to α -carbon) followed by a CO insertion to form **4**, an η^3 -vinylketene (or phenylketene) complex. Then, electrocyclic ring closure in **5** followed by tautomerization generates **6**, an η^6 -benzenic (or naphthalenic) Cr(CO)₃ complex (see Scheme 16). A decade ago, it was proposed that from vinylcarbene **3a**, the π -interaction with the ending C=C double bond of the carbene affords a chromahexatriene complex that allows an earlier C(α)-CO interaction in **8** which will lead to the η^4 -cyclohexadienone **5** in the next step.³⁶ A third possibility suggested by Casey,⁴⁶ where the metallation of **3a** occurs directly and then the CO insertion takes place originating a chromacycloheptadienone species, will not be discussed here because for all our previous^{34,47} and present calculations this reaction mechanism is significantly much higher in energy than the aforementioned proposals.



Scheme 16. Benzannulation reaction mechanisms of Fischer carbenes.

The reaction mechanisms leading to the 5- and 6-MRs formation match each other until complex **3a** is reached. From this point there is a ramification and 6- or 5-MRs are obtained depending on the incorporation or not of carbon monoxide into the ring. Scheme 17 illustrates the 5-MR competition reaction that we also broach in this work. By closing the ring (**9**) and subsequent removal of CO, indene **10** product is obtained. For phenylcarbenes, 1,2 H-shift to a more stabilized position, which can be assisted or not by the solvent, leads to **13**^{9,10,28,48} and finally a haptotropic rearrangement

results in the formation of **14** as the final product. Recent advances about the versatility of both reactions⁴⁹ have prompted us to investigate the reaction mechanisms for the formation of phenols and indenenes in the Dötz reaction.



Scheme 17. Cyclopentannulation reaction in competition for Fischer carbene **3a**.

Therefore, we have carried out a theoretical mechanistic investigation of the reaction pathways leading to the two more usual products of the Dötz reaction (phenols and indenenes) by using density-functional theory (DFT) on representative substituents (**R** = CH=CH₂, Ph) and heteroatom ligands (**X** = OH, NH₂, OCH₃, N(CH₃)₂) of Fischer carbenes with a twofold purpose: (i) to investigate the effect of heteroatom and the substituent in these reaction mechanisms, see Schemes 16 and 17, and (ii) to discuss the origin of the experimental product distributions found in these species. Gleichmann, Dötz, and Hess (GDH)³⁹ investigated the 6-MR formation reaction assisted by Fischer carbenes having **X** = OH and NH₂ and **R** = CH=CH₂ and Ph. However, they analyzed only the Dötz route in Scheme 16. So, in this work we extend their previous study by including four new systems (the species with **X** = OCH₃ and N(CH₃)₂) and by analyzing two new reaction pathways: the chromahexatriene route and the cyclopentannulation route. In that way, we expect to get a deeper understanding of the reasons that explain the product distributions obtained experimentally.

3.2 Computational Methodology.

We have used the Gaussian03 computational package⁵⁰ for modeling the gas-phase reaction mechanisms reported here. We have employed the hybrid density-functional B3LYP⁵¹ to perform geometry optimizations and compute energy differences. The B3LYP method has been shown to be suitable for calculating reaction mechanisms in chromium metal complexes.⁵² A mixed basis sets consisting in 6-31G(d,p)⁵² for C, O, N, and H atoms and a Wachters' basis set⁵³ of the type (14s9p5d3f)/[8s4p3d1f] using the *df*-expanded contraction scheme (62111111/3312/311/3) for chromium was employed. Table A1 of the Appendix shows that the mixed basis set used gives the same quality of results as 6-311G(d,p) basis set. Stationary points were located using the Berny algorithm.⁵⁴ For transition states (TSs) where the potential energy surface (PES) was not explored yet, we utilized the SQTN method.⁵⁵ Frequency calculations indicated that we got the correct stationary points characterized by the number of negative eigenvalues of its analytic Hessian matrix (this number is zero for minima and one for any true TS). We also checked that imaginary frequencies exhibit the expected motion and TSs were connected to the corresponding minima by following the minimum energy path through intrinsic reaction coordinate (IRC) calculations.⁵⁶ We are reporting here, along with enthalpy values, Gibbs free-energies at 298 K obtained by adding zero-point energies (ZPE), thermal corrections, and entropic terms into electronic energies for all species. Entropy effects are especially important in the initial part of the reaction where dissociation processes take place and they become relatively constant for the central part. We considered only closed-shell states (previous calculations on metal carbenes **1** and **3** showed that triplet states are far away of singlet ones by more than 15 kcal·mol⁻¹ in all cases). Relativistic effects were ignored in our study because it was demonstrated that they are very small in chromium Fischer carbene complexes.⁵⁷ Finally, solvent effects were not treated in this work because the Dötz reaction is carried out in many cases in rather nonpolar solvents such as heptane, benzene, ethers or tetrahydrofuran, although, in other cases, relatively polar solvents such as acetonitrile have also been used.

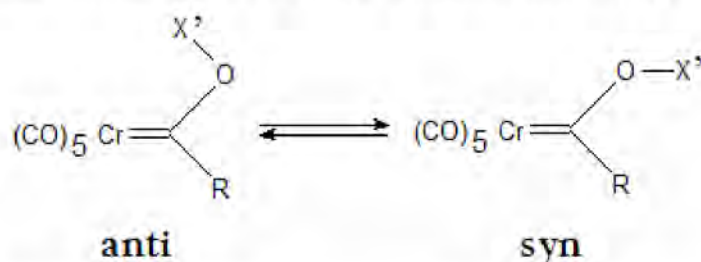
3.3 Results and Discussion.

This section is divided as follows: first, the results for the initial part of the reaction (**1** → **3a**) are presented; and second, we discuss the product distributions in cycloannulation reactions with special emphasis on the three reaction mechanisms analyzed (Schemes 16 and 17).

3.3.1. Initial Part of the Reaction.

Pentacarbonylchromium carbenes (**1**) as starting points of this reaction have been discussed in terms of reactivity and bonding in the literature.^{4,6,58} In the present work, we have performed a conformational study for the studied alkoxy Fischer carbenes following the previous work done for the [pentacarbonyl(hydroxyvinyl)chromium(0)]carbene.³⁷ Alkoxy metal carbenes present two conformations: *anti* (alkoxy ligand towards Cr(CO)₅ in a staggered position with respect to the carbonyls) and *syn* (alkoxy ligand pointing to the **R** substituent). Table 1 shows the calculated Gibbs free-energies for both kinds of isomers. Clearly, the *anti*-conformer prevails over *syn*-orientation as it was already found experimentally for the methoxy(methyl)carbene complex.⁵⁹ Fernández and coworkers⁶⁰ have demonstrated that this bias in the case of X' = CH₃ is due to a two-electron stabilizing donation from the σ_{CH} orbital of the alkoxy group to the π*_{CO} of the closer CO ligand and back-donation from the π_{CO} orbital to the σ*_{CH} in the *anti*-isomer as well as to the stronger destabilizing repulsion between the OX' group and the **R** substituent present in the *syn*-conformer. Both experimental data and theoretical calculations show that there is a free rotation around the C_{carbene}-OX' bond under mild conditions with energy barriers of about 11-14 kcal·mol⁻¹.^{37,59,60} There is also an almost free rotation around the Cr=C_{carbene} bond where the staggered conformation (the plane of the carbene bisects two carbonyl's plane) is somewhat more stable than the eclipsed conformation.^{37,57,61}

Table 1. Relative Gibbs free-energies (ΔG_{298}^0 ,^a kcal·mol⁻¹) of *anti* and *syn* conformations of hydroxycarbenes studied here calculated at the B3LYP/(Wachters' basis, 6-31G(d,p)) level of theory.



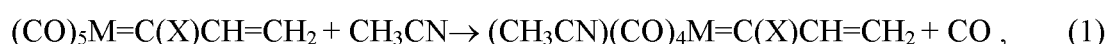
X' = H		X' = CH ₃	
R = CH=CH ₂	3.6	R = CH=CH ₂	4.8
R = Ph	2.9	R = Ph	2.1

^a Values computed as $\Delta G = G_{\text{syn}} - G_{\text{anti}}$.

We have analyzed both the dissociative and associative scenarios shown in Scheme 16 (*vide supra*). In the case of the dissociative pathway, where carbon monoxide loss takes place, we explored all the possible intermediates, *i.e.*, elimination of *trans*-CO ligand with respect to the carbene or the four *cis*-CO positions. We found that removing a *trans*-CO is higher in energy by ca. 7 kcal·mol⁻¹ (in average) than *cis*-carbon monoxides in agreement with experimental and theoretical observations.^{18,37,39,62} Two square pyramidal conformers result from *cis*-elimination depending on whether the CO removed was closed to the heteroatom (**2a-1**) or the **R** substituent (**2a-2**) (see Figure 5). The energy difference between **2a-1** and **2a-2** isomers is in (CO)₄Cr=C(**X**)CHCH₂ carbenes 3.9, 2.3, 2.2 and 0.4 kcal·mol⁻¹ for **X** = OH, NH₂, OCH₃ and N(CH₃)₂, respectively, whereas for (CO)₄Cr=C(**X**)Ph it corresponds to 5.2, 4.0, 2.4 and 3.9 kcal·mol⁻¹ in the same order of **X** ligands and interestingly, differences between alkyl- and arylaminocarbenes being bigger (1.7 – 3.5 kcal·mol⁻¹) than for the corresponding alkoxy-carbenes (less than 1.3 kcal·mol⁻¹). The dissociation leading to **2a-2** is more favorable because of the agostic interaction formed between the C–H bond of the vinyl group (or phenyl for alkoxy-carbenes) and the vacant side in the chromium Fischer carbene complex,³⁷ except for phenylaminocarbenes where this interaction is not well achieved. Thus, taking into account this second isomer of **2a**, C–H bond distance increases by about 0.015 – 0.032 Å when going from **1** to **2a-2** depending on the Fischer carbene considered. This agostic interaction is responsible for a gain of stability,

which is estimated to be about 5 – 10 kcal·mol⁻¹ from the values obtained in similar complexes,⁶³ thus explaining the higher stability of species **2a-2**. The X-ray data of a [tetracarbonyl(methoxyaryl)chromium(0)]carbene complex equivalent to **2a-2** was reported by Dötz and coworkers in 1997.⁶⁴ Table 2 gathers the Gibbs' free-energies (enthalpies in parenthesis) and energy barriers for the dissociation process **1** → **2a-2**. For the (CO)₅Cr=C(OCH₃)Ph complex, the experimental value⁴² for the dissociation enthalpy and entropy of 26 ± 0.5 kcal·mol⁻¹ and 6 ± 1.5 cal (K mol)⁻¹ is in good agreement with our 23.5 kcal·mol⁻¹ and 7.0 cal (K mol)⁻¹ values. As GDH found for **X** = OH and NH₂,³⁹ our results also show that substitution of **X** = OX' by **X** = NX'₂ has a minor effect (change of 1 – 2 kcal·mol⁻¹ in ΔG or ΔH) on the dissociation energy of *cis*-CO. The so-called heteroatom effect is clearly seen in the dissociation of *trans*-CO that increases in the expected order of increasing π-donor character of the **X** groups: OH < OCH₃ < NH₂ < N(CH₃)₂ (with the only exception of the change between OCH₃ and NH₂ in the ordering for **R** = Ph) but not in the *cis*-CO dissociation. It is worth mentioning that substitution of H by CH₃ in alkoxy **X** ligands reduces the dissociation energy by about 6 kcal·mol⁻¹. It is quite likely that a bulkier group in the alkoxy substituent helps the vinyl or the phenyl **R** group to be closer to the metal and form stronger agostic interactions (for instance, the Cr...H_{phenyl} bond in (CO)₄Cr=C(**X**)Ph changes from 2.524 to 2.312 Å when going from **X** = OH to **X** = OCH₃). Note also that dissociation is somewhat easier in phenylcarbenes than in vinylcarbenes, which in this case concurs with the fact that vinylcarbenes are stronger π-donors than phenylcarbenes. Unlike GDH who did not find TSs for these dissociation processes,³⁹ we have located the TSs for the eight *cis*-CO dissociation processes. The trends observed in energy barriers are similar to those found for the dissociation energies (Table 2). The most important difference due to the heteroatom effect in the energy required to surmount energy barriers is now more evident as Gibbs' free-energy and enthalpy barriers to withdraw carbon monoxides from alkoxy-carbenes are 5 – 10 kcal·mol⁻¹ larger than those of aminocarbenes. The energy barriers required to remove out one *cis*-CO from chromium in these carbenes follows the sequence: N(CH₃)₂ < NH₂ < OH ≈ OCH₃. This result does not conform the experimental observation that stronger π-donors in chromium carbenes require harsher conditions for the initial decarbonylation step of the Dötz reaction.^{13,14} For this reason, we have calculated *cis*-CO dissociation energies in the case of (CO)₅Cr=C(**X**)CH=CH₂ for **X** = OH and NH₂ with different methods and

basis sets. The results collected in Table A1 of the Appendix confirm that differences in dissociation Gibbs' free-energies are less than 2 kcal·mol⁻¹ when going from **X** = OH to **X** = NH₂. Apparently, this discrepancy between experimental and theoretical results is solved when one considers the presence of donating solvents such as tetrahydrofuran, acetonitrile or ether. In this case, the *cis*-CO–solvent exchange process clearly favors dissociation in Fischer carbenes having the stronger π-donors as demonstrated by GDH.³⁹ We have confirmed this result by calculating the Gibbs' free-energy of the dissociation process:



for **X** = OH and NH₂. We have found that this exchange process requires 12.7 kcal·mol⁻¹ for **X** = OH and 14.5 kcal·mol⁻¹ for **X** = NH₂. The endergonicity of this process indicates that the interaction of (CO)₄M=C(**X**)CH=CH₂ with CO is larger than with CH₃CN as one could expect from the higher σ-donor plus π-acceptor character of the former.⁶⁵ The difference in the interaction energy between CO and CH₃CN coordination increases in less electron-poor carbenes, *i.e.*, when going from **X** = OH to NH₂.

Table 2. Reaction free-energies (ΔG_{298}^0) and activation barriers ($\Delta G_{298}^{\ddagger}$) for all steps in the initial stages of the reaction calculated at the B3LYP/(Wachters' basis, 6-31G(d,p)) level (enthalpy values, ΔH_{298}^0 and $\Delta H_{298}^{\ddagger}$, are in parenthesis). For notation of the structures, see Scheme 16. All energies are in kcal·mol⁻¹.

Route	Step	ΔG_{298}^0 (ΔH_{298}^0)		TS	$\Delta G_{298}^{\ddagger}$ ($\Delta H_{298}^{\ddagger}$)	
		X = OH	X = NH ₂		X = OH	X = NH ₂
	R = CH=CH ₂					
Ds	1 → 2a	19.2 (30.3)	19.0 (31.6)	TS(1 → 2a)	31.3 (35.1)	26.1 (32.1)
	2a → 21	3.8 (-4.7)	4.2 (-3.3)			
	21 → 2	0.9 (-1.6)	-3.1 (-6.2)			
	2 → 3	-29.7 (-30.0)	-25.5 (-25.6)	TS(2 → 3)	4.5 (2.3)	10.1 (8.2)
As	1 → 20	7.5 (1.2)	3.1 (-0.4)			
	20 → 2b	-24.0 (-29.4)	-19.9 (-25.7)	TS(20 → 2b)	34.2 (29.1)	31.5 (28.0)
	2b → 3	10.8 (22.2)	11.3 (22.7)	TS(2b → 3)	23.2 (26.6)	25.2 (27.6)
	3 → 3a	0.5 (1.5)	1.7 (0.1)			

		X = OCH ₃	X = N(CH ₃) ₂			X = OCH ₃	X = N(CH ₃) ₂
Ds	1 → 2a	15.2 (26.3)	15.0 (26.2)	TS(1 → 2a)		32.1 (36.0)	22.0 (26.8)
	2a → 21	6.1 (-0.2)	6.0 (0.2)				
	21 → 2	4.0 (0.2)	2.2 (-2.4)				
	2 → 3	-33.4 (-34.2)	-31.4 (-31.4)	TS(2 → 3)		3.9 (1.8)	11.6 (10.0)
As	1 → 20	9.9 (3.9)	5.5 (-0.1)				
	20 → 2b	-30.8 (-36.1)	-22.5 (-28.0)	TS(20 → 2b)		35.8 (35.6)	32.0 (31.8)
	2b → 3	12.8 (24.2)	8.8 (20.7)	TS(2b → 3)		23.0 (26.1)	25.5 (27.9)
	3 → 3a	-0.1 (-2.1)	2.7 (1.4)				
R = Ph							
		X = OH	X = NH ₂			X = OH	X = NH ₂
Ds	1 → 2a	15.6 (27.6)	17.0 (28.8)	TS(1 → 2a)		29.5 (33.3)	24.3 (29.6)
	2a → 21	4.1 (-3.8)	5.6 (-1.1)				
	21 → 2	4.4 (0.6)	-0.4 (-5.4)				
	2 → 3	-32.6 (-32.8)	-28.4 (-28.1)	TS(2 → 3)		4.8 (3.1)	10.6 (9.1)
As	1 → 20	8.3 (1.1)	5.7 (-1.2)				
	20 → 2b	-23.4 (-27.4)	-19.9 (-23.5)	TS(20 → 2b)		42.1 (43.5)	37.3 (37.4)
	2b → 3	6.7 (17.9)	7.9 (29.3)	TS(2b → 3)		27.4 (29.1)	28.1 (29.3)
	3 → 3a	2.4 (1.1)	2.7 (2.0)				
X = OCH ₃ X = N(CH ₃) ₂							
Ds	1 → 2a	11.2 (23.5)	10.5 (22.0)	TS(1 → 2a)		25.2 (31.1)	18.7 (22.8)
	2a → 21	6.0 (-0.1)	6.0 (-1.4)				
	21 → 2	4.1 (0.5)	7.1 (3.2)				
	2 → 3	-25.4 (-28.7)	-32.3 (-32.2)	TS(2 → 3)		5.2 (2.3)	10.9 (9.0)
As	1 → 20	6.5 (0.5)	6.0 (-1.1)				
	20 → 2b	-24.2 (-27.7)	-22.2 (-26.6)	TS(20 → 2b)		42.5 (43.3)	31.4 (32.4)
	2b → 3	13.6 (22.4)	7.5 (19.2)	TS(2b → 3)		23.7 (26.0)	19.9 (22.2)
	3 → 3a	-6.5 (-6.1)	3.1 (2.0)				

Once **2a-2** is formed, the acetylene molecule approaches to the metal complex forming the van der Waals complex **21** (see Figure 5) and preactivating the following scenario of insertion. This complex **21** is stabilized with respect to **2a-2** and acetylene

from -4.7 to 0.2 kcal·mol⁻¹ in terms of enthalpy, although it is thermodynamically unstable according to Gibbs' free-energy values (from 3.8 to 6.1 kcal·mol⁻¹). This chromium – acetylene interaction is generally a little more favored for alkoxy- than aminocarbenes and also for vinyl- than phenylcarbenes. Subsequent coordination of acetylene leads to species **2**. Note the hydrogen twisting to a *syn*-position in **2**; some time ago *anti* → *syn* conversion before loss of CO was reported.⁶⁶ Therefore, the substitution of CO by C₂H₂ in complex **1** to give **2** is an endothermic and endergonic process indicating that CO is a better σ -donor and π -acceptor than acetylene. Finally, **2** evolves to **3** through a chromacyclobutadiene-like **TS(2→3)** structure. The barrier associated to this transformation is relatively low and increases by $5 - 7$ kcal·mol⁻¹ from alkoxy to aminocarbenes (as expected more electron deficient C_{carbene} atoms insert acetylene easier).

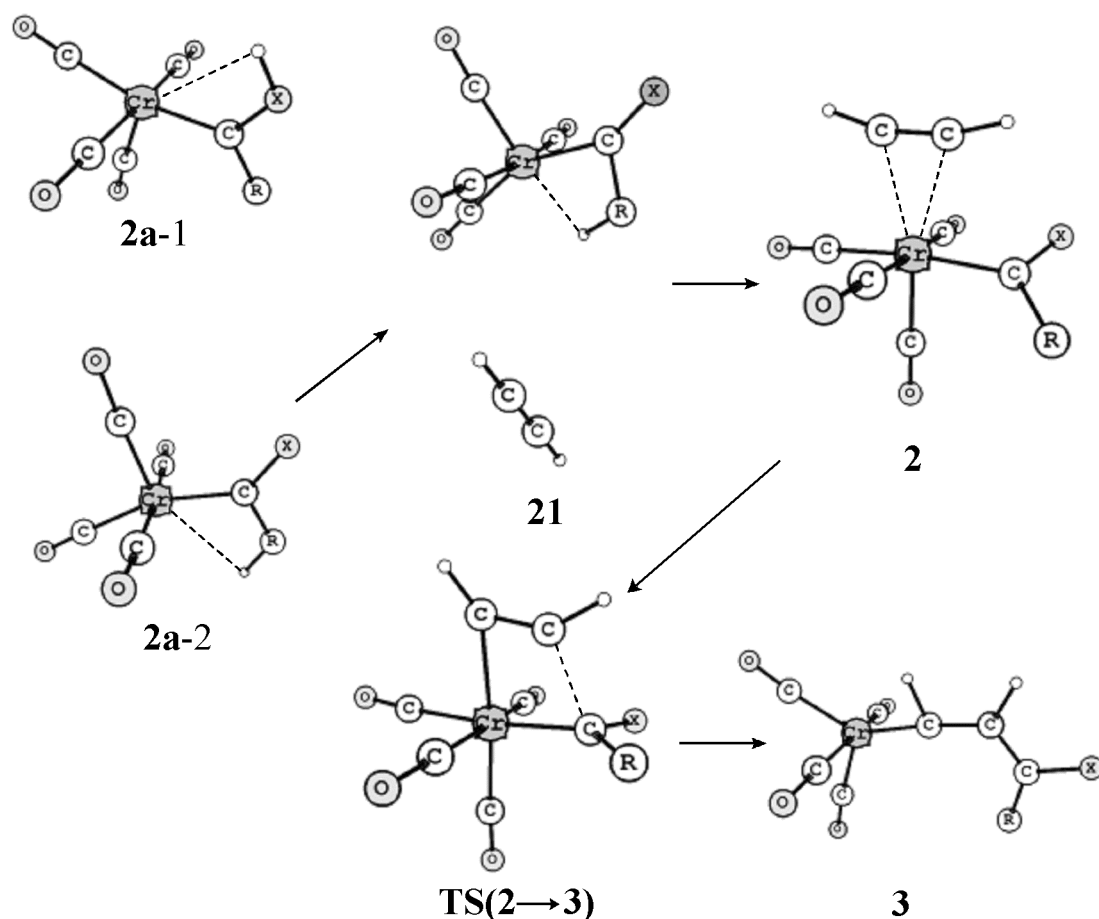


Figure 5. Sketched acetylene insertion in Cr(CO)₄ carbenes for the dissociative route when X = OH, OCH₃, NH₂, N(CH₃)₂ and R = CHCH₂ and Ph. For **2a-1**, **2a-2** and **21** structures, H atoms are shown explicitly from X or R groups.

In the associative pathway, first thermodynamically unstable (basically for entropic reasons) structure **20** corresponding to the interaction between $\text{Cr}(\text{CO})_5$ -carbene **1** and weakly interacting acetylene is formed (see Figure 6). Direct insertion of acetylene from **20** through $\text{TS}(\mathbf{20} \rightarrow \mathbf{2b})$ leads to intermediate **2b**, which is the lowest minimum in energy for this initial part of the reaction in all cases. For the Fischer carbenes with $\mathbf{R} = \text{Ph}$, the Gibbs' free-energy and enthalpy barriers for the $\mathbf{20} \rightarrow \mathbf{2b}$ transformation are higher than those corresponding to the whole $\mathbf{2a} \rightarrow \mathbf{3}$ conversion, thus making this associative pathway unlikely for these cases. However, for $\mathbf{R} = \text{CH}=\text{CH}_2$ the TSs are less congested and differences between associative and dissociative pathways become smaller.⁴⁷ Indeed, in general, the dissociative pathway presents lower Gibbs' free-energy barriers but higher enthalpy barriers. Therefore, conclusions are less clear in this case, and the associative path may be perfectly operative. This is in line with the experimental finding that usually the Dötz reaction is first-order in carbene complex and zero-order in alkyne,^{42,43,67} as expected in a dissociative mechanism, although, depending on reaction conditions, the reaction can be bimolecular with a first-order dependence on both the carbene complex and the alkyne.⁴⁵ Finally, it is worth mentioning that the preference for the associative pathway increases for π -donor substituted alkynes.⁴²

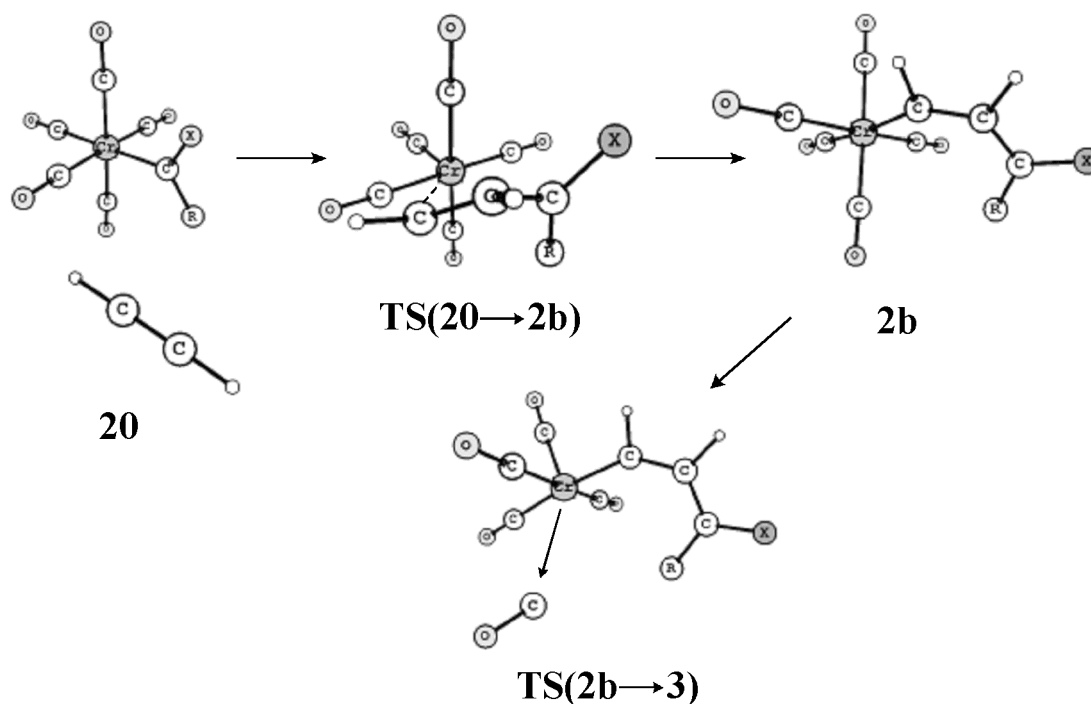


Figure 6. Sketched acetylene insertion in $\text{Cr}(\text{CO})_4$ carbenes for the associative route when $\mathbf{X} = \text{OH}$, OCH_3 , NH_2 , $\text{N}(\text{CH}_3)_2$ and $\mathbf{R} = \text{CHCH}_2$ and Ph.

Vinyl- or phenylcarbene **3** rearranges then into an agostic complex **3a** (*vide infra*, Figure 11) where the tail of **R** substituent interacts agostically with the chromium atom. This barrierless conversion is a slightly endothermic and endergonic process for most of the cases (see Table 2). Alkoxy-carbenes undergo more easily this transformation than aminocarbenes. Indeed the Cr–H and Cr–C(methylene) distances in **3a** are shorter for alkoxy-carbenes (1.909 and 2.426 ± 0.02 Å in average, respectively) than for aminocarbenes (1.934 and 2.441 ± 0.02 Å in average, respectively). This is especially true for the case of phenyl substituents. Thus, tetracarbonyl(hydroxyphenyl)chromium has a clear agostic interaction with the C(ε)-H bond: distances Cr–H, 2.060 Å, and Cr–C(arene) 2.655 Å; whereas for tetracarbonyl(aminophenyl)chromium the interaction is minor: distances Cr–H, 2.875 Å, and Cr–C(arene) 2.855 Å. This behavior is even more pronounced between tetracarbonyl(methoxyphenyl)chromium and tetracarbonyl(dimethylaminophenyl)-chromium where distances Cr–H and Cr–C(arene) are 2.091 and 2.650 Å against 3.022 and 2.892 Å, in that order of carbenes. Moreover, Cr(CO)₄-methoxyphenyl carbene involves an exothermic and exergonic step to get **3a** structure in a clear opposite trend to the amino derivative: -6.1 kcal·mol⁻¹ (-6.5) against 2.0 kcal·mol⁻¹ (3.1) as enthalpies (Gibbs' free-energies), respectively. Thus, this point deserves special attention since it can be seen that alkoxy-carbenes ensemble better than aminocarbenes into the coordinatively unsaturated metal center once a carbon monoxide is lost. **3a** constitutes the bottleneck point where the next competition reactions of cycloannulation diverge. As we will show in next sections, all following reaction steps have relatively low-energy barriers, and, therefore, the *cis*-CO dissociation (involving or not solvent exchange) must be considered as the rate-determining step.

3.3.2. Chromium-mediated cycloannulation reactions of Fischer carbenes.

We have split the presentation of the results of the second part of the reaction mechanism into two subsections. First, the reactions pathways of the benzannulation and cyclopentannulation are discussed in the case of vinylcarbenes and for the different **X** groups considered. Then, the same analysis is done for the case of phenylcarbenes.

3.3.2.1. Vinylcarbenes

Let us consider first the case of vinylcarbenes. Figures 7 and 8 depict the Gibbs' free-energy diagrams for hydroxyvinylcarbene and aminovinylcarbene **1** whereas Figures 9 and 10 correspond to the methoxyvinylcarbene and dimethylaminovinylcarbene cases. In the classic Dötz proposal, the so-called vinylketene route (route **A** in Figures 7 to 10), entails an endothermic and endergonic arrangement of the η^1 -vinylcarbene **3a** to yield **3b**, which can be described as an η^3 -vinylcarbene (see Figure 11), prior to CO insertion into the Cr–C(α) bond. Conversion from **3a** to **3b** involves rotation and folding of the organic chain. In this rearrangement the agostic interaction present in **3a** is lost and the vacant coordination site is partially filled with the π interaction with the C(β)–C(δ) double bond. This isomerization is characterized by $\angle\text{CrC}(\alpha)\text{C}(\beta)$ angles of 88 (alkoxy derivatives) and 92 (amino derivatives) degrees. This step has similar energy requirements for alkoxy- and aminocarbenes (see Table 3). This is probably because the **3a**→**3b** transformation does not involve strong bond breaking/formation processes. Indirect support for intermediates **3a** and **3b** was provided by Barluenga et al. who isolated a chromium vinylaminocarbene complex having a molecular structure intermediate between a rigorous η^1 - and η^3 -bonded species.^{5,31,68} The step **3b**→**4** is clearly favored for alkoxy- over aminocarbene species (barriers are lower by as much as 8 kcal·mol⁻¹ as shown in Table 3). This clear heteroatom effect is the result of stronger π -donors leading to strong CO bonds in **3b**.²⁷ In fact, we have calculated the Cr–CO bond strength in **3b** to be ca. 4 kcal·mol⁻¹ stronger in aminocarbenes than in alkoxy-carbenes. Next steps from η^4 -vinylketene **4** to the benzannulated product **6** show relatively minor heteroatom effects with almost no difference in reaction energies and barriers for alkoxy- and aminocarbenes. This route has been sustained through experimental observations of structures akin to **4**^{68,69} and the Wheland intermediate **5**¹⁸ in the past years. Finally, an 1,3-H shift in **5** leads to **6** with a significant energy barrier. It is likely that the solvent can help in this process by subtracting the transferred proton and attaching it to the oxygen atom of the carbonyl group. In this way, the **5**→**6** energy barrier could be reduced considerably.

It has been proposed another mechanistic possibility some years ago: the so-called chromahexatriene route.³⁶ Looking at the values in Table 3, we can say this alternative pathway is slightly more favorable than Dötz reaction mechanism for

benzannulation. The chromahexatriene intermediate **8** (*vide infra*, Figure 17) is formed from **3a** through very small energy barriers (less than 1 kcal·mol⁻¹) in a clearly exothermic and exergonic process. This kind of intermediates with an η²-coordination mode⁷⁰ cannot be discarded since it has been suggested from literature that insertion of alkynes into Cr=C bond readily leads to such structures undergoing cyclizations subsequently.⁷⁰ Further evidence supporting this route comes from an investigation by Barluenga et al.³¹ where an analogous species to the chromahexatriene intermediate **8** was synthesized from the reaction of a tetracarbonyl aminovinylcarbene chromium(0) complex with dimethyl acetylenedicarboxylate and characterized through ¹H and ¹³C NMR spectroscopy. The authors also showed that decomposition of this intermediate produced cyclopentadienes and phenol derivatives.³¹ The next step in this chromahexatriene route is the **8**→**5** conversion (*vide infra*, Figure 17), that is, closing the formed ring and the displacement of tricarbonylchromium to its center. This step is somewhat more favored for alkoxy- than aminocarbenes.

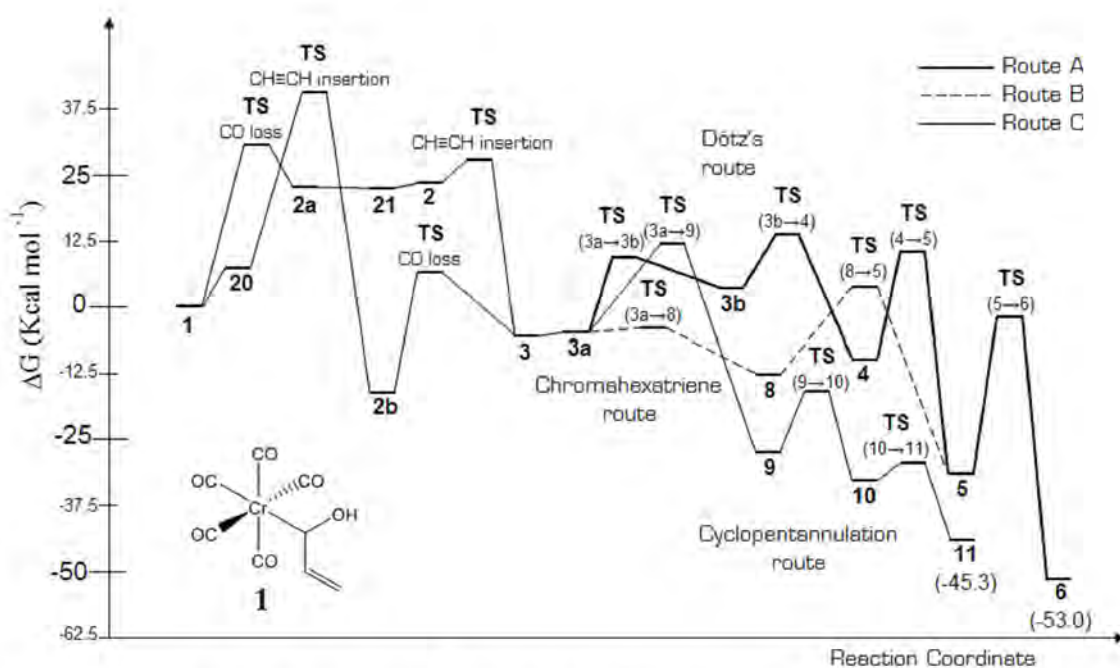


Figure 7. Gibbs free-energy profiles of the (CO)₅Cr=C(OH)CHCH₂ Fischer carbene: comparison of the studied mechanisms (benzannulation – route A, solid line; route B, dashed line; cyclopentannulation – route C, normal line). Relative energies are in kcal·mol⁻¹.

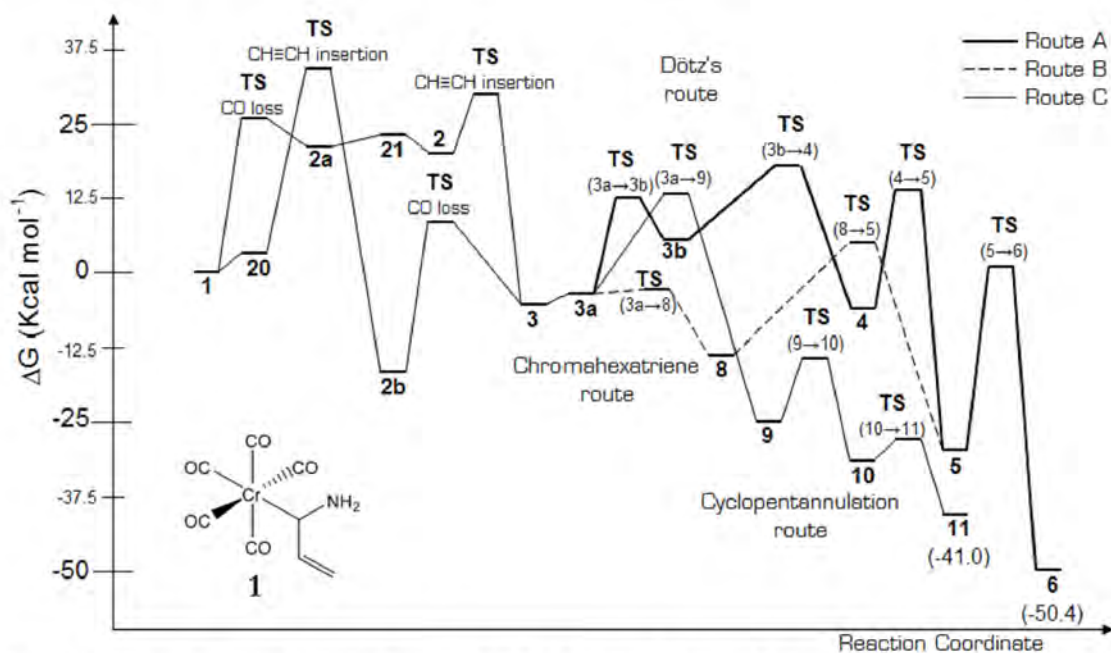


Figure 8. Gibbs free-energy profiles of the $(\text{CO})_5\text{Cr}=\text{C}(\text{NH}_2)\text{CHCH}_2$ Fischer carbene: comparison of the studied mechanisms (benzannulation – route A, solid line; route B, dashed line; cyclopentannulation – route C, normal line). Relative energies are in kcal·mol⁻¹.

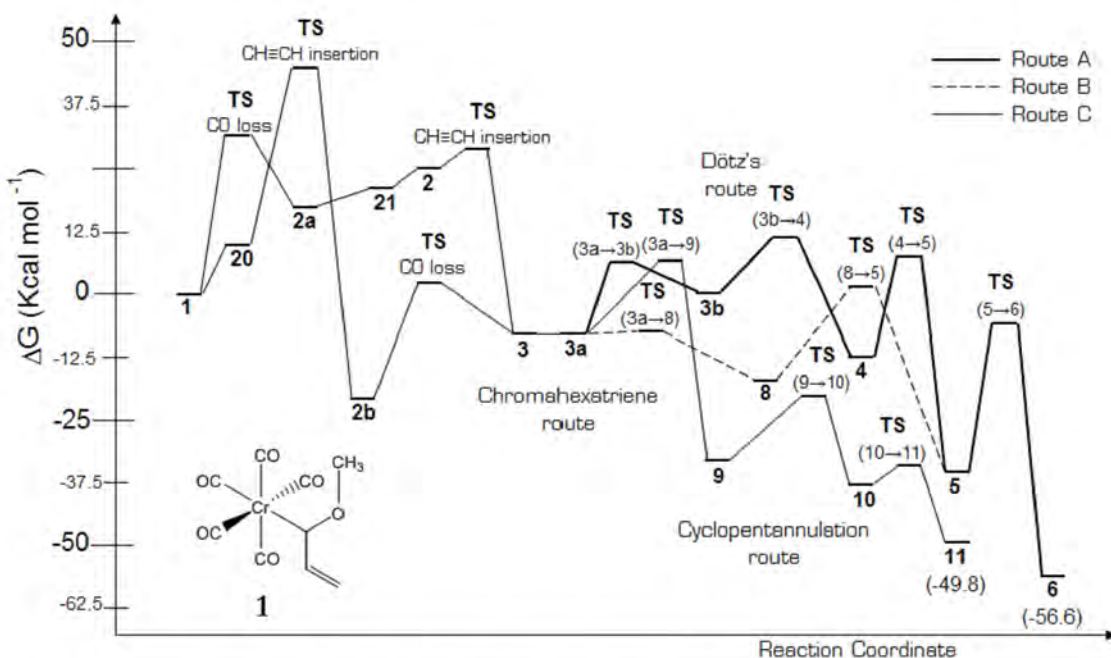


Figure 9. Gibbs free-energy profiles of the $(\text{CO})_5\text{Cr}=\text{C}(\text{OMe})\text{CHCH}_2$ Fischer carbene for the main studied mechanisms (benzannulation – route A, solid line; route B, dashed line; cyclopentannulation – route C, normal line). Relative energies are in kcal·mol⁻¹.

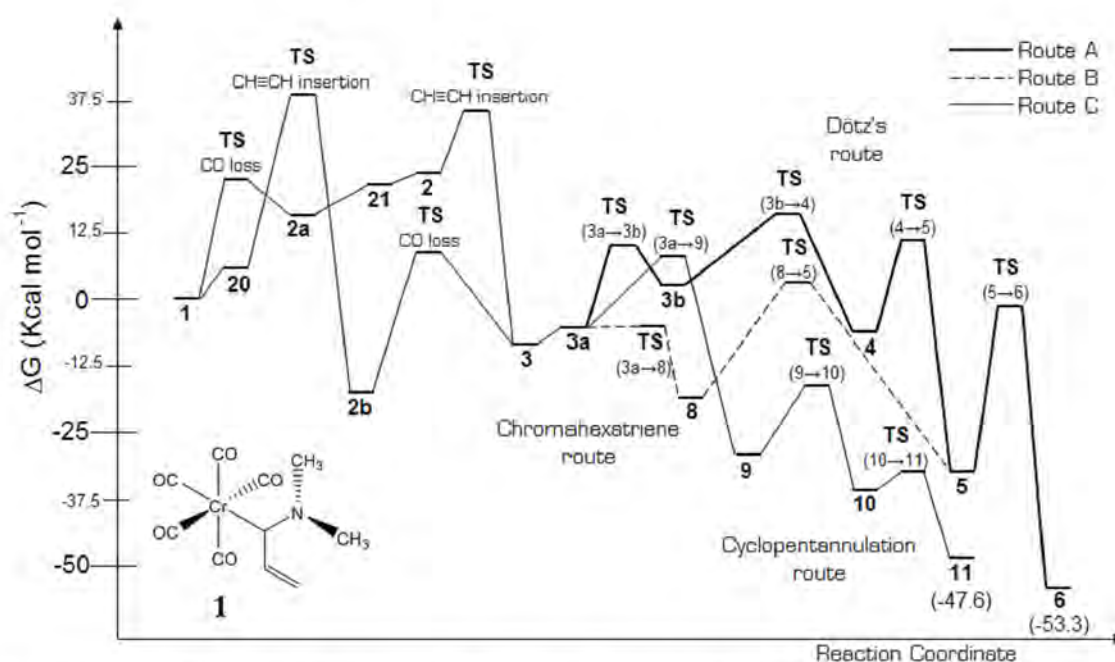


Figure 10. Gibbs free-energy profiles of the $(\text{CO})_5\text{Cr}=\text{C}(\text{NMe}_2)\text{CHCH}_2$ Fischer carbene for the main studied mechanisms (benzannulation – route A, solid line; route B, dashed line; cyclopentannulation – route C, normal line). Relative energies are in $\text{kcal}\cdot\text{mol}^{-1}$.

Table 3. Reaction free-energies (ΔG_{298}^0) and activation barriers ($\Delta G_{298}^{\ddagger}$) for all steps in the benzannulation (Dötz route, **A**, and chromahexatriene route, **B**) and cyclopentannulation (**C**) reaction pathways calculated at the B3LYP/(Wachters' basis, 6-31G(d,p)) level (enthalpy values, ΔH_{298}^0 and $\Delta H_{298}^{\ddagger}$, are in parenthesis). Results are presented for $\text{R} = \text{CH}=\text{CH}_2$ and for the different X substituents studied. For notation of the structures, see schemes 16 and 18. All energies are in $\text{kcal}\cdot\text{mol}^{-1}$.

Route	Step	ΔG_{298}^0 (ΔH_{298}^0)		TS	$\Delta G_{298}^{\ddagger}$ ($\Delta H_{298}^{\ddagger}$)	
		X= OH	X= NH ₂		X= OH	X= NH ₂
A	3a → 3b	8.5 (9.6)	9.2 (10.2)	TS(3a → 3b)	14.5 (14.6)	16.2 (16.1)
	3b → 4	-13.7 (-15.8)	-11.8 (-14.2)	TS(3b → 4)	10.6 (9.4)	18.2 (16.5)
	4 → 5	-22.2 (-24.3)	-23.6 (-25.7)	TS(4 → 5)	20.8 (20.1)	20.3 (19.7)
	5 → 6	-20.4 (-19.7)	-20.5 (-19.7)	TS(5 → 6)	30.5 (30.0)	30.7 (30.4)
B	3a → 8	-8.1 (-9.2)	-10.3 (-11.7)	TS(3a → 8)	0.9 (0.4)	0.6 (0.1)
	8 → 5	-19.3 (-21.3)	-15.9 (-18.0)	TS(8 → 5)	16.9 (15.4)	18.9 (17.3)
C	3a → 9	-23.2 (-23.2)	-21.5 (-22.0)	TS(3a → 9)	17.3 (17.0)	16.9 (16.3)
	9 → 10	-5.5 (3.1)	-6.6 (2.0)	TS(9 → 10)	12.1 (11.7)	10.8 (10.1)

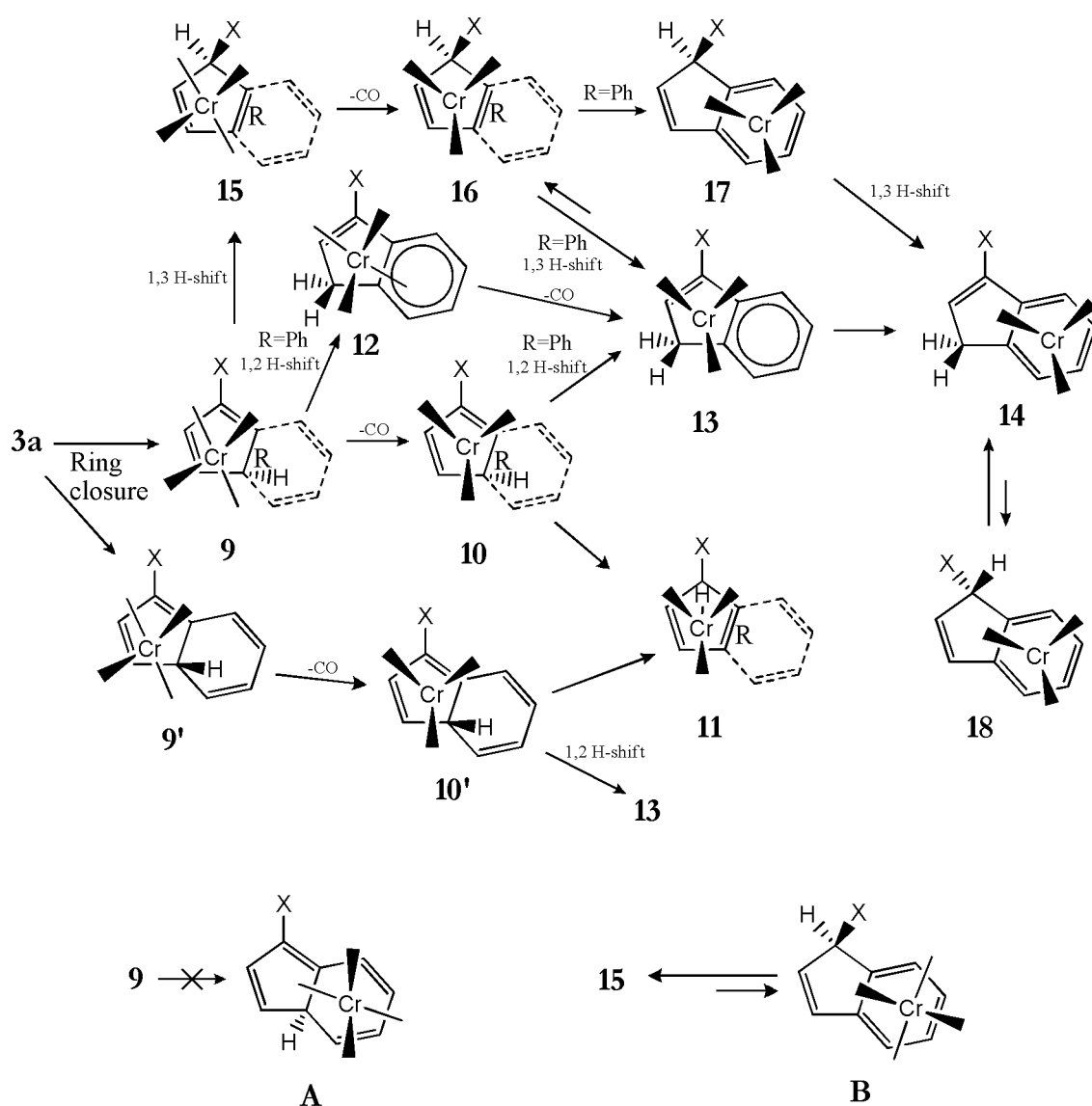
	10 → 11	-11.5 (-11.1)	-9.2 (-8.6)	TS(10 → 11)	3.5 (3.0)	3.7 (3.0)
	9 → 15	-4.6 (-6.6)	-0.3 (-2.4)	TS(9 → 15)	27.6 (27.7)	26.0 (26.0)
	15 → 16	6.9 (17.4)	-0.3 (9.8)			
		X= OCH ₃	X=N(CH ₃) ₂		X= OCH ₃	X=N(CH ₃) ₂
A	3a → 3b	8.1 (8.9)	8.0 (8.4)	TS(3a → 3b)	14.5 (14.4)	15.2 (15.3)
	3b → 4	-12.4 (-14.3)	-8.6 (-10.6)	TS(3b → 4)	8.3 (7.8)	13.1 (12.4)
	4 → 5	-23.2 (-25.2)	-25.8 (-28.1)	TS(4 → 5)	20.0 (19.4)	16.8 (15.2)
	5 → 6	-21.0 (-20.3)	-21.4 (-19.3)	TS(5 → 6)	29.7 (29.3)	30.4 (30.2)
B	3a → 8	-9.2 (-10.2)	-12.7 (-14.1)	TS(3a → 8)	0.6 (0.3)	0.5 (0.1)
	8 → 5	-18.2 (-20.4)	-13.7 (-16.2)	TS(8 → 5)	18.7 (17.3)	21.2 (19.1)
C	3a → 9	-25.1 (-25.1)	-23.2 (-24.0)	TS(3a → 9)	14.9 (14.4)	13.4 (13.0)
	9 → 10	-5.0 (3.6)	-6.6 (2.0)	TS(9 → 10)	12.9 (13.1)	12.9 (11.5)
	10 → 11	-11.6 (-11.1)	-12.3 (-11.8)	TS(10 → 11)	4.0 (3.4)	3.5 (2.6)
	9 → 15	-4.4 (-6.3)	-0.8 (-3.1)	TS(9 → 15)	27.9 (28.0)	25.3 (24.4)
	15 → 16	7.6 (18.0)	1.8 (11.7)			

As found by GDH,³⁹ our results also indicate that phenol formation is more exothermic for hydroxycarbenes than for aminocarbenes. Thus, full transformation from **1**→**6** releases -53.0 ($X' = \text{H}$) and -56.6 ($X' = \text{CH}_3$) $\text{kcal}\cdot\text{mol}^{-1}$ in $(\text{CO})_5\text{Cr}=\text{C}(\text{OX}')\text{CHCH}_2$ as compared to -50.4 ($X' = \text{H}$) and -53.3 ($X' = \text{CH}_3$) $\text{kcal}\cdot\text{mol}^{-1}$ in $(\text{CO})_5\text{Cr}=\text{C}(\text{NX}'_2)\text{CHCH}_2$. To discuss about the most viable reaction mechanism, we have to take into account that differences in energy between TSs and intermediates (and not between TSs and initial reactants) are decisive in reactions carried out in solvents. In this case, molecular collisions are sufficiently efficient to cool the reactant complex (if this is stable enough to survive for several vibrations), causing it to be in thermal equilibrium with the environment. Thus, looking at the barriers between TSs and intermediates, it is found, first, that all involved enthalpy barriers are lower than the barrier that has to be surmounted in the initial step of the Dötz reaction (CO dissociation), and, second, that the chromahexatriene route is the minimum reaction pathway for the transformation from **3a** to **5** in alkoxyvinyl- and aminovinylcarbenes with the exception of $(\text{CO})_4\text{Cr}=\text{C}(\text{N}(\text{CH}_3)_2)\text{CHCH}_2$. For instance, for $(\text{CO})_4\text{Cr}=\text{C}(\text{OH})\text{CHCH}_2$, the highest barrier in the Dötz reaction mechanism

corresponding to the **4**→**5** step is 20.8 kcal·mol⁻¹ whereas the chromahexatriene alternative proposal the highest barrier is just 16.9 kcal·mol⁻¹ (**8**→**5**). Energy differences between the two mechanisms are smaller for the bulkier **X** substituents and even the Dötz mechanism becomes the most favorable in the case of the (CO)₄Cr=C(N(CH₃)₂)CHCH₂ complex. Since differences in enthalpy barriers for the two mechanisms of 6-MR formation are relatively small, it is likely that the two mechanisms can be operative in vinylcarbenes with some preference for the chromahexatriene route.

Finally, the third studied route (route C, Scheme 18) corresponds to the formation of the 5-MR product. Some authors have suggested the possibility that indene formation takes place from **3a** via an electrocyclic ring closure to give a chromacyclohexadiene intermediate.^{13,21,27,31} We have been unable to find such an intermediate and all geometry optimizations carried out starting from a chromacyclohexadiene structure lead to η^2 -vinylcarbenes structures. So, according to our results the cyclopentannulation reaction proceeds with the formation of tetracarbonyl η^4 -cyclopentannulated complex **9** from **3a**. By comparing the barriers of electrocyclization **3a**→**9** for the different **X** substituents studied, we can see that this process is somewhat favored for bulkier **X** ligands. This is attributed to the shorter distance between the C atoms in **3a** that form the new bond due to steric effects. For instance, this distance decreases from 2.139 and 2.128 Å in (CO)₄Cr=CHCHC(OH)CHCH₂ and (CO)₄Cr=CHCHC(NH₂)CHCH₂ to 2.124 and 2.115 Å in (CO)₄Cr=CHCHC(OCH₃)CHCH₂ and (CO)₄Cr=CHCHC(N(CH₃)₂)CHCH₂, respectively. The electrocyclization **3a**→**9** is also favored for amino- as compared to alkoxy-carbenes, the larger π -population in aminocarbenes helping to some extent this electrocyclization process. From complex **9**, we have explored the PES in detail looking for all intermediates present in the reaction pathways shown in Scheme 18. In the case of vinylcarbenes depending on the order of carbon-monoxide loss and 1,3-H migration, we found two possible routes: **9**→**10**→**11** or **9**→**15**→**16**. From data in Table 3, we can see both initial steps are exergonic, but **9**→**15** is exothermic whereas **9**→**10** is slightly endothermic. On the other hand, migrating the hydrogen to the better stabilized position in **9**→**15** costs more than twice of a first CO removal followed by H migration, so it is clear that the most favorable reaction path in this case is **9**→**10**→**11**. In the (tricarbonylchromium)cyclopentadiene complex **10** a hydrogen atom is transferred to

the chromium atom to form the metal hydride **11** through a small barrier of less than 5 kcal·mol⁻¹. Figures 7 to 10 display only the minimum energy path (**9**→**10**→**11**) found for cyclopentannulation. The **3a**→**9** step is the one having the largest barrier in route C and it is somewhat favored in the case of aminocarbenes as compared to alkoxy-carbenes. This is in contrast to the **8**→**5** transformation in chromahexatriene route that has slightly smaller barriers in the case of alkoxy-carbenes. This concurs with the experimental evidence that the ratio of 5-MR formation increases by substitution of an alkoxy group by a better electron donor such as the amino group.^{13,14,27,31}



Scheme 18. Cyclopentannulation reaction (route C) pathways studied in the present work ($X = \text{OH}, \text{NH}_2, \text{OCH}_3$ and $\text{N}(\text{CH}_3)_2$; $R = \text{CH}=\text{CH}_2$ and Ph).

Since all the routes (A, B, and C) start from the same intermediate **3a**, the product distribution should be explained based on the kinetic parameters of these three routes after the generation of **3a**. The selectivity on this ramification is then determined by the difference in activation free-energy between two reaction routes. From Figures 7 to 10, the most energy demanding step from **3a** for the generation of benzannulated product **6** is via **TS(8→5)** (except for $X = N(CH_3)_2$ where the **TS(8→5)** must be considered instead), requiring activation free-energies of 16.9, 18.9, 18.7, and 16.8 kcal·mol⁻¹ for $X = OH, NH_2, OCH_3,$ and $N(CH_3)_2$, respectively. The activation free energies for the generation of cyclopentannulated product **11** should be calculated from intermediate **8** to the highest transition state **TS(3a→9)** (this is because the generation of **8** from **3a** is very easy, which has an energy barrier of nearly 1 kcal/mol, and **8** is thermodynamically favored over **3a**), and they are 25.4, 27.2, 24.1, and 26.1 kcal·mol⁻¹, respectively. Due to the difference of at least 5 kcal·mol⁻¹ between the most accessible pathways, we can derive that 6-MR formation is kinetically preferred over 5-MR product in these cases. This is in line with experimental observation that vinylcarbenes gives exclusively phenols and cyclohexadienones (with few exceptions).^{29,31,71}

3.3.2.2 Phenylcarbenes

The optimized structures of intermediates and TSs in the Dötz benzannulation route for $X = OH$ and $R = Ph$ are drawn in Figure 11. Figures 12 to 15 show energy diagrams for the alkoxyphenyl- and aminophenylcarbenes **1** studied in this work, while Table 4 reports energy values. In accordance with GDH results,³⁹ we also find that 6-MR formation is more exothermic for vinyl- than phenylcarbenes (by about 10 kcal·mol⁻¹) since in the former case a new aromatic system is created. Our results show that not only 6-MR but also 5-MR product formation is more exergonic for vinylcarbenes.

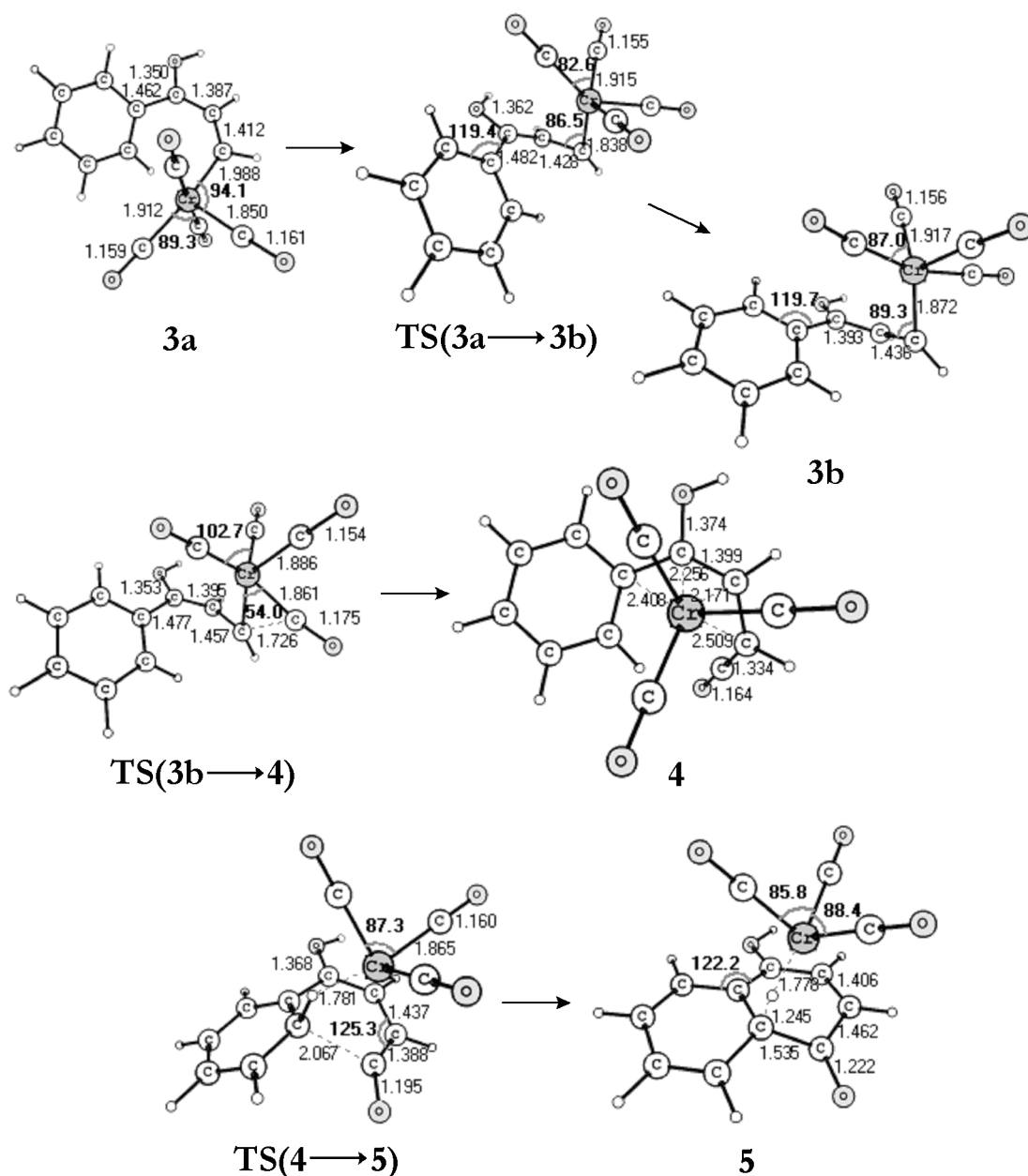


Figure 11. Optimized structures of intermediates and transition states in the Dötz benzannulation route for the case of X = OH and R = Ph. Distances in Å and angles in degrees.

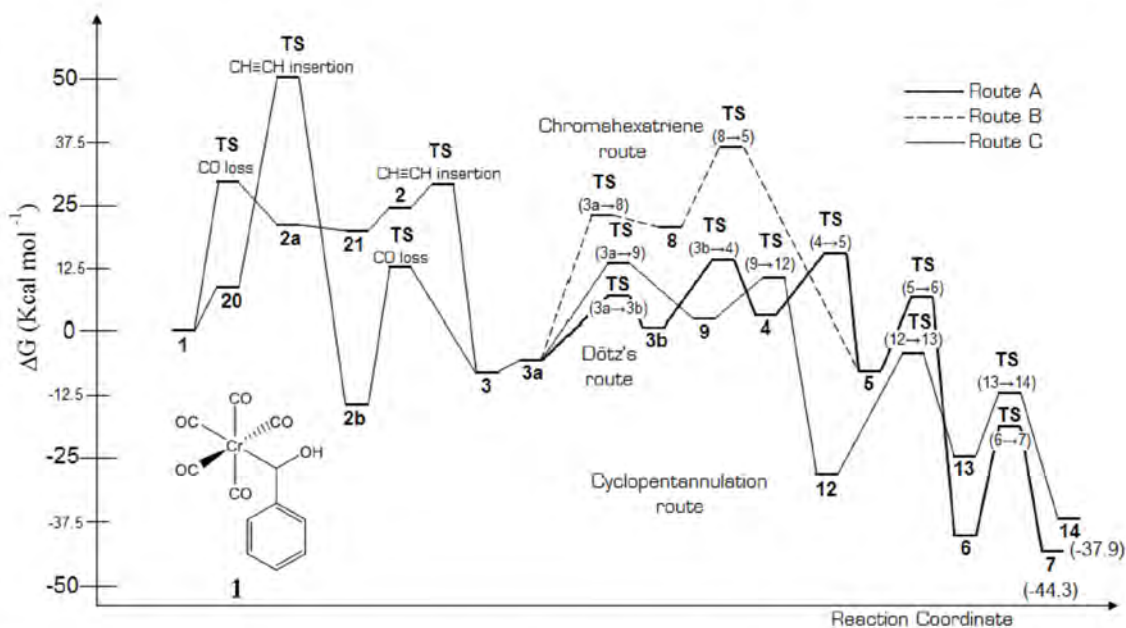


Figure 12. Gibbs free-energy profiles of the $(\text{CO})_5\text{Cr}=\text{C}(\text{OH})\text{Ph}$ Fischer carbene for the main studied mechanisms (benzannulation – route A, solid line; route B, dashed line; cyclopentannulation – route C, normal line). Relative energies are in $\text{kcal}\cdot\text{mol}^{-1}$.

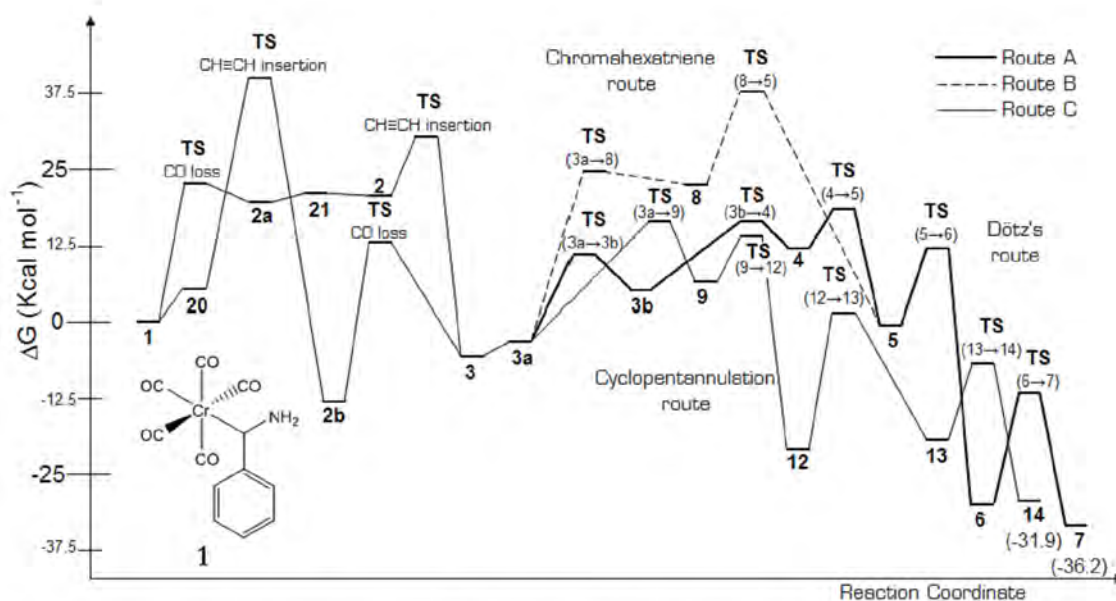


Figure 13. Gibbs free-energy profiles of the $(\text{CO})_5\text{Cr}=\text{C}(\text{NH}_2)\text{Ph}$ Fischer carbene for the main studied mechanisms (benzannulation – route A, solid line; route B, dashed line; cyclopentannulation – route C, normal line). Relative energies are in $\text{kcal}\cdot\text{mol}^{-1}$.

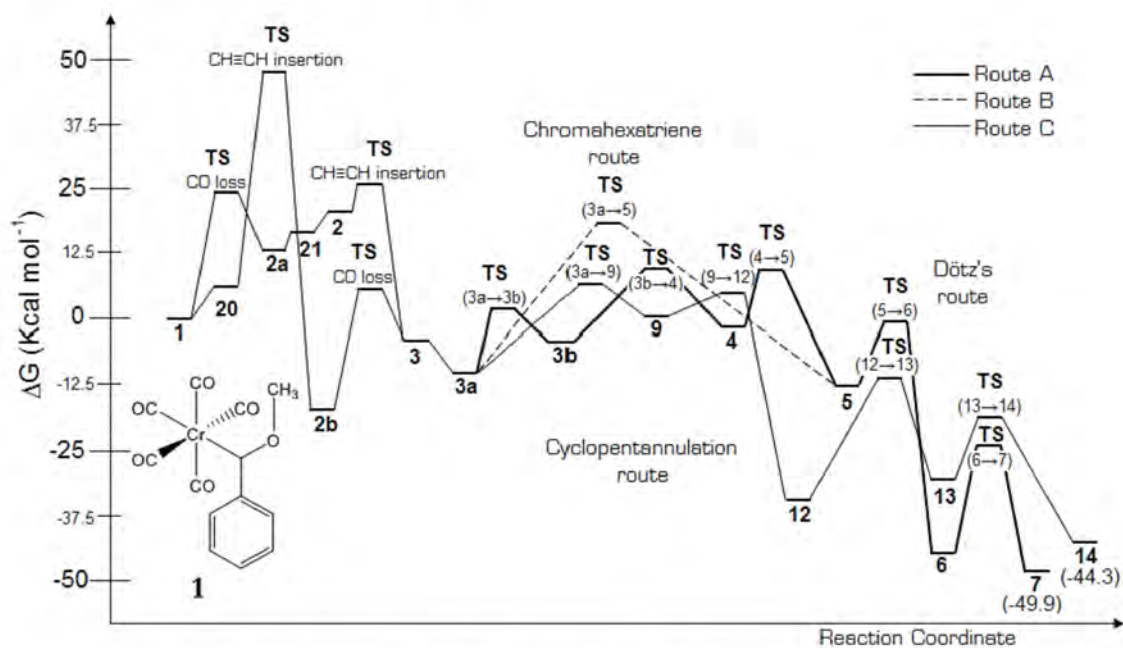


Figure 14. Gibbs free-energy profiles of the $(\text{CO})_5\text{Cr}=\text{C}(\text{OMe})\text{Ph}$ Fischer carbene for the main studied mechanisms (benzannulation – route A, solid line; route B, dashed line; cyclopentannulation – route C, normal line). Relative energies are in $\text{kcal}\cdot\text{mol}^{-1}$.

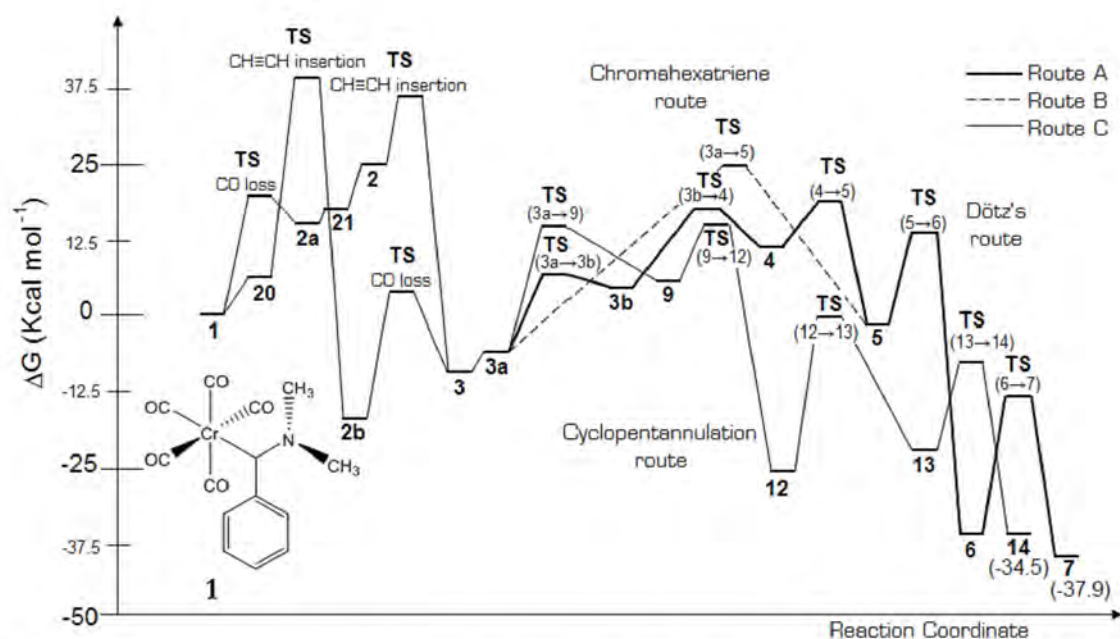


Figure 15. Gibbs free-energy of the $(\text{CO})_5\text{Cr}=\text{C}(\text{NMe}_2)\text{Ph}$ Fischer carbene for the main studied mechanisms (benzannulation – route A, dashed line; route B, dashed line; cyclopentannulation – route C, normal line). Relative energies are in $\text{kcal}\cdot\text{mol}^{-1}$.

Table 4. Reaction free-energies (ΔG_{298}^0) and activation barriers ($\Delta G_{298}^0 \ddagger$) for all steps in the benzannulation (Dötz route, **A**, and chromahexatriene route, **B**) and cyclopentannulation (**C**) reaction pathways calculated at the B3LYP/(Wachters' basis, 6-31G(d,p)) level (enthalpy values, ΔH_{298}^0 and $\Delta H_{298}^0 \ddagger$, are in parenthesis). Results are presented for R = Ph and for the different X substituents studied. For notation of the structures, see Schemes 16 and 18. All energies are in kcal·mol⁻¹.

Route	Step	ΔG_{298}^0 (ΔH_{298}^0)		TS	$\Delta G_{298}^0 \ddagger$ ($\Delta H_{298}^0 \ddagger$)	
		X = OH	X = NH ₂		X = OH	X = NH ₂
A	3a → 3b	6.5 (7.5)	8.8 (9.0)	TS(3a → 3b)	12.7 (12.0)	15.2 (12.6)
	3b → 4	2.2 (1.0)	7.4 (6.0)	TS(3b → 4)	13.3 (11.5)	12.3 (11.1)
	4 → 5	-10.9 (-14.1)	-13.4 (-16.4)	TS(4 → 5)	12.3 (9.6)	7.1 (4.3)
	5 → 6	-32.8 (-32.3)	-31.8 (-31.4)	TS(5 → 6)	14.6 (14.4)	13.4 (13.0)
B	3a → 8	26.4 (25.8)	27.7 (25.7)	TS(3a → 8)	28.8 (27.5)	30.1 (28.4)
	8 → 5	-28.6 (-31.3)	-24.9 (-27.0)	TS(8 → 5)	16.0 (14.6)	16.4 (15.6)
C	3a → 9	8.1 (7.8)	10.4 (9.0)	TS(3a → 9)	19.2 (17.0)	21.2 (18.2)
	9 → 10	2.9 (12.7)	2.3 (12.2)	TS(9 → 10)	23.3 (24.6)	22.2 (24.1)
	10 → 13	-30.3 (-31.0)	-30.1 (-30.6)	TS(10 → 13)	14.6 (14.3)	15.0 (14.7)
	9 → 12	-31.1 (-31.8)	-29.7 (-30.1)	TS(9 → 12)	8.1 (8.5)	8.1 (8.6)
	12 → 13	3.7 (13.5)	1.9 (11.6)	TS(12 → 13)	24.4 (27.2)	24.2 (26.6)
	13 → 14	-12.7 (-12.6)	-11.0 (-11.1)	TS(13 → 14)	12.8 (13.6)	13.4 (14.1)
	14 → 18	9.3 (9.5)	9.3 (9.2)			
	9 → 15	-31.1 (-31.8)	-37.1 (-38.7)	TS(9 → 15)	8.6 (8.2)	6.7 (6.3)
	15 → 16	8.7 (18.5)	12.1 (22.8)	TS(15 → 16)	31.9 (31.4)	22.9 (24.6)
	16 → 13	-4.9 (-5.0)	-2.7 (-2.5)	TS(16 → 13)	36.2 (36.1)	38.0 (38.5)
	16 → 17	-7.7 (-7.7)	-1.3 (-1.2)	TS(16 → 17)	16.6 (17.4)	21.4 (22.4)
	17 → 14	-9.9 (-9.9)	-12.5 (-12.5)	TS(17 → 14)	33.8 (43.6)	29.7 (29.7)
	3a → 9'	10.4 (10.6)	12.4 (11.4)			
	9' → 10'	-33.9 (-25.0)	-33.0 (-24.0)	TS(9' → 10')	16.1 (15.7)	16.6 (16.0)
	10' → 11	11.6 (11.2)	11.9 (11.7)			
	10' → 13	4.3 (3.9)	3.3 (3.2)			
		X = OCH ₃	X = N(CH ₃) ₂		X = OCH ₃	X = N(CH ₃) ₂
A	3a → 3b	6.3 (6.8)	9.8 (9.9)	TS(3a → 3b)	12.7 (11.9)	12.0 (12.0)
	3b → 4	2.8 (1.8)	6.4 (4.8)	TS(3b → 4)	14.2 (12.2)	12.5 (11.3)

Heteroatom and Substituent Effects

	4 → 5	-14.2 (-14.9)	-12.2 (-15.6)	TS(4 → 5)	11.2 (8.5)	7.3 (4.3)
	5 → 6	-34.8 (-32.7)	-32.9 (-32.2)	TS(5 → 6)	12.5 (12.4)	14.5 (14.6)
B	3a → 5	-6.1 (-6.2)	4.0 (-0.8)	TS(3a → 5)	29.4 (28.0)	29.2 (27.8)
C	3a → 9	11.0 (7.1)	10.9 (10.5)	TS(3a → 9)	17.5 (15.2)	19.5 (16.7)
	9 → 10	-0.2 (12.8)	2.9 (12.2)	TS(9 → 10)	19.3 (24.7)	21.1 (23.0)
	10 → 13	-31.8 (-32.2)	-29.4 (-30.1)	TS(10 → 13)	13.9 (13.5)	15.6 (15.1)
	9 → 12	-36.0 (-33.2)	-30.0 (-31.5)	TS(9 → 12)	4.8 (8.8)	8.9 (8.9)
	12 → 13	4.1 (13.9)	3.5 (13.6)	TS(12 → 13)	23.9 (27.4)	24.3 (27.2)
	13 → 14	-12.7 (-13.0)	-13.4 (-13.3)	TS(13 → 14)	12.3 (13.2)	13.8 (13.8)
	14 → 18	9.4 (9.5)	8.1 (7.4)			
	9 → 15	-35.7 (-33.0)	-25.4 (-26.8)	TS(9 → 15)	5.2 (7.2)	7.4 (6.2)
	15 → 16	9.3 (19.2)	1.3 (10.3)	TS(15 → 16)	47.2 (46.3)	37.4 (36.3)
	16 → 13	-5.6 (-5.5)	-2.4 (-1.4)	TS(16 → 13)	37.8 (37.9)	37.3 (37.9)
	16 → 17	-8.7 (-8.5)	-2.8 (-2.4)	TS(16 → 17)	15.8 (16.6)	20.4 (21.5)
	17 → 14	-9.6 (-10.0)	-13.0 (-12.3)	TS(17 → 14)	34.1 (33.8)	30.6(31.0)
	3a → 9'	9.6 (9.4)	9.7 (8.9)			
	9' → 10'	-34.0 (-25.2)	-29.3 (-21.4)	TS(9' → 10')	16.6 (16.0)	19.4 (19.4)
	10' → 11	10.9 (10.9)	8.5 (8.9)			
	10' → 13	3.5 (3.5)	4.1 (5.1)			

For the Dötz benzannulation mechanism, the main difference with respect to the vinyl substituent is that most of energy barriers are now significantly lower, which is not unexpected given the fact that Cr–CO bonds in phenylcarbenes are weaker than in vinylcarbenes (Table 2), and the reaction pathway for 6-MR formation is clearly favored over the chromahexatriene route. At variance with the vinyl case, there is almost no heteroatom effect and, in particular, the barrier of the insertion of CO corresponding to **TS(3b→4)** has similar energy requirements for alkoxy- and aminocarbenes. In addition, this CO insertion is exothermic and exergonic in vinylcarbenes and the other way around for phenylcarbenes. These results point out that the higher production of cyclopentannulated products in aminoarylcarbenes cannot be attributed to the stronger C–O bonds due to the higher π -donor character of the amino as compared to the alkoxy groups. There are remarkable differences between the vinyl and phenyl cases in steps **4→5** and **5→6**. Both the energy barriers of ring closure, **TS(4→5)**,

and tautomerization from keto to enol form, **TS(5→6)**, are significantly reduced for the phenyl substituent. In the case of the **4→5** transformation, the reason behind these changes can be found by inspecting the structure of the Wheland intermediate **5**, where the electrocyclization leads to the formation of a relatively strong agostic interaction between C–H bond of the C atom in the ring junction and the Cr(CO)₃ group that stabilizes intermediate **5** and favors the **4→5** conversion. Such agostic interaction is not present in the vinyl analogues. Depending on which side of the phenyl group is attacked by the ketene, below the ring with respect to the location of the tricarbonylchromium tripod (**5a**) or above this (**5b**, see Figure 16), we find two possible intermediates. Our results show that isomer **5a** is lower in energy (4 kcal·mol⁻¹ in average) than **5b**. In **5b**, the central carbon in the junction of both rings is more pyramidalized and the naphthalenic fragment is less aromatic than in **5a**. Moreover, in **5a** there is the abovementioned stabilizing agostic interaction. In the case of the keto to enol tautomerization, the energy barrier is also lower in phenylcarbenes than vinylcarbenes because the hydrogen transfer is assisted by the chromium metal through the agostic interaction formed. In addition, the keto to enol tautomerization is more exergonic (exothermic) in phenylcarbenes than for vinylcarbenes because in the final product **6** one recovers aromaticity in two 6-MRs as compared to a single 6-MR in vinylcarbenes.

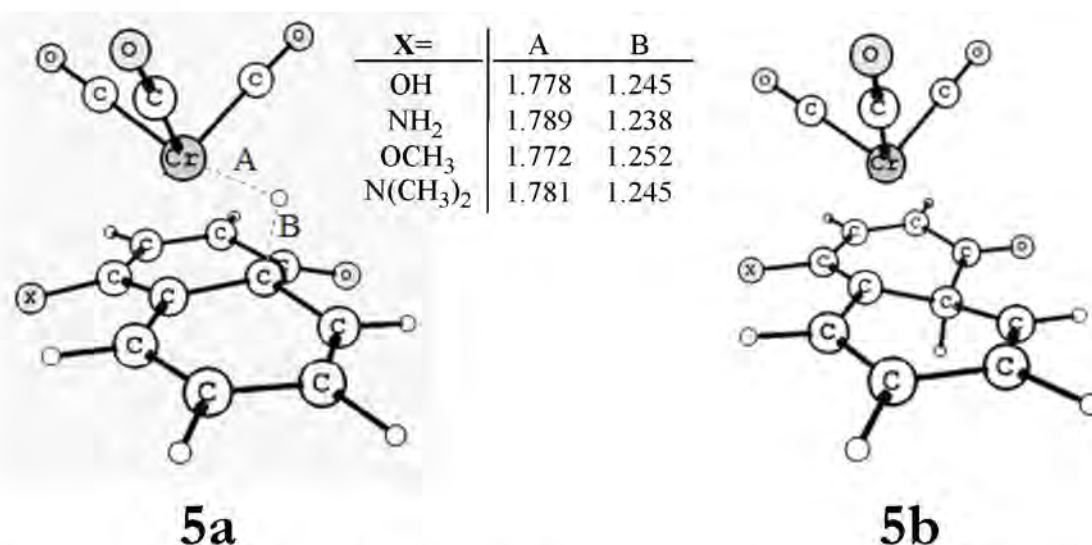


Figure 16. The naphthoquinone derivative prefers **5a** structure over **5b** because of an agostic stabilizing interaction.

Inspecting values in Table 4 about the proposed chromahexatriene route B, we observe dramatic changes when going from vinylcarbenes to phenylcarbenes. Figure 17 resumes the modifications undergone on this reaction mechanism dependent of the kind of Fischer carbene used. As mentioned above, η^1 -vinylcarbene complex **3a** rearranges to an η^2 -species **8** looking for a first C(carbene)-C(carbonyl) interaction and then a concerted reaction step is followed where the carbon monoxide ensembles directly into the ring when metal complex is “walking” to its center (**R1** mechanism). But for the case of hydroxyphenyl and aminophenyl carbenes, this η^2 -conformation is not achieved (the phenyl suffers steric hindrance from the nearest CO ligands when approaching its π -system to the chromium atom) and a Cr–H bond is formed instead. So the benzannulation proceeds through a hydride complex **8** (not a chromahexatriene intermediate) and the CO insertion is performed by the aromatic carbon and not from the carbene carbon atom as in the case of vinylcarbenes to generate again the Wheland intermediate **5** (**5a**) compound (**R2** mechanism). Such intermediate **8** in phenylcarbenes is quite unstable, and for the case of bulkier functional groups (**X** = OCH₃, N(CH₃)₂) we have even been unable to locate such intermediate in the PES. Since intermediate **8** is unstable, the barrier for the transformation from **3a** to **5** corresponds to the energy difference between the highest TS found in the path, **TS(3a→5)** or **TS(8→5)**, and the energy of **3a**. Thus, route B in phenylcarbenes has barriers of about 30 – 40 kcal·mol⁻¹ and, consequently, the Dötz reaction mechanism is then confirmed as the more feasible proposal for benzannulation in the four *phenylcarbenes* studied.

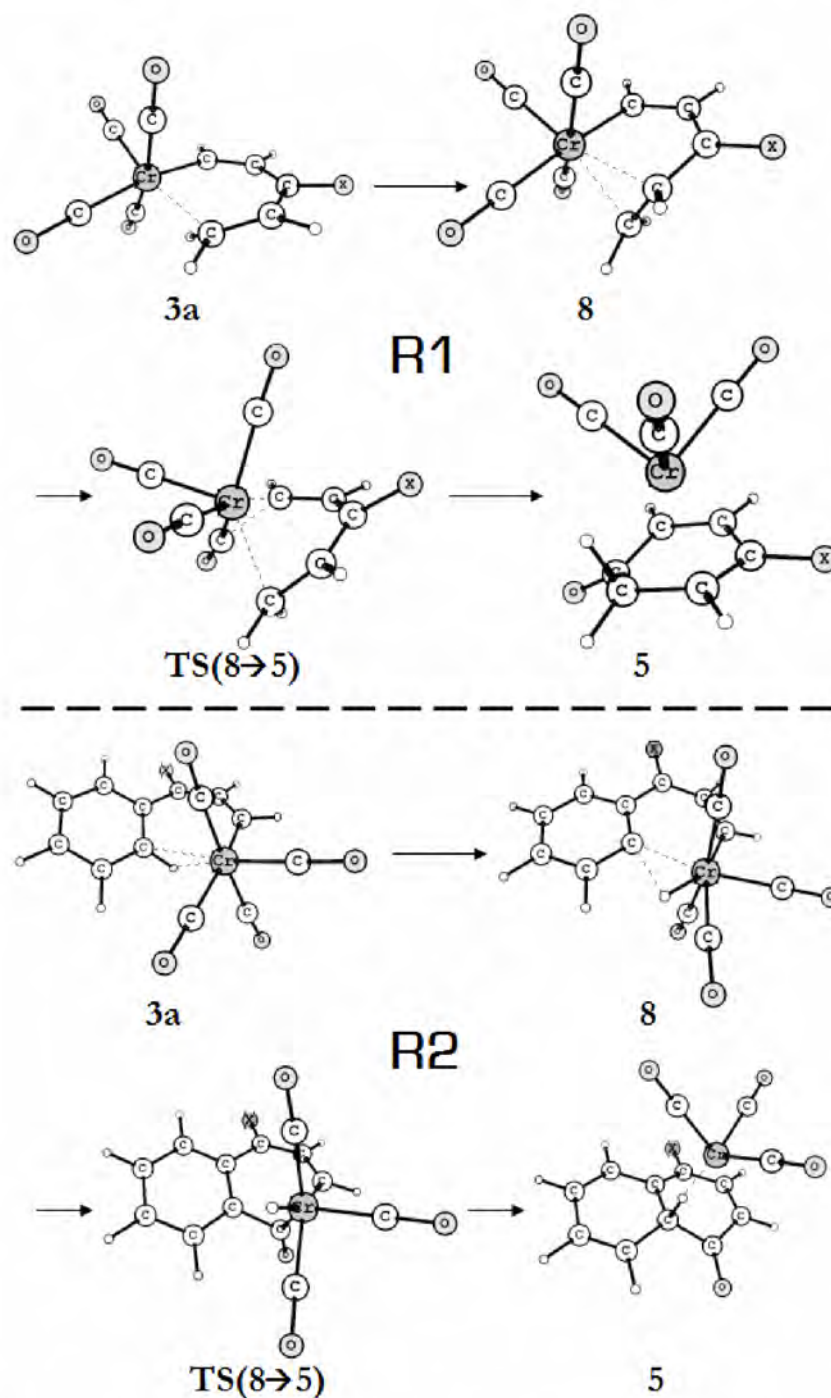


Figure 17. The chromahexatriene pathway is modified depending on which substituents are used: **R1** is the path followed for all **X** ligands and **R = CH=CH₂** and **R2** is the one that occurs when **X = OH, NH₂** and **R = Ph**.

Our mechanism for the formation of 5-MRs (see Figure 18 where we have exemplified the involved structures for the case of $(\text{CO})_4\text{Cr}=\text{C}(\text{OH})\text{Ph}$) differs from some proposals in the literature where is supposed the existence of a

chromacyclohexadiene intermediate by which chromahexatriene **3a** is converted into **9**.^{13,20,33,72} However, as said before such intermediate was not possible to obtain and instead the **TS(3a→9)** directly connecting both structures was located (see Figure 18). Such chromacyclohexadiene intermediate is more likely to be present in the [3+2] cycloaddition of imines⁷³ due to the more electron-donating character of imine. From **9**, we have tested several prospects (see Scheme 18) together with the two routes already explored for vinylcarbenes. In the case of phenyl derivatives, the hydrogen atom of the phenyl group depicted in Scheme 18 can be positioned in the same or in the opposite face of the ring with respect to the chromium carbonyl fragment when the cyclization is performed. In the latter case, the hydrogen atom can first migrate to a vicinal carbon in **12** and thus connecting to **13** by CO elimination apart from the already discussed routes **9→10** and **9→15**. From **10**, it is not possible now to follow a proton shift to **11** as for vinylcarbenes, because of the location of the hydrogen atom that should be transferred. Instead, the modified route from **10** goes to **13** complex through a 1,2 H-shift (see Scheme 18). Moreover, this latter tautomer can also suffer a haptotropic migration of the tricarbonylchromium unit to yield **14** as well as **16** to the corresponding **17** haptoisomer. From our calculated energy values, **14** can be regarded as the final product of the reaction since it presents the minor energy compared with all the other discussed intermediates (see Figures A1 to A4 in Appendix). On the other hand, we also checked the energy route of isomers of **9** and **10**, namely **9'** and **10'**, respectively, as we did previously for **5a** and **5b** (see Figure 16) to discard possible minimum energy paths leading to **13** or **11** species by tautomerization. Very interestingly, **9** is more stable than **9'** for the less congested **X** ligands ($\sim 4 \text{ kcal}\cdot\text{mol}^{-1}$) but the order is inverted when **X** becomes bulkier by a difference of ca. $3 \text{ kcal}\cdot\text{mol}^{-1}$. The η^3 -conformation of the $\text{Cr}(\text{CO})_4$ moiety creates a steric hindrance of the hydrogen atom with one equatorial CO in **9'** when **X** = OH and NH_2 , but for bulkier **X** ligands the repulsion of methyl group rotates the $\text{Cr}(\text{CO})_4$ group and allows a stabilizing Cr–H agostic interaction favoring **9'** isomer in this case. Furthermore, **10'** is more stable than **10** by more than $25 \text{ kcal}\cdot\text{mol}^{-1}$, the reason being the same as discussed for Figure 16 but for a more dense 5-MR instead of 6-MR. Figures 12 to 15 show only reaction pathways for the minimum energy path to **14**. We also proved haptomigration paths from tetracarbonylchromium species **9** or **15** (and **12**) but whereas we were unable to optimized a hypothetical complex **A** (Scheme 18), from the structure **15** we located a haptotropic isomer **B**, $23 \text{ kcal}\cdot\text{mol}^{-1}$ (alkoxycarbenes) – $30 \text{ kcal}\cdot\text{mol}^{-1}$ (aminocarbenes) uphill. This unfavorable $\text{Cr}(\text{CO})_4$

haptotropic rearrangement distorts the benzene ring losing its aromaticity and therefore, we did not include species **A** and **B** in Table 4.

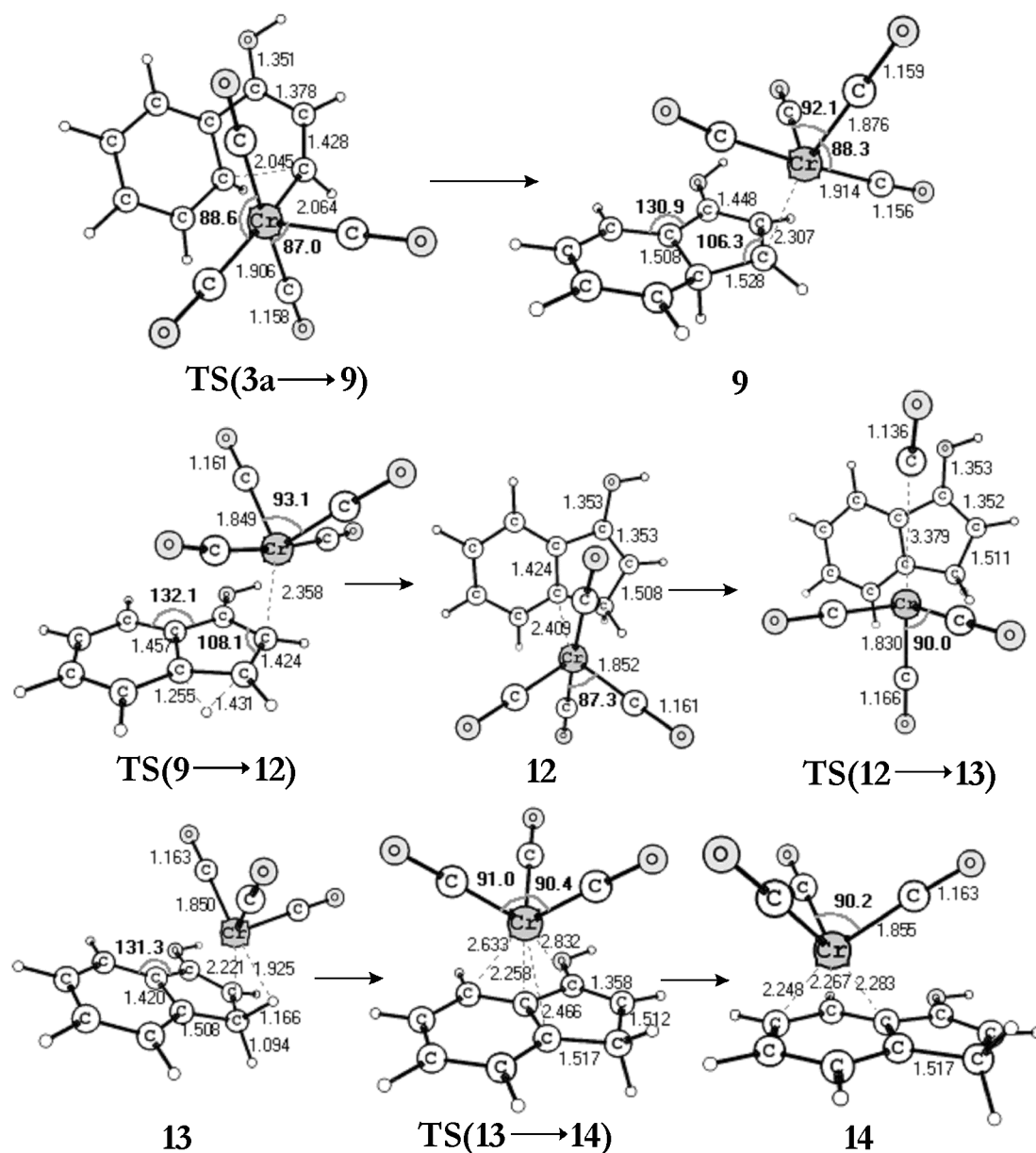


Figure 18. Optimized intermediates and transition state structures for the most suitable cyclopentannulation routes for the case of X = OH and R = Ph. Distances in Å and angles in degrees.

From the cyclopentannulation reaction values in Tables 3 and 4, it can be seen that route *C* is *thermodynamically* somewhat more competitive for phenyl- than vinylcarbenes. Thus, the smallest Gibbs' free-energy differences between the most stable 6- and 5-MR products are 5.7 kcal·mol⁻¹ (dimethylaminovinylcarbene) and 3.4

kcal·mol⁻¹ (dimethylaminophenylcarbene). At the B3LYP/6-311G++(d,p) level of theory, these energy differences are 1.2 and 0.4 kcal·mol⁻¹. Therefore, in the case of the dimethylaminophenylcarbene differences between 5- and 6-MR formation are insignificant and this is in line with the experimental observation that cyclopentannulation is favored in this case.¹³ Figure 19 sketches the steric hindrance that amino derivatives suffer in the benzannulation reaction in phenylcarbenes. Starting from the carbene skeleton of **3a**, namely **3ax**, one can form the 6-MRs **6'x/6x** or the 5-MRs **14ax**. There is a reduction of 10 degrees in the external junction angle between the two rings for the naphthalenic as compared to the indenic structure. In **6'x** there is a steric repulsion coming from X' substituents in amine position that is not present in vinylcarbenes and alkoxyphenylcarbenes. To avoid it, the amino group rotates around the C–N bond to yield **6x**. In this conformation, the lone electron pair of the N atom cannot intervene in the π -delocalized structure, although it can interact with the nearest H atom of the nonsubstituted ring. This loss of planarity is not attained when the 5-MR is formed like in **14ax** and π -delocalization of the N lone pair is in this case possible. The destabilization of **6'x/6x** with respect to **14ax** in dialkylaminocarbenes is in part explained by this steric effect. Our results indicate that the cyclopentannulation route **3a**→**9**→**12**→**13**→**14** is the most favored pathway to 5-MR products both from kinetic and thermodynamic points of view.

From Figures 12 to 15, it can be seen that the most favored reaction pathway leading to 6-MR products after the generation of **3a** requires activation free energies (calculated as the Gibbs free energy needed to reach **TS(4**→**5)** from **3a**) of 21.0, 23.3, 20.3, and 23.5 kcal·mol⁻¹ for X = OH, NH₂, OCH₃, and N(CH₃)₂, respectively. The activation free energies for the generation of 5-MR products are slightly lower (19.2, 21.1, 17.5, and 19.5 kcal·mol⁻¹ in the same order corresponding to the barrier **TS(3a**→**9)**) than those for 6-MR products. This could explain why the generation of 6- and 5-MR products is very competitive for phenylcarbenes. In addition, in the case of dimethylaminophenylcarbene (Figure 15), route C (cyclopentannulation) is favored over route A (Dötz benzannulation pathway) by the highest difference (4 kcal·mol⁻¹), which is in good agreement with the experimental observation that cyclopentannulation is particularly favored in this case.^{13,14,27,31}

As a whole, from a kinetic point of view, our results show that in all cases there are operative routes leading to 6- and 5-MR products with energy barriers smaller than the initial CO loss and, therefore, both 6- and 5-MR products are kinetically feasible for all Fischer carbenes analyzed. Reaction pathways leading to 6-MR products have smaller barriers than those yielding 5-MRs for vinylcarbenes, whereas the opposite holds for phenylcarbenes in agreement with experimental findings. From a thermodynamic point of view, 6-MR products are generally favored over 5-MR adducts (especially for vinylcarbenes and alkoxy-carbenes), although for the dimethylaminophenylcarbene complex the difference between 6- and 5-MR formation is negligible. Thus we obtain that bulky X substituents with high π -donor character reduce the thermodynamic stability difference between the 5- and 6-MR products. Our results show that the reaction mechanism is complex with many accessible intermediates and TSs and the kinetic and thermodynamic driving forces are similar for routes A and C in phenylcarbenes, although kinetically route C is somewhat favored. In this situation, minor modifications in the reaction conditions can lead to very different product distributions. For instance, the experimental product distribution²¹ in the case of the Dötz reaction between 3-hexyne and [pentacarbonyl(methoxyphenyl)-chromium(0)]carbene 0.005 M in THF at 45 °C is 88% of quinone and less than 1% of indene. When CH₃CN is used as solvent instead of THF, the percentages change to 24% and 14%, respectively.

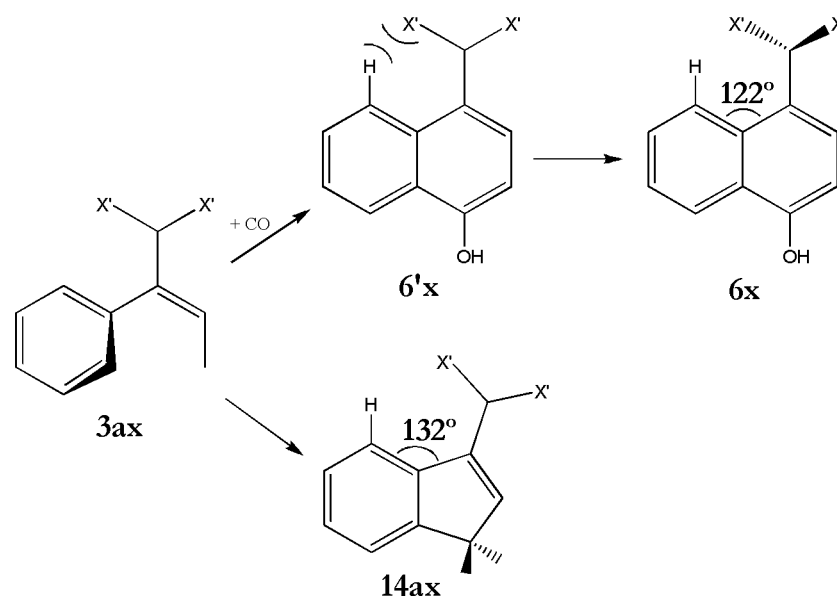


Figure 19. Steric hindrance found in aminocarbenes in the benzannulation product **6x** ($\text{Cr}(\text{CO})_3$ is omitted here for the sake of clarity). **6'x** tends to migrate to **6x** intermediate to avoid $\text{X}'\text{-H}$ repulsion ($\text{X}' = \text{H}, \text{CH}_3$).

Finally, for benzannulated product **6** the phenyl substituent also opens the possibility to exchange the tricarbonylchromium unit between rings like for the case of 5-MRs in cyclopentannulation reactions discussed above. Figure 20 exemplifies the haptotropic rearrangement for the [tricarbonyl(4-naphthohydroquinone)chromium(0)] species and Table 5 lists the energetic data computed for both haptoisomers. Recently, we have reported on the reaction mechanisms found for the haptotropic migrations in a series of small linear, kinked, fused, and curved polycyclic aromatic hydrocarbons coordinated to a Cr(CO)₃ tripod.^{74,75} We had not considered yet the haptotropic migrations between a functional-group substituted ring (**6**) and a non-substituted fused one (**7**) until now. As found experimentally in similar cases,⁷⁶ coordination to the non-substituted ring is more favorable than coordination to the substituted ring. In terms of relative energies with respect to **6** complex, the stability of **7** increases marginally from -OH to -OCH₃ substituents and decreases from -NH₂ to -N(CH₃)₂ ligands. TSs correspond more to η^2 - than η^1 -structures and are akin to that found for naphthalene.⁷⁴ The TS is structurally closer to the more substituted ring and not exactly at the half of the distance between ring centers as expected from the Hammond's postulate.⁷⁷ In the same way as for the naphthalene case,⁷⁵ no intermediates were located on the route from **6**→**7**. The barriers found of about 20 kcal·mol⁻¹ are in perfect agreement with those found experimentally in molecules having the same naphthohydroquinone skeleton but different substituents on the substituted ring.⁷⁶ Although haptotropic migration is only symmetric for 4-naphthohydroquinone, other substitutions in *para*-position do not seem to affect energetically the preference of Cr(CO)₃ to move from one side or the other onto the less-substituted ring. A very small difference is noted for the amino side in 4-dimethylamine-1-naphthol where the organic skeleton adopted the **6x** spatial orientation showed in Figure 19 but no amino-interaction was observed as a possible stabilizing factor. It seems that the barrier for haptomigration is not very sensitive to neither electronic nor steric effects induced by substituents.

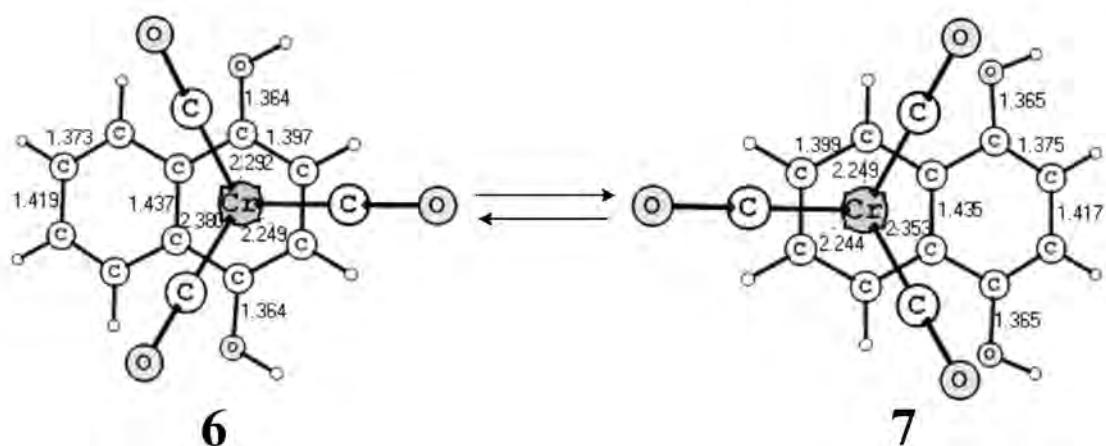
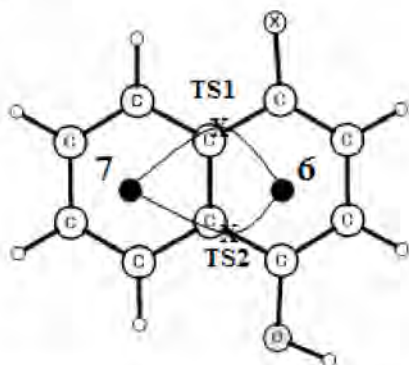


Figure 20. Haptotropic rearrangement reaction found when R = Ph for the benzannulated product **6** (for the case of X = OH). Distances are in Å and angles in degrees.

Table 5. Reaction Gibbs free-energies and activation barriers for all the haptotropic rearrangements resulted in the naphthol derivative **6** (for R = Ph), calculated at B3LYP/(Wachters' basis, 6-31G(d,p)) level. All energies are in kcal·mol⁻¹.



X	OH	NH ₂	OCH ₃	N(CH ₃) ₂
6 → 7	-3.3	-3.6	-3.7	-3.4
TS1 (6 → 7)	21.7	19.7	21.2	21.1
TS2 (6 → 7)	21.7	19.7	21.2	21.7

Dötz and coworkers have suggested that these haptotropic migrations can be used as novel organometallic molecular switches,⁷⁸ where this rearrangement has been tuned depending on whether reaction conditions or photoinduction are applied into these

chemical species. They have also reviewed a variety of benzannulation reactions where this haptotropic migration plays an important role in the synthesis and regioselectivity of organic compounds.¹⁴ Thus, this last step is one of the most interesting stages of the Dötz benzannulation reaction since an initial choice/preparation of the Fischer carbene can derive into a regioselective haptoisomer complex in a systematic procedure of synthesis. We hope the present work will stimulate experimental organic research in the future when considering mechanistic aspects of this fascinating organometallic reaction.

3.3 Concluding Remarks.

Classical chromium-mediated Dötz benzannulation proposal has been examined here for some representative Fischer carbenes via acetylene insertion together with other competitive reaction mechanisms. The benzannulation and cyclopentannulation reactions are very exothermic and exergonic (30 – 50 kcal·mol⁻¹). Our results indicate that reactions leading to benzannulated and cyclopentannulated products are more exothermic in vinyl- than phenylcarbenes and also more exothermic for alkoxy- as compared to aminocarbenes.

The present study confirms that the CO loss in the initial part of the reaction is the rate-limiting step of reaction. For phenylcarbenes, the dissociative pathway corresponding to loss of CO prior acetylene addition is the most plausible route to phenylcarbenes **3a** since it has lower enthalpy barriers than the associative path (first addition of acetylene followed by CO loss). In the case of vinylcarbenes, both the dissociative and associative pathways can be operative since they have similar energy requirements.

From the two postulated reaction pathways leading to 6-MR products studied here, we have found that the reaction mechanism followed depends on the kind of Fischer carbenes used. Thus, vinylcarbenes explain better this reaction through a chromahexatriene intermediate route whereas phenylcarbenes are best rationalized to undergo benzannulation through Dötz reaction mechanism. From a thermodynamic point of view, 6-MR products are generally favored over 5-MR adducts, especially in the case of vinylcarbenes and alkoxy-carbenes, although for the dimethylaminophenylcarbene complex the difference between 6- and 5-MR formation is negligible. Thus, bulky X substituents with high π -donor character reduce the thermodynamic stability difference between 5- and 6-MR products. From a kinetic point of view, our results show that in all cases there are operative routes leading to the 6- and 5-MR products with smaller energy barriers than the initial CO loss. Starting from complex **3a** as the ramification point, it is found that 6-MR formation is favored in the case of vinylcarbenes, while 5-MR production is preferred in the case of

phenylcarbenes. It has been found that differences in barriers for CO insertion (**8**→**5** in vinylcarbenes and **3b**→**4** in phenylcarbenes) between alkoxy and amino groups are small and not critical to explain the differences found in the 5- and 6-MR formation ratio.

Finally, we discussed the last but not less important step in Dötz benzannulation reaction of phenylcarbenes corresponding to the haptotropic rearrangement. In this rearrangement, the $\text{Cr}(\text{CO})_3$ tripod migrates from the functional-group substituted aromatic ring to the non-substituted one.

APPENDIX

Table A1. Performance of different basis sets and selected density-functionals in the relative energies (enthalpy, ΔH_{298}^0 , and free-energy, ΔG_{298}^0) of the decarbonylation step (**1**→**2a**) for $\text{Cr}(\text{CO})_5\text{Cr}=\text{C}(\text{X})\text{CHCH}_2$ carbenes. Reaction energies are expressed in kcal mol^{-1} .

B3LYP/basis set	X= OH		X= NH ₂	
	1 → 2a		1 → 2a	
	$\Delta\mathbf{H}$	$\Delta\mathbf{G}$	$\Delta\mathbf{H}$	$\Delta\mathbf{G}$
Wachters/6-31G(d,p)	34.4	23.2	34.5	21.3
6-311G(d,p)	34.3	22.7	33.4	22.5
TZVP	32.3	20.6	31.5	20.4
Stuttgart	39.7	28.1	39.0	27.7
CEP-31G	6.1	-5.6	5.3	-5.9
BP86/basis set				
Wachters/6-31G(d,p)	41.0	29.5	40.3	29.6
6-311G(d,p)	41.1	29.8	40.1	29.2
TZVP	39.3	27.5	38.4	27.6
Stuttgart	45.5	34.0	44.7	34.7
CEP-31G	15.9	4.0	15.0	3.9
PBE0 ^a	40.7	29.5	40.2	29.2
OLYP ^a	32.2	21.0	31.7	20.7
BB95 ^a	41.2	29.3	40.5	29.5

^aBasis set used: Wachters/6-31G(d,p)

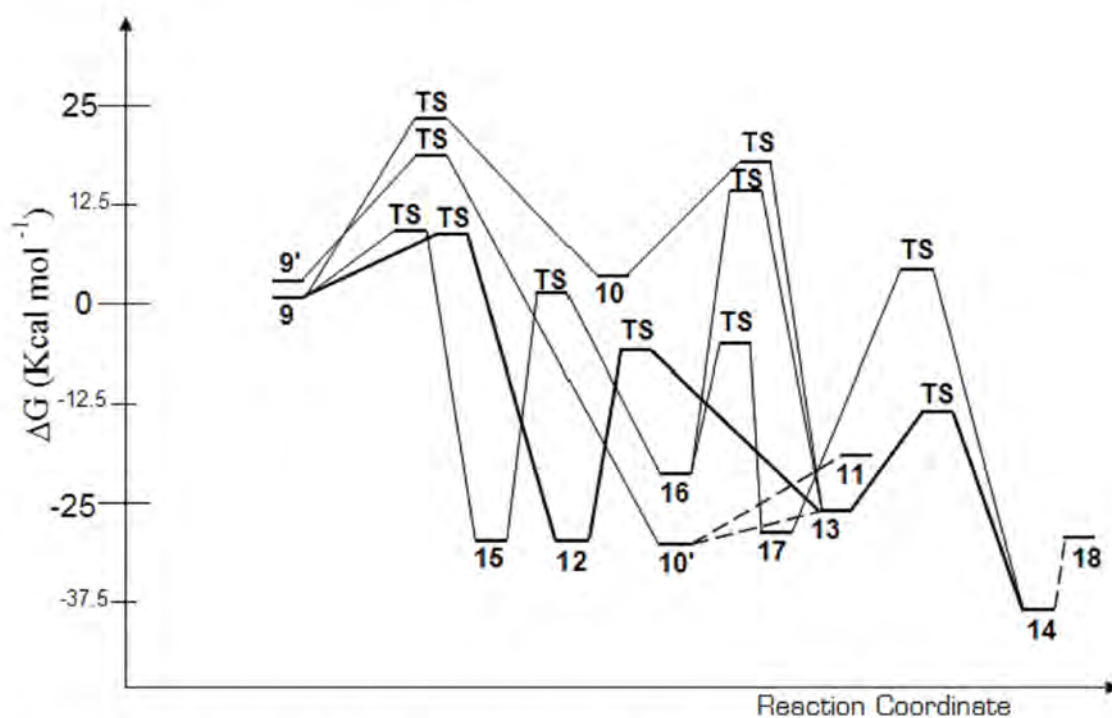


Figure A1. Energy profiles of all the routes explored for cyclopentannulation reaction mechanism in $(\text{CO})_5\text{Cr}=\text{C}(\text{OH})\text{Ph}$ Fischer carbene. Solid lines are connecting transition states with minima whereas dotted lines are just indicating the pathways established in Scheme 18.

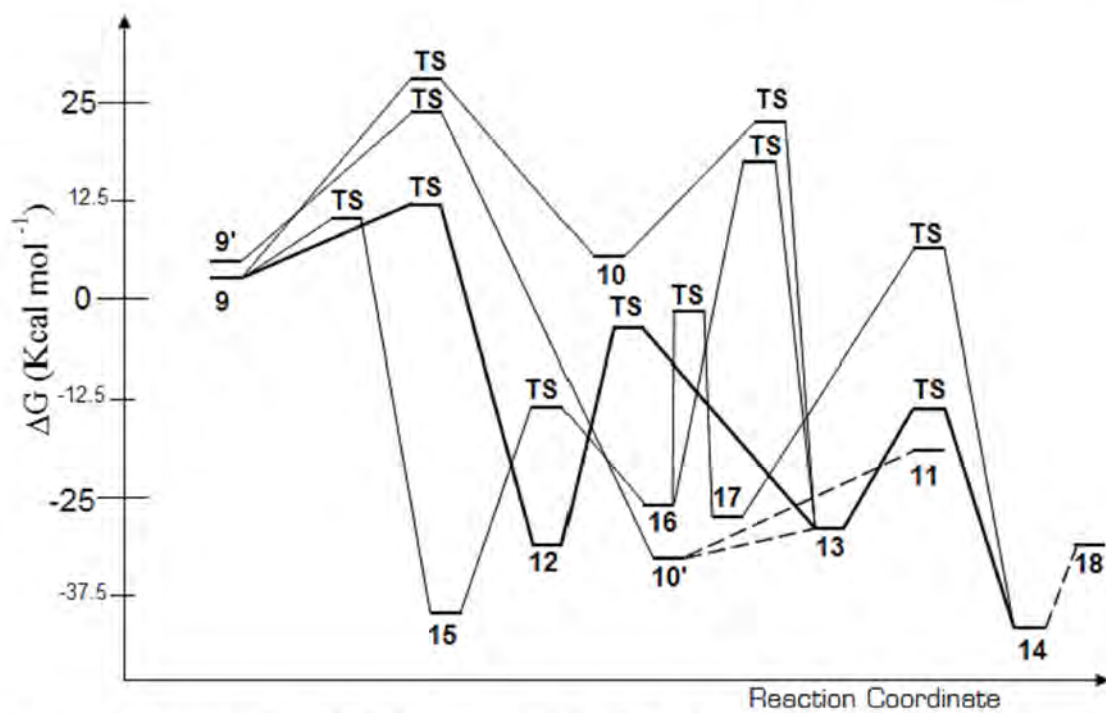


Figure A2. Energy profiles of all the routes explored for cyclopentannulation reaction mechanism in $(\text{CO})_5\text{Cr}=\text{C}(\text{NH}_2)\text{Ph}$ Fischer carbene. Solid lines are connecting transition states with minima whereas dotted lines are just indicating the pathways established in Scheme 18.

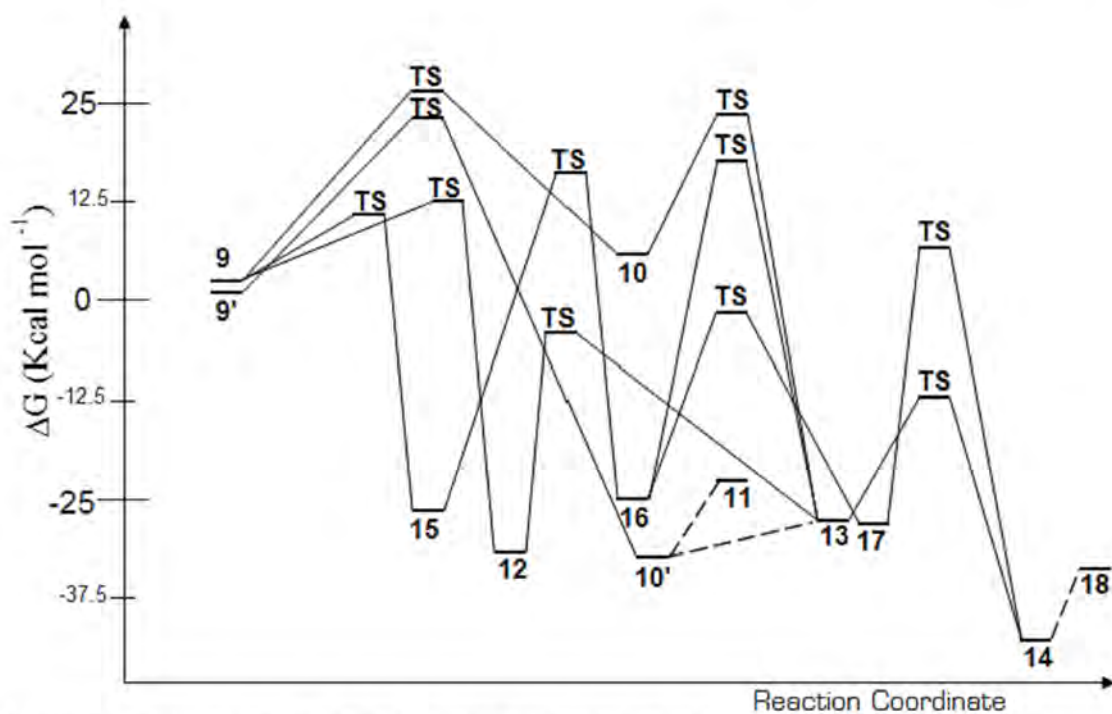


Figure A4. Energy profiles of all the routes explored for cyclopentannulation reaction mechanism in $(\text{CO})_5\text{Cr}=\text{C}(\text{N}(\text{CH}_3)_2)\text{Ph}$ Fischer carbene. Solid lines are connecting transition states with minima whereas dotted lines are just indicating the pathways established in Scheme 18.

References.

- (1) E. O. Fischer, A. Maasböl, *Angew. Chem. Int. Ed. Eng.* **1964**, *3*, 580.
- (2) (a) C. F. Bernasconi, *Chem. Soc. Rev.* **1997**, *26*, 299; (b) D. Bourissou, O. Guerret, F. P. Gabbaï, G. Bertrand, *Chem. Rev.* **2000**, *100*, 39; (c) F. Z. Dörwald, *Metal Carbenes in Organic Synthesis*; Wiley-VCH: Weinheim, **1999**; (d) J. W. Herndon, *Coord. Chem. Rev.* **2005**, *249*, 999; (e) W. Kirmse, *Eur. J. Org. Chem.* **2005**, 237; (f) M. F. Lappert, *J. Organomet. Chem.* **2005**, *690*, 5467; (g) A. Minatti, K. H. Dötz, *Metal Carbenes in Organic Synthesis*; Springer-Verlag: Berlin, Heidelberg, **2004**; Vol. 13; (h) T. Strassner, *Topics Organomet. Chem.* **2004**, *13*, 1; (i) W. D. Wulff, *Advances in Metal-Organic Chemistry*; JAI Press: Greenwich, CT, **1989**; Vol. 1; (j) W. D. Wulff, *Comprehensive Organometallic Chemistry II*; Pergamon: Oxford, **1995**; Vol. 12.
- (3) G. Frenking, M. Solà, S. F. Vyboishchikov, *J. Organomet. Chem.* **2005**, *690*, 6178.
- (4) M. Cases, G. Frenking, M. Duran, M. Solà, *Organometallics* **2002**, *21*, 4182.
- (5) J. Barluenga, *Pure & Appl. Chem.* **1996**, *68*, 543.
- (6) J. Poater, M. Cases, X. Fradera, M. Duran, M. Solà, *Chem. Phys.* **2003**, *294*, 129.
- (7) (a) C. P. Casey, R. L. Anderson, *J. Am. Chem. Soc.* **1971**, *93*, 3554; (b) C. P. Casey, R. L. Anderson, *J. Chem. Soc., Chem. Commun.* **1975**, 895.
- (8) (a) J. Barluenga, F. J. Fañanás, *Tetrahedron* **2000**, *56*, 4597; (b) A. de Meijere, H. Schirmer, M. Duetsch, *Angew. Chem. Int. Ed.* **2000**, *39*, 3964; (c) M. A. Sierra, *Chem. Rev.* **2000**, *100*, 3591.
- (9) J. Barluenga, J. Santamaría, M. Tomás, *Chem. Rev.* **2004**, *104*, 2259.
- (10) J. W. Herndon, *Tetrahedron* **2000**, *56*, 1257.
- (11) K. H. Dötz, *Angew. Chem. Int. Ed. Eng.* **1975**, *14*, 644.
- (12) D. F. Harvey, D. M. Sigano, *Chem. Rev.* **1996**, *96*, 271.
- (13) K. H. Dötz, P. Tomuschat, *Chem. Soc. Rev.* **1999**, *28*, 187.
- (14) K. H. Dötz, B. Wenzel, H. C. Jahr, *Top. Curr. Chem.* **2004**, *248*, 63.
- (15) (a) D. L. Boger, O. Huter, K. Mbiya, M. S. Zhang, *J. Am. Chem. Soc.* **1995**, *117*, 11839; (b) S. A. Eastham, J. Herbert, S. P. Ingham, P. Quayle, M. Wolfendale, *Tetrahedron Lett.* **2006**, *47*, 6627; (c) S. A. Eastham, S. P. Ingham, M. R. Hallett, J. Herbert, P. Quayle, J. Raftery, *Tetrahedron Lett.* **2006**, *47*, 2299; (d)

- R. A. Fernandes, V. P. Chavan, *Tetrahedron Lett.* **2008**, *49*, 3899; (e) R. A. Fernandes, V. P. Chavan, A. B. Ingle, *Tetrahedron Lett.* **2008**, *49*, 6341; (f) M. Rawat, W. D. Wulff, *Org. Lett.* **2004**, *6*, 329; (g) W. R. Roush, R. J. Neitz, *J. Org. Chem.* **2004**, *69*, 4906; (h) W. D. Wulff, P.-C. Tang, *J. Am. Chem. Soc.* **1984**, *106*, 434.
- (16) (a) J. C. Anderson, R. M. Denton, H. G. Hickin, C. Wilson, *Tetrahedron* **2004**, *60*, 2327; (b) M. W. Giese, W. H. Möser, *J. Org. Chem.* **2005**, *70*, 6222; (c) A. Minatti, K. H. Dötz, *J. Org. Chem.* **2005**, *70*, 3745; (d) S. R. Pulley, B. Czako, *Tetrahedron Lett.* **2004**, *45*, 5511; (e) M. X.-W. Jiang, M. Rawat, W. D. Wulff, *J. Am. Chem. Soc.* **2004**, *126*, 5970.
- (17) (a) K. H. Dötz, W. Kuhn, *Angew. Chem. Int. Ed. Eng.* **1983**, *22*, 732; (b) K. H. Dötz, I. Pruskil, *J. Organomet. Chem.* **1981**, *209*, C4; (c) K. H. Dötz, I. Pruskil, J. Muhlemeier, *Chem. Ber.* **1982**, *115*, 1278; (d) A. Gupta, S. Sen, M. Harmata, S. R. Pulley, *J. Org. Chem.* **2005**, *70*, 7422; (e) S. R. Pulley, B. Czako, G. D. Brown, *Tetrahedron Lett.* **2005**, *46*, 9039; (f) J. D. White, H. Smits, *Org. Lett.* **2005**, *7*, 235; (g) E. Janes, M. Nieger, P. Saarenketo, K. H. Dötz, *Eur. J. Org. Chem.* **2003**, 2276.
- (18) (a) W. D. Wulff, B. M. Bax, T. A. Brandvold, K. S. Chan, A. M. Gilbert, R. P. Hsung, J. Mitchell, J. Clardy, *Organometallics* **1994**, *13*, 102.
- (19) (a) B. Alcaide, L. Casarrubios, G. Domínguez, M. A. Sierra, J. Jiménez-Barbero, *Organometallics* **1994**, *13*, 2934; (b) A. de Meijere, H. Schirner, F. Stein, F. Funke, M. Duetsch, Y. T. Wu, M. Noltemeyer, T. Belgardt, B. Knieriem, *Chem. Eur. J.* **2005**, *11*, 4132; (c) A. Longen, M. Nieger, K. Airola, K. H. Dotz, *Organometallics* **1998**, *17*, 1538; (d) A. Parlier, M. Rudler, H. Rudler, R. Goumont, J.-C. Daran, J. Vaissermann, *Organometallics* **1995**, *14*, 2760; (e) B. C. G. Söderberg, J. A. Shriver, S. H. Cooper, T. L. Shrout, E. S. Helton, L. R. Austin, H. H. Odens, B. R. Hearn, P. C. Jones, T. N. Kouadio, T. H. Ngi, R. Baswell, H. J. Caprara, M. D. Meritt, T. T. Mai, *Tetrahedron* **2003**, *59*, 8775; (f) W. D. Wulff, P.-C. Tang, K. S. Chan, J. S. McCallum, D. C. Yang, S. R. Gilbertson, *Tetrahedron* **1985**, *41*, 5813.
- (20) K. H. Dötz, *Angew. Chem. Int. Ed. Eng.* **1984**, *23*, 587.
- (21) M. E. Bos, W. D. Wulff, R. A. Miller, S. Chamberlin, T. A. Brandvold, *J. Am. Chem. Soc.* **1991**, *113*, 9293.

- (22) M. L. Waters, T. A. Brandvold, L. Isaacs, W. D. Wulff, A. L. Rheingold, *Organometallics* **1998**, *17*, 4298.
- (23) (a) M. J. S. Dewar, *Bull. Soc. Chim. Fr. (Paris)* **1951**, *18*, C79; (b) J. Chatt, J. S. Duncanson, *J. Chem. Soc.* **1953**, 2929.
- (24) E. Matito, M. Solà, *Coord. Chem. Rev.* **2009**, *253*, 647.
- (25) Y.-T. Wu, T. Kurahashi, A. de Meijere, *J. Organomet. Chem.* **2005**, *690*, 5900.
- (26) (a) J. Barluenga, R. Vicente, P. Barrio, L. A. López, M. Tomás, *J. Am. Chem. Soc.* **2004**, *126*, 5974; (b) H. Rudler, A. Parlier, M. P. Peregrina, J. Vaissermann, *Organometallics* **2005**, *24*, 1.
- (27) B. L. Flynn, H. Schirmer, M. Duetsch, A. de Meijere, *J. Org. Chem.* **2001**, *66*, 1747.
- (28) J. Barluenga, L. A. López, S. Martínez, M. Tomás, *Tetrahedron* **2000**, *56*, 4967.
- (29) J. Barluenga, L. A. López, S. Martínez, M. Tomás, *J. Org. Chem.* **1998**, *63*, 7588.
- (30) C. Hansch, A. Leo, R. W. Taft, *Chem. Rev.* **1991**, *91*, 165.
- (31) J. Barluenga, F. Aznar, I. Gutiérrez, A. Martín, S. García-Granda, M.A. Llorca-Baragaño, *J. Am. Chem. Soc.* **2000**, *122*, 1314.
- (32) (a) J. Barluenga, *Pure & Appl. Chem.* **2002**, *74*, 1317; (b) J. Barluenga, M. A. Fernández-Rodríguez, E. Aguilar, *J. Organomet. Chem.* **2005**, *690*, 539; (c) A. de Meijere, *Pure & Appl. Chem.* **1996**, *68*, 61; (d) C. B. de Koning, A. L. Rousseau, W. A. L. van Otterlo, *Tetrahedron* **2003**, *59*, 7.
- (33) K. H. Dötz, *Pure & Appl. Chem.* **1983**, *55*, 1689.
- (34) M. Torrent, M. Solà, G. Frenking, *Chem. Rev.* **2000**, *100*, 439.
- (35) M. A. Sierra, I. Fernández, F. P. Cossío, *Chem. Commun.* **2008**, 4671.
- (36) M. Torrent, M. Duran, M. Solà, *Chem. Commun.* **1998**, 999.
- (37) M. Torrent, M. Duran, M. Solà, *Organometallics* **1998**, *17*, 1492.
- (38) M. Torrent, M. Duran, M. Solà, *J. Am. Chem. Soc.* **1999**, *121*, 1309.
- (39) M. M. Gleichmann, K. H. Dötz, B. A. Hess, *J. Am. Chem. Soc.* **1996**, *118*, 10551.
- (40) (a) P. Hofmann, M. Hämmerle, *Angew. Chem. Int. Ed. Eng.* **1989**, *28*, 908; (b) P. Hofmann, M. Hämmerle, G. Unfried, *New J. Chem.* **1991**, *15*, 769.
- (41) W. D. Wulff, *Comprehensive Organic Synthesis*; Pergamon: New York, **1991**; Vol. 5.
- (42) H. Fischer, P. Hofmann, *Organometallics* **1999**, *18*, 2590.

- (43) H. Fischer, J. Mühlemeier, R. Märkl, K. H. Dötz, *Chem. Ber.-Recl.* **1982**, *115*, 1355.
- (44) H. Fischer, J. Hofmann, E. Mauz, *Angew. Chem. Int. Ed. Eng.* **1991**, *30*, 998.
- (45) M. L. Waters, M. E. Bos, W. D. Wulff, *J. Am. Chem. Soc.* **1999**, *121*, 6403.
- (46) C. P. Casey, *Reactive Intermediates*; Wiley: New York, **1981**; Vol. 2.
- (47) M. Solà, M. Duran, M. Torrent, *Computational Modeling of Homogeneous Catalysis*; Kluwer Academic: Amsterdam, **2002**; Vol. 25.
- (48) F. Z. Dörwald, *Angew. Chem. Int. Ed.* **2003**, *42*, 1332.
- (49) (a) J. Barluenga, F. Aznar, M.A. Palomero, *J. Org. Chem.* **2003**, *68*, 537; (b) J. Barluenga, S. Martínez, A.L. Suárez-Sobrino, M. Tomás, *Organometallics* **2006**, *25*, 2337; (c) J.W. Zhang, Y.S. Zhang, W.F.K. Schnatter, J.W. Herndon, *Organometallics* **2006**, *25*, 1279.
- (50) M. J. Frisch, G. W. Trucks, H. B. Schlegel, G. E. Scuseria, M. A. Robb, J. R. Cheeseman, J. A. Montgomery Jr., T. Vreven, K. N. Kudin, J. C. Burant, J. M. Millam, S. S. Iyengar, J. Tomasi, V. Barone, B. Mennucci, M. Cossi, G. Scalmani, N. Rega, G. A. Petersson, H. Nakatsuji, M. Hada, M. Ehara, K. Toyota, R. Fukuda, J. Hasegawa, M. Ishida, T. Nakajima, Y. Honda, O. Kitao, H. Nakai, M. Klene, X. Li, J. E. Knox, H. P. Hratchian, J. B. Cross, C. Adamo, J. Jaramillo, R. Gomperts, R. E. Stratmann, O. Yazyev, A. J. Austin, R. Cammi, C. Pomelli, J. Ochterski, P. Y. Ayala, K. Morokuma, G. A. Voth, P. Salvador, J. J. Dannenberg, V. G. Zakrzewski, S. Dapprich, A. D. Daniels, M. C. Strain, O. Farkas, D. K. Malick, A. D. Rabuck, K. Raghavachari, J. B. Foresman, J. V. Ortiz, Q. Cui, A. G. Baboul, S. Clifford, J. Cioslowski, B. B. Stefanov, G. Liu, A. Liashenko, P. Piskorz, I. Komaromi, R. L. Martin, D. J. Fox, T. Keith, M. Al-Laham, C. Peng, A. Nanayakkara, M. Challacombe, P. M. W. Gill, B. G. Johnson, W. Chen, M. W. Wong, C. González, J. A. Pople, *Gaussian 03, rev. B03*, Pittsburgh, PA, **2003**.
- (51) (a) A. D. Becke, *J. Chem. Phys.* **1993**, *98*, 5648; (b) C. T. Lee, W. T. Yang, R. G. Parr, *Phys. Rev. B* **1988**, *37*, 785.
- (52) (a) J. S. Binkley, J. A. Pople, W. J. Hehre, *J. Am. Chem. Soc.* **1980**, *102*, 939; (b) M. S. Gordon, J. S. Binkley, J. A. Pople, W. J. Pietro, W. J. Hehre, *J. Am. Chem. Soc.* **1982**, *104*, 2797; (c) W. J. Pietro, M. M. Francl, W. J. Hehre, D. J. Defrees, J. A. Pople, J. S. Binkley, *J. Am. Chem. Soc.* **1982**, *104*, 5039.
- (53) A. J. Wachters, *J. Chem. Phys.* **1970**, *52*, 1033.

- (54) C. Y. Peng, P. Y. Ayala, H. B. Schlegel, M. J. Frisch, *J. Comput. Chem.* **1996**, *17*, 49.
- (55) C. Y. Peng, H. B. Schlegel, *Israel J. Chem.* **1994**, *33*, 449.
- (56) (a) C. González, H. B. Schlegel, *J. Chem. Phys.* **1989**, *90*, 2154; (b) C. González, H. B. Schlegel, *J. Phys. Chem.* **1990**, *94*, 5523.
- (57) H. Jacobsen, G. Schreckenbach, T. Ziegler, *J. Phys. Chem.* **1994**, *98*, 11406.
- (58) (a) T. F. Block, R. F. Fenske, C. P. Casey, *J. Am. Chem. Soc.* **1976**, *98*, 441; (b) D. J. Cardin, B. Çetinkaya, M. J. Doyle, M. F. Lappert, *Chem. Soc. Rev.* **1973**, *2*, 99; (c) C.-C. Wang, Y. Wang, H.-J. Liu, K.-J. Lin, L.-K. Chou, K.-S. Chan, *J. Phys. Chem. A* **1997**, *101*, 8887.
- (59) C. G. Kreiter, E. O. Fischer, *Angew. Chem. Int. Ed. Eng.* **1969**, *8*, 761.
- (60) I. Fernández, F. P. Cossío, A. Arrieta, B. Lecea, M. J. Mancheño, M. A. Sierra, *Organometallics* **2004**, *23*, 1065.
- (61) (a) H. Jacobsen, T. Ziegler, *Organometallics* **1995**, *14*, 224; (b) H. Jacobsen, T. Ziegler, *Inorg. Chem.* **1996**, *35*, 775.
- (62) C. P. Casey, M. C. Cesa, *Organometallics* **1982**, *1*, 87.
- (63) M. Solà, T. Ziegler, *Organometallics* **1996**, *15*, 2611.
- (64) F. Hohmann, S. Siemoneit, M. Nieger, S. Kotila, K. H. Dötz, *Chem. Eur. J.* **1997**, *3*, 853.
- (65) G. M. Bancroft, K. D. Butler, L. E. Manzer, A. Shaver, J. E. H. Ward, *Can. J. Chem.* **1974**, *52*, 782.
- (66) J. R. Knorr, T. L. Brown, *Organometallics* **1994**, *13*, 2178.
- (67) (a) J. N. Bechara, S. E. J. Bell, J. J. McGarvey, J. J. Rooney, *J. Chem. Soc. - Chem. Commun.* **1986**, 1785; (b) H. C. Foley, L. M. Strubinger, T. S. Targos, G. L. Geoffroy, *J. Am. Chem. Soc.* **1983**, *105*, 3064.
- (68) J. Barluenga, F. Aznar, A. Martín, S. García-Granda, E. Pérez-Carreño, *J. Am. Chem. Soc.* **1994**, *116*, 11191.
- (69) (a) K. H. Dötz, B. Fügen-Köster, *Chem. Ber.* **1980**, *113*, 1449; (b) B. A. Anderson, W. D. Wulff, A. L. Rheingold, *J. Am. Chem. Soc.* **1990**, *112*, 8615; (c) W. A. Herrmann, J. Gimeno, J. Weichmann, M. L. Ziegler, B. Balbach, *J. Organomet. Chem.* **1981**, *213*, C26.
- (70) R. Aumann, *Eur. J. Org. Chem.* **2000**, 17.
- (71) W. D. Wulff, A. M. Gilbert, R. P. Hsung, A. Rahm, *J. Org. Chem.* **1995**, *60*, 4566.

- (72) K. H. Dötz, *Organometallics in Organic Synthesis: Aspects of a Modern Interdisciplinary Field*, Springer: Berlin, **1988**.
- (73) H. Kagoshima, T. Okamura, T. Akiyama, *J. Am. Chem. Soc.* **2001**, *123*, 7182.
- (74) J. O. C. Jimenez-Halla, J. Robles, M. Solà, *J. Phys. Chem. A* **2008**, *112*, 1202.
- (75) J. O. C. Jimenez-Halla, J. Robles, M. Solà, *Organometallics* **2008**, *27*, 5230.
- (76) (a) H. C. Jahr, M. Nieger, K. H. Dötz, *Chem. Commun.* **2003**, 2866; (b) H. C. Jahr, M. Nieger, K. H. Dötz, *Chem. Eur. J.* **2005**, *11*, 5333.
- (77) G. S. Hammond, *J. Am. Chem. Soc.* **1955**, *77*, 334.
- (78) K. H. Dötz, H. C. Jahr, *Chem. Rec.* **2004**, *4*, 61.

CHAPTER 4

REACTIVITY OF
 TpRu(L)(NCMe)R (L= CO;
R= Me, Ph) SYSTEMS
WITH ISONITRILES

John P. Lee, J. Oscar C. Jimenez-Halla, Thomas R. Cundari and T. Brent Gunnoe.
“Reactivity of TpRu(L)(NCMe)R (L = CO, PMe₃; R = Me, Ph) systems with isonitriles: Experimental and computational studies toward the intra- and intermolecular hydroarylation of isonitriles”. *Journal of Organometallic Chemistry*.
Vol. 692, issue 11 (1 May 2007) : p. 2175-2186.

[doi:10.1016/j.jorganchem.2007.01.037](https://doi.org/10.1016/j.jorganchem.2007.01.037)

Department of Chemistry, North Carolina State University, Raleigh, NC 27695-8204, United States

Center for Advanced Scientific Computing and Modeling (CASCaM), Department of Chemistry, University of North Texas, Box 305070, Denton, TX 76203-5070, United States

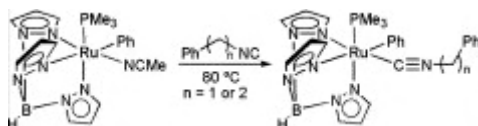
Received 21 December 2006; revised 22 January 2007; accepted 22 January 2007.
Available online 30 January 2007.

Abstract

The Ru(II) phenyl complex TpRu(PMe₃)(NCMe)Ph {Tp = hydridotris(pyrazolyl)borate} reacts with isonitriles to form complexes of the type TpRu(PMe₃)(C≡NR)Ph (R = ^tBu, CH₂Ph, CH₂CH₂Ph). Neither thermal nor photolytic reactions of these systems with excess isonitrile and benzene resulted in the production of corresponding imines. DFT studies that probed the energetics of the desired catalytic transformations revealed that (Tab)Ru(PH₃)(C≡NCH₂CH₂Ph)Ph {Tab = tris(azo)borate} is the most stable species in a proposed catalytic cycle. Exclusive of calculated transition states, the highest points on the calculated free energy surface are 34 kcal/mol, for (Tab)Ru(PH₃)(*o*,η²-C,C-CNCH₂CH₂Ph)Ph {relative to the starting material (Tab)Ru(PH₃)(C≡NCH₂CH₂Ph)Ph}, and 27 kcal/mol for the C–H activation product (Tab)Ru(PH₃)(*o*-C₆H₄CH₂CH₂NC) and benzene. The substantial increases in free energy result primarily from the loss of the stable ruthenium–η¹-isonitrile interaction.

Graphical abstract

The Ru(II) phenyl complex $\text{TpRu}(\text{PMe}_3)(\text{NCMe})\text{Ph}$ {Tp = hydridotris(pyrazolyl)borate} reacts with isocyanides to form complexes of the type $\text{TpRu}(\text{PMe}_3)(\text{C}\equiv\text{NR})\text{Ph}$ ($\text{R} = t\text{Bu}, \text{CH}_2\text{Ph}, \text{CH}_2\text{CH}_2\text{Ph}$). Consistent with experimental studies, DFT calculations revealed that intramolecular hydroarylation of β -phenethylisonitrile to produce imine is a high energy process due to the strong coordinating nature of the isocyanide.



Keywords: Ruthenium; Hydroarylation; Isonitrile; Density Functional Theory studies

CHAPTER 5

COORDINATION AND
HAPTOTROPIC
MIGRATION OF $\text{Cr}(\text{CO})_3$
IN POLYCYCLIC
AROMATIC
HYDROCARBONS

J. Oscar C. Jiménez-Halla, Juvencio Robles, and Miquel Solà. "Coordination and Haptotropic Migration of Cr(CO)₃ in Polycyclic Aromatic Hydrocarbons: The Effect of the Size and the Curvature of the Substrate". *Journal of physical chemistry A*. Vol. 112, issue 6 (2008) : p. 1202–1213.

DOI: 10.1021/jp077553h

<http://pubs.acs.org/doi/abs/10.1021/jp077553h>

Institut de Química Computacional and Departament de Química, Universitat de Girona, Campus de Montilivi, 17071 Girona, Catalonia, Spain, and Facultad de Química, Universidad de Guanajuato, Noria Alta s/n 36050 Guanajuato, Gto. Mexico

Abstract

In this work, we study the reaction mechanism of the tricarbonylchromium complex haptotropic rearrangement between two six-membered rings arranged like in naphthalene of four polycyclic aromatic hydrocarbons (PAHs). It has been found that the reaction mechanism of this haptotropic migration can either occur in a single step or stepwise depending on the interaction between the orbitals of the Cr(CO)₃ and the PAH fragments. Our results show that the size of the cyclic system favors the metal migration whereas the curvature of the organic substrate tends to slow down the rearrangement. We discuss the key factors that help to explain this behavior through orbital and energy decomposition analysis.

CHAPTER 6

INTRAMOLECULAR
HAPTOTROPIC
REARRANGEMENTS OF
THE TRICARBONYL-
CHROMIUM COMPLEX
IN SMALL POLYCYCLIC
AROMATIC
HYDROCARBONS

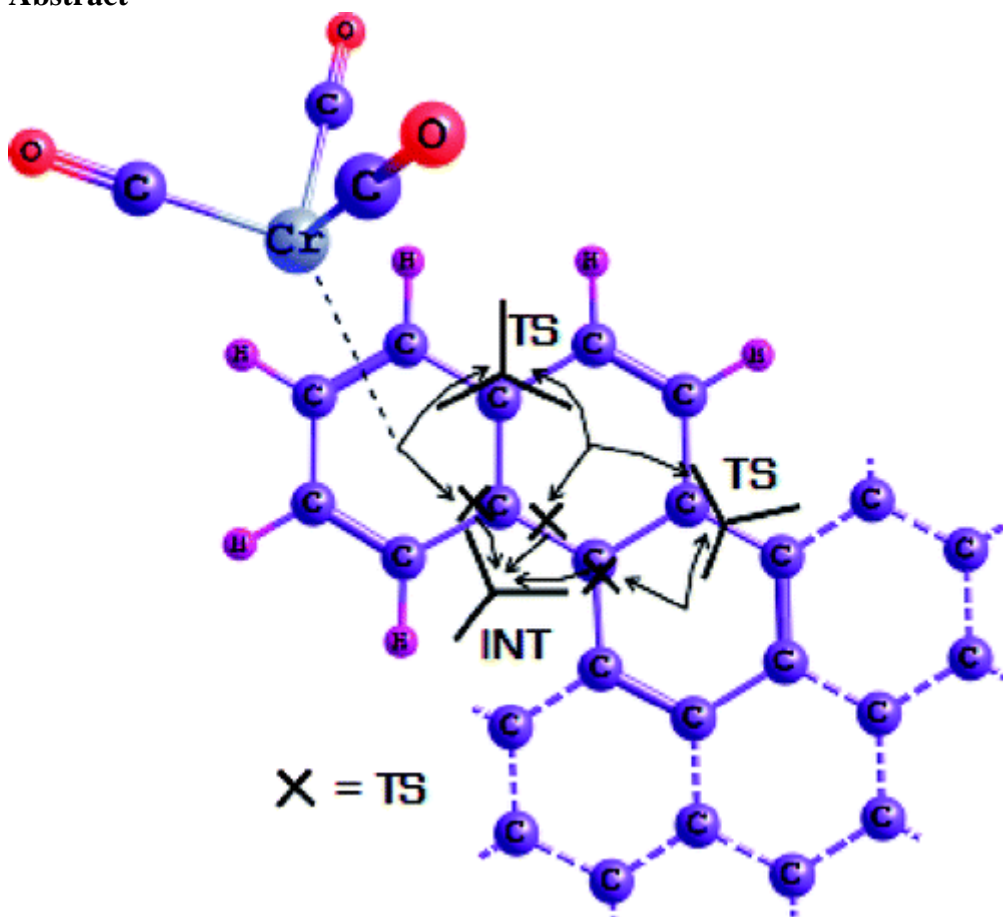
J. Oscar C. Jiménez-Halla, Juvencio Robles and Miquel Solà. "Intramolecular Haptotropic Rearrangements of the Tricarbonylchromium Complex in Small Polycyclic Aromatic Hydrocarbons". *Organometallics*. Vol. 27, issue 20 (Oct. 2008) : p. 5230–5240.

DOI: 10.1021/om800505j

<http://pubs.acs.org/doi/abs/10.1021/om800505j>

Institut de Química Computacional and Department de Química, Universitat de Girona, Campus de Montilivi, 17071 Girona, Catalonia, Spain, and Facultad de Química, Universidad de Guanajuato, Noria Alta s/n 36010 Guanajuato, Gto. Mexico

Abstract



Haptotropic rearrangement reaction mechanisms for a series of polycyclic aromatic hydrocarbons (PAHs) of three and four fused six-membered rings attached to a tricarbonylchromium complex were investigated by theoretical methods. All possible ways by which haptomigrations can occur were explored, as for the less symmetric PAHs there are nonequivalent reaction pathways. The metal complex prefers to be coordinated on the less substituted rings (the more aromatic ones) and tends to avoid the migration to the more substituted ring. A paradigmatic example of this behavior is the case of triphenylene, where the coordination with the outer rings is $17.4 \text{ kcal}\cdot\text{mol}^{-1}$ more favored than complexation with the inner ring. The energy barriers for

haptomigration vary from 16.4 (phenalene) to 24.5 kcal·mol⁻¹ (triphenylene). In general, small energy differences are found between energy barriers of the so-called *exo* and *endo* pathways.

CHAPTER 7

COORDINATION OF
BIS(TRICARBONYL-
CHROMIUM)
COMPLEXES TO SMALL
POLYCYCLIC AROMATIC
HYDROCARBONS:
STRUCTURE, RELATIVE
STABILITIES AND
BONDING

J. Oscar C. Jiménez-Halla, Juvencio Robles, Miquel Solà. "Coordination of bis(tricarbonylchromium) complexes to small polycyclic aromatic hydrocarbons: Structure, relative stabilities, and bonding". *Chemical Physics Letters*. Vol. 465, issues 4-6 (13 november 2008) : p. 181-189.

[doi:10.1016/j.cplett.2008.10.001](https://doi.org/10.1016/j.cplett.2008.10.001)

Institut de Química Computacional and Departament de Química, Universitat de Girona, Campus de Montilivi, 17071 Girona, Catalonia, Spain

Facultad de Química, Universidad de Guanajuato, Noria Alta s/n 36010 Guanajuato, Gto., Mexico

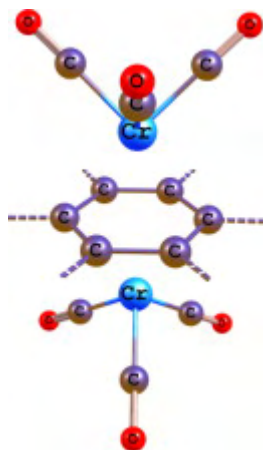
Received 21 July 2008; accepted 1 October 2008; Available online 7 October 2008.

Abstract

Bis(tricarbonylchromium) complexes of two- to four-fused benzenoid rings were investigated by means of the B3LYP method. Our analysis was focused on both the molecular structure of the different isomers and their relative energies. For all the studied cases, the isomer with the lowest energy resulted to be the *anti* where both $\text{Cr}(\text{CO})_3$ units are bonded to the most external rings. According to the calculated dissociation energies for the lowest energy isomers, stabilization due to metal bicomplexation is similar in angular and linear polycyclic aromatic hydrocarbons (PAH), while the less energetically favorable complexation occurs in PAH with a compact arrangement of six-membered rings like in pyrene.

Graphical abstract

Bis(tricarbonylchromium) complexes of small benzenoids were investigated by means of density-functional theory.



CHAPTER 8

DISCUSSION OF RESULTS

From the results obtained in this Thesis, I will discuss the most important aspects learned from Fischer carbene chemistry throughout my last years. It can be divided into two main branches: i) the whole process concerning to the cycloannulation reactions of Fischer carbenes focusing specially on Dötz benzannulation reaction because of the interest in diverse applications already exposed at the Introduction and ii) the last isomerization step of this reaction when more than one ring are present in the final product of cycloaddition. Due to the close relationship with N-heterocyclic carbene (NHC) chemistry, there is also a short study of a somewhat related RNC ligand (R= Me, Ph) or isonitrile that I also explored as a part of this work. In fact, apart of other very interesting and promising topics about phosphino- and thio-carbenes which also deserve to be studied through mechanistic explorations, NHC have demonstrated to possess a similar reactivity like Schrock carbene catalysis.¹ In fact, the advantages of NHCs as ancillary ligands are that: 1) they are stronger σ -donors than alkoxy-carbenes enabling favorable rates of metal catalyzed oxidative addition of aryl complexes, 2) the strong metal-carbenoid bond of the NHC complex favors tight binding kinetics, therefore lessening ligand dissociation, 3) the presence of sterically encumbering groups bound to the N-atoms facilitates reductive elimination of the product from the metal catalyst, and 4) the activity of NHC ligands can be modified by the introduction of electronic directing substituents remotely, as witnessed in the synthesis of benzimidazolidines that contain electronically dissimilar groups on the aromatic backbone.² Thus, the research of molecules containing a N-C(carbenoid) bond like isonitrile species is very interesting to test such hypothesis with respect to the FCCs.

8.1 Effects of heteroatom, substituents and asymmetric acetylene for Fischer carbenes in cycloannulation reactions.

From our results, we have obtained a very detailed outlook of every reaction mechanism for all the studied Fischer carbenes. In Figures 21 to 24, the complete reaction mechanisms for the competition between benzannulation and cyclopentannulation for (pentacarbonylchromium)phenylaminocarbene are shown. It was possible to expand on the initial part of the reaction which had been studied in our

group.³ In this previous research it was stated that “due to the lower energy of intermediate **2b**, in comparison with the route leading to species **2a**, it seems to be more feasible the associative route (**1**→**2b**→**3**) than the dissociative one (**1**→**2a**→**3**)”, even when it was not possible to find the TS structures this affirmation was supposed to be correct. But there were some contradictions with most experimental observations (although in some cases, experiments favor the associative route). For phenylcarbenes, we computed the free-energy barriers for **20**→**2b** step to be 31.4 – 42.5 kcal·mol⁻¹ (32.4 – 43.5 kcal·mol⁻¹ in enthalpy) against those 26.5 – 28.5 kcal·mol⁻¹ (25.8 – 30.7 kcal·mol⁻¹ in enthalpy) for **2a**→**3** step; thus proving that dissociative route is more favored than associative one for this case. However, we found for vinylcarbenes that the dissociative pathway has lower free-energy barriers but higher enthalpy barriers as compared with the associative route (free energy barriers: 28.4 – 34.8 kcal·mol⁻¹ (28.0 – 35.6 kcal·mol⁻¹ in enthalpy) against 31.5 – 35.8 kcal·mol⁻¹ (26.3 – 34.0 kcal·mol⁻¹ in enthalpy) for dissociative and associative routes, respectively). Thus, both paths are almost equally weighted, so route **1**→**2a**→**3** may be perfectly feasible in this way. Therefore, we have corroborated the experimental points of view satisfactorily.

On the other hand, we have rationalized the results obtained since one decade ago when just calculations for (CO)₅Cr=C(OH)CHCH₂ complex had been made. However, these results gave an unprecedented prediction: it seemed like the chromahexatriene route is more feasible than that proposed in Dötz mechanism because of intermediates and TS from the former, clearly had lower energies than Dötz structures.⁴ This work shows that according to the results presented in Chapter 3 noticeably alkylcarbenes proceed through a more favored mechanism like chromahexatriene route and phenylcarbenes, on the contrary, are more reactive following Dötz proposal (as can be seen from Figure 24). The main reason can be regarded to stability of complex **8**: whereas for η¹-vinylcarbene complexes **3a** rearranges to an η²-species **8** looking for a first C(carbene)-C(carbonyl) interaction and then a concerted reaction step is followed where the carbon monoxide ensembles directly into the ring when metal complex is “walking” to its center, for phenylcarbene species **3a**, the phenyl group suffers steric hindrance from the nearest CO ligands when approaching its π-system to the chromium atom and thus it forms a Cr-H bond instead which a structure higher in energy. So the preference for the reaction mechanism changes depending on the **R** substituent.

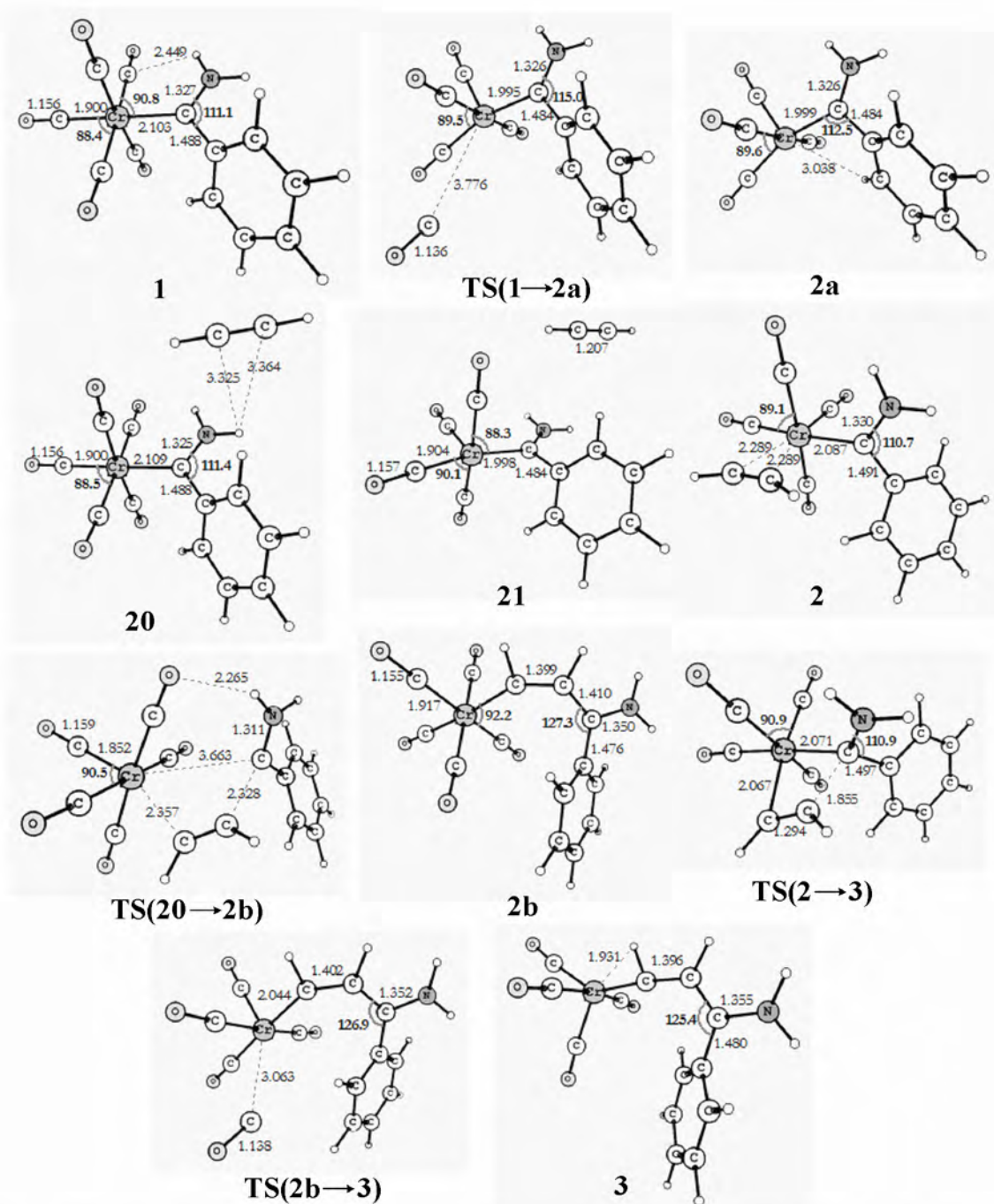


Figure 21. It is shown the intermediates and transition states structures involved on the first stage common to all the cycloannulation reactions. This example corresponds to the $(\text{CO})_5\text{Cr}=\text{C}(\text{NH}_2)\text{Ph}$ Fischer carbene calculated at B3LYP/(Wachters' basis, 6-31G(d,p)) level. Distances are in angstroms and angles (bold) in degrees.

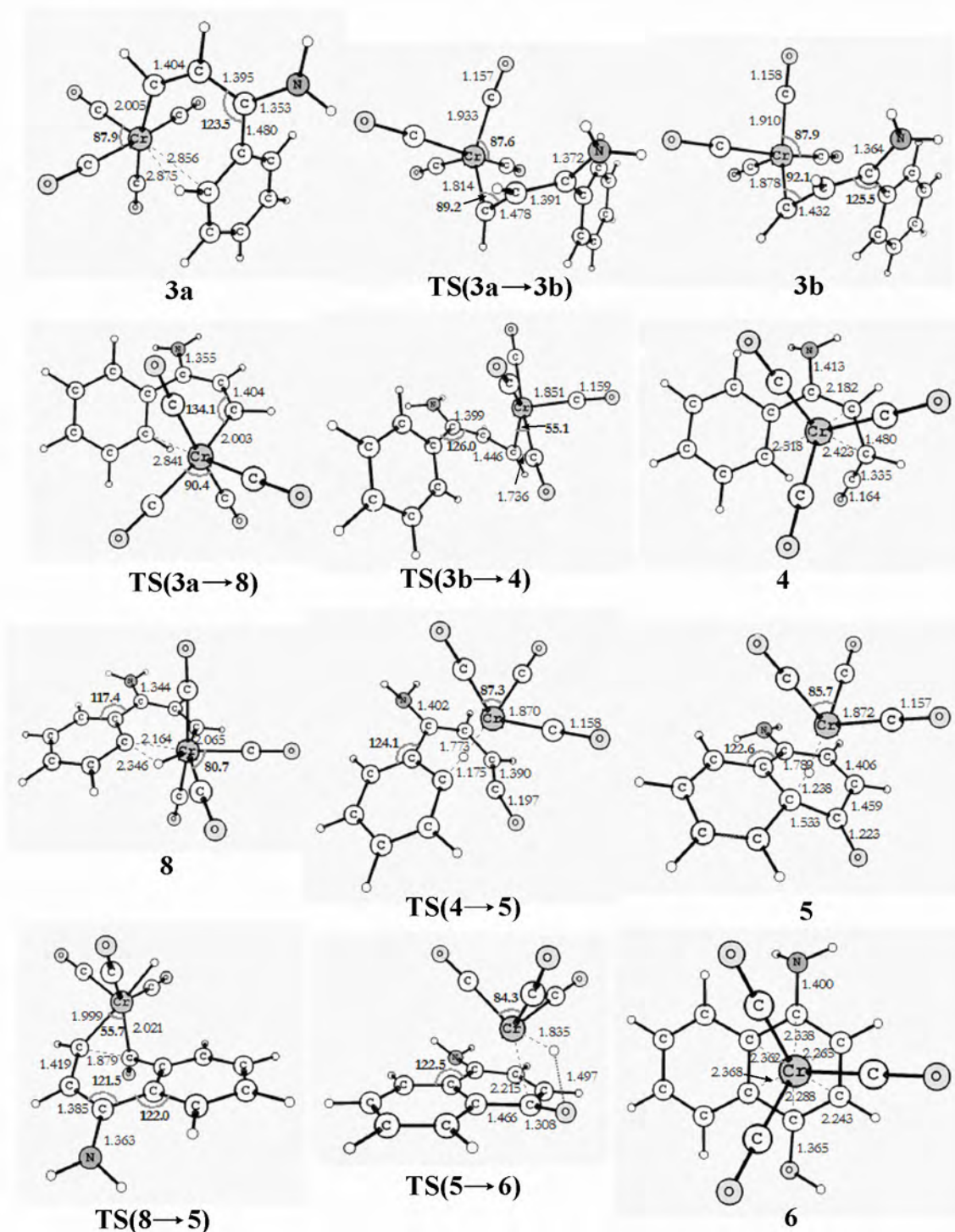


Figure 22. It is shown the intermediates and transition states structures involved on both proposed routes of Dötz benzannulation reaction. This example corresponds to the $(\text{CO})_5\text{Cr}=\text{C}(\text{NH}_2)\text{Ph}$ Fischer carbene calculated at B3LYP/(Wachters' basis, 6-31G(d,p)) level. Distances are in angstroms and angles (bold) in degrees.

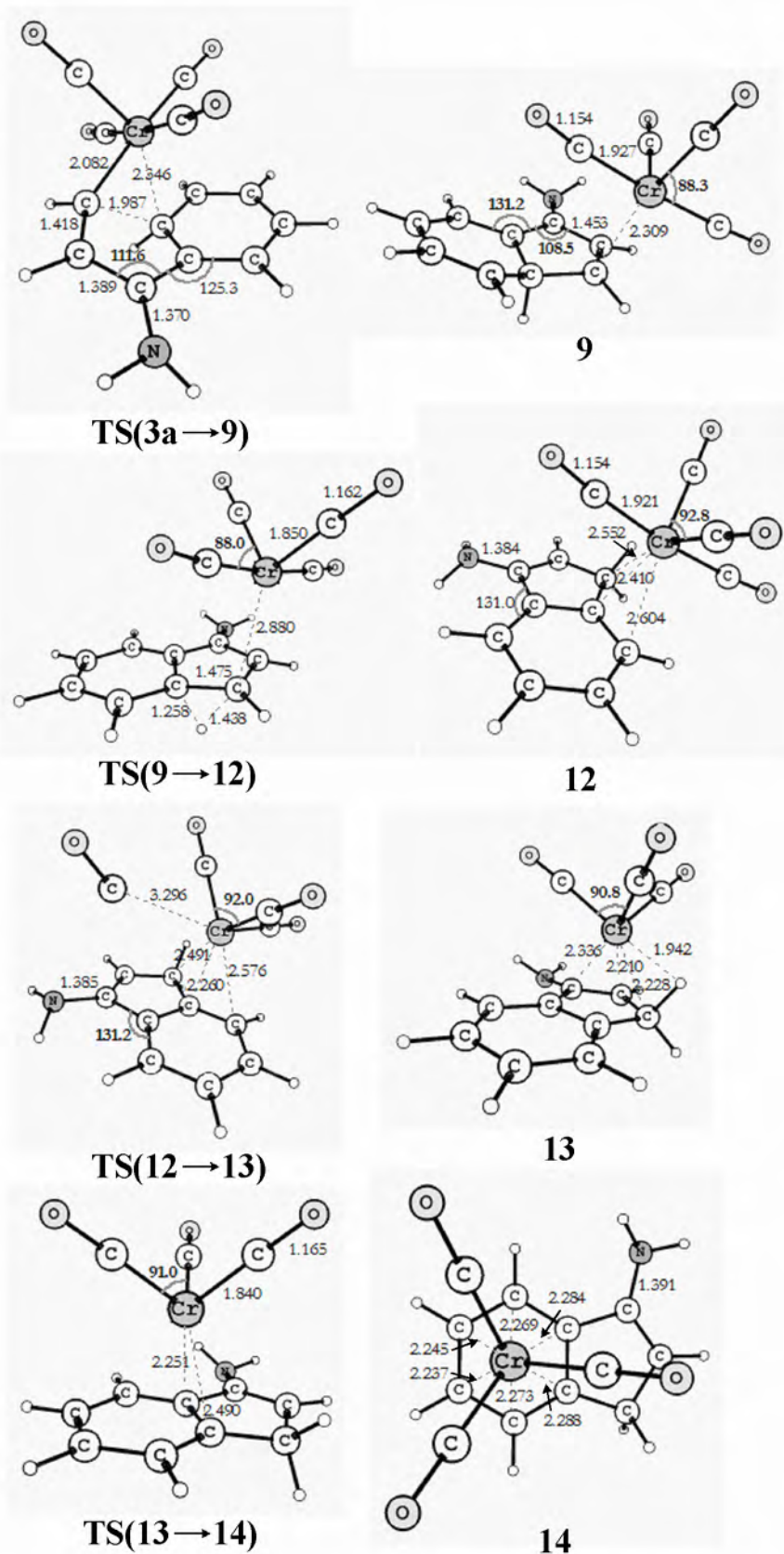


Figure 23. It is shown the intermediates and transition states structures involved on cyclopentannulation reaction. This example corresponds to the $(\text{CO})_5\text{Cr}=\text{C}(\text{NH}_2)\text{Ph}$ Fischer carbene calculated at B3LYP/(Wachters' basis, 6-31G(d,p)) level. Distances are in angstroms and angles (bold) in degrees.

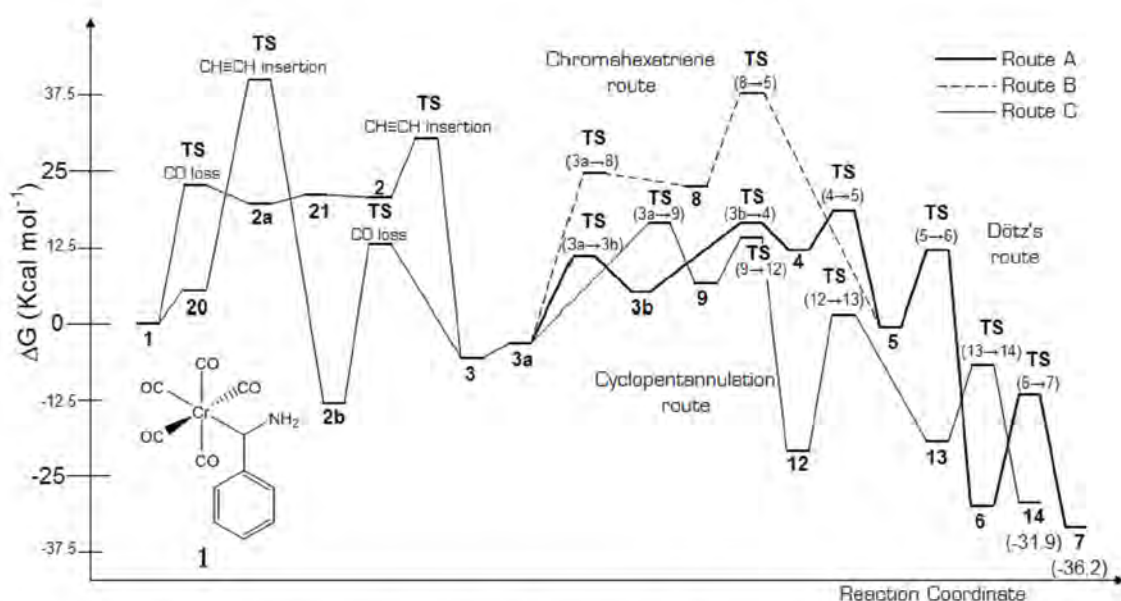


Figure 24. Gibbs free-energy profiles of the $(\text{CO})_5\text{Cr}=\text{C}(\text{NH}_2)\text{Ph}$ Fischer carbene for the main studied mechanisms (benzannulation – route A, solid line; route B, dashed line; cyclopentannulation – route C, normal line). Relative energies are in $\text{kcal}\cdot\text{mol}^{-1}$.

The difference between alkoxy- and amino carbenes is essentially through the influence that the heteroatom can afford into the Cr-C(α) and Cr-CO bonds. Alkoxy groups are stronger π -donors than amino groups; thus, Cr-C(α) bond becomes stronger and Cr-CO bond turns out weaker for alkoxy-carbenes and vice versa for aminocarbenes. This behavior is reflected in some key points in the reaction mechanism: 1) Rearrangement of vinyl- or phenylcarbenes **3** into the agostic complex **3a** (see Figures 21 and 22 for the case of $(\text{CO})_5\text{Cr}=\text{C}(\text{NH}_2)\text{Ph}$ species) is less energetic for alkoxy derivatives than for amino counterparts, being in some cases exothermic processes for the former cases and endothermic for the latter ones (see Table 2 in Chapter 3). In fact, this is because alkoxy-carbenes form an agostic interaction between chromium and the carbene tail (it is stronger for vinylcarbenes than for phenylcarbenes as can be expected) whereas for aminocarbenes this interaction is minor or it is not present. 2) Just considering Dötz benzannulation mechanism (*vide supra*, Figure 22, route **3a** \rightarrow **3b** \rightarrow **4** \rightarrow **5**), the reaction step that entails to the six-membered cycloannulation, **3b** \rightarrow **4**, for the case of vinylcarbenes is clearly more favored for alkoxy- over aminocarbenes species (differences in energy barriers are lower by more than $5 \text{ kcal}\cdot\text{mol}^{-1}$ comparing between X= OR' and X= NR'₂ ligands). This is not achieved for phenylcarbenes where we concluded that bulky heteroatom ligands with high π -donor character reduce the

thermodynamic stability difference between products of cyclopentannulation and benzannulation.

8.2 Catalytic reaction of an isonitrile cyclization reaction.

Experimentally, it has been attempted the intramolecular hydroarylation of isonitriles catalyzed by $\text{TpRu}(\text{PMe}_3)(\text{C}\equiv\text{NR})\text{Ph}$.⁵ Even when reactions of oxidative additions in front of heteroaryl systems under photolytic conditions have been reported in literature,⁶ C-H bond activation mediated by $\text{TpRu}(\text{L})\text{R}$ complexes are best described as σ -bond metathesis transformations.⁷ We pursue to explain why this situation could not be accessible for such complexes despite of using a more effective σ -donor ligand *e.g.* PMe_3 instead of CO. Thus, after a first reaction of complex **28** (see Figure 25) by heating in cyclohexane-*d*₁₂ for a prolonged time, the formation of **29** or **30** (characterized by NMR and IR spectroscopy) did not give any signals of C-H activation of the tethered phenyl group of isonitrile (hydroarylation).

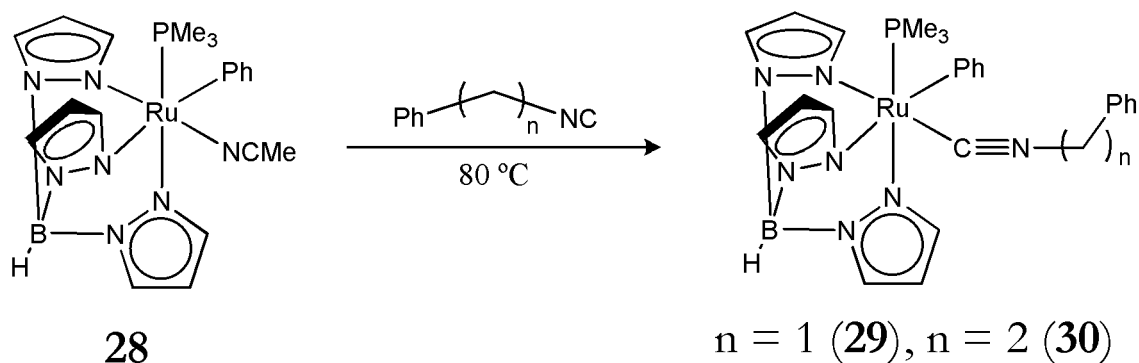


Figure 25. Initially, a substitution reaction produces intermediates **7** and **8** when benzylisonitrile and β -phenethylisonitrile react with ruthenium complex **2**, respectively.

Therefore, we started a theoretical investigation with a model complex of $\text{TpRu}(\text{PMe}_3)\text{NCMe}(\text{Ph})$ by changing the bulkier Tp ligand by “Tab” (Tris(azo)borate) and PMe_3 converted into PH_3 to simplify calculations, as was done previously for other calculations involving C-H bond activations, giving good estimations in agreement with the original ligand.⁸ Scheme 19 shows the proposed intermediates by which the full exploration of PES was performed later.

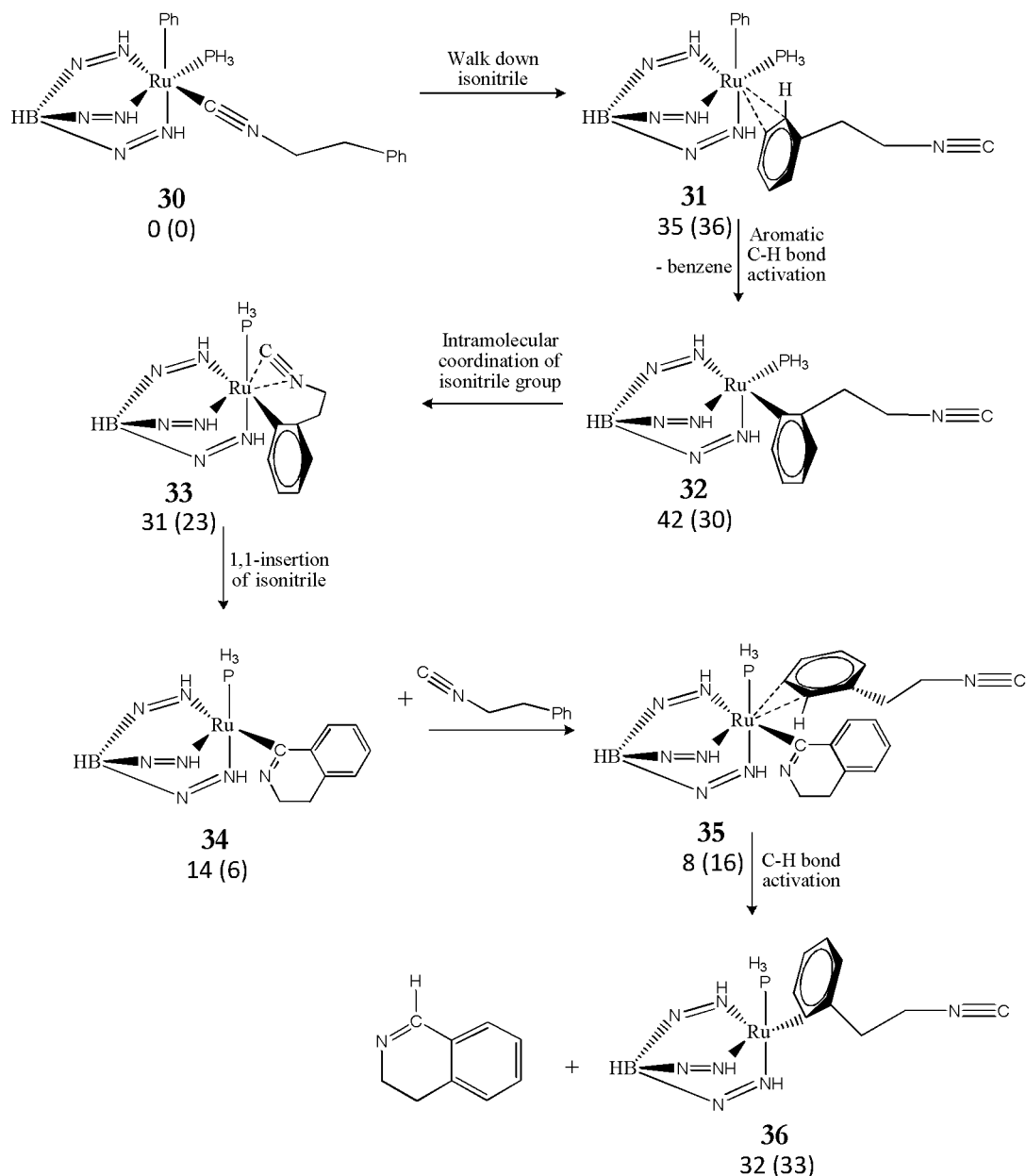
First step (**30** → **31**) is an endothermic isomerization of about 36 kcal·mol⁻¹. Calculating the binding enthalpy to TabRu(PH₃)(Ph) for a simple methylisonitrile model, a value of 39 kcal·mol⁻¹ is obtained. Thus, the interaction is very weak (~3 kcal·mol⁻¹ using the present calculations). Moreover, the geometry obtained upon DFT optimization of **31** corresponds more closely to a weak η²-C-C adduct of benzene. Hence, the calculated enthalpy difference for the **30** → **31** transformation corresponds almost entirely to the energetics of dissociating the isonitrile reactant from the ruthenium complex compensated minimally by a weak π-arene interaction.

It follows the dissociation of benzene. This step is calculated close to be thermoneutral (ΔH_{rxn} = +4 kcal·mol⁻¹), which implies that the Ru-C bond strengths for the phenyl (**31**) and C₆H₄CH₂CH₂NC (**32**) ligands are approximately the same. This result seems inherently reasonable as both are ruthenium-aryl bonds. As many groups have noted linear correlations between corresponding M-R and R-H bond energies, the BDE(C-H) for benzene and BDE(C_{ortho}-H) for C₆H₅CH₂CH₂NC were calculated and yielded values of 109 kcal·mol⁻¹ for both of these bond dissociation enthalpies, further supporting the calculated thermoneutrality of this reaction.

The ligation of the pendant isonitrile functionality in a side-on, η²-NC fashion is calculated to be exothermic by 10 kcal·mol⁻¹. Examples of isonitriles coordinated in a η²-NC fashion are rare.⁹ The binding energy gained by side-on ligation (which we estimate at ~15-16 kcal·mol⁻¹) of the isonitrile moiety to a 16-electron complex (**32**) to yield a formally 18-electron species (**33**) is partially offset by the energetic expense of rotating the CH₂CH₂NC arm of the isonitrile into a conformation suitable for binding to ruthenium (~ 1 kcal·mol⁻¹) and bending of the C-N≡C group from 178° (**32**) to 151° (**33**), which is calculated to cost ~ 4 kcal·mol⁻¹ for the C₆H₄CH₂CH₂NC fragment.

The **33** → **34** reaction step (see Scheme 19) is calculated to be exothermic by 17 kcal·mol⁻¹, and largely reflects the greater stability of the dihydroisoquinoliny (Q) radical versus the C₆H₄CH₂CH₂NC (Z) radical (calculated ΔH_{Q-Z} for the organic fragments is -31 kcal·mol⁻¹). This enthalpy gain from the 1,1-insertion of the isonitrile is countermanded to a certain degree by a stronger ruthenium-carbon bond for Ru-Z as

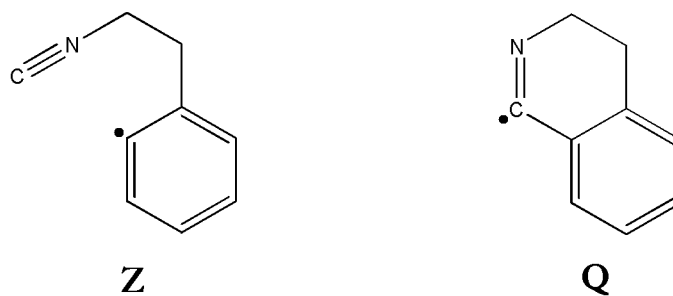
compared to Ru-Q (calculated $\Delta\text{BDE}(\text{C-H})_{\text{Q-Z}} = +10 \text{ kcal}\cdot\text{mol}^{-1}$) and the loss of the weak $\eta^2\text{-NC}$ interaction in **33**.



Scheme 19. Sketched reaction mechanism proposed for the hydroarylation of isonitrile compound **30**. Enthalpies (and Gibbs free-energies in parenthesis) are shown relative to the starting complex **30** in $\text{kcal}\cdot\text{mol}^{-1}$. These data were calculated at B3LYP/ CEP-31G+(5d,7f) level of theory.

The rearrangement in **34** to get the new coordinated **35** complex is mildly exothermic ($\Delta H_{\text{rxn}} = -3 \text{ kcal}\cdot\text{mol}^{-1}$), reflecting the weak binding enthalpy of $\text{C}_6\text{H}_5\text{CH}_2\text{CH}_2\text{NC}$ reactant to the Ru-Q complex, which was estimated at $\sim 3 \text{ kcal}\cdot\text{mol}^{-1}$

in the **30** → **31** step of the process (see above). As with complex **32**, complex **35** is best described as a η^2 -C-C adduct.



The extrusion of product (Q-H) by transfer of a hydrogen atom from the isonitrile reactant to the Q ligand is $24 \text{ kcal}\cdot\text{mol}^{-1}$ uphill (**35** → **36**), reflecting the intrinsically lower bond strength of Q-H versus Z-H (calculated $\Delta\text{BDE}(\text{C-H})_{\text{Q-Z}} = +10 \text{ kcal}\cdot\text{mol}^{-1}$). Furthermore, a complete outlook of the reaction mechanism is displayed in Figures 26 to 29 where the energy barriers are shown for each reaction step. Finding all the transition states of the PES scan gives us a broader perspective of the reaction. The **31** → **I-32** reaction step proceeds through a hydride ruthenium complex where the imaginary frequency was computed to be -1298 cm^{-1} . This reaction coordinate involves purely the H-exchange from isonitrile group to the benzene ring. It means that the energetic barrier of $28 \text{ kcal}\cdot\text{mol}^{-1}$ is due entirely to the arene C-H bond activation. The reverse reaction has a lower cost (C-H activation of benzene: $24 \text{ kcal}\cdot\text{mol}^{-1}$), noting the benzene C-Ru distance is smaller than dihydroisoquinoliny radical (Q) C-Ru bond by $\sim 0.1 \text{ \AA}$. This is indicating the little preference on the aromatic ring over Q species, perhaps due to the better π -arene interaction with the free-rotating phenyl ligand than the impeded isonitrile arm of Q.

Complete dissociation of benzene to release **32** for undergoing intramolecular isomerization is calculated endothermic by $2.5 \text{ kcal}\cdot\text{mol}^{-1}$. This corresponds to vanish the weak interaction H-Ru when the benzene is fully formed from the adduct **I-32**. In addition, isonitrile rearrangement previous to the 1,1-insertion step requires bending up the isonitrile group for the closure of the ring. This stage is calculated to be exothermic by $15 \text{ kcal}\cdot\text{mol}^{-1}$. This is absolutely reflecting the most basic character of the carbene carbon at the extreme of the nitrile. This explains why the formed Ru-C bond is better stabilized over the previous η^2 -NC species **33**.

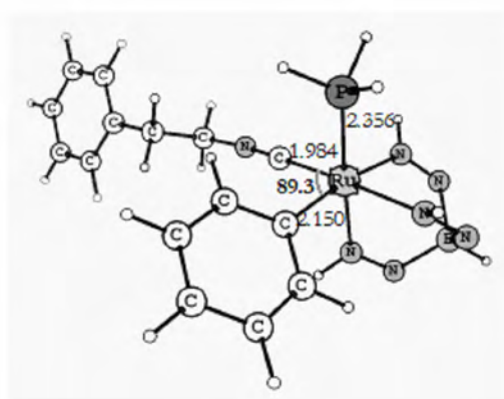
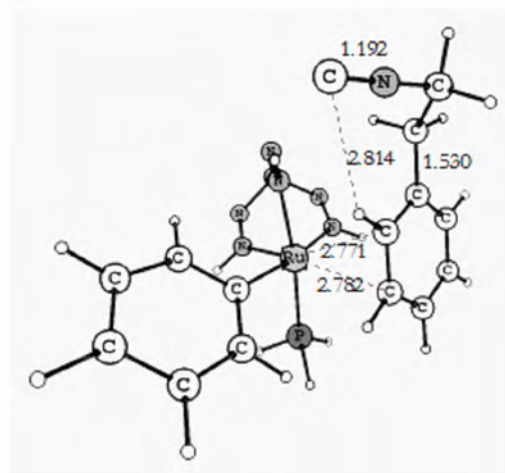
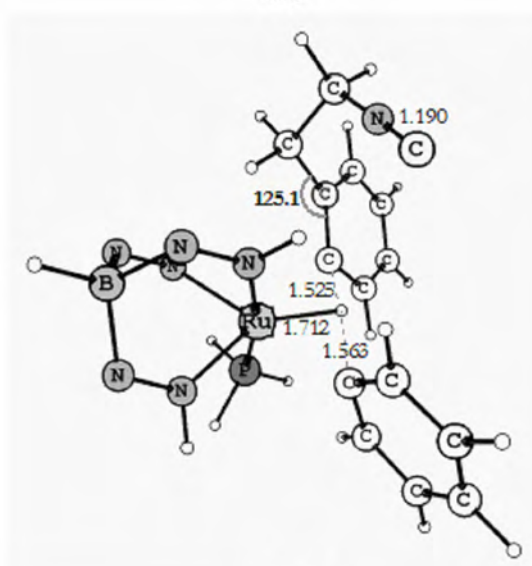
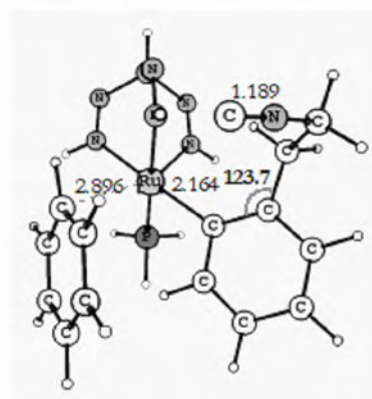
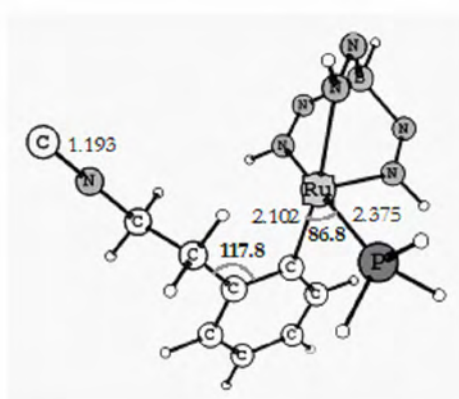
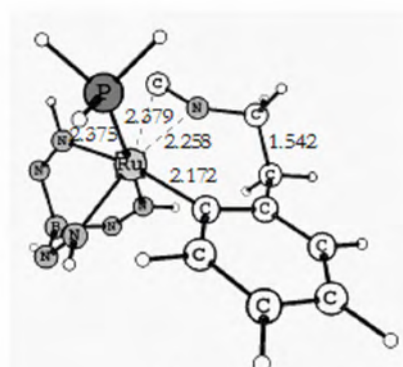
**30****31****TS31****I-32****32****33**

Figure 26. Optimized geometries of the involved intermediates and transition states of the first half of hydroarylation of isonitrile complex **30** calculated at B3LYP/CEP-31G+(5d,7f) level of theory.

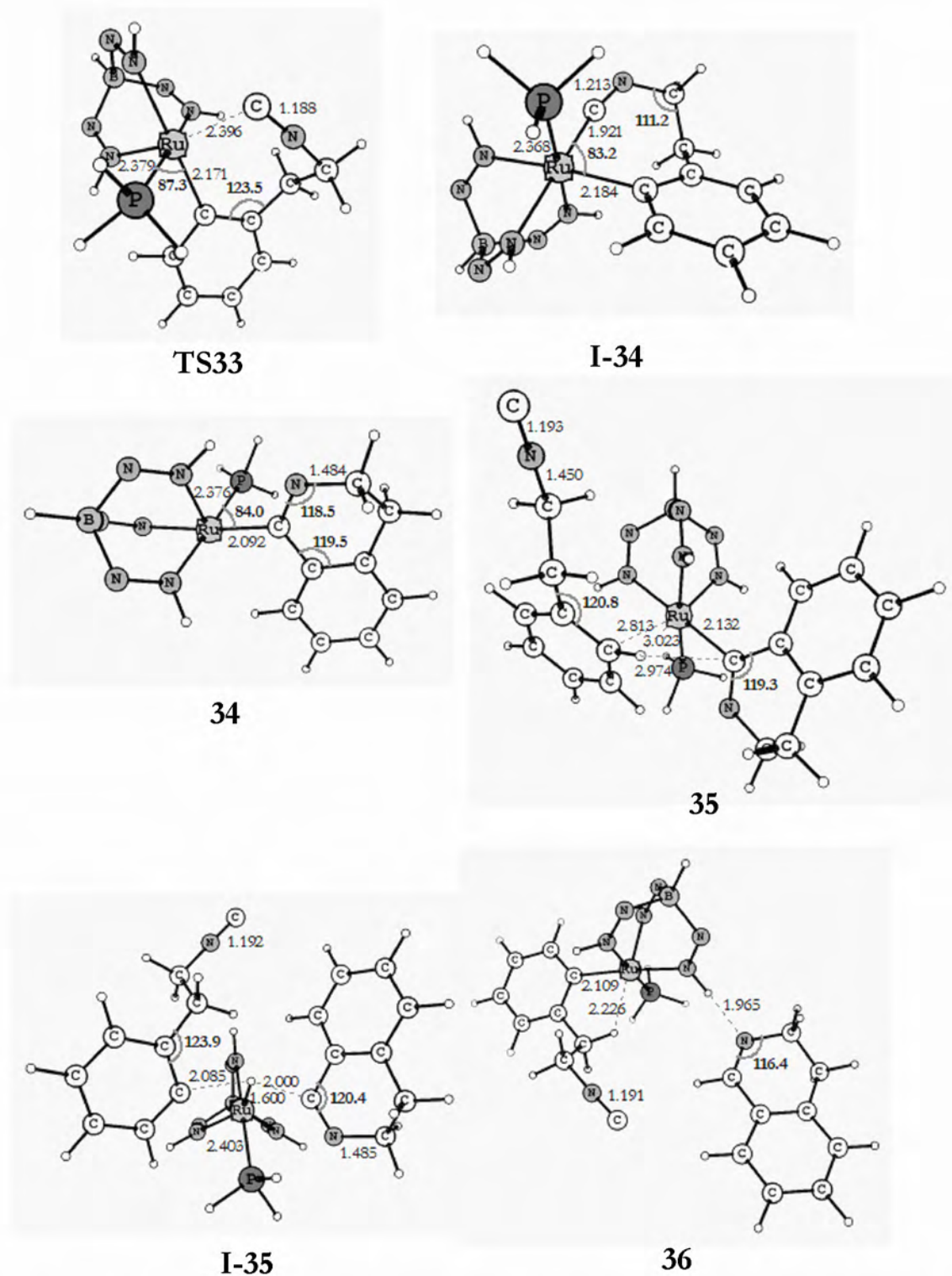


Figure 27. Optimized geometries of the involved intermediates and transition states of the second half when is regenerated the catalytic circle at complex 36 calculated at B3LYP/CEP-31G+(5d,7f) level of theory.

Following the **33** → **I-34** route (see Figure 27), we calculated the associated TS at -185 cm^{-1} in the reaction coordinate. The intrinsic reaction barrier is just $4.8\text{ kcal}\cdot\text{mol}^{-1}$ and the spatial reorientation of the p -orbitals (opening the Ru-C-N angle from 69 to 167°) of the carbene carbon ($p_x \rightarrow p_y$) to form the Ru-C bond takes $20.3\text{ kcal}\cdot\text{mol}^{-1}$. Moreover, since we calculated that the Ru-C(arene) bond break turns out the piperidine ring to be only $1.5\text{ kcal}\cdot\text{mol}^{-1}$ exothermic, no TS was searched for as we thought this step proceeds without a significant energetic barrier. By inspecting the Mulliken charges over this complex, we discovered this is the most significant step where the metal donates more charge. For almost all the reaction pathway, ruthenium has a 1.1 electron population mean but for structure **34** is decreased to 0.68. Also, the carbon and nitrogen atoms of isonitrile are better stabilized in charge as they turn into this position, which explains the more favored the product is.

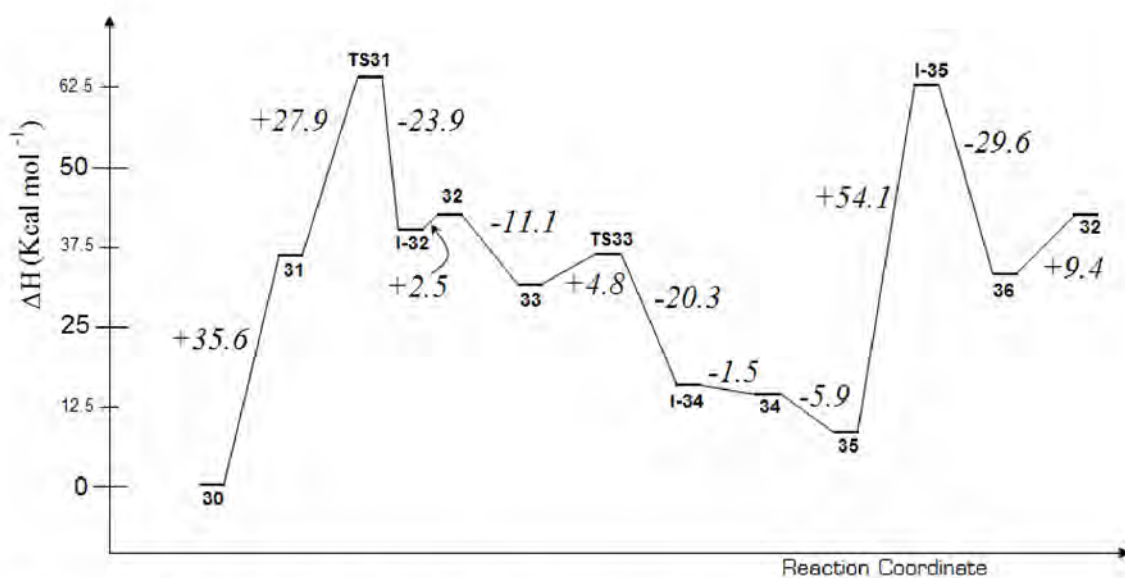


Figure 28. Energy barriers for the studied reaction mechanism of hydroarylation calculated at B3LYP/CEP-31G+(5d,7f) level of theory. Enthalpies are in $\text{kcal}\cdot\text{mol}^{-1}$.

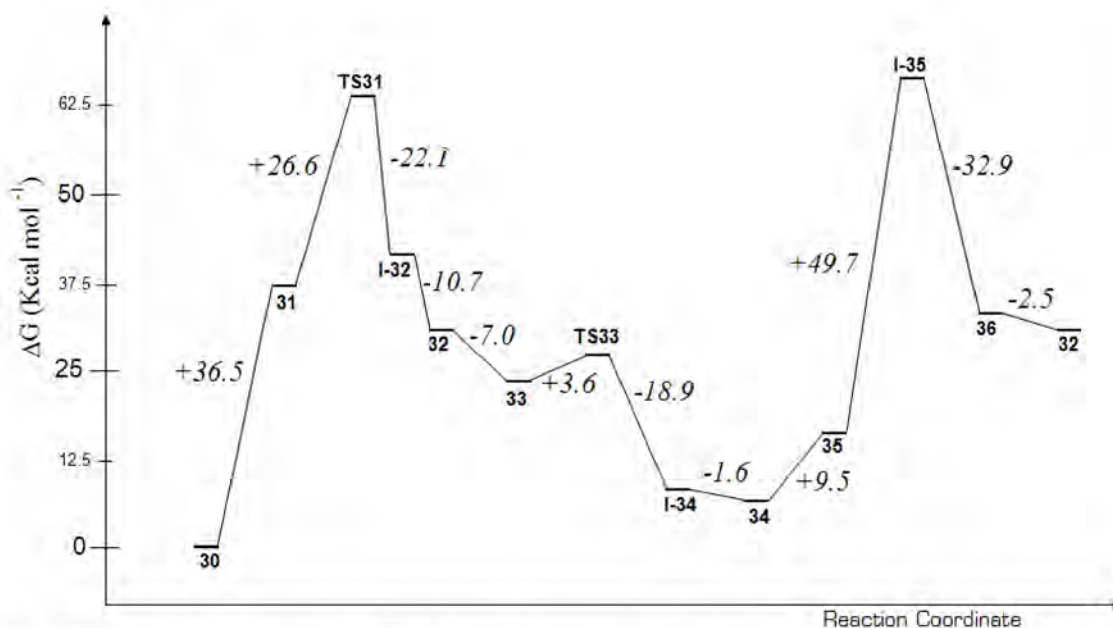


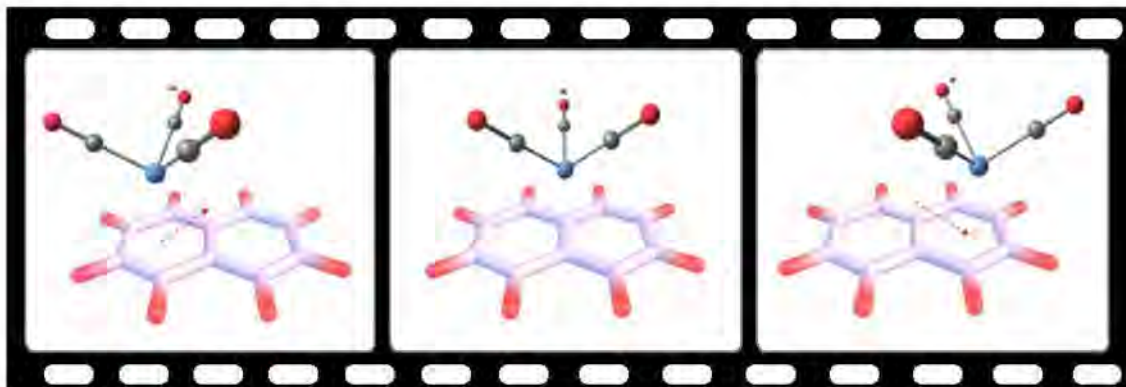
Figure 29. Energy barriers for the studied reaction mechanism of hydroarylation calculated at B3LYP/CEP-31G+(5d,7f) level of theory. Gibbs' free energies are in kcal·mol⁻¹.

Turning our attention to **35** → **I-35** (see Figure 27), this reaction step is highly endothermic, involving a C-H bond activation from the new coordinated phenyl isocyanoethane fragment and producing a hydride Ru intermediate. No TS was found connecting both extremes of this step. It seems like this is a less stable intermediate on the PES, since the energy difference is 54.1 kcal·mol⁻¹ and the reaction goes downhill once the hydride is released. Hence the demanded energy for reaching at this point can be decomposed as follows: ~28-30 kcal·mol⁻¹ for the C-H rupture, 6 kcal·mol⁻¹ for the destabilization of the Ru-C(aryl) bond from piperidine ring and the remaining 17 kcal·mol⁻¹ perhaps are due to the deformed octahedral geometry in this complex.

Next step is the formation of 1,2-dihydroisoquinoline. When the new Ru-C(aryl) bond and the product are obtained, the hydride intermediate **I-35** is then stabilized by 29.6 kcal·mol⁻¹. It is noteworthy that for the latter two steps, no TSs were found in this pathway for our best intent. Perhaps due to the higher energy required to get the C-H bond activation or the main steric impediment for the coordination mode of complex **36** for this case. Thus, boundless dihydroisoquinoline **36** has a weak interaction N---H at one face of the Tab ligand before the catalytic cycle to **32** be completed.

8.3 Haptotropic rearrangements as the last step in Dötz reaction.

An intramolecular haptotropic rearrangement is formally defined as the sequence of migration of a metal coordinated over a polycyclic system, from one ring to another, by changing its π -arene coordination mode.



When exploring the PES of the studied benzannulation reaction mechanism in FCCs, we found that the last step (**6** \rightarrow **7**) always corresponded to a haptotropic migration of tricarboxylchromium if carbene contained other 6-MR apart of the already formed one. Indeed, Dötz and co-workers¹⁰ pointed out this must be true since metal migration is faster than the 1,3-H shift of the *endo*-hydrogen atom when electrocyclization is taking place (and then it tends to lose a CO if the case for other cycloannulations to evolve into tricarboxylchromium species). Moreover, $\text{Cr}(\text{CO})_3$ decomplexation from the new benzenoid system proceeds by two orders of magnitude slower than the haptomigration.¹¹ Then, we computed the energy barriers of all of these products shown in Figure 30. For the four formed naphthalenic systems (case **a**), these barriers were found to be 21.7, 19.7, 21.2 and 21.1 kcal \cdot mol⁻¹ for the η^6 -[4-X-naphthoquinone] $\text{Cr}(\text{CO})_3$ complexes (X= OH, NH₂, OCH₃ and N(CH₃)₂, respectively). Moreover, for biphenyl systems this metal shift corresponds to 26.6 kcal \cdot mol⁻¹ for case **b** and to 25.0 and 29.1 kcal \cdot mol⁻¹ for the isomeric cases **c** and **d**. This notable increase by 5 kcal \cdot mol⁻¹ at least between planar aryl and twisted biaryl chromium complexes is due to the $\text{Cr}(\text{CO})_3$ – phenyl repulsion in the second case when phenyl ring is rotating over the C-C bond, avoiding a free ‘walking’ of metal center through the arene surface. Our reasoning is in agreement with experimental observations reporting different chromium biphenol complexes.¹²

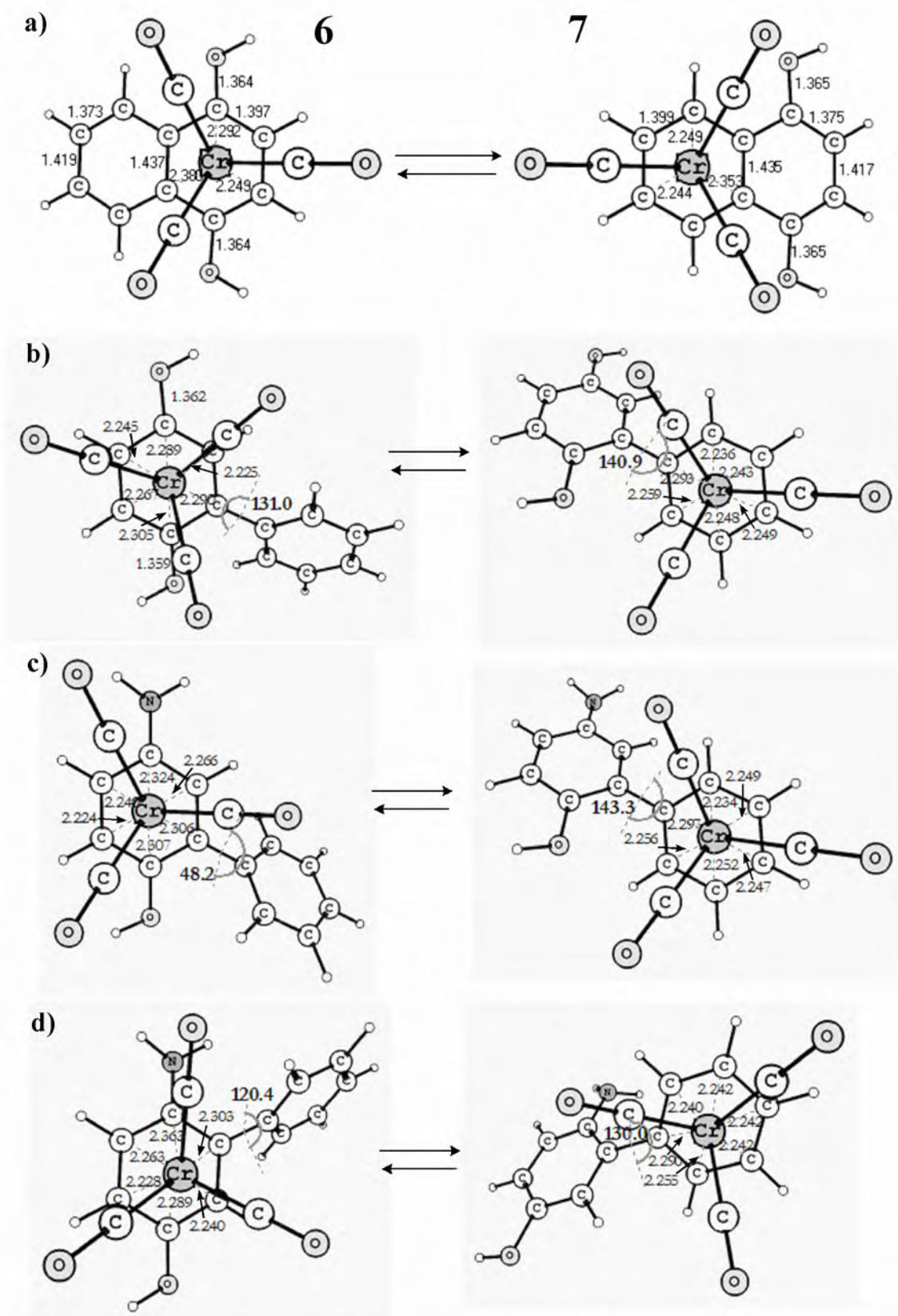
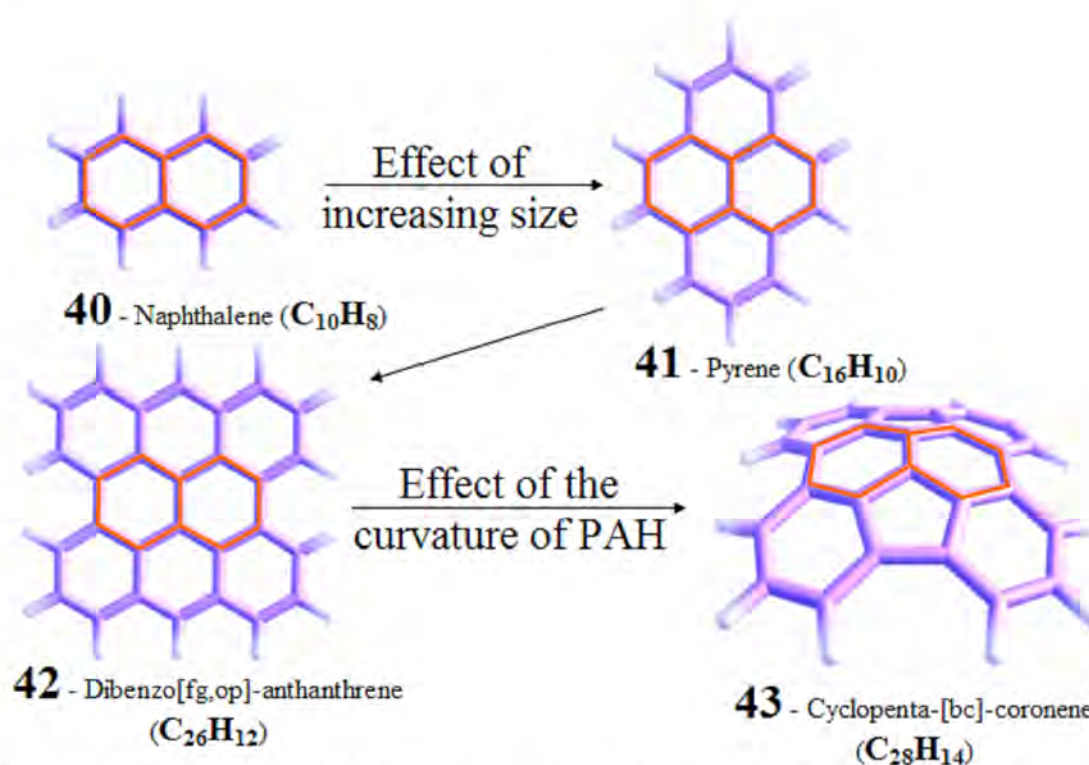


Figure 30. Representative haptotropic rearrangements of $\text{Cr}(\text{CO})_3$ complex found for Dötz benzannulation products for (a) acetylene-inserted hydroxyphenylcarbene, (b) aminophenylcarbene, (c) phenylacetylene-inserted hydroxyvinylcarbene and (d) phenylacetylene-inserted aminovinylcarbene calculated at B3LYP/(Wachters' Basis, 6-31G(d,p)) level.

Furthermore, haptotropic rearrangements of $\text{Cr}(\text{CO})_3$ on naphthalenic substrates occurred in a single step whereas for biphenyl systems proceeded through a stepwise reaction mechanism (energy barriers are referred to the first TS which was the highest in energy on the path). A striking difference came between both isomers of aminonaphthoquinone derivative: the metal migration in case **d** is $4 \text{ kcal}\cdot\text{mol}^{-1}$ higher than for case **c** (see Figure 30). Interestingly, it is observed an intermediate assisted by the hydroxylic oxygen in **c** whereas for **d** chromium avoids the pathway through the amine nitrogen. Thus, we started to think about the possible reaction pathways of haptotropic rearrangements and how can they be modified as the size of arene changes in order to gain an insight into control of the last step of the Dötz reaction.

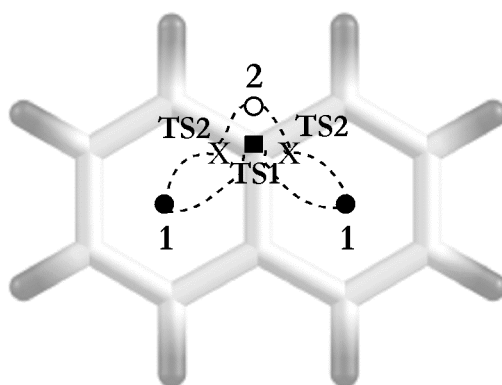


Scheme 20. It is shown the naphthalenic skeleton of the molecules where the haptotropic rearrangements of tricarbonylchromium complex occurred to investigate the effect of increasing the number of rings and curvature.

We studied the effect of the size in energy barriers going from naphthalene to pyrene over the rings in the middle (Scheme 20, compounds **40** and **41**) and from this to a bigger polycyclic system, anthanthrene **42** –Scheme 20– where we chose also a coronene derivative **43** to investigate the migration consequences for a curved molecule. We planned this way because we knew that a majority of studies deals with haptotropic

rearrangements involving π -ligands derived from naphthalene which represents the simplest fused aromatic system available. The first example was reported by Deubzer and coworkers for $\text{Cr}(\text{CO})_3$ complexes of methyl-substituted naphthalenes.¹³ Thus, this point of reference in our research could be used to compare with systems sharing the same naphthalenic skeleton. Furthermore, next studies on the kinetics of this reaction pointed out that the energy barriers decrease notoriously when the size of polycyclic aromatic hydrocarbons (PAHs) increases.¹⁴ Experimental kinetic parameters goes from 21.1 to 26.6 $\text{kcal}\cdot\text{mol}^{-1}$ for naphthalene substituted derivatives in haptomigrations and our calculated value is 23.4 $\text{kcal}\cdot\text{mol}^{-1}$ which fitted very well with previous studies. Table 6 resumes our initial effort in exploring these PESs which were first time compared between planar and curved PAHs. This allowed us to confirm the experimental hypothesis about the influence of the number of rings in energy barriers for the same studied fragment onto the PAH surface and additionally, we realized that the curvature recovers at some extent this barrier (approximately the double with respect to the planar analogous).

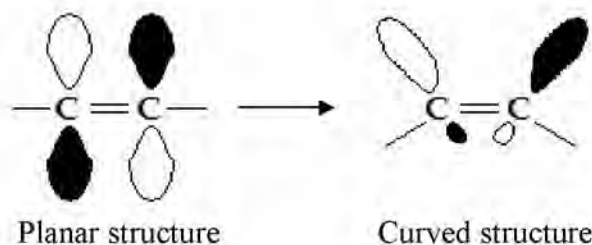
Table 6. Binding energies (ΔE), activation barriers (ΔE^\ddagger), and relative energy of the intermediate **2** (ΔE_2) with respect to the $(\eta^6\text{-PAH})\text{Cr}(\text{CO})_3$ reactant for the two reaction routes found at level B3LYP/(Wachters' basis, 6-31G(d,p)). All energies (in kcal/mol) are corrected by BSSE. **Route A** goes through $1 \rightarrow \text{TS2} \rightarrow 2 \rightarrow \text{TS2} \rightarrow 1$ and **Route B** stands for $1 \rightarrow \text{TS1} \rightarrow 1$.



ROUTE A	ΔE	ΔE_2	$\Delta E^\ddagger_{(1 \rightarrow \text{TS2})}$
$\text{C}_{16}\text{H}_{10}$	-27.05	17.76	18.24
$\text{C}_{28}\text{H}_{14}$	-10.74	4.01	4.40
ROUTE B			$\Delta E^\ddagger_{(1 \rightarrow \text{TS1})}$
C_{10}H_8	-39.26	–	23.40
$\text{C}_{26}\text{H}_{12}$	-18.58	–	10.44

In order to discuss about the bonding mechanism in the $(\eta^6\text{-arene})\text{Cr}(\text{CO})_3$ complexes we made orbital interaction diagrams defining the dominant bonding contributions. Figure 31 shows those between the planar $\text{C}_{26}\text{H}_{12}$ and the curved $\text{C}_{28}\text{H}_{14}$ complexes. On the left and right sides the highest-lying filled π orbitals of cyclopenta-[bc]-coronene and dibenzo-[fg,op]-anthanthrene, respectively, are displayed whereas in the center of Figure 31 the LUMOs (a_1 and e) of the $\text{Cr}(\text{CO})_3$ fragment are shown. We have adopted the notation used by Hoffmann and coworkers¹⁵ of s and a subscripts according to whether the orbital is symmetric or antisymmetric with respect to the plane of C_s symmetry (yz) of the initial $(\eta^6\text{-C}_{10}\text{H}_8)\text{Cr}(\text{CO})_3$ complex. The numbers in Figure 31 represent the composition of the MOs of the $(\eta^6\text{-PAH})\text{Cr}(\text{CO})_3$ complex in terms of Gross Mulliken contributions. There are two factors that explain the higher binding energy in $(\eta^6\text{-C}_{26}\text{H}_{12})\text{-Cr}(\text{CO})_3$ as compared to $(\eta^6\text{-C}_{28}\text{H}_{14})\text{-Cr}(\text{CO})_3$. First, the HOMOs of the curved PAH that intervene more in the bonding mechanism are higher in energy than those of the planar species with the only exception of the HOMO of $\text{C}_{28}\text{H}_{14}$. Second, the HOMOs present larger lobes in the convex surface leading to better MO overlaps: the overlaps of the LUMOs of $\text{Cr}(\text{CO})_3$ with the HOMOs of the planar $\text{C}_{28}\text{H}_{14}$ and the curved $\text{C}_{26}\text{H}_{12}$ are in the range 0.02 – 0.05 and 0.10 – 0.16, respectively.

In other words, when increasing the number of rings, energy barriers for haptotropic migration become lower because of the diminution of overlapping between HOMO of PAHs and the LUMO of $\text{Cr}(\text{CO})_3$. By other hand, curving an arene makes the π bonds larger at the convex face of it (and vice versa at the concave side) which leads to stronger metal - π interactions and this entails a major cost to undergo haptotropic shifts.

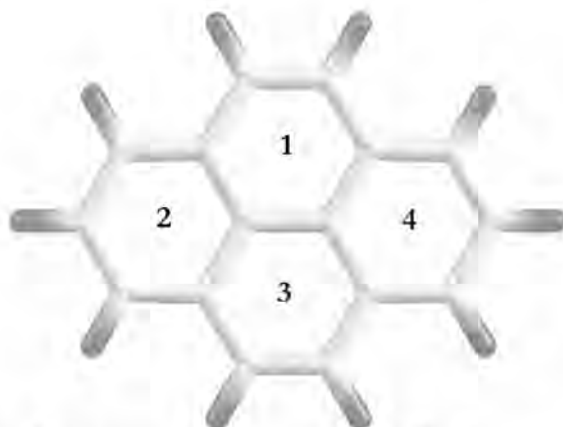


Apart from discussions based on MOs, we quoted some considerations in aromaticity about this topic. In fact, we extended our research on to well-known PAHs of two-, three-, and four-membered rings. According to Mitchell and coworkers,¹⁶ the

benzene ring in tricarbonylchromium-complexed benzene is about 30-40% more aromatic than benzene itself. Schleyer and co-workers¹⁷ using nucleus-independent chemical shifts (NICS) and ¹H NMR chemical shifts data found that the aromaticity of the benzene ring in (η^6 -C₆H₆)Cr(CO)₃ is similar to that of the free benzene molecule. Besides of this, Simion and Sorensen¹⁸ concluded from diamagnetic susceptibility exaltation data that the benzene ring coordinated to the chromium tricarbonyl complex is antiaromatic. A similar opinion is hold by Hubig and co-workers¹⁹ who consider that the charge transfer from the arene to the transition metal in metal-arene coordination leads to a complete loss of aromaticity of the π -system. We have recently shown by means of different indicators of aromaticity that there is an important reduction of the aromaticity of benzene when coordinated to Cr(CO)₃.²⁰ Then, we decided to tackle this controversial issue by calculating the more accepted electronic, structural and magnetic indices of aromaticity²¹ for the isolated PAHs and coordinated to the tricarbonylchromium complex. NICS_{*mn*}(*x*) represents the value of the chemical shift at *x* Å up or down of the position of the ring center (subscript *mn* involves the *mn*-component of the tensor in the perpendicular direction of the ring center; conventionally it is *zz*). Negative NICS values indicate aromaticity whereas positive NICS values are for antiaromatic rings. The more negative the NICS value, the more aromatic the ring is. On the other hand, the FLU values near to zero are pointing out aromaticity and vice versa; the higher the PDI value, the more aromatic the ring is; the same as PDI stands for MCI values. Finally, HOMA structural index of aromaticity has a scale from zero to one by definition: the more aromatic rings present values close to one whereas the more antiaromatic ones have values almost equal to zero. In this way, we can establish an aromatic criterion for every ring of PAHs coordinated or non-coordinated to the metal center.

For instance, Tables 7 to 9 show these indices for the cases of pyrene, compared with the linear tetracene and the helicoidal four-membered tetrahelicene, respectively. In general, we observed in the analyzed PAHs that there is a reduction in aromaticity in all the rings coordinated to Cr(CO)₃ moiety. In most cases, the reduction of aromaticity was also accompanied by the neighboring rings.

Table 7. Aromaticity indices calculated at B3LYP/(Wachters' Basis, 6-31G(d,p)) showed for both the isolated pyrene and the coordinated-Cr(CO)₃ moieties. The Cr-n (n = 1, 2) notation stands for the ring where the Cr(CO)₃ is positioned at. NICS(1) were measured at the opposite side of the ring where chromium is complexed.



	Isolated system		Cr-1			
	Ring 1 (3)	Ring 2 (4)	Ring 1	Ring 2	Ring 3	Ring 4
NICS(0)	-5.180	-12.861	-19.411	-11.853	-3.102	-11.834
NICS(1)	-7.963	-14.121	-11.591	-12.814	-5.824	-12.810
NICS_{zz}(1)	-16.594	-35.726	-16.208	-32.996	-11.252	-33.106
FLU	0.017	0.006	0.032	0.012	0.027	0.012
PDI	0.044	0.069	0.023	0.063	0.035	0.063
MCI	0.015	0.030	0.005	0.022	0.009	0.022
HOMA	0.550	0.832	0.436	0.758	0.388	0.758

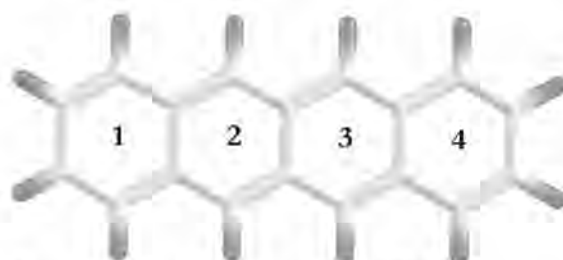
	Cr-2			
	Ring 1	Ring 2	Ring 3	Ring 4
NICS(0)	-1.349	-25.442	-4.503	-10.885
NICS(1)	-4.243	-14.634	-6.761	-12.480
NICS_{zz}(1)	-7.379	-24.963	-14.269	-31.257
FLU	0.027	0.025	0.023	0.005
PDI	0.036	0.030	0.041	0.071
MCI	0.009	0.008	0.012	0.032
HOMA	0.390	0.632	0.490	0.865

Unexpectedly, however, for pyrene HOMA and FLU indicate a larger reduction at the non-coordinated rings than for the coordinated one when this is achieved at one of the central rings (Cr-1, Table 7). For HOMA, the same is found in the (η^6 -C₂₆H₁₂)Cr(CO)₃ species, although in general the neighboring rings are more aromatic than the Cr(CO)₃-complexed one, as one could expect from the fact that the coordinated ring is the one interacting more strongly with the Cr(CO)₃ moiety. Although we include NICS values, it has been suggested in literature they follow the same trend as ring currents where the effect on the local aromaticity (*i.e.* for every ring) is mixed with the

effects of the surrounding rings and therefore, it cannot split up the different contributions discerning between the coordinated and non-coordinated rings.²² Anyway, these values can be compared between the isolated and the coordinated complex to give some estimation of the change in the global aromaticity.

Comparing pyrene system with respect to the linear tetracene below, it can be seen that the coordination of tricarbonylchromium at one extreme ring does not affect any to the aromaticity of the other opposite ring. Very interestingly, the coordination on an inner ring is predicted in some cases like naphthalene to strength aromaticity of the more distant ring by FLU, PDI and HOMA (rings 2 and 4, Table 8). This effect can be addressed to the electron distribution as waves when metal coordination displaces equilibrium and accumulates delocalization in other regions (damped alternation).²³

Table 8. Aromaticity indices calculated at B3LYP/(Wachters' Basis, 6-31G(d,p)) showed for both the isolated naphthalene and the coordinated-Cr(CO)₃ moieties. The Cr-n (n = 1, 2) notation stands for the ring where the Cr(CO)₃ is positioned at. NICS(1) were measured at the opposite side of the ring where chromium is complexed.



	Isolated system		Cr-1			
	Ring 1 (4)	Ring 2 (3)	Ring 1	Ring 2	Ring 3	Ring 4
NICS(0)	-7.966	-12.703	-18.834	-12.787	-12.697	-8.009
NICS(1)	-9.876	-13.948	-11.012	-13.512	-13.927	-9.939
NICS_{zz}(1)	-23.402	-34.668	-16.517	-33.342	-34.382	-23.800
FLU	0.018	0.010	0.027	0.014	0.011	0.017
PDI	0.063	0.062	0.025	0.058	0.061	0.063
MCI	0.021	0.018	0.039	0.015	0.018	0.021
HOMA	0.527	0.603	0.419	0.573	0.599	0.530

	Cr-2			
	Ring 1	Ring 2	Ring 3	Ring 4
NICS(0)	-5.452	-22.354	-12.877	-8.584
NICS(1)	-7.045	-13.670	-13.552	-10.409
NICS_{zz}(1)	-18.119	-21.588	-32.868	-25.082
FLU	0.026	0.034	0.013	0.016
PDI	0.060	0.025	0.061	0.065
MCI	0.016	0.005	0.017	0.023
HOMA	0.448	0.386	0.641	0.588

Table 9. Aromaticity indices calculated at B3LYP/(Wachters' Basis, 6-31G(d,p)) showed for both the isolated tetrahelicene and the coordinated-Cr(CO)₃ moieties. The Cr-n (n = 1, 2, 3, 4) notation stands for the ring where the Cr(CO)₃ is positioned at. NICS(1) were measured at the opposite helicoidal face where chromium is complexed.



	Isolated system				Cr-1			
	Ring 1	Ring 2	Ring 3	Ring 4	Ring 1	Ring 2	Ring 3	Ring 4
NICS(0)	-10.146	-7.729	-7.729	-10.146	-10.101	-7.751	-7.675	-24.103
NICS(1)	-10.677	-9.572	-10.292	-12.721	-12.770	-10.367	-8.929	-12.341
NICS_{zz}(1)	-24.360	-22.318	-22.217	-29.782	-30.337	-22.650	-21.312	-19.299
FLU	0.006	0.014	0.014	0.006	0.006	0.014	0.020	0.022
PDI	0.079	0.054	0.054	0.079	0.078	0.054	0.050	0.030
MCI	0.037	0.018	0.018	0.037	0.036	0.018	0.015	0.008
HOMA	0.806	0.493	0.493	0.806	0.802	0.510	0.444	0.579

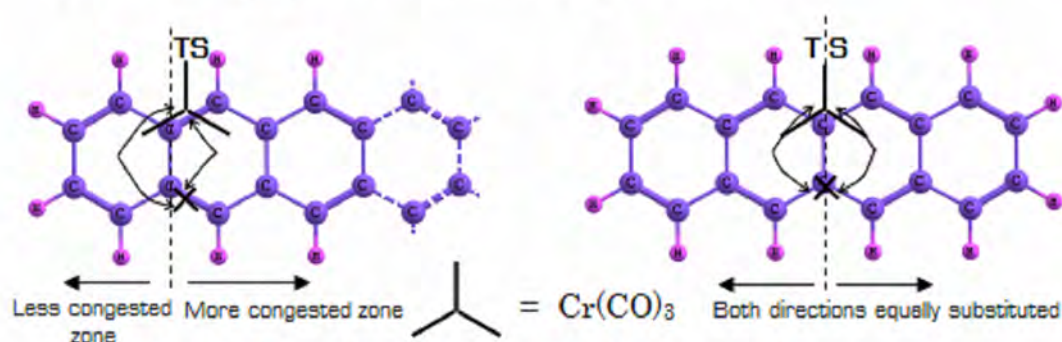
	Cr-2				Cr-3			
	Ring 1	Ring 2	Ring 3	Ring 4	Ring 1	Ring 2	Ring 3	Ring 4
NICS(0)	-10.067	-6.587	-22.176	-8.905	-9.862	-21.895	-5.849	-9.936
NICS(1)	-12.702	-8.609	-12.610	-9.171	-11.698	-13.210	-7.176	-10.743
NICS_{zz}(1)	-30.166	-18.309	-19.455	-23.064	-27.480	-19.530	-16.143	-25.632
FLU	0.005	0.023	0.032	0.016	0.012	0.032	0.025	0.004
PDI	0.081	0.046	0.026	0.069	0.073	0.026	0.043	0.082
MCI	0.039	0.012	0.006	0.024	0.029	0.005	0.011	0.040
HOMA	0.842	0.327	0.300	0.655	0.718	0.300	0.288	0.858

	Cr-4			
	Ring 1	Ring 2	Ring 3	Ring 4
NICS(0)	-24.826	-7.939	-8.099	-10.202
NICS(1)	-14.163	-9.683	-10.059	-10.980
NICS_{zz}(1)	-23.106	-21.079	-22.834	-26.005
FLU	0.021	0.020	0.014	0.006
PDI	0.032	0.049	0.054	0.078
MCI	0.008	0.014	0.019	0.036
HOMA	0.606	0.394	0.492	0.793

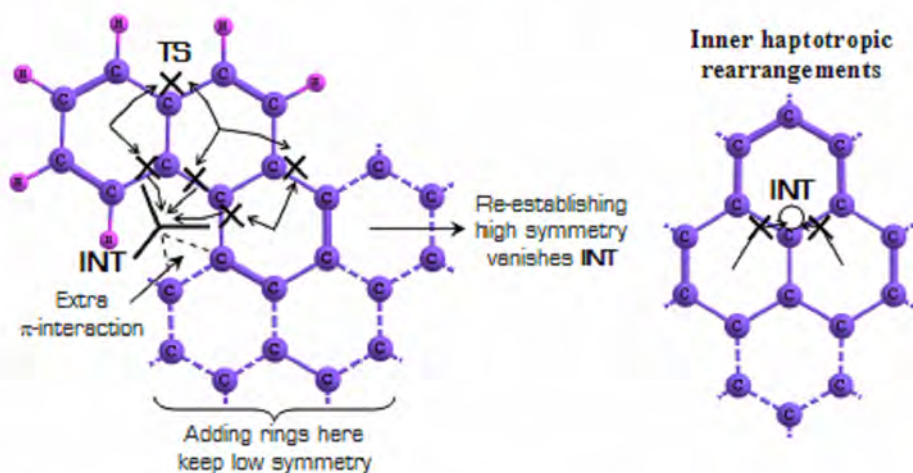
A different pattern of aromaticity can also be observed for tetrahelicene. Comparing isolated PAHs, electronic indices (FLU, PDI, MCI and HOMA) give inverse trends than magnetic indices (NICS variants) but whereas for acenes like naphthacene (Table 8), electronic indices predict the inner rings to be more aromatic than the external ones, this behavior is reverted for the rings of tetrahelicene. Moreover,

when $\text{Cr}(\text{CO})_3$ is complexed onto rings 2 and 3 of tetrahelicene (see Table 9), tendency is very similar as for planar PAHs but it is radically contrasting when complexation is on ring 1 has almost nothing to do with aromaticity of rings 2 and 3 but decreases notoriously that one from ring 4 and vice versa. For bigger helicenes, this effect had been attributed to the π - π interaction between two rings due to the helicoidal twisting that exert magnetic couplings so there a direct connexion between them,²⁴ and also for [3.3]orthocyclophanes, which revealed an important decrease of the dihedral angle between the two aromatic rings because of the $\text{Cr}(\text{CO})_3$ complexation.²⁵

Linear Polycyclic Aromatic Hydrocarbons



Angular Polycyclic Aromatic Hydrocarbons

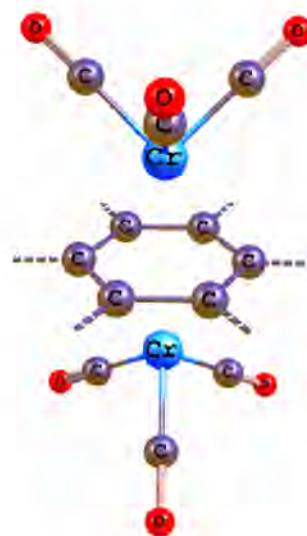


Scheme 21. Summary of the different reaction pathways found for intramolecular haptotropic rearrangements of $\text{Cr}(\text{CO})_3$ species over two, three and four six-membered rings.

Coming back to the haptotropic reaction mechanisms, we got no distinctions of rings to take all the possibilities of haptomigrations pathways; some cases presented

equivalent reaction mechanisms due to the symmetry of arene but others had a dissimilar route. All the intermediates and TSs found for the $\text{Cr}(\text{CO})_3$ migration over three and four 6-MRs can be found at the Appendix of this Chapter. Scheme 21 resumes the task of finding all the haptotropic rearrangement pathways of $\text{Cr}(\text{CO})_3$ over the polycyclic systems that were calculated and discussed in terms of reactivity and aromaticity. We found out that straight PAHs (*i.e.* acenes) share the same reaction mechanisms of inter-ring haptotropic rearrangements (IRHR) (one TS connecting both minima of $\text{Cr}(\text{CO})_3$ – acene coordination on the neighboring rings); the TS can be a η^1 -species or displaced towards η^2 -interaction depending on the symmetry of both sides in the pathway to migrate to and the even or odd number of rings of PAHs. Angular PAHs, by the other side, usually form a η^4 -intermediate that is common between three rings when the haptotropic shift is performed on the curved border side (*endo* pathway), but they have similar energy requirements as for the external side contour (*exo* pathway). However, for chrysene this intermediate is not present since this benzenoid recovers a high symmetry and the most important π -HOMO interactions are contained at the *exo* carbons, where tricarbonylchromium forms the η^1 -intermediate (**I-1**) shown in Figure A10 of Appendix. For the cases of pyrene and phenalene (and must be for bigger PAH systems) sharing common C-C bonds between rings, they possess a η^2 -TS in a position located between the two rings where the metal migration is taking place. When the arene is more symmetric like for phenalene, it appears a η^1 -intermediate located at the shared methylenic C atom. Nevertheless, this situation is less favored than haptomigrations through the periphery of these systems.

Finally, we studied which were the rings more favored to undergo a second coordination with other tricarbonylchromium complex on the same PAHs of two, three, and four six-membered rings. To accomplish with this, we searched all the possible isomers that result from the complexation of two $\text{Cr}(\text{CO})_3$ in the different positions (*anti* and *syn*) at the rings.



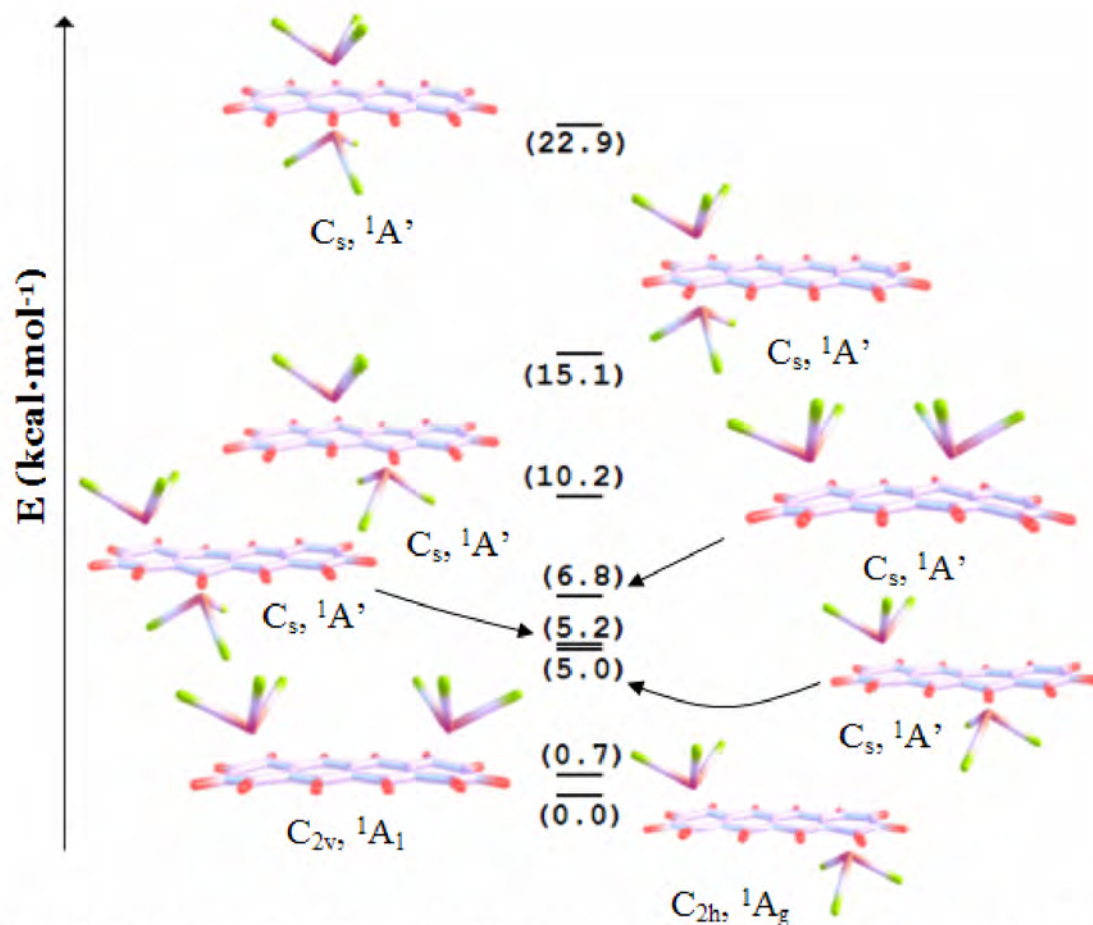


Figure 32. B3LYP/(Wachters' basis, 6-31G(d,p)) calculated geometries and relative energies for the possible isomers of $[\mu-(\eta^6:\eta^6)\text{naphthacene}]\text{bistricarbonylchromium}(0)$ complex. Molecular symmetry and electronic state are shown below each bicoordinated complex.

The aim here was about discussing which is the relative stability between linear and kinked PAHs in terms of structure when more electron-withdrawing groups were added. Drawn isomers of the optimized structures for some bi-coordinated 4-MRs are shown in Figures 32 to 35, ordered in a relative energy scale. We found that the coordination was favored at the more external rings (in *anti*-position) for all the cases. It is also possible to find $\text{Cr}(\text{CO})_3$ complexes in the same face of PAH but it makes the system a bit pyramidalized to avoid repulsions from the carbonyl arms of chromium complex.

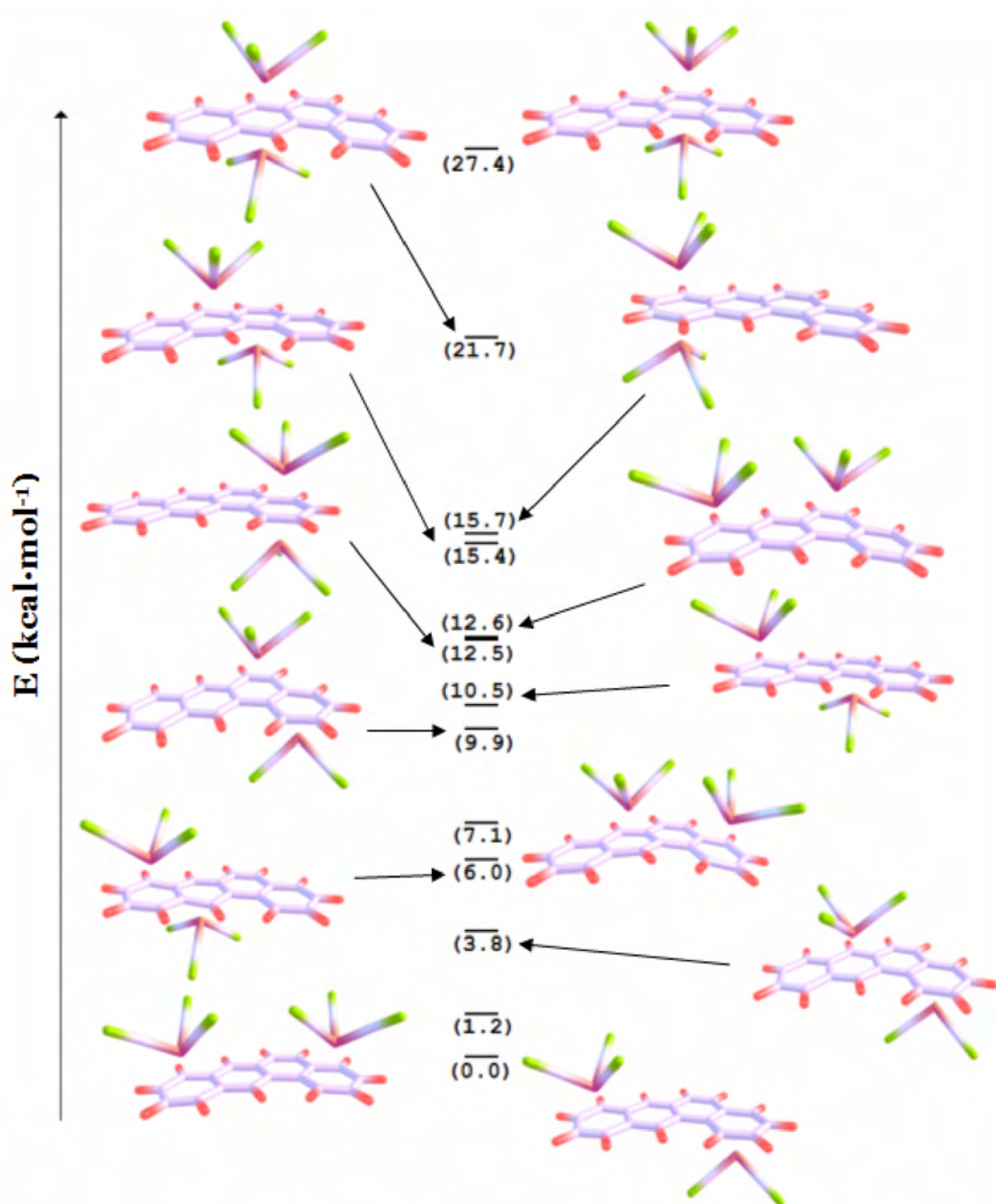


Figure 33. B3LYP/(Wachters' basis, 6-31G(d,p)) calculated geometries and relative energies for the possible isomers of $[\mu-(\eta^6:\eta^6)\text{tetraphene}]\text{bistricarbonylchromium}(0)$ complex. All the bicoordinated complexes possess C_1 symmetry and electronic state 1A .

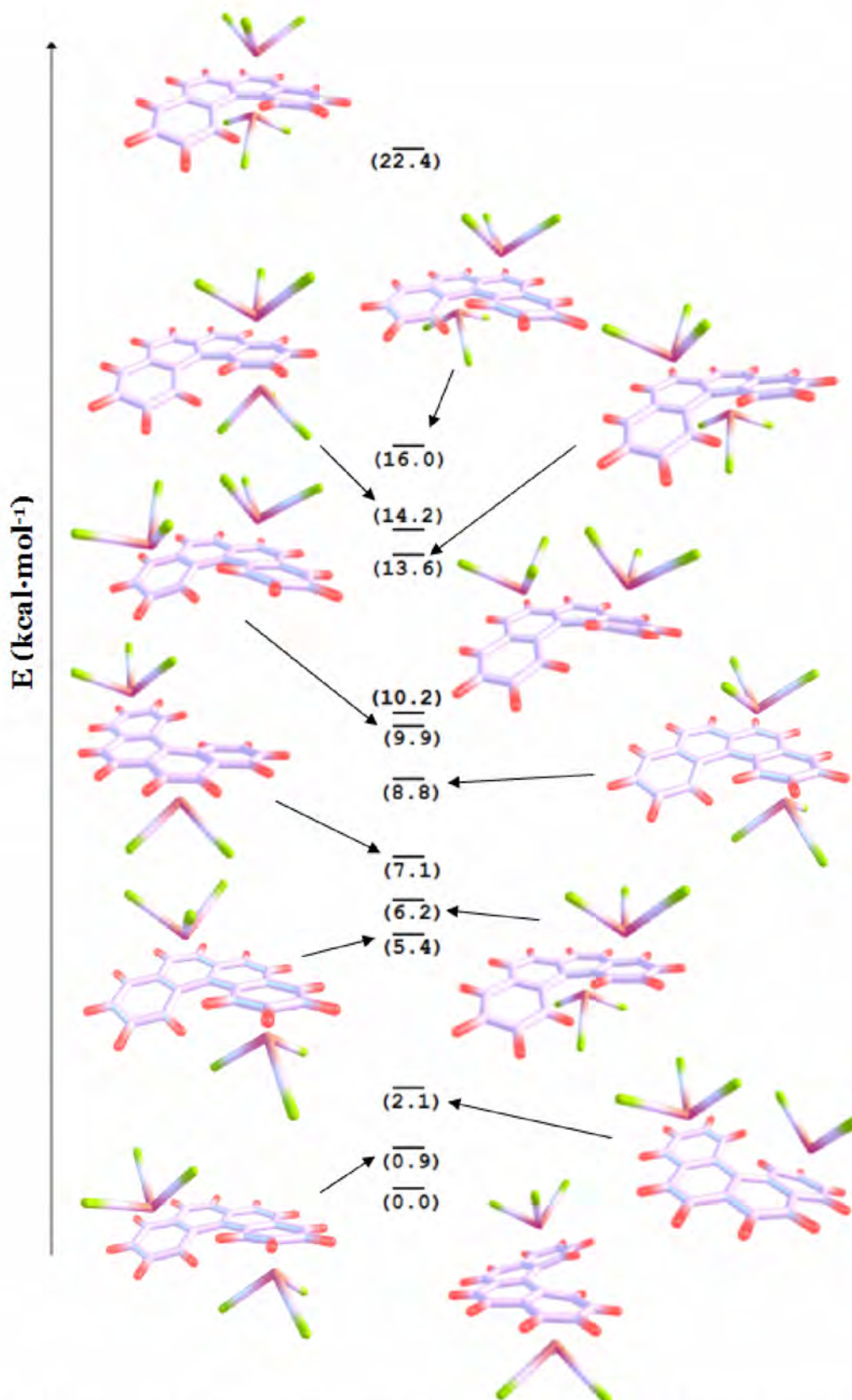


Figure 34. B3LYP/(Wachters' basis, 6-31G(d,p)) calculated geometries and relative energies for the possible isomers of $[\mu-(\eta^6:\eta^6)\text{tetrahelicene}]\text{bistricarbonylchromium}(0)$ complex. All the bicoordinated complexes possess C_1 symmetry and electronic state 1A .

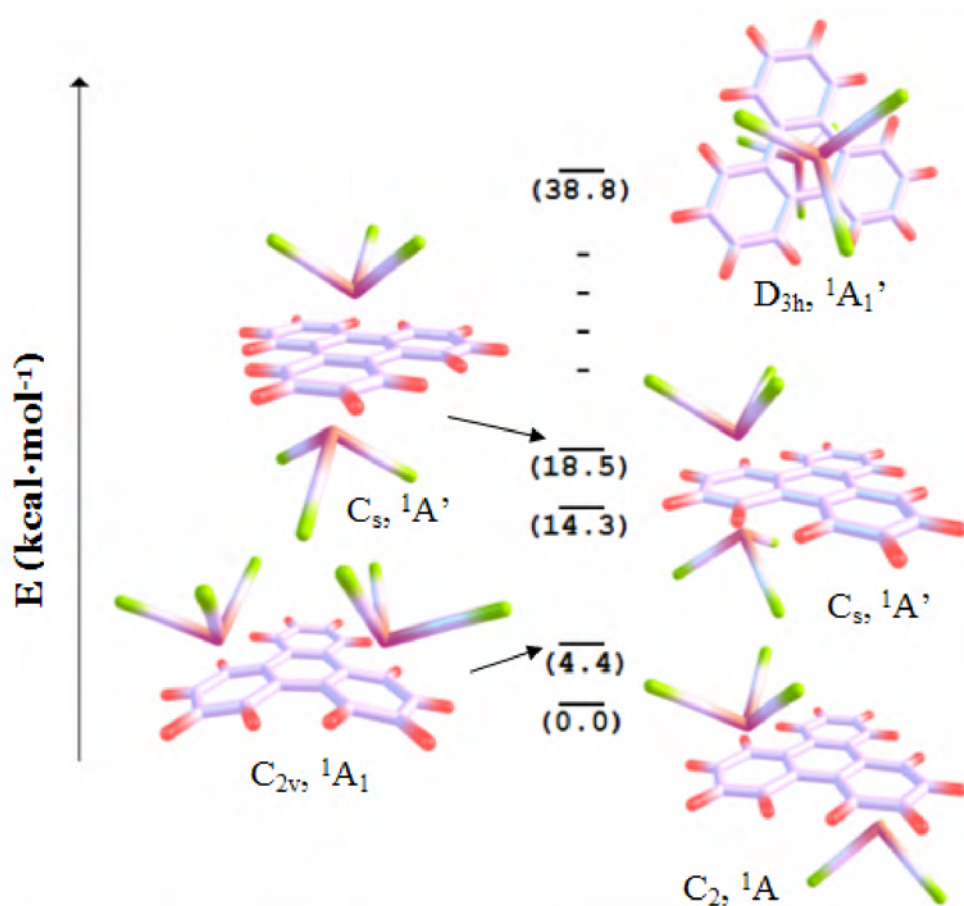


Figure 35. B3LYP/(Wachters' basis, 6-31G(d,p)) calculated geometries and relative energies for the possible isomers of $[\mu-(\eta^6:\eta^6)\text{triphenylene}]\text{bistricarbonylchromium}(0)$ complex. Molecular symmetry and electronic state are shown below each bicoordinated complex.

Appendix.

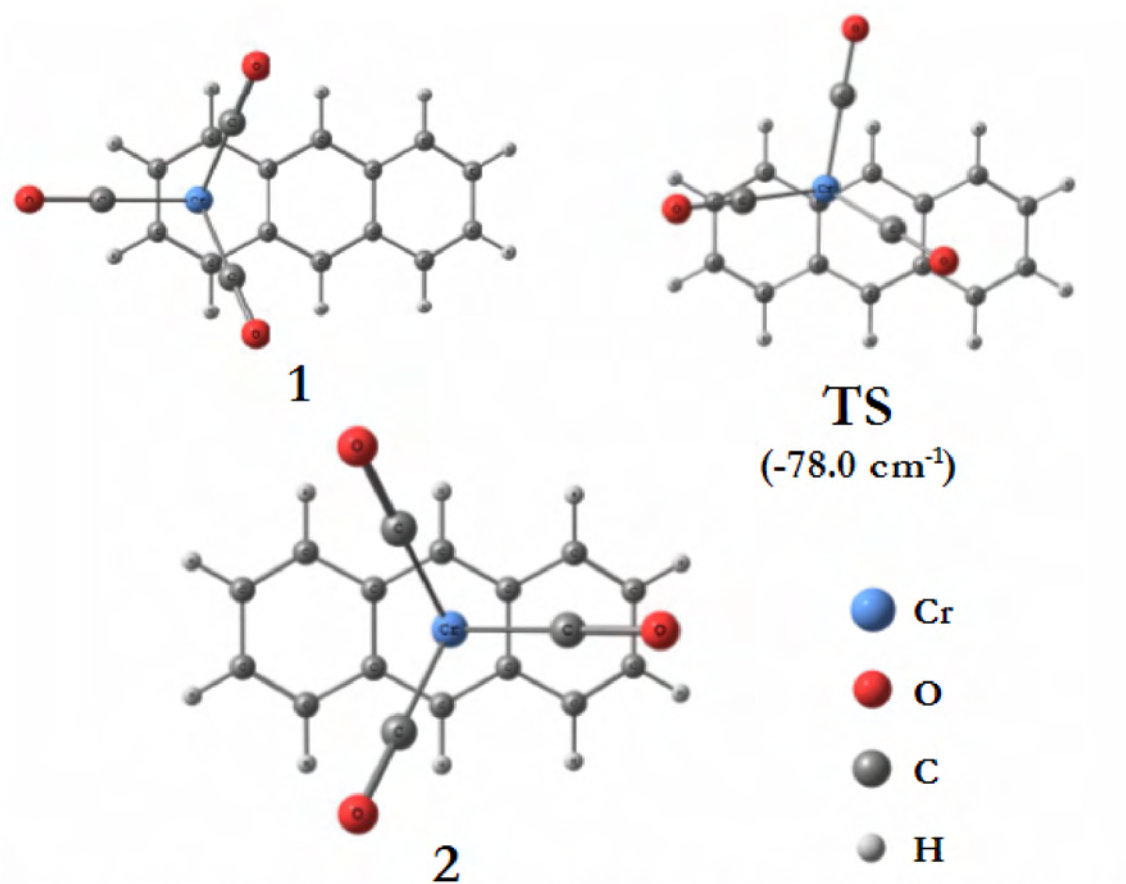


Figure A5. Optimized critical points found at the B3LYP/(Watchers' basis/6-31G(d,p)) level of theory in the PES of the $\text{Cr}(\text{CO})_3$ migration over anthracene.

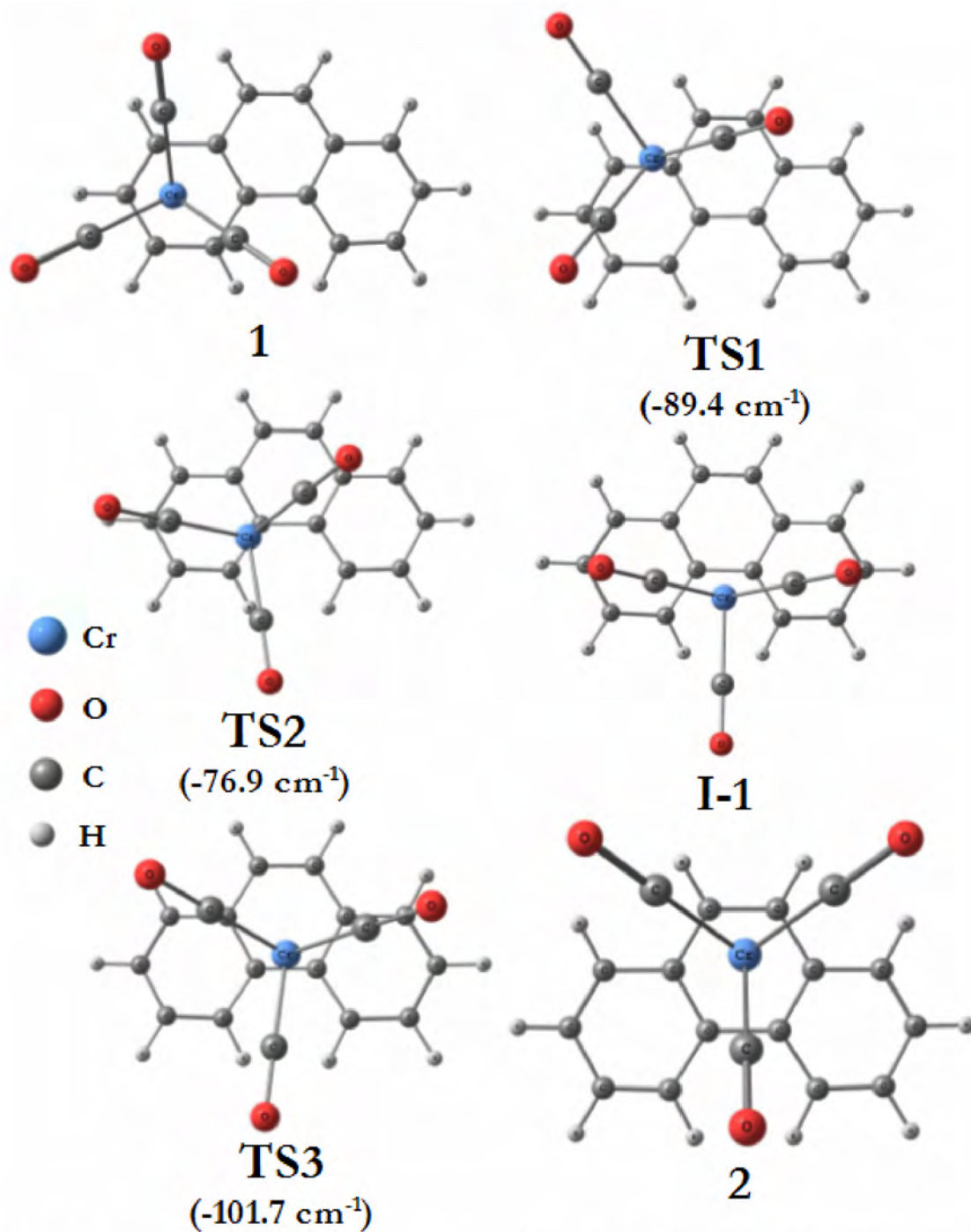


Figure A6. Optimized critical points found at the B3LYP/(Walters' basis/6-31G(d,p)) level of theory in the PES of the $\text{Cr}(\text{CO})_3$ migration over phenanthrene.

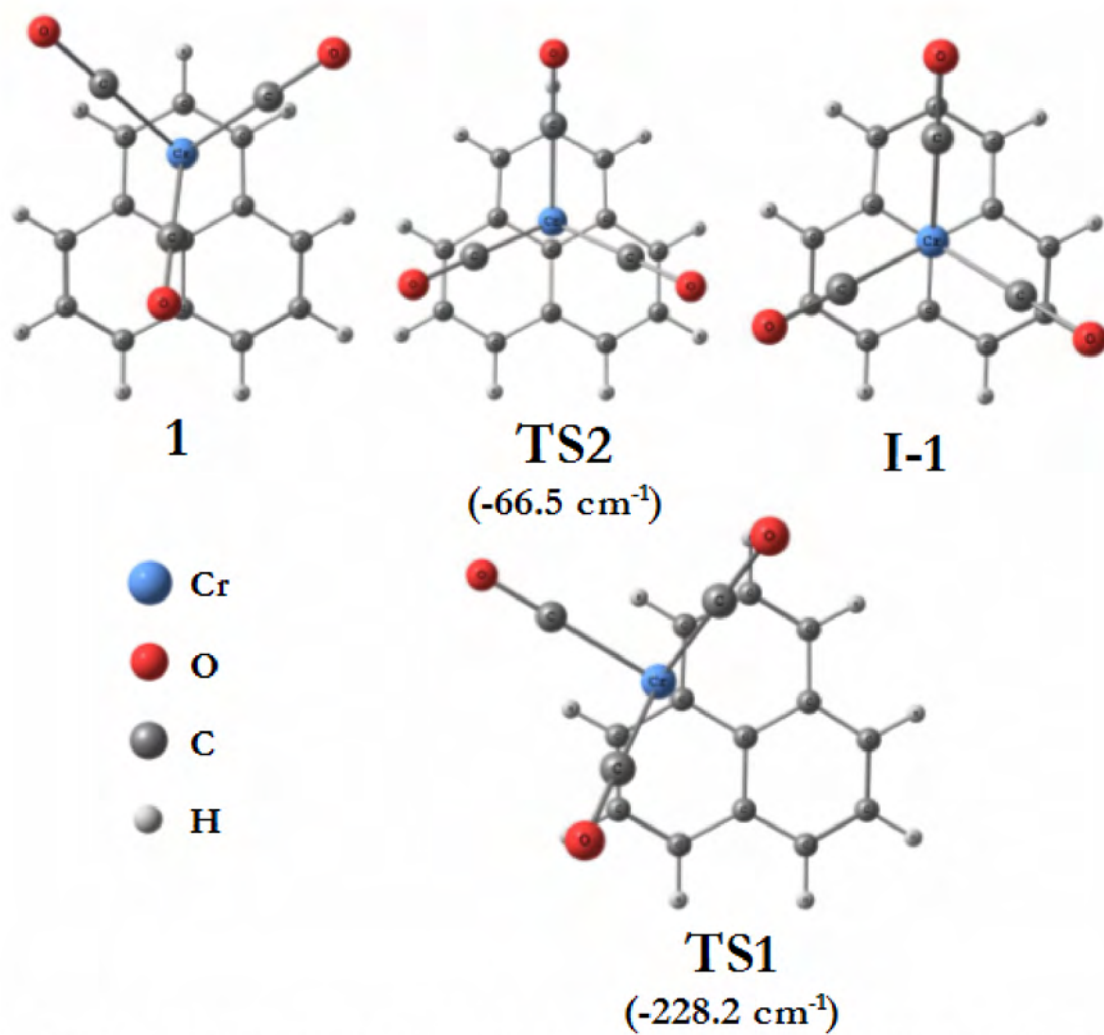


Figure A7. Optimized critical points found at the B3LYP/(Watchers' basis/6-31G(d,p)) level of theory in the PES of the $\text{Cr}(\text{CO})_3$ migration over phenalene.

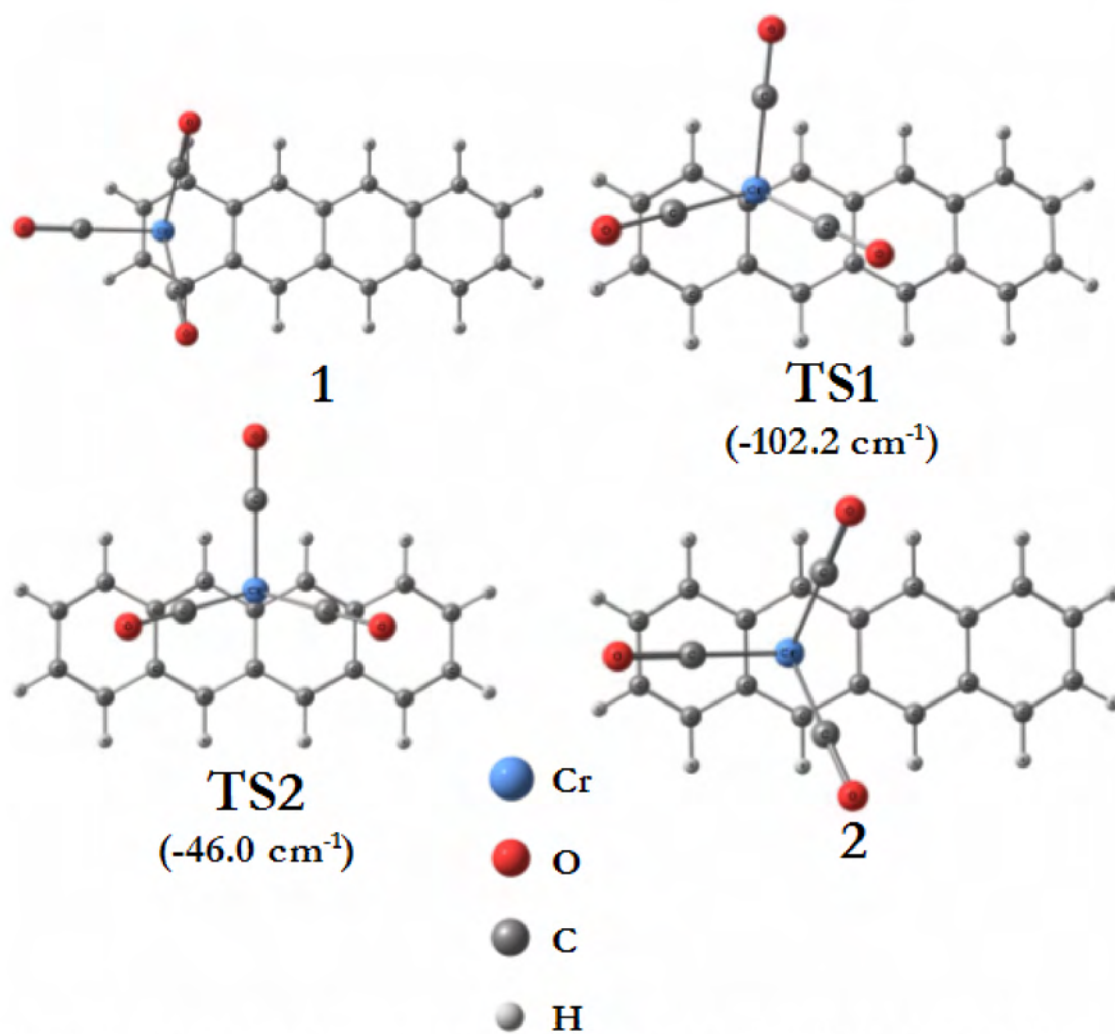


Figure A8. Optimized critical points found at the B3LYP/(Walters' basis/6-31G(d,p)) level of theory in the PES of the $\text{Cr}(\text{CO})_3$ migration over tetracene.

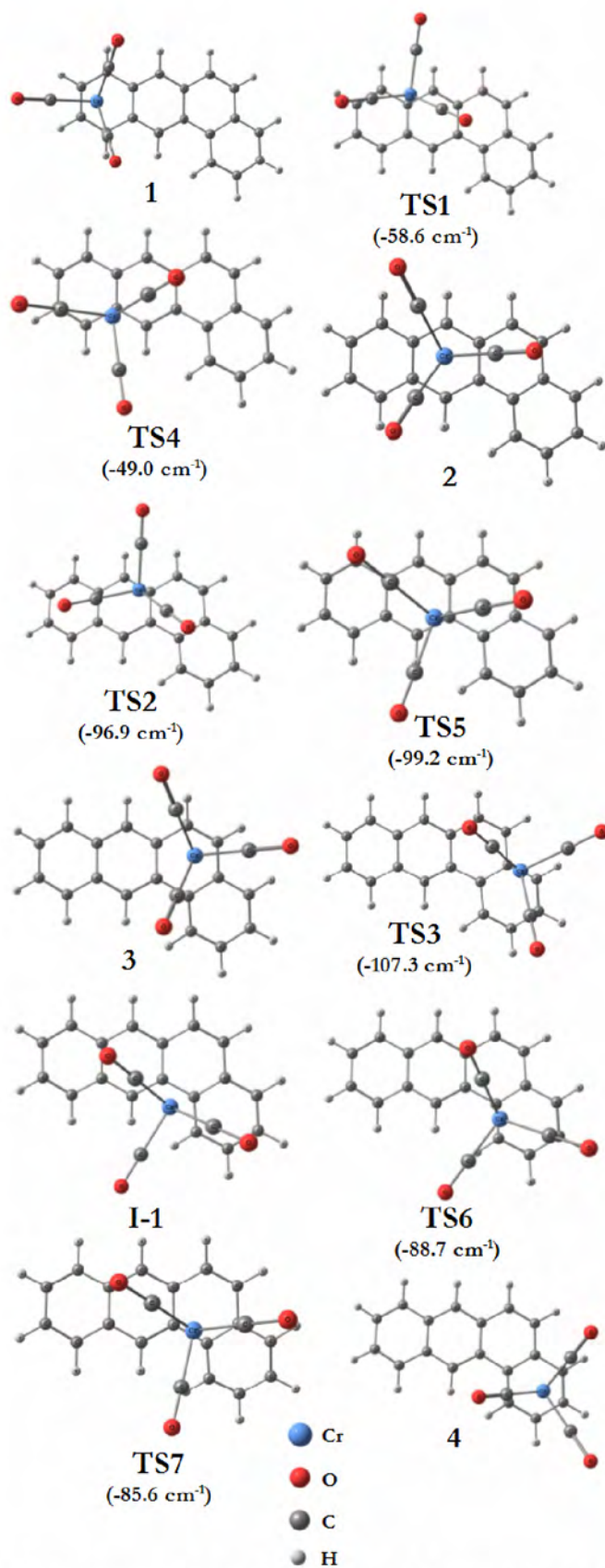


Figure A9. Optimized critical points found at the B3LYP/(Watchers' basis/6-31G(d,p)) level of theory in the PES of the $\text{Cr}(\text{CO})_3$ migration over tetraphene.

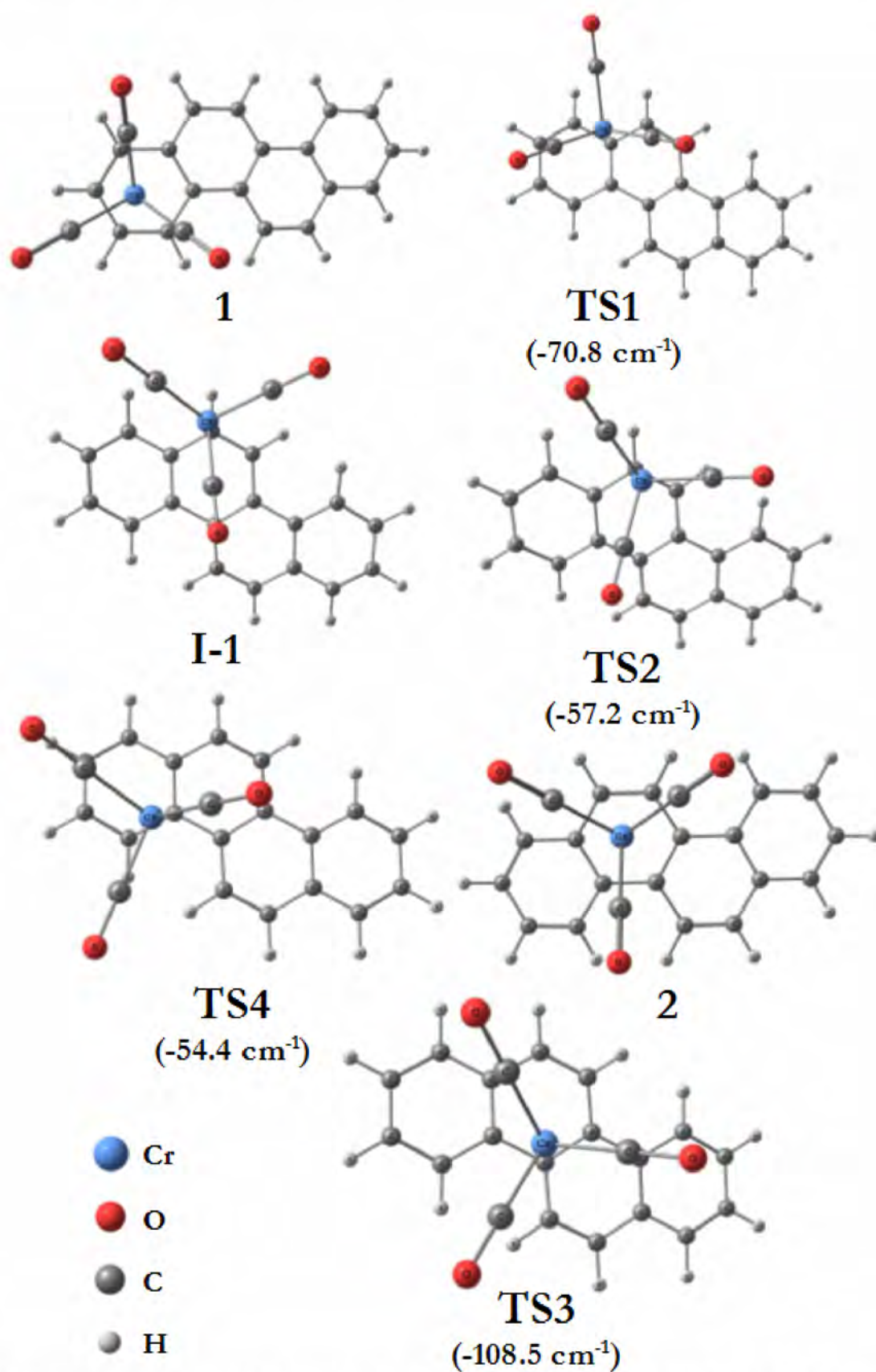


Figure A10. Optimized critical points found at the B3LYP/(Watchers' basis/6-31G(d,p)) level of theory in the PES of the $\text{Cr}(\text{CO})_3$ migration over chrysene.

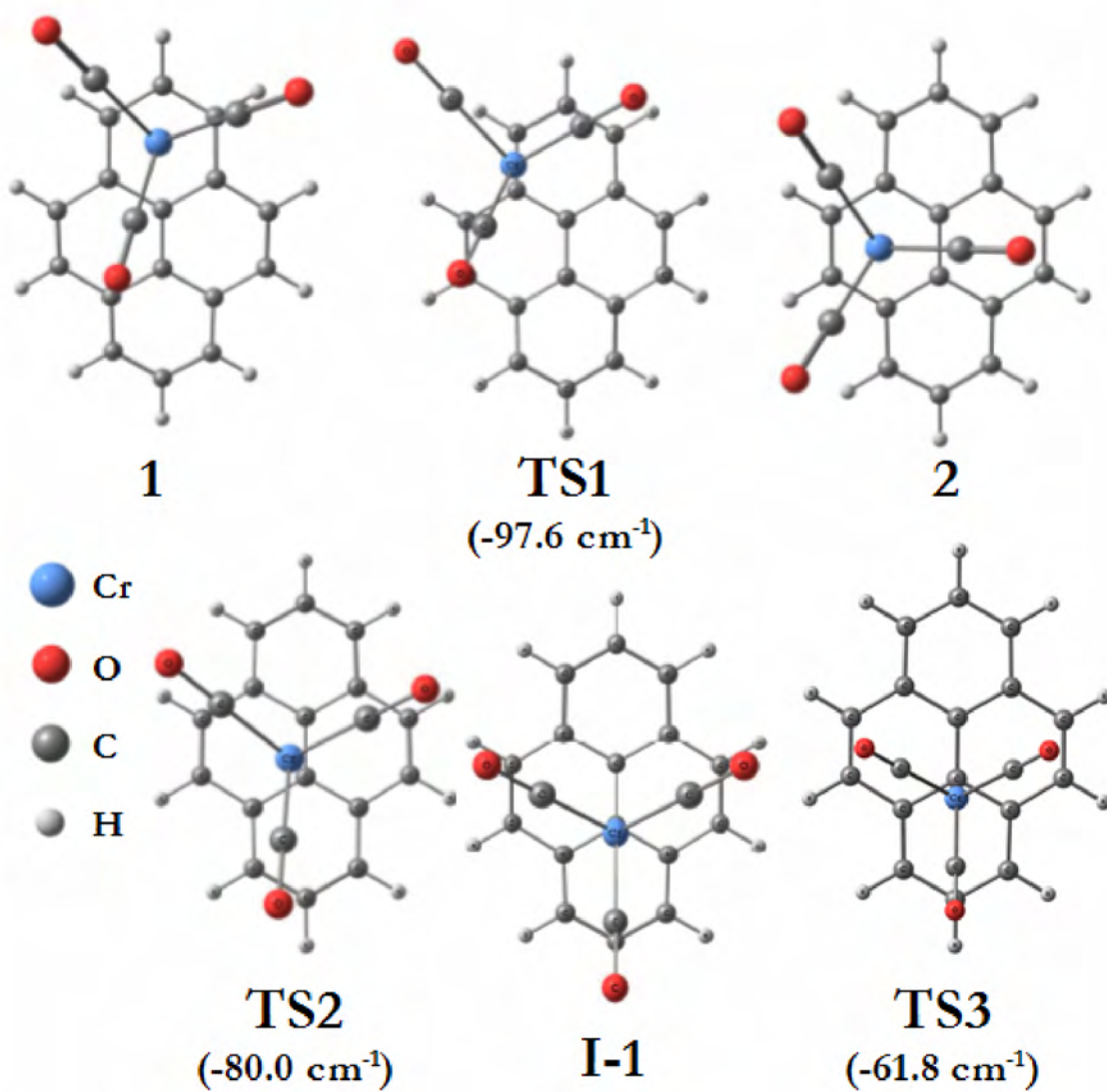


Figure A11. Optimized critical points found at the B3LYP/(Watchers' basis/6-31G(d,p)) level of theory in the PES of the $\text{Cr}(\text{CO})_3$ migration over pyrene.

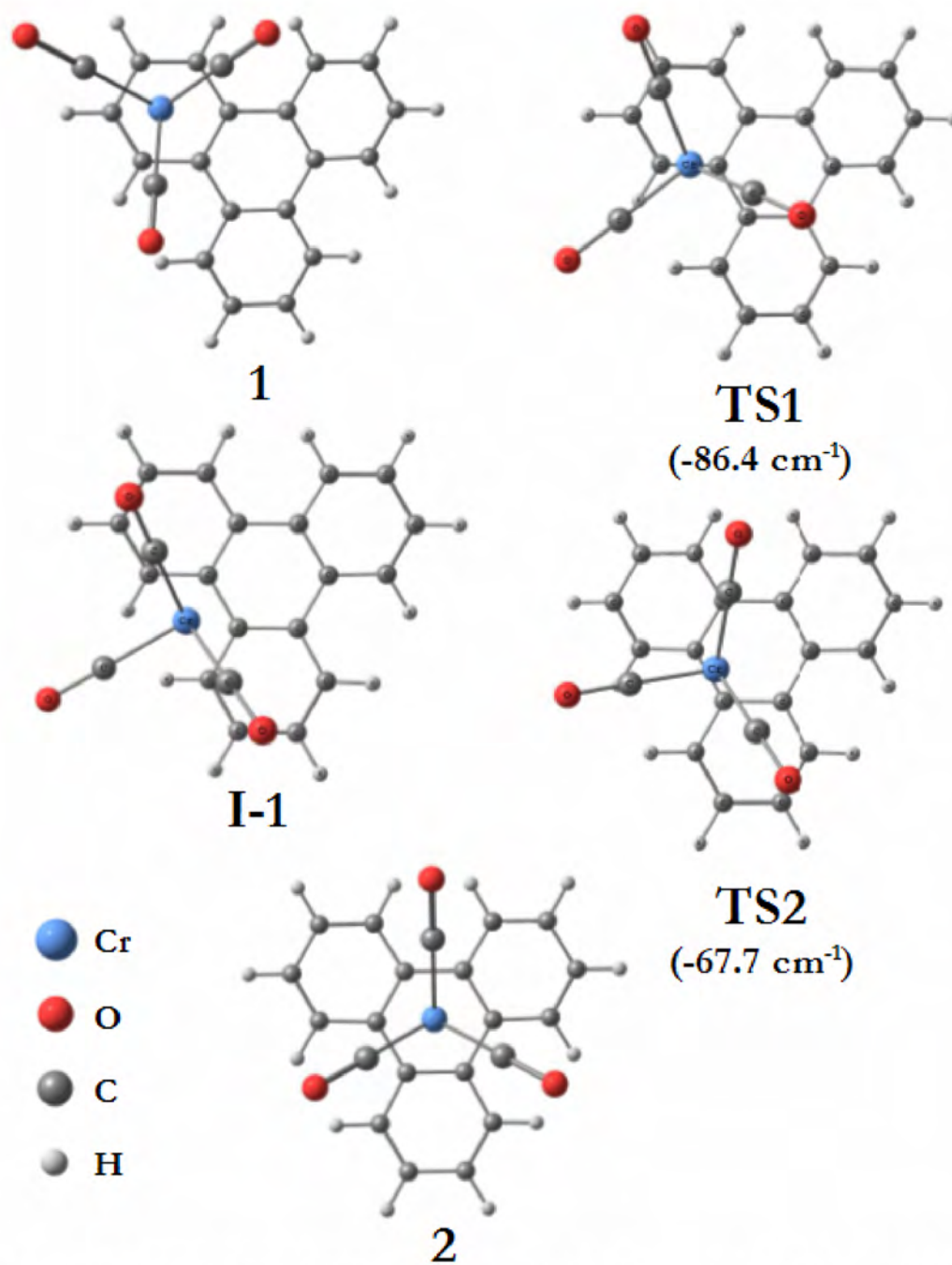


Figure A12. Optimized critical points found at the B3LYP/(Watchers' basis/6-31G(d,p)) level of theory in the PES of the $\text{Cr}(\text{CO})_3$ migration over triphenylene.

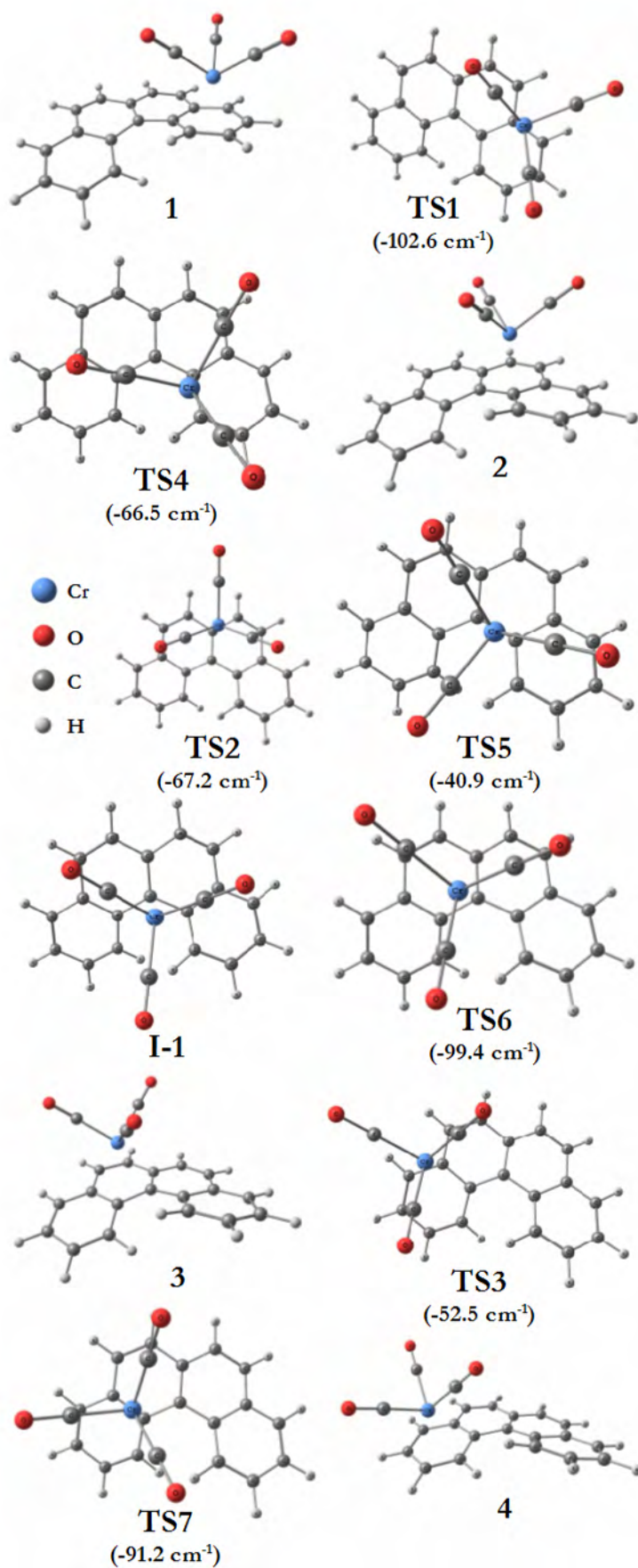


Figure A13. Optimized critical points found at the B3LYP/(Watchers' basis/6-31G(d,p)) level of theory in the PES of the $\text{Cr}(\text{CO})_3$ migration over tetrahelicene.

References.

- (1) (a) R. R. Schrock, J. S. Murdzek, G. C. Bazan, J. Robbins, M. DiMare, M. O'Regan, *J. Am. Chem. Soc.* **1990**, *112*, 3875; (b) R. R. Schrock *Top. Organomet. Chem.* **1998**, *1*, 1.
- (2) N. Hadei, E. A. B. Kantchev, C. J. O'Brien, M. G. Organ, *Org. Lett.* **2005**, *7*, 1991.
- (3) M. Torrent, M. Duran, M. Solà, *Organometallics* **1998**, *17*, 1492.
- (4) (a) M. Torrent, M. Duran, M. Solà, *Chem. Commun.* **1998**, 999; (b) M. Torrent, M. Duran, M. Solà, *J. Am. Chem. Soc.* **1999**, *121*, 1309.
- (5) J. P. Lee, K. A. Pittard, N. J. De Yonker, T. R. Cundari, T. B. Gunnoe, J. L. Petersen, *Organometallics* **2006**, *25*, 1500.
- (6) (a) W. D. Jones, R. P. Duttweiler, F. J. Feher, E. T. Hessell, *New J. Chem.* **1989**, *13*, 725; (b) W. D. Jones, F. J. Feher, *Organometallics* **1983**, *2*, 686; (c) W. D. Jones, G. P. Foster, J. M. Putinas, *J. Am. Chem. Soc.* **1987**, *109*, 5047; (d) W. D. Jones, G. P. Foster, J. M. Putinas, *Inorg. Chem.* **1987**, *26*, 2120; (e) W. D. Jones, E. T. Hessell, *Organometallics* **1990**, *9*, 718.
- (7) M. Lail, C. M. Bell, D. Conner, T. R. Cundari, T. B. Gunnoe, J. L. Petersen, *Organometallics* **2004**, *23*, 5007.
- (8) R. G. Bergman, T. R. Cundari, A. M. Gillespie, T. B. Gunnoe, W. D. Harman, T. R. Klinckman, M. D. Temple, D. P. White, *Organometallics* **2003**, *22*, 2331.
- (9) (a) J. Barrera, M. Sabat, W. D. Harman, *Organometallics* **1993**, *12*, 4381; (b) C. G. Young, S. Thomas, R. W. Gable, *Inorg. Chem.* **1998**, *37*, 1299; (c) J. J. García, A. Arevalo, N. M. Brunkan, W. D. Jones, *Organometallics* **2004**, *23*, 3997; (d) J. J. García, W. D. Jones, *Organometallics* **2000**, *19*, 5544; (e) J. L. Kiplinger, A. M. Arif, T. G. Richmond, *Chem. Commun.* **1996**, 1691; (f) J. L. Kiplinger, A. M. Arif, T. G. Richmond, *Organometallics* **1997**, *16*, 246.
- (10) K. H. Dötz, in: *Topics in Organometallic Chemistry*, K. H. Dötz ed., Springer-Verlag: Berlin/Heidelberg, **2004** vol. 13, p. 123
- (11) N. G. Akhmedov, S. G. Malyugina, V. I. Mstislavsky, Y. F. Oprunenko, V. A. Roznyatovsky, Y. A. Ustynyuk, A. S. Batsanov, N. A. Ustynyuk, *Organometallics* **1998**, *17*, 4607.

- (12) See for instance: (a) L. Fogel, R. P. Hsung, W. D. Wulff, *J. Am. Chem. Soc.* **2001**, *123*, 5580; (b) K. Kamikawa, K. Nishino, T. Sakamoto, S. Kinoshita, H. Matsuzaka, M. Uemura, *J. Organomet. Chem.* **2007**, *692*, 678.
- (13) B. Deubzer, H. P. Fritz, C. G. Kreiter, K. Öfele, *J. Organomet. Chem.* **1967**, *7*, 289.
- (14) (a) C. A. Bradley, E. Lobkovsky, I. Keresztes, P. J. Chirik, *J. Am. Chem. Soc.* **2005**, *127*, 10291; (b) H. C. Jahr, M. Nieger, K. H. Dötz, *Chem. Commun.* **2003**, 2866; (c) K. H. Dötz, C. Stinner, M. Nieger, *J. Chem. Soc., Chem. Commun.* **1995**, 2535; (d) H. C. Jahr, M. Nieger, K. H. Dötz, *Chem. Eur. J.* **2005**, *11*, 5333; (e) E. P. Kündig, V. Desobry, C. Grivet, B. Rudolph, S. Spichiger, *Organometallics* **1987**, *6*, 1173.
- (15) T. A. Albright, P. Hofmann, R. Hoffmann, C. P. Lillya, P. A. Dobosh, *J. Am. Chem. Soc.* **1983**, *105*, 3396.
- (16) (a) R. H. Mitchell, Y. S. Chen, N. Khalifa, P. Z. Zhou, *J. Am. Chem. Soc.* **1998**, *120*, 1785; (b) R. H. Mitchell, *Chem. Rev.* **2001**, *101*, 1301; (c) R. H. Mitchell, Z. Brkic, D. J. Berg, T. M. Barclay, *J. Am. Chem. Soc.* **2002**, *124*, 11983; (d) R. H. Mitchell, P. Z. Zhou, S. Venugopalan, T. W. Dingle, *J. Am. Chem. Soc.* **1990**, *112*, 7812.
- (17) P. v. R. Schleyer, B. Kiran, D. V. Simion, T. S. Sorensen, *J. Am. Chem. Soc.* **2000**, *122*, 510.
- (18) D. V. Simion, T. S. Sorensen, *J. Am. Chem. Soc.* **1996**, *118*, 7345.
- (19) S. M. Hubig, S. V. Lindeman, J. K. Kochi, *Coord. Chem. Rev.* **2006**, *200*, 831.
- (20) F. Feixas, J. O. C. Jimenez-Halla, E. Matito, J. Poater, M. Solà, *Pol. J. Chem.* **2007**, *81*, 783.
- (21) To consult mathematical details in methodology, please see J. O. C. Jiménez-Halla, in: *Quantifying Aromaticity in a Series of Cyclic Planar Inorganic Compounds*, Research Workshop, Universitat de Girona, Catalunya, **2006**.
- (22) P. Bultinck, *Faraday Discuss.* **2007**, *135*, 347.
- (23) (a) J. Poater, J. M. Bofill, P. Alemany, M. Solà, *J. Phys. Chem. A.* **2005**, *109*, 10629; (b) G. Portella, J. Poater, M. Solà, *J. Phys. Org. Chem.* **2005**, *18*, 785.
- (24) G. Portella, J. Poater, J. M. Bofill, P. Alemany, M. Solà, *J. Org. Chem.* **2005**, *70*, 2509.
- (25) M. Taniguchi, T. Thiemann, T. Sawada, S. Mataka, *Z. Anorg. Allg. Chem.* **1999**, *625*, 1249.

**GENERAL
CONCLUSIONS OF
THIS THESIS**

The most relevant results derived from this work on the catalytic reactions of Fischer carbenes, in particular from Dötz benzannulation and other cycloannulation reactions and haptotropic rearrangements as well, can be summarized as follows:

- I) The effect of substituents in FCCs for Dötz benzannulation and cyclopentannulation reactions has been investigated. Heteroatom ligands (X= alkoxy or alkylamino group) are the responsible of tuning the electronic properties of carbenes; thus, even when alkoxy-carbenes and aminocarbenes seem to be comparable π -donors, the amino groups favor the cyclopentannulation, especially if they are alkylated. Hindrance effects play a significant role because a bulkier aminocarbene is more congested to form a 6-MR than a 5-MR and must bend out of plane for the former case losing the in-plane aromatic π -system. Alkyl- or aryl-substituents (R= vinyl, phenyl) are more responsible of tuning the steric effects, *i.e.*, vinylcarbenes go through the chromahexatriene pathway of benzannulation whereas phenylcarbenes fit better into the classical Dötz reaction mechanism because of the geometrical position at the key intermediate **3a** occurring just before electrocyclic ring closure.
- II) The results also point out that benzannulation and cyclopentannulation are more exothermic reactions for vinylcarbenes than for phenylcarbenes but also more exothermic for alkoxy-carbenes than for aminocarbenes. Moreover, it has been confirmed that for phenylcarbenes, the first dissociation of carbon monoxide is the rate-limiting step of reaction, following the dissociative pathway in the initial part of the reaction. Vinylcarbenes, less congested, shown energetically more equivalent routes between dissociative and associative pathway even though the former one is also favored.
- III) From the first part of the Thesis, it is proven the importance of the metal assistance to cycloannulation reactions. Phenylcarbenes follow a reaction pathway through hydride intermediates and without chromium complex no C-H bond cleavage could be possible. Furthermore, the transport of a proton to construct the furan ring and the hydroarylation of 3,4-dihydroisoquinolinyll

ligand were computationally found to be metal-mediated catalytic reactions. However, several pathways for the intramolecular hydroarylation of isonitriles were tested along the proposed catalytic cycle where both the initial deinsertion of isonitrile from the Ru complex and the regeneration (that is, the coordination of a second isonitrile ligand after formation of the desired product) were found to be processes of very high energy.

- IV) Haptotropic rearrangements go through a change in coordination mode to the system of fused rings according to the sequence: $\eta^6 \rightarrow \eta^1 (\eta^3) \rightarrow \eta^6$ for all the studied cases. Depending on the favorable orbital interactions bumped into the way or not, we rationalized the existence of an intermediate (η^3 -complex) at the middle of the path or just one η^1 -transition state located anywhere between the distance of one of ring centers and the carbon in the ring junction. As the size of the arene increases in number of rings, the π -system is more delocalized and Cr-C interactions are weaker so therefore it reduces the reaction barrier. By other hand, the curvature of the system increases the reaction barrier of haptomigration because it favors again the metal-arene interactions.
- V) It was found that the tricarbonylchromium prefers to be coordinated on the less substituted rings due to reduced steric hindrance. The $\text{Cr}(\text{CO})_3$ tripod is a withdrawing-electron group and when coordinated to a benzenoid ring, it decreases the aromaticity of the ring. Thus, metal complex coordination is favored on more aromatic rings and with the higher π -density.
- VI) Symmetry of PAHs also makes the existence of an intermediate possible or not when there are *peri*-fused rings. For the case of bridged rings, there is a η^2 -intermediate between the bond common to both rings. Furthermore, when heteroatoms are present near to the rings where haptotropic shift evolves in, chromium complex was observed to interact better with the less π -donor oxygen and avoid the more σ -acceptor nitrogen during this process.
- VII) Regarding to the calculated dissociation energies between the tricarbonylchromium complex and PAHs, it was shown that the stabilization due to complexation is high but get lower as the system of fused rings grows up. It decreases notoriously when the benzenoid rings are grouped in an *ortho*, *peri*-

fused way like in phenalene or pyrene. For all the studied cases of bis-Cr(CO)₃ complexes, the *anti* isomer where the both metallic complexes are bonded to the most external and distant rings, resulted as the more stable one.

ACKNOWLEDGEMENTS

Runi sti binniee' xquenda' ni zani'

(My spirit shall talk for my race)

José Vasconcelos

The author of this Thesis wants to show gratitude for all the people that contribute somehow with his professional and cultural formation during his doctoral stay at Girona. To whom they assisted me to Live and supported me for my best and my worst moments, I don't want to forget anyone of you.

Gracias mamá y papa por haber creído en mi y por apoyarme a realizar este sueño que ahora es realidad. A mis hermanos Johann, Gerardo, Rodolfo y Luis que mucho han hecho intentando comprender porque tuvo que ser así mi ejemplo para alejarme de casa y saber si aún les quiero como siempre.

Vull fer un reconeixement a tot el poble de Catalunya que me'n va acollir a casa seva durant més de quatre anys i que me'n va fer sentir com si fora part d'ells. Havent conegut tant a gent força intel·ligent i culta així com joves de futur prometedor, estic agraït primer que tot amb Déu per donar-me aquesta oportunitat per ampliar la meva visió del món i portar-me a casa més d'una forma de pensar diferent d'aquest país.

Primer he de començar pel grup de recerca que em va veure superar-me com investigador: el Institut de Química Computacional (IQC). Hi seré sempre agraït amb les dues persones responsables de la meva arribada i adaptació a Girona: En Miquel Solà i la Carme López. Sense l'organització, la diligència i fer unes quantes vegades de 'mamà Carme' no hagués estat possible sobreviure als embats administratius i 'burucrates' de la vida. Però sobretot, de tota la gent maca de Catalunya, agraeixo els quatre anys d'oportunitats que me'n va donar en Professor Miquel Solà: moltes gràcies per la teva paciència, per tota la teva comprensió, per la teva visió del projectes de recerca als que me'n vas involucrar i perquè sempre vas estar per a mi com pare acadèmic. Fins i tot t'estic agraït per apel·lar davant d'altres per mi i segurament enyoraré les clàssiques reunions de cada dilluns per discutir treball i mantenir els punts clars al estudiant i el to de bona col·laboració científica.

De primer cop, vull expressar molts sentiments grats pels professors al IQC: Professor Ramon Carbó-Dorca, al qui en tinc bona admiració pel seus treballs matemàtics i la seva persona; Professor Joan Miró que sempre portava cafè o el diari a

la mà; Professor Miquel Duran que ara se'm queda gravat a la ment com tot un professional divulgador de la ciència a Girona i estimulador de la gent jove a acostar-se a la Química a través de trucs químics que parlen de màgia real; Professor Lluís Blancafort pel que després d'unes quantes interseccions còniques vaig quedar marejat :D ja en serio, amb la seva aportació vaig tenir una altra visió de l'aromaticitat als cúmuls de magnesi que hi vàrem estudiar; Professor Josep Maria Luis, em porto a la memòria la benvinguda al principi i que hem fet bon equip (congrés a Loutraki), gràcies per la teva assistència i assessorament en activitats com l'última de fer contracte; Professora Sílvia Simon, encara que vaig fer poca conversa amb tu, crec que si ens hem caigut molt bé; Professor Emili Besalú, gràcies pel suport als tràmits administratius :) . I also thanks to Professor Alexander Voityuk who was very friendly and I enjoyed his questions at the group seminars, it was stimulating to know about someone's research handling with semiempirical methods since in my school, they taught me to look ahead for *ab initio* methods; Professor Sergei Vyboishchikov, thanks for all your advices even when I could not keep continue with meetings at lunch time, to my regret; a mi querido compadre Profesor Pedro Salvador, que me hizo conocer junto con los demás compañeros a mi llegada, el espíritu de colaboración IQCino –en aspectos comunes y no tan comunes– ¡Larga vida a los *Starky&Hutchers!* a quienes también debo un par de felices noches roqueras uuuuuu.

Life is not clearly well defined without friendship; everywhere I go, happily I must say I find somebody whom I share good and bad days, and nights fully of fun! (So I stay alive yet) Thank you, dear Samat Tussupbayeb(sake) not only as a fellow worker but also as my best friend. Спасибо маленький брат, эта диссертация также идет из-за тебя. Я буду скучать эти ночи excalibur или мы обратно в дом передвигаясь по улице и обсуждая научные идеи или ежедневной жизни.

Per descomptat, no vaig a deixar enrere a la resta de companys i companyes que em van acompanyar a través d'aquests anys. Començant pel meu col·laborador estrella: mi compadre Eduard Matito al que deu molta ajuda amb els càlculs d'índexs d'aromaticitat (ESI, BAD) i en bona part, enriquir els papers amb les seves discussions descobrint que tenim el mateix interès de recerca. Sense la teva dedicació i esforç conjuminat a la perseverança d'en Miquel Solà, no haguéssim pogut publicar aquell paper mil·lenari. A més, en faig un gran agraïment pels IQCins: David Asturiol, Mireia Güell, JuanMa Barroso, Quim Chaves, David Hugas, els germans Poater: Jordi i Albert, Ferran Feixas, Cristina Butchosa i les adorables Annas (3). Gràcies a tothom per obrir-

me els ulls a Catalunya, per la companya, els germanors emotius, els sopars estil IQC – amb el nostre bunker de batalla, *Luxury*, l'última frontera del infinit i més enllà–, les jornades jodete que em porto en concepte cap a casa. Potser no hauré estat el mexicà més tranquil i reservat però si el oxaqueny més característic que us trobarà a faltar alguna vegada, salut. No em podria deixar mai al benvolgut Miquel Torrent amb qui he tingut bona química i se'm va comparar amb els mateixos horaris nocturns; gràcies a tu pels consells ben encertats i per ser dels primers amics que vaig necessitar al principi de tota aquesta aventura. Aquells que són anomenats al final no significa que siguin els menys importants, grazie per tutti Annapaola Migani; dank u Marcel Swart, la teva ajuda fent servir el ADF va ser molt útil per mi. Aquest quatre anys i mig fent servir les cues del cràpula i oblidar-me del nostre informàtic de capçalera no pot ser: gràcies per tota l'ajuda tècnica Daniel Masó (la cia mexicana t'estarà molt agraïda pels informes de Banyoles que t'he pres prestats) ;D. Finalmente, hago un llamado a las futuras generaciones IQCinas a superarse y representar orgullosamente nuestra institución, los que leemos tesis ahora os dejamos la batuta, mucha suerte! Eugeni Horbatenko, Luz Dary Mercado, Eloy Ramos, Sergi Ruiz, Martin Felix, Laia Guillaumes i el més distingit per mi, el bon Lluís Armangué.

També vull recordar als químics experimentals, que més que cares conegudes, hi són els amics divertits de les nits lux-úriques: la comadre Montse Rodríguez, Isabel Serrano, el bon compadre meu Rafael Ferrer, Jordi Rich, Anna Company i perdoneu-me les omissions d'altres noms (no vull deixar-hi sense cognoms a uns) d'aquesta gent tan maca i bona amb mi.

Esta tesis también va para el 'grupo de los elementales', los primeros amigos que conocí durante mi primera vez en Catalunya. Dejo aquí constancia que jamás me olvidé tan sólo una vez de mis apreciados valencianos o granadinos –en su mayoría– (creo que decían que había un italiano :D ese es el mejor de todos!): Daniel Roca, Juanjo Serrano, Gloria Olaso, Issac Vidal, Miquel Adrover, Javier Ruiz, Joaquín Ortiz, Noemi Hernández, Pamela Moles, Natal Kanaan, y gracias también a Adrián Varela por su amistad y haber sido mi guía de lujo en mi paso por Marburg, y por supuesto a mi querida comadre Merche Alonso, que quedó grabada en el recuerdo de la noche internacional gironina más exitosa. I also thank to my good friend Marcin Palusiak, who shared with me valuable scientific discussion and daily life tales, Dziękuję, mój przyjaciel.

I moltes gràcies de veritat a tota la gent que ha compartit amb mi tant de temps rodant els carrers de Girona i als companys de pis dels que també hi ha moltes històries gravades al meu cap: Germán Ávila, Miquel Maldonado, Fernando Vázquez, Laia Boadas, Montse Fort, Sandra Den Braber i Xavi Vilaseca. Seguidament, he d'agrair a un tio molt guai, en Miquel Huix, que es mereix el quadre d'honor dels Guardianes de la Bahia, ja saps de quin peu calço ;) en sóc més paisà que tú :D :D y lo mismo para mi querido Ramoncito Valencia, que es el máster #1 con las arepas.

Esto también va para toda la raza bonita que hay por éstos lares, sean naturalizados-por-conveniencia o de origen: Iria Cajiao y Antonio Mortera, muchas gracias por su amistad tan sincera e incondicional, por todos los paros que me hicieron (por los sustos de medianoche) y porque fueron mis mayores confidentes en Girona, los quiero mucho; a los chavos que son la neta, puro chamaco desma: Carmen Vázquez, Roel Martínez, Verónica Leyva, Reina Marisol Linares, Enrique Rodríguez, Yolanda Godó, David Alesanco, Alejandra Flores, Ricardo Medina, Raúl Alcántara, Edgar Mixcoha, Oscar Arias, Rocio López, Elisa Vázquez, Silvia González, Héctor Núñez, Manuel Vial y César González.

“Em vaig topar amb els estudiants més capaços, imaginatius, organitzadors i sensacionals de Catalunya. Estic flipant! Es fan cridar el Esquadró Vermell i en van convidar a unir-me a les seves files... però fa una estona que he desertat perquè no tinc bona confiança en mi mateix. De totes maneres, agraeixo deixar-me les portes obertes: Albert Orriols, Núria Mach, Leanid Kazyrytski, Anna Lluveras, Marilena de Chiara, Judith Baos, Rut Fado, Raquel Camprubí, Aida Míguez, Estela Romero, Ping Xiao, Mónica Antequera i Jordi Marrugat. (*Diari de JOC, Girona 2007*)”.

Aquesta tesi difícilment s'hagués pogut solucionar sense el suport econòmic sempre puntual de l'Agència de Gestió d'Ajuts Universitaris i de Recerca (AGAUR). Vull agrair responsablement als senyors i senyores Antoni Morell, Bernat Xancó, Montse Boada i Cristina Rivas per la seva assistència respecte de la beca que vaig gaudir durant la meva estada del doctorat. A més, vull expressar agraïment a l'eficàcia dels meus banquers de capçalera que van resoldre els meus problemes més com veritables amics abans que funcionaris grises: Joan del Pozo i Jordi Fàbregas, gràcies per la vostra col·laboració al llarg d'aquests anys.

También he de agradecer todo el apoyo moral que siempre he tenido de mis amigos en México, que a pesar de la distancia no nos hemos alejado ni un pelo a través del contacto que mantenemos. Gracias a Mavis Bautista, Luis Salvachúa, José Eduardo

Báez, Jorge Hernández, Roberto Horacio Herrera, Yunuén Ordaz, Tanya Ramírez, Rubén Jiménez y Luis Bernardino. Ustedes también son parte motivadora de esta tesis; me ha alegrado mucho compartir mis logros y que siempre hayan estado al pendiente de mis trabajos pidiendo ser los primeros en leerlos y que hubieran más :-). Hago una mención especial al maestro Heliodoro Canseco cuya afirmación sobre la posibilidad de encontrar un cúmulo inorgánico que cambie sus propiedades electromagnéticas al acomplejarse con otros metales dio origen a la idea central de nuestro trabajo publicado en *J. Comput. Chem.*

Un agradecimiento más, a la persona responsable de mi primer viaje a Girona y quien me puso en contacto con el IQC, mi codirector de tesis Profesor Juvencio Robles que además de introducirme al fascinante mundo de los funcionales de la densidad, me dió un curso intensivo de cultura catalana y las primeras nociones de catalán pa' mexicanos. El reporte al final de esta tesis, doc Juve, es que faltó la ida a Toloriu para honrar el vínculo espacio-temporal entre aztecas y catalanes.

I want to thank also to Professor Thomas Cundari and his group, Adriana Dinescu, Sridhar Vaddadi, Aaron Pierpont, Khaldoon Barakat, Nathan DeYonker, from University of North Texas for a very warm welcome to Denton. I really appreciate the opportunity you gave me for my formation, the stay was a real pleasure for me and that barbecue time was so fun since I recover some old links between neighboring countries, which makes sense on the common past we had. Also in Denton and Dallas, I met really good friends: thanks for your help Maria Asencio, al compa Gustavo Garza, que es raza a toda madre, a mis cuates Angel Bravo, Iris Nelly Gómez y doña Eulalia, que bien nos encariñamos y fué difícil la despedida. Yall are in my heart, amigos, God bless you.

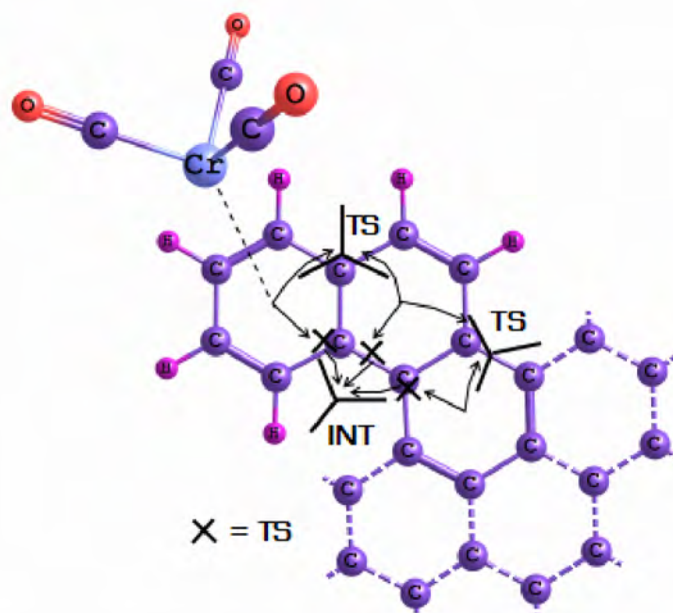
I am in debt with Professor Gernot Frenking and his group in Marburg, Gerda Jansonius, Israel Fernández, Taka Shimizu, Nozomi Takagi, Ralf Tonner, Robin Haunschild, Professor Oleg Poleshuk, Giovanni Caramori and Greta Heydenrych whose fellowship and solidarity for the worst moment I passed through were well motivating. Thank you for your kind welcome but emotive farewell and be sure you contribute so well in my formation.

Moreover, my best wishes for some friends I met last year and to whom I thank for some mischievous moments we had: Israel Alfaro, Fernando Rascón, Roberta Bomparola, Andrew Suirman, Irma Sánchez, Gemma Christian, Paulina Dreyse, Mauricio Cattaneo and Pietro Vidossich. It was my pleasure to meet you all.

Finally, I thank to all my referees and the members of the committee of this dissertation for your time, your effort to read this Thesis and your patience, Prof. Luigi Cavallo, for all the time you was waiting for my response. And in general, thanks to the reader who not only jumped into these lines but took a look on the chemistry I had been working during these years. Have a nice day! :D

J. Oscar C. Jimenez-Halla

In this thesis, several reaction mechanisms of cycloannulation reactions in Fischer carbenes were studied by means of theoretical methods, namely B3LYP/(Wachters' basis / 6-31G**) level of theory. Vinylic or aromatic alkoxy- and amino pentacarbonyl chromium carbenes react with acetylene to give Cr(CO)₃-coordinated substituted phenols, naphthols or cyclopentadiene and indene derivatives in a regioselective fashion. The aim of this work is to discuss both of the competitive reactions focusing on the Dötz benzannulation which during past years has been explored experimentally by W. D. Wulff, C. P. Casey, R. Aumann, and J. Barluenga among others with mechanistic proposals. Moreover, K. H. Dötz proved that coordination of Cr(CO)₃, once the ring is formed, can undergo haptotropic rearrangements, *i.e.*, walking of the metal complex from one ring to another –usually less substituted– changing its hapticity (π -coordination with the members of the ring). Thus, intramolecular haptotropic migrations in small polycyclic aromatic hydrocarbons were also studied in order to analyze the reaction pathways by which these reactions are carried out.



Català:

En aquesta tesi s'han estudiat mecanismes de reaccions de cicloannul·lació en carbens de Fischer a través de mètodes teòrics, concretament fent servir el nivell de teoria B3LYP/(Wachters' basis / 6-31G**). Els alcoxi- i amino carbens de pentacarbonil crom, ja siguin vinílics o aromàtics, reaccionen amb acetilè per produir fenols, naftols o derivats ciclopentadiè o índè substituïts amb el Cr(CO)₃ coordinat, d'una manera regioselectiva. L'objectiu d'aquest treball és discutir ambdues reaccions competitives particularment a la reacció de Dötz, la qual durant els darrers anys ha estat explorada experimentalment per W. D. Wulff, C. P. Casey, R. Aumann i J. Barluenga entre altres amb diferents propostes mecanístiques. A més, K. H. Dötz va demostrar que la coordinació del Cr(CO)₃, un cop l'anell ja està format, pot patir canvis haptotòpics, és a dir, la caminada del complex metàl·lic d'un anell a un altre –generalment al menys substituït – canviant la seva hapticitat (coordinació π amb els membres de l'anell). Llavors, s'han estudiat les migracions haptotòpiques intramoleculares en petits hidrocarbons aromàtics policíclics amb l'objectiu d'analitzar les rutes de reacció per les quals aquestes reaccions es porten a terme.